Comparative analysis of the nuclear receptors CAR, PXR and PPARα in the regulation of hepatic energy homeostasis and xenobiotic metabolism

EDITED BY
DR MOHAMMAD MAHMOUD

**FOR MY DAUGHTER
LYNAH**

Table of content

Abbreviations

ACAA	acetyl-CoA acyltransferase
ACAD	acyl-CoA dehydrogenase
ACSL	acyl-CoA synthetase long-chain
ADH	alcohol dehydrogenase
AF	activation function
AKR	aldoketoreductase
ALAS	aminolevulinate, delta-, synthase 1
ALDH	aldehyde dehydrogenase
AMPK	AMP-activated protein kinase
ANGPTL4	angiopoietin-like 4
ARG	arginase
cAMP	cyclic adenosine monophosphate
CAR	constitutive androstane receptor
CCRP	CAR cytoplasmic retention protein
CD36	CD36 Molecule (Thrombospondin Receptor)
Cdk	cyclin-dependent kinases
CES	carboxylesterase
CITCO	6-(4-Chlorophenyl)imidazo[2,1-b][1,3]thiazole-5-carbaldehyde O-(3,4-dichlorobenzyl)oxime copy
CNV	number variation
CV	coefficient of variation
CPT	carnitine palmitoyltransferase
CREB	cAMP responsive element binding protein
CXCL	chemokine (C-X-C motif) ligand
CYBB	cytochrome b-245, beta polypeptide
CYP	cytochrome P450
DAPK	death-associated protein kinase 1
DBD	DNA-binding domain drug-
DDI	drug interaction
DMET	drug metabolizing enzymes and transporter
EGF	epidermal growth factor
EPHX	epoxide hydrolase 2
ERK	extracellular-signal-regulated kinases
FABP	fatty acid binding protein
FADS	fatty acid desaturase
FMO	flavin containing monooxygenase
FOX	forkhead box
FXR	farnesoid X receptor
G6PC	glucose-6-phosphatase, catalytic subunit
GO	Gene ontology
GR	glucocorticoid receptor
GRB	growth factor receptor-bound protein
GSK	glycogen synthase kinase
GST	glutathione S-transferase
GYS	glycogen synthase
HADH	hydroxyacyl-CoA dehydrogenase
HMGCS	3-hydroxy-3-methylglutaryl-CoA synthase
HNF	hepatocyte nuclear factor
IRS	insulin receptor substrate
IRS	insulin response sequence
KEGG	Kyoto Encyclopedia of Genes and Genomes

LBD	ligand-binding domain
LXR	liver X receptor
MAPK	mitogen-activated protein kinases
MASP	mannan-binding lectin serine peptidase
MDR	multi drug resistance protein
ME	malic enzyme
MGST	microsomal glutathione S-transferase
NAFL	non-alcoholic fatty liver disease
D	nuclear factor kappa-light-chain-enhancer of activated B cells
NFκB	nuclear receptor
NR	organic solute transporter
OST	phenobarbital responsive enhancer module
PBREM	phosphoenolpyruvate carboxykinase
PCK	pregnenolone-16α-carbonitrile
PCN	programmed cell death 1 ligand
PDCD1LG	pyruvate dehydrogenase kinase
PDK	6-phosphofructo-2-kinase/fructose-2,6-biphosphatase
PFKFB	peroxisome proliferator-activated receptor gamma, coactivator
PGC	protein kinase A
PKA	protein kinase C
PKC	perilipin
PLIN	proline-rich nuclear receptor coactivator
PNRC2	cytochrome P450 reductase or P450 (cytochrome) oxidoreductase
POR	protein phosphatase
PP	peroxisome proliferator activator receptor
PPAR	peroxisome proliferator response elements
PPRE	PRAME family member
PRAMEF	PR domain containing PR
PRDM	domain containing
PRDM2	patched
PTCH	post-translational modification
PTM	pregnane X receptor
PXR	quantitative real-time polymerase chain reaction
qRT-PCR	retinol dehydrogenase
RDH	retinoid X receptor
RXR	stearoyl-CoA desaturase
SCD	serotonin re-uptake inhibitor
SERT	sulforaphane
SFN	small interfering RNA
siRNA	St John's wort
SJW	solute carrier
SLC	snail family zinc finger
SNAI	single nucleotide polymorphism
SNP	STEAP family member
STEAP	sulfotransferases
SULT	transducin (beta)-like 1X-linked
TBL1X	transcription factor
TF	thyroid hormone responsive
THRSP	tumor necrosis factor receptor superfamily
TNFRSF	transient receptor potential cation channels
TRPC	uridine diphosphoglucuronosyl
UDP	UDP-glucuronosyltransferase
UGT	xenobiotic responsive enhancer module
XREM	

Zusammenfassung

Kernrezeptoren, allen voran der Constitutive Androstane Receptor (CAR) und der Pregnane X Receptor (PXR), regulieren die Transkription zahlreicher Arzeimittel-metabolisierender Enzyme und Transporter (engl. drug metabolizing enzymes and transporters / DMET) und stellen damit wichtige Regulatoren der Entgiftungs-prozesse in der Leber dar. Folglich trägt die Liganden-abhängige Aktivierung dieser Rezeptoren, durch Arzneimittel und andere körperfremde Stoffe, zur intra- und inter-individuellen Variabilität des Arzneimittelstoffwechsels bei. CAR und PXR sind zudem in die Regulation des Fett- und Glukosestoffwechsels involviert. Auch für den Kernrezeptor Peroxisome Proliferator-activating Receptor Alpha (PPARα), ein Schlüsselregulator des Fettsäure-Abbaus und Ansatzpunkt von Fibraten, wurde kürzlich gezeigt, dass dieser die Expression von Cytochrom P450 3A4 (*CYP3A4*) direkt reguliert und darüber hinaus mit der Regulation weiterer wichtiger DMET-Gene assoziiert ist. In diesem Zusammenhang stellen CAR, PXR und PPARα wichtige Determinanten von Leberfunktionen wie Arzneimittel-Metabolismus und Energie-homöostase dar und stehen dadurch in Verbindung mit Arzneimittelnebenwirkungen, sowie Lebererkrankungen, wie beispielsweise Steatose.

Bis jetzt gibt es keine vergleichenden Studien, welche die Transkriptome der Kernrezeptoren CAR, PXR und PPARα im Menschen untersucht haben. Deshalb war ein Hauptaspekt dieser Arbeit, die genomweiten transkriptionellen Veränderungen, welche durch diese Kernrezeptoren in humanen Leberzellen hervorgerufen werden, zu untersuchen. Diese Untersuchungen wurden mit primären humanen Hepatozyten durchgeführt, da diese Zellen das geeignetste verfügbare Zell-Modell zur Untersuchung der leberspezifischen Gen-Expression und deren Regulation darstellen. Um die CAR-, PXR- und PPARα-spezifischen, genomweiten Expressions-änderungen zu bestimmen, wurden Hepatozyten-Kulturen von sechs verschiedenen Spendern mit den prototypischen Liganden für CAR (CITCO), PXR (Rifampicin) und PPARα (WY-14643), sowie mit DMSO, der Vehikel-Kontrolle, behandelt. Im Folgenden wurde die mRNA-Expression in diesen Proben mittels Affymetrix® Microarrays bestimmt. Die Expressions-Daten wurden statistischen Analysen unterzogen, um die Gene zu identifizieren, die eine signifikant veränderte Expression

durch die Agonisten-Behandlungen zeigen; des Weiteren wurde untersucht, mit welchen metabolischen Funktionen diese Gene assoziiert sind.

Die so gewonnenen Resultate bestätigten, dass CAR, PXR und PPARα unterschiedliche, aber dennoch teilweise überlappende Gruppen von DMET-Genen regulieren. Durch KEGG- (Kyoto Encyclopedia of Genes and Genomes) Pathway-Analysen wurde beispielsweise gezeigt, dass eine Gruppe von zehn DMET-Genen gleichermaßen durch CAR, PXR und PPARα reguliert wurden, wohingegen die Expression weiterer DMET-Gene exklusive durch die Aktivierung einer der drei Rezeptoren beeinflusst wurde. Für eine Reihe dieser Gene wurde hierbei eine Regulation durch die Rezeptoren CAR [z.B. *CYP2E1*, Sulfotransferase 1B1 (*SULT1B1*), UDP-Glucuronosyltransferase 2B4 (*UGT2B4*) und Cytochrom P450 Reductase (*POR*)], PXR z.B. *CYP2E1*, Alkohol Dehydrogenasen (*ADH*s), Flavin-abhängige Monooxygenase 5 (*FMO5*) und Glutathion Peroxidase 2 (*GPX2*)] und PPARα [z.B. *UBT2B4*, *ADH1s* und *FMO5*] erstmals gezeigt. Für CAR und PXR erweitert dies die Liste der Gene, durch welche diese Kernrezeptoren den Arzneimittel-Metabolismus beeinflussen und potenziell zu Arzneimittelwechsel- wirkungen beitragen. Die erhaltenen Daten konkretisieren darüber hinaus die Funktion von PPARα als Regulator von DMET-Genen *in vitro,* beispielsweise durch eine Erhöhung der Expression von CYPs *3A4*, *2B6*, *2C8* und *UGT1A1*. Dies lässt auch auf eine Beteiligung von PPARα bei Arzneimittelnebenwirkungen *in vivo* schließen. Des Weiteren zeigten die Analysen, dass Gene, wie beispielsweise Pyruvat Dehydrogenase Kinase 4 (*PDK4*), Glycogen Synthase 2 (*GYS2*) und Carnitin Palmitoyltransferase 2 (*CPT2*), deren Proteine an der Energiehomöostase beteiligt
sind, in Folge einer PXR Aktivierung differenziell exprimiert wurden. Ein solcher Zusammenhang war für diese Gene bisher unbekannt. Diese Resultate erweitern die bestehenden Kenntnisse der potenziellen Mechanismen über die PXR Stoffwechselprozesse wie Fettsäure-Abbau, Glukoneogenese und *de novo* Lipogenese beeinflusst und somit PXR zu Veränderungen von Lipid- und Glukose-Spiegeln oder Erkrankungen wie hepatischer Steatose beitragen kann.

Neben einer Liganden-abhängigen Regulation von Kernrezeptoren wurde auch für post-translationale Modifikationen gezeigt, dass diese Einfluss auf die Aktivität von Kernrezeptoren und deren Zielgen-Expression nehmen. So wurde für die

Proteinkinase A (PKA) eine Repression der *CPY3A4* Expression, als Folge einer PXR-Phosphorylierung, gezeigt. Ein Einfluss der PKA auf die Expression anderer humaner DMET-Gene hingegen ist bislang kaum untersucht. Der zweite Teil dieser Arbeit beschäftigte sich daher mit der Untersuchung des Einflusses einer PKA-Aktivierung auf die Expression und Aktivität von Arzneimittel-metabolisierenden Enzymen, in Abhängigkeit von PXR und dessen nächstverwandtem Kernrezeptor CAR. In dieser Arbeit wurde durch qRT-PCR Analysen der mRNA-Expression und CYP-Aktivitätsmessungen, mittels eines Cocktail-Assays, in primären humanen Hepatozyten gezeigt, dass eine PKA-Aktivierung durch 8-bromo cAMP eine Determinante des Arzneimittelstoffwechsels *in vitro* darstellt. Diese Analysen zeigten eine Repression der CAR und PXR vermittelten, sowie der basalen Expression und Aktivität von CYP1A1, CYP2B6, CYP2C8 und CYP3A4 als auch der Expression von ATP-binding cassette Transporter B1 (*ABCB1*) und *UGT1A1*. Reporter-Gen Experimente zeigten zudem, dass die beobachteten Effekte in Verbindung mit einer erniedrigten PXR- und CAR-Aktivität standen. Des Weiteren wurde aufgezeigt, dass die Expression von DMET-Genen auch durch das Hormon Glucagon, ein physiologisch relevanter Aktivator des PKA-Signalweges, reprimiert wurde, was bisher in dieser Form noch nicht untersucht worden war.

Auf Grund der breiten Liganden-Spezifität von PXR führen Behandlungen mit Arzneimitteln, sowie mit sogenannt „natürlichen" Heilmitteln wie Johanniskraut, oft zu einer unerwünschten PXR-Aktivierung. Diese PXR-Aktivierung und die dadurch hervorgerufene veränderte Expression und Aktivität von DMET stehen im Zusammenhang mit einer Vielzahl von Arzneimittelnebenwirkungen. Solche Arzneimittelnebenwirkungen sind auch für Johanniskraut-Präparate beschrieben, die auf den potenten PXR-Agonisten Hyperforin zurückzuführen sind. Hyperforin, die stärkste aktive Komponente der Johanniskrautpflanze, welche zur Behandlung von Depressionen verwendet wird, vermittelt seine antidepressive Wirkung über eine selektive Aktivierung des TRPC6-Kanals und in Folge dessen eine Inhibierung der Serotonin-Wiederaufnahme. Zur Vermeidung solcher Arzneistoffnebenwirkungen wäre es daher von großem Vorteil, wenn bei der Arzneimittelentwicklung Strategien zur Verfügung ständen, mit denen man eine PXR-Aktivierung verhindern könnte, ohne den pharmakologischen Effekt zu beeinträchtigen. Als Beispiel für eine solche

Strategie wurde im letzten Teil dieser Arbeit eine *in vitro* Studie durchgeführt, um synthetische, acylierte Phloroglucinole, welche als Ersatzstoffe für Hyperforin entwickelt wurden, auf ihr PXR-Aktivierungspotential im Vergleich zu Hyperforin und Rifampicin, hin zu untersuchen. Eine frühere *in vitro* Studie konnte bereits zeigen, dass fünf dieser synthetischen acylierten Phloroglucinole einen mit Hyperforin vergleichbaren pharmakologischen Effekt besitzen.

Eine Hyperforin- und Rifampicin-Behandlung von HepG2 Zellen, die mit einem Expressions-Vektor für humanes PXR, sowie einem *CYP3A4*-Reporter-Konstrukt transfiziert waren, resultierte in einer potenten PXR-abhängigen Induktion des *CYP3A4*-Promotors, während die TRPC6-aktivierenden Substanzen keine PXR-Aktivierung und *CYP3A4*-Promotor Induktion zeigten. Die Behandlung von primären humanen Hepatozyten mit Hyperforin und Rifampicin führte zu einer stark korrelierenden Induktion von PXR-Zielgenen; die Behandlung mit den Phloroglucinol-Derivaten hingegen rief nur moderate Expressions-Änderungen hervor, welche nur schwach mit den durch Rifampicin-Behandlung vermittelten Effekten korrelierten. Das in dieser *in vitro* Studie beobachtete Fehlen einer PXR-Aktivierung durch die TRPC6-aktivierenden Phloroglucinole wurde weiter unterstützt durch die im Rahmen einer Kooperation von Prof. Ekins durchgeführten *in silico* Pharmakophor-Modellierungen und Bindungsstudien, die nur schwache Interaktionen der TRPC6-aktivierenden Derivate mit PXR vorhersagten (Kandel et al., 2014). Diese Herangehensweise zeigte, dass Strategien mit dem Ziel, eine PXR-Aktivierung zu untersuchen und diese zu vermeiden, einen denkbaren Ansatz bieten, um in der Arzneimittelentwicklung dem Auftreten von Arzneimittelwechselwirkungen vorzubeugen und damit die Sicherheit von Medikamenten zu verbessern.

Zusammenfassend lässt sich sagen, dass in der hier präsentierten genomweiten Studie an humanen Hepatozyten zahlreiche neue Zielgene der NRs CAR, PXR und PPARα identifiziert wurden, welche zu einer Beeinflussung des Arzneimittelstoffwechsels und der Energiehomöostase durch diese NRs beitragen könnten. Darüber hinaus wurde gezeigt, dass die PKA, die unter anderem die Effekte des Hormons Glucagon vermittelt, eine Einflussgröße für die Arzneimittelentgiftung im Menschen darstellt. Des Weiteren wurde am Beispiel von Hyperforin-Derivaten eine Strategie präsentiert, die zur Untersuchung und Vermeidung von Arzneimittel-

interaktionen in der Medikamentenentwicklung beitragen kann. Im Hinblick auf die personalisierte Medizin und die allgegenwärtige Polypharmazie werden solche Informationen in Zukunft unerlässlich sein, um Probleme, die durch intra- und interindividuelle Variabilität hervorgerufen werden, zu berücksichtigen und um das Auftreten von Therapieversagen und Arzneimittelwechselwirkungen zu minimieren.

Summary

Nuclear receptors (NRs), most notably the constitutive androstane receptor (CAR) and the pregnane X receptor (PXR), regulate the transcription of several drug metabolizing enzymes and transporters (DMET) and thus represent important regulators of drug metabolism in the liver. Accordingly, the ligand dependent activation of these NRs by drugs and other xenobiotics contributes to the intra- and inter-individual variability of the drug detoxifying system. CAR and PXR were further shown to regulate the transcription of key enzymes involved in lipid and glucose metabolism. The NR peroxisome proliferator-activated receptor alpha (PPARα), a key regulator of fatty acid catabolism and target of lipid lowering fibrates, was recently identified as a direct regulator of cytochrome P450 3A4 (*CYP3A4*) and also potentially of other DMET genes. In this respect, CAR, PXR and PPARα are determinants of an overlapping number of liver functions including drug metabolism and energy homeostasis and are therefore associated with adverse drug reactions as well as liver disease like steatosis.

Until now there have been no comparative studies investigating the transcriptomes of CAR, PXR and PPARα in humans. Therefore, a major focus of this study was to assess the genome-wide transcriptional changes provoked by these NRs in primary human hepatocytes (PHHs). To investigate human liver-specific gene expression and its regulation PHHs represent the most suitable available *in vitro* cell system. To identify the CAR-, PXR- and PPARα-specific genome-wide expression changes, hepatocyte cultures from six individual donors were treated with the prototypical ligands for CAR (CITCO), PXR (rifampicin) and PPARα (WY-14643) as well as DMSO (vehicle control). Afterwards, the mRNA expression in these samples was determined utilizing Affymetrix® microarrays. The obtained expression data were statistically evaluated to identify the genes that showed a differential expression in response to the agonist treatments and to investigate to which metabolic functions these genes contribute. The results of these experiments confirmed that CAR, PXR and PPARα regulated a highly overlapping but distinct set of genes coding for DMET. For example, according to KEGG (Kyoto Encyclopedia of Genes and Genomes) pathway analyses expression of 10 DMET genes were shown to be regulated by all

three NRs, whereas other DMET genes responded exclusively to the activation of one of the NRs. In addition several DMET related genes previously not shown to be regulated by CAR [like *CYP2E1*, sulfotransferase 1B1 (*SULT1B1*), UDP-glucuronosyltransferase 2B4 (*UGT2B4*) and cytochrome P450 reductase (*POR*)], PXR [like *CYP2E1*, alcohol dehydrogenases (*ADHs*), flavin containing monooxygenase 5 (*FMO5*) and glutathione peroxidase 2 (*GPX2*)] or PPARα like *UBT2B4*, *ADH1s* and *FMO5*) were identified to respond to the respective agonists. For PXR and CAR, this extends the list of genes by which these NRs influence drug metabolism and potentially contribute to drug-drug interactions (DDIs). The results obtained further specify the role of PPARα as a regulator of drug metabolism *in vitro* by increasing expression of, e.g., *CYP3A4*, *2B6*, *2C8* and *UGT1A1*, thus pointing to a potential role of PPARα in adverse drug reactions *in vivo*. Furthermore, several genes coding for proteins involved in energy homeostasis, were identified as differentially expressed in response to PXR activation [e.g., pyruvate dehydrogenase kinase 4 (*PDK4*), glycogen synthase 2 (*GYS2*), carnitine palmitoyltransferase 2 (*CPT2*)], where such a relation was not reported so far. These results further expanded the knowledge of how PXR potentially impact fatty acid catabolism, gluconeogenesis and lipid *de novo* synthesis and provide interesting starting points to investigate how PXR activation contributes to altered glucose and lipid levels or disease like hepatic steatosis.

Besides ligand-dependent regulation of nuclear receptors, post-translational modification has also been shown to influence the activity of liver-enriched NRs and expression of their target genes. In this context, protein kinase A (PKA) had been shown to repress *CYP3A4* expression via PXR in a species-dependent manner, whereas the influence of PKA on the expression of other DMET genes had not been investigated in detail so far. The second part of this work therefore investigated the impact of PKA activation on the expression and activity of important drug metabolizing enzymes in a PXR- as well as a CAR-dependent manner. In this work PKA activation in primary human hepatocytes was identified as a determinant of drug metabolism *in vitro* by repressing PXR- and CAR-mediated or reducing basal expression and activity of CYP1A1, CYP2B6, CYP2C8 and CYP3A4, but also expression of ATP-binding cassette B1 (*ABCB1*) and *UGT1A1*. Using reporter gene

assays, these observed effects could be linked to PKA-mediated repression of PXR and CAR activity that may involve phosphorylation of these NRs. It could be further shown that expression of DMET genes was also repressed by the fasting hormone glucagon, a physiologically relevant activator of PKA signaling, which was not investigated in humans so far.

Due to the promiscuous ligand-specificity of PXR, which includes numerous compounds, drug treatment often leads to PXR activation, even with so-called "natural" compounds like St. John's wort (SJW). It would thus be highly desirable to develop strategies in drug development to assess or circumvent the activation of NRs without compromising the pharmacological effects. Therefore, the last part of this work consists of an *in vitro* study to investigate synthetic acylated phloroglucinols, designed as substitutes for hyperforin, regarding their potential to activate PXR. Hyperforin the major active constituent of the plant SJW used to treat depressions was shown to exert its antidepressant properties via indirect inhibition of serotonin reuptake by selectively activating the canonical transient receptor potential channel 6 (TRPC6). In addition, hyperforin is associated with clinically relevant drug-drug interactions in patients that had taken SJW concomitantly with other drugs due to potent activation of the nuclear receptor PXR by hyperforin. The phloroglucinol derivatives investigated in this thesis had previously been evaluated for their bioactivity. It had been reported that five of the nine synthetic acylated phloroglucinols activate TRPC6 with similar potency as hyperforin.

In this work, all these nine synthetic phloroglucinol derivatives were investigated in comparison to hyperforin and rifampicin for their potential to activate PXR. Hyperforin and rifampicin treatment of HepG2 cells co-transfected with a human PXR expression vector and a *CYP3A4* promoter reporter construct resulted in potent PXR-dependent induction, while all TRPC6-activating compounds failed to show any PXR activation or to antagonize rifampicin-mediated *CYP3A4* promoter induction. Hyperforin and rifampicin treatment of primary human hepatocytes resulted in highly correlated induction of PXR target genes, whereas treatment with the phloroglucinol derivatives elicited moderate gene expression changes that only weakly correlated to those of rifampicin treatment. The herein observed lack of PXR activation by the TRPC6 activating phloroglucinols was further supported by *in silico* pharmacophore

modeling that did not indicate potent agonist or antagonist interactions for the TRPC6 activating derivatives and docking studies that suggested interaction of only one of these compounds. These *in silico* studies performed by Prof. Sean Ekins are published together with the results presented in this work (Kandel et al., 2014). This approach shows that strategies avoiding PXR activation are conceivable in drug development in order to prevent DDIs and improve drug safety.

Taken together, these results further increase the number of genes by which CAR, PXR, and PPARα contribute to the regulation of drug metabolism and energy homeostasis. Moreover it was demonstrated that the PKA, which is involved in the transduction of the effects of, e.g., the hormone glucagon, represents a determinant of the drug detoxifying system in humans. Furthermore, a strategy could be presented, taking the example of the hyperforin derivates, which can be used to investigate and avoid DDIs in drug development. Such information will become imperative in future personalized medicine and the ever-present polypharmacy in order to handle intra- and inter-individual variability and to minimize drug failure or drug-drug interactions.

1   Introduction

1.1 Drug metabolism and its regulation

Many nutritional components foreign to the human body including plant secondary metabolites like monoterpenoids or alkaloids as well as other xenobiotic substances including various environmental pollutants, orally ingested, are of lipophilic nature and can thus, be easily absorbed. Due to their hydrophobic properties, xenobiotics tend to accumulate in fat deposits and cell membranes and therefore require biotransformation making them accessible for renal and biliary excretion in order to prevent increasing concentrations and toxicity. Most orally administered drugs have similar chemical properties and also undergo the same biotransformation processes prior to their excretion (Anzenbacher and Zanger, 2012).

After absorption from the gastrointestinal lumen by passive diffusion or specific uptake-transporters such as members of the solute carrier family (SLC), drugs and other xenobiotics are transported via the portal vein into the liver, where drug metabolism mainly takes place. The so called "first pass" metabolism of drugs in liver as well as in the intestine is an important factor influencing the pharmacokinetics and availability of drugs before they enter systemic circulation (Anzenbacher and Zanger, 2012). The transport of drugs from blood into the liver and hepatocytes is again facilitated by passive diffusion or SLC transporters also termed phase 0 transporters (Hagenbuch and Meier, 2004). Within hepatocytes, phase I enzymes, most notably cytochrome P450 monooxygenases (CYPs), as well as flavin-containing monooxygenases (FMOs) and alcohol and aldehyde dehydrogenases (ADHs, ALDHs), facilitate the oxidation of hydrophobic drugs by introducing functional groups and increasing their water solubility. Phase II conjugating enzymes like UDP-glucuronosyltransferases (UGTs), glutathione S-transferases (GSTs) and sulfotransferases (SULTs) further increase hydrophilicity by adding polar molecules to such functional groups. The products of phase I and II reactions are finally exported via efflux transporters (phase III), e.g., members of the ATP-binding cassette family into blood or bile, and undergo renal or biliary excretion (Wang et al., 2012). The proteins facilitating the phase I, II and 0/III reactions can be summarized as drug metabolizing enzymes and transporters (DMET).

Inter- and intra-individual variability in the expression and activity of drug metabolizing enzymes and transporters has been identified as a major determinant of drug response and toxicity. Besides genetic factors like single nucleotide polymorphisms (SNPs) and copy number variations (CNVs), which contribute to the inter-individual variability, the expression of drug metabolizing enzymes can vary several-fold within a single individual at different time points, depending on external and internal stimuli (Zanger and Schwab, 2013). For example, several xenobiotics like environmental pollutants, nutritional ingredients and drugs have been shown to alter the expression of DMET genes by interacting with a class of transcription factors (TFs) called xenosensors. These TFs belong to the superfamily of ligand dependent nuclear receptors (NRs). Upon ligand dependent activation, these NRs bind to specific recognition sites within the promoters or enhancers of their genes and thereby regulate the transcription of these genes (Figure 1.1). The major xenosensors pregnane x receptor (PXR) and constitutive androstane receptor (CAR) have been shown to regulate the expression of several cytochrome P450 genes including CYP3A4, which metabolizes more than 50% of all prescribed drugs, as well as other important drug metabolizing enzymes like UGTs and drug transporters (Moore et al., 2006; Timsit and Negishi, 2007; Wang et al., 2012). Moreover, the farnesoid X receptor (FXR), the liver X receptors α and β (LXRα, β), the peroxisome proliferator-activated receptors α, β and γ (PPARα, β, γ) and other NRs have been shown to regulate expression of drug metabolizing enzymes and transporters (Nakata et al., 2006). Thus, NRs are an important part of the drug and xenobiotic detoxification system by adapting the assembly and activity of this system to various external chemical stimuli. On the other hand, the fact that NRs regulate the expression of enzymes and transporters responsible for the detoxification of most drugs, implies that drug-dependent activation of NRs can provoke undesirable drug-drug interactions and adverse drug reactions (Tolson and Wang, 2010; Wang et al., 2012). For example, numerous studies showed that drugs that activate PXR like the antibiotic rifampicin, increased the expression and activity of CYP3A4. In combination therapy, these led to reduced half-life and efficacy of drugs metabolized by CYP3A4 (Niemi et al., 2003; Sousa et al., 2008).

1.2 Nuclear receptors

1.2.1 Nuclear receptors: general background, structure and way of action

Nuclear receptors (NR) are a family of ligand-dependent TFs with 48 members in humans, categorized into six subfamilies NR1, NR2, NR3, NR4, NR5 and NR0 according to sequence homology (Germain et al., 2006). Nuclear receptors are involved in a variety of biological processes like proliferation, differentiation and development by adjusting the transcriptional activity of cells in response to small hydrophobic ligands, which may originate either from the endocrine system (e.g., steroids, steroid hormones and other lipophilic hormones), the metabolic transformation of dietary compounds (e.g., cholesterol and fatty acid and their derivatives) or external sources (e.g., environmental chemicals and drugs) (Chawla et al., 2001; Mangelsdorf et al., 1995). Based on their ligands, nuclear receptors can be further grouped into receptors that bind to hormones or lipids like the estrogen receptor (ER) or the hepatocyte nuclear factor 4 α (HNF4α) and into orphan receptors that lack an endogenous ligand, which controls their physiological function. For some orphan receptors, low affinity endogenous ligands have been identified in recent years. These receptors, including several members of the NR1C family like the peroxisome proliferator-activated receptor α (PPARα or NR1C1), the NR1H family like the liver X receptor (LXR or NR1H3) and the NR1I family like the pregnane x receptor (PXR or NR1I2) or the constitutive androstane receptor (CAR or NR1I3), are termed adopted orphan nuclear receptors. Most of these adopted orphan receptors form heterodimers with the NR retinoic X receptor (NR2B1, RXRα) (Mangelsdorf and Evans, 1995; Mukherjee and Mani, 2010).

Nuclear receptors share a common protein structure, which is composed of four functional domains. The N-terminal domain A/B includes the ligand independent activation function 1 (AF-1), which is important for a ligand independent activation of the nuclear receptor. The ligand dependent activation function 2 (AF-2) is located close to the C-terminus at the end of the ligand-binding domain (LBD) in domain E. The domain C contains the DNA binding domain (DBD), which is comprised of two conserved C4-type zinc-finger motifs. These zinc-finger motifs facilitate the binding of the NRs to specific hexameric DNA sequences within the promoter or enhancer of

genes. The domains C and E are connected via the highly flexible hinge region (domain D) (Mukherjee and Mani, 2010).
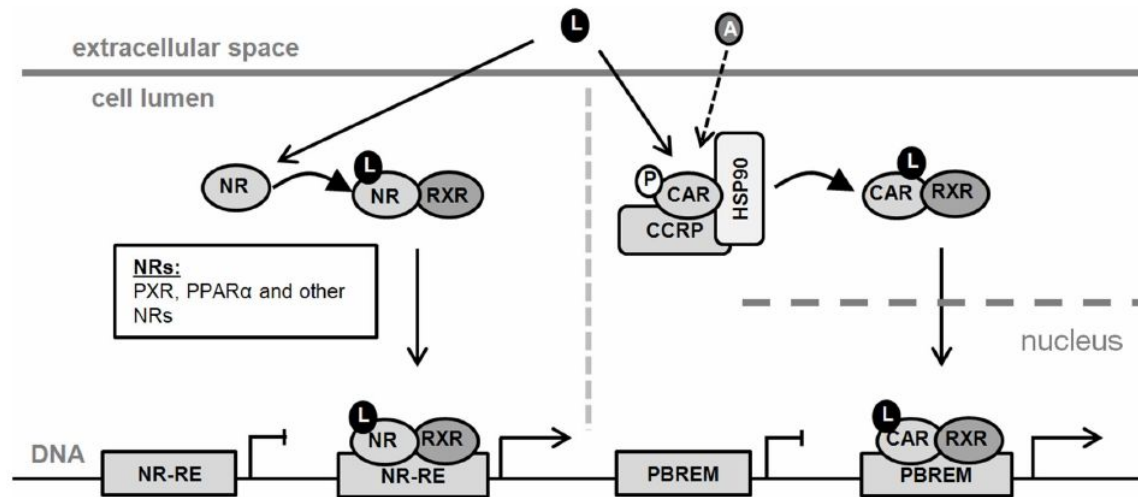

Figure 1.1 Direct regulation of gene expression by nuclear receptors (NR). Upon ligand (L) binding NR bind to their specific responsive elements (NR-RE) within the promoters or enhancers of their target genes and increase the expression of these genes. In its non-activated state, CAR is located in the cytoplasm in a complex with CCRP and HSP90. In response to a ligand or CAR activator (A), CAR translocates into the nucleus, binds to its specific responsive elements (phenobarbital responsive enhancer module; PBREM) and initiates the transcription of its target genes.

The classical transcriptional regulation by nuclear receptors occurs via ligand binding to the NR, which leads in most cases to the recruitment of co-activator proteins to the DNA bound NR ligand complex and an initiation of transcription by RNA polymerase II (Figure 1.1). NR ligands are lipophilic molecules including steroids and other lipid hormones, fatty acid, drugs and xenobiotics. Most NRs bind as homodimers to their specific target sequences, also termed responsive elements, but there are also NRs, which bind as heterodimers or monomers (Germain et al., 2006). Besides the classical way of transcriptional regulation, NRs have been also shown to bind to other TFs or their co-activator proteins and thereby modulate target gene expression of these TFs (Kodama et al., 2004, 2007) (Figure 1.2). Moreover, NRs have been reported to mutually regulate their expression. For example, the expression of the NRs CAR and PXR was shown to be regulated by HNF4α and GR.

Also, other TFs like NFκB are involved in expression of NRs, revealing that nuclear receptors are part of a highly complex and hierarchical network of transcriptional regulators sensitive to various external and internal stimuli (Lim and Huang, 2008; Pascussi et al., 2004).

1.2.2 Pregnane X receptor (PXR)

The pregnane X receptor (*NR1I2*, PXR) belongs to the group of adopted orphan receptors and is predominantly expressed in the liver and intestine (Kliewer et al., 2002). Possessing a large and flexible ligand-binding pocket (Watkins et al., 2001), PXR binds to and is activated by a broad variety of structurally diverse substances including drugs (e.g., rifampicin, dexamethasone, ritonavir, tamoxifen and lovastation), herbal contents (e.g., hyperforin and numerous herbal extracts), environmental pollutants (e.g., bisphenol A) and endogenous compounds like bile acids (e.g., lithocholic acid). Its promiscuous ligand specificity makes PXR one of the most important xenosensors in humans (Chang, 2009; Kliewer et al., 2002; Kretschmer and Baldwin, 2005; Moore et al., 2000a; Staudinger et al., 2001; Sui et al., 2012).

Upon ligand-dependent activation, PXR binds together with its heterodimer partner RXRα to its specific recognition sites within the promoter or enhancer of its target genes and recruits co-activating proteins and initiate transcription (Ihunnah et al., 2011) (Figure 1.1). PXR has been shown to directly bind to and regulate several human phase I enzymes like CYP3A4, CYP2B6, CYP2C8 and CYP2C9 (Chen and Goldstein, 2009; Goodwin et al., 1999, 2001), phase II enzymes like UGT1A1 (Sugatani et al., 2008) and SULT2A1 (Fang et al., 2007) and phase III drug transporters like MDR1 (Geick et al., 2001).

Besides drug metabolism, PXR is also involved in the regulation of glucocorticoid, androgen, bile acid, vitamin and retinoic acid metabolism and homeostasis, either by regulation of the above mentioned phase I, II and 0/III enzymes and transporters, or by regulating other enzymes (Ihunnah et al., 2011). For example, PXR has been shown to bind to the promoter of CYP7A1, encoding for the rate-limiting step in bile acid metabolism, and to downregulate its expression (Li and Chiang, 2005).

Additionally, numerous other genes involved in drug detoxification and a multitude of other biological processes have been reported to be regulated by PXR and its ligands. However, many of these studies were conducted in animal models. The extrapolation of these findings to humans is not straightforward because murine PXR has been shown to have a rather narrow ligand specificity compared to the human ortholog, which was reported to have very promiscuous ligand specificity, including very large compounds like rifampicin, which do not activate mouse PXR. On the other hand the murine PXR agonist PCN shows no effect on human PXR activity. (Iyer et al., 2006; Moore et al., 2002). Additionally, due to the lack of genome-wide expression data following the activation of PXR in humans, the differences between mouse and human PXR target gene profiles are currently unknown, whereas such a divergence was suggested by Rosenfeld and colleagues in a genome-wide approach comparing PXR-humanized and wild type mice (Rosenfeld et al., 2003).

1.2.3 Constitutive androstane receptor (CAR)

The constitutive androstane receptor (*NR1I3*, CAR) is predominantly expressed in liver and is the most closely related NR to PXR with an amino acid homology of 70% and 50% in their DBD and LBD, respectively. Moreover, CAR is the second most important xeno-sensing NR apart from PXR and is implicated in the regulation of genes involved in cell growth, apoptosis, tumor genesis and drug and xenobiotic metabolism. Upon activation, CAR, like other adopted orphan nuclear receptors, hetero-dimerizes with RXRα (Kliewer et al., 2002; Ueda et al., 2002) (Figure 1.1). CAR has been shown to transcriptionally regulate several genes involved in drug metabolism and transport including *CYP1A1*, *CYP1A2*, *CYP2B6*, *CYP2C8*, *CYP2C9* and *CYP3A4* (Ferguson et al., 2002, 2005; Goodwin et al., 2002; Sueyoshi et al., 1999; Yoshinari et al., 2010), *UGT1A1* (Sugatani et al., 2001) and *ABCB1* (Burk et al., 2005), which are in part also established target genes of PXR (Tolson and Wang, 2010). Therefore, CAR binds to the same or very similar recognition sites within the promoters or enhancers of these genes (Wang et al., 2012).

As illustrated in Figure 1.1, CAR can be activated by two different mechanisms, ligand-dependent and independent. In the absence of ligands or other activating stimuli, CAR is retained as a phospho-protein in the cytoplasm in a complex together

with the heat shock protein 90 (HSP90) and the cytoplasmic CAR retention protein (CCRP) (Kobayashi et al., 2003). Ligand-independent activation, e.g., by the anticonvulsant phenobarbital, has been shown to inhibit EGF signaling, which leads to protein phosphatase 2A (PP2A) mediated dephosphorylation of CAR and subsequently, its translocation into the nucleus (Mutoh et al., 2013). In the nucleus, CAR binds to its responsive elements and initiates transcription of its target genes in the absence of a ligand (Tolson and Wang, 2010). Ligand binding also leads to the dissociation of the cytoplasmic complex and the translocation of CAR into the nucleus (Kobayashi et al., 2003; Timsit and Negishi, 2007). CAR ligands including the compound CITCO, drugs like meclizine and endogenous substances like 5 β-pregnane-3,20-dione could behave as agonists, inverse agonists or antagonists, depending on the experimental setup and species. Several compounds have been shown to activate both CAR and PXR in a species-dependent manner, which complicates the differentiation between CAR and PXR activation and the extrapolation of mouse data to human (Maglich et al., 2003; Moore et al., 2000b; Xie et al., 2000). For example, phenobarbital is assumed to be a specific activator of murine CAR, whereas it also activates PXR in humans (Chen et al., 2004). Furthermore, most human CAR ligands or activators do not activate murine CAR (e.g., CITCO) or show inverse agonist properties (e.g., 5β-pregnanedione). By contrast the compound TCPOBOP activates murine but not human CAR (Molnár et al., 2013).

1.2.4 Peroxisome proliferator-activated receptor alpha (PPARα)

The members of the NR1C family peroxisome proliferator activated receptor alpha (NR1C1, PPARα), PPARβ/δ (NR1C2), and PPARγ (NR1C3) are the most important class of NRs for the regulation of lipid homeostasis. These NRs are lipid sensors and regulate the expression of genes involved in energy and lipid homeostasis, adipocyte differentiation, and inflammation (Lalloyer and Staels, 2010; Wahli and Michalik, 2012). PPARα is predominantly expressed in tissues with high rates of fatty acid catabolism, like liver, heart, intestine and muscle. In these tissues, PPARα transcriptionally regulates genes important for fatty acid intracellular trafficking, peroxisomal β-oxidation, microsomal ω-oxidation, but also genes involved in bile acid and cholesterol metabolism (Pyper et al., 2010). Besides various endogenous lipids,

PPARα ligands include fibrates used to treat hyperlipidemia, and the explorative synthetic compound WY-14643 (4-chloro-6-(2,3-xylidino)- 2-pyrimidinylthio acetic acid) (Chakravarthy et al., 2009; Forman et al., 1997; Kliewer et al., 1997). Upon ligand-dependent activation, PPARα together with RXRα binds to its recognitions sites, the peroxisome proliferator response elements (PPREs) and activates the transcription of its target genes (Pyper et al., 2010) (Figure 1.1).

Identification of PPARα target genes by comparative transcriptome analysis in human and mouse hepatocytes treated with WY-14643, indicate that regulation of genes involved in hepatic lipid metabolism and energy homeostasis like CPT1A, FABP1, ASCL1, PDK4 and HMGCS2 (Figure 1.2) appears to be mostly conserved between species, whereas other regulated genes were found to be largely divergent between mouse and human (Rakhshandehroo et al., 2009). The list of human-specific PPARα target genes that had been identified by Rakhshandehroo and colleagues contained several *CYP*s involved in drug metabolism, such as *CYP3A4*, *CYP2B6* and *CYP2C8* (Rakhshandehroo et al., 2009). Previously, Prueksaritanont and colleagues had reported that fibrates induced the expression of *CYP3A4*, *CYP2C8* and *UGT1A1* in primary human hepatocytes, whereas the contribution of PPARα to these gene expression changes was not investigated in this study (Prueksaritanont et al., 2005). A potential role of PPARα as a regulator of DMET genes was further supported by a study performed in cooperation with our institute that investigated regulatory mechanisms responsible for pleiotropic effects of atorvastatin (Schröder et al., 2011). Schröder and colleagues suggested, based on expression data from primary human hepatocytes (PHHs) treated with atorvastatin, a regulatory impact of PPARα on *CYP3A4*, which was validated by knock-down and ligand-mediated activation of PPARα in primary human hepatocytes. Moreover, in a pharmacogenetic candidate genes approach, performed in our institute, the PPARA SNP rs4253728 (G>A) was identified to significantly correlate with decreased CYP3A4 mRNA and protein expression as well as in vitro and in vivo CYP3A4 atorvastatin 2-hydroxylation activity (Klein et al., 2012). These findings together with the observations from Rakhshandehroo and colleagues (Rakhshandehroo et al., 2009) clearly revealed a regulatory impact of PPARα on CYP3A4. Recently, Thomas and colleagues could demonstrate that PPARα binds the *CYP3A4* promoter and

thereby directly regulates *CYP3A4* expression via two distinct PPARα response elements (Thomas et al., 2013). Additionally, in the same study, based on PPARα knock-down and induction experiments in PHHs, it was further demonstrated that PPARα is involved in the regulation of *CYP2B6* and *CYP2C8*. De Keyser and colleagues investigated, based on the findings of Klein et al., 2012, the impact of the PPARA SNP rs4253728 and another strongly linked PPARA SNP (rs4823613) on the response to simvastatin treatment in 123 incident statin users (de Keyser et al., 2013). They showed that both SNPs were associated with the total LDL-lowering effect of simvastatin, possibly through influence on CYP3A4. Moreover, in a pharmacokinetic model for simvastatin and its active metabolite simvastatin acid, the PPARA SNP (rs4253728) was identified to significantly decrease simvastatin acid plasma concentration (Tsamandouras et al., 2014). Both studies clearly demonstrate that PPARα impacts metabolism of simvastatin *in vivo*. Besides CYP3A4, several UGTs have been identified as PPARα target genes (Barbier et al., 2003; Senekeo-Effenberger et al., 2007).

1.2.5 The role of CAR and PXR in energy homeostasis

Besides their importance as major regulators of DMETs, CAR and PXR were also shown to impact hepatic lipid and glucose metabolism by interfering with important transcriptional regulators of these metabolic functions (Konno et al., 2008). For example, in mice, both CAR and PXR repress the expression of G6pc and Pck1, involved in gluconeogenesis, by binding to forkhead transcription factor o1 (Foxo1) (Figure 1.2). In the absence of insulin, Foxo1 is bound to insulin response sequence (IRS) within the promoters of its target genes and activates their expression (Nakae et al., 2001). Additionally, in mice, PXR binds to the cAMP-response element binding protein (Creb), which is activated upon PKA-mediated phosphorylation in a glucagon-dependent manner, and prevents its binding to the cAMP response elements within the promoters of G6pc and Pck1 (Kodama et al., 2007) (Figure 1.2). PXR and CAR were also shown to dissociate the peroxisome proliferator-activated receptor γ co-activator 1 (Pgc-1) α from Hnf4α (Figure 1.2), which together also regulate G6pc and Pck1 (Miao et al., 2006). Moreover, as illustrated in Figure 1.2, PXR was identified to repress expression of the rate-limiting enzymes of β-oxidation and ketogenesis Cpt1a and Hmgcs2 by tethering the TF Foxa2 via direct protein-protein interaction in mouse

(Nakamura et al., 2007). On the other hand, in mice expressing a constitutive active PXR, Cd36, involved in fatty acid absorption, and Scd1, an important enzyme for *de novo* lipogenesis, and Fae (Elovl6), also involved in *de novo* lipogenesis, were found to be upregulated compared to mice expressing wild type PXR (Zhou et al., 2006) (Figure 1.2). Moreau and colleagues also reported an increased expression of the fatty acid synthase (FASN) following PXR activation in primary human hepatocytes (Moreau et al., 2009). All in all, activation of PXR as well as CAR lead to transcriptional repression of important genes involved in energy providing pathways like gluconeogenesis, β-oxidation and ketogenesis. On the other hand, PXR induces expression of *de novo* lipogenesis genes promoting lipid deposition in liver and hepatic steatosis in mice, which can be a source of non-alcoholic fatty liver disease (NAFLD) (Konno et al., 2008; Moreau et al., 2009; Nakamura et al., 2007). Furthermore, Moya and colleagues showed that PXR and CAR ligands induce steatosis in primary human hepatocytes (Moya et al., 2010).
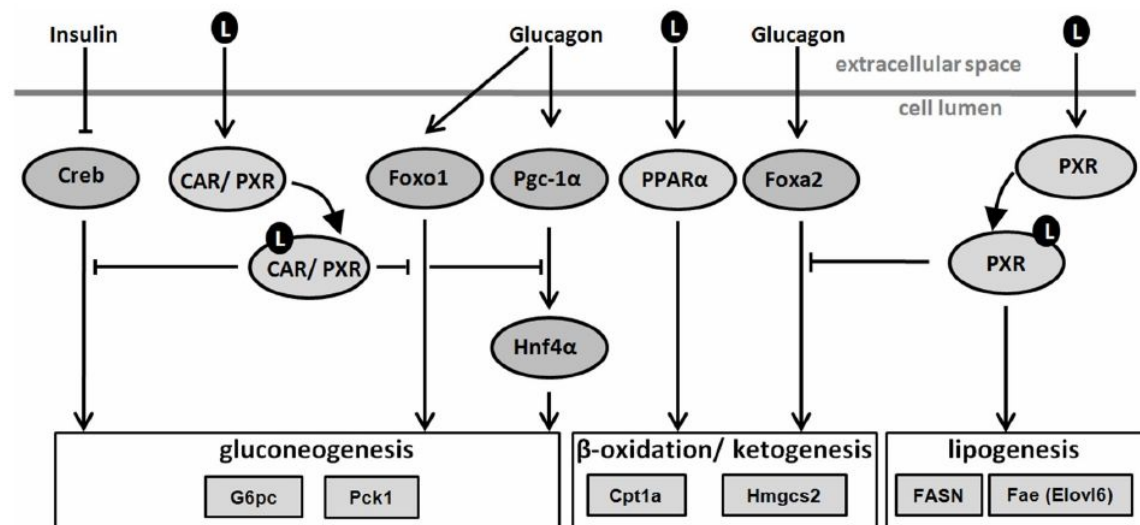
Figure 1.2 Schematic representation of the role of CAR, PXR and PPARα in energy homeostasis. CAR and PXR interact with Foxo1 Creb, and the Pgc-1α and Hnf4α hetero-dimerization, which leads to decreased expression of target genes involved in gluconeogenesis (G6pc and Pck1) and β-oxidation or ketogenesis (Cpt1a and Hmgcs2). PPARα activation by ligands (L), leads to increased expression of CPT1A involved in β- oxidation and HMGCS2 involved in ketogenesis. Activation of PXR induces lipogenesis by increasing expression of FASN and Fae (Elovl6) and represses β-oxidation and ketogenesis by tethering the glucagon-sensitive TF Foxa2 and thereby decreasing the expression of the Foxa2 target genes Cpt1a and Hmgcs2.

1.2.6 Phosphorylation of PXR and CAR

As described in 1.2.1, nuclear receptors adjust the transcriptional activity of cells to signals mediated by small lipophilic molecules, which originate from endogenous as well as exogenous sources in order to adapt the organism to changing conditions. However, as nuclear receptors are involved in the regulation of fundamental cell functions, their activity requires further fine tuning to meet the organisms' needs. Therefore, upon post-translational modifications (PTMs), NRs are able to integrate cellular signals arising from various other signaling events. These PTMs include phosphorylation, acetylation, ubiquitination and sumoylation. In this regard, phosphorylation of NRs by protein kinases like protein kinase C (PKC), protein kinase A (PKA), AMP-activated protein kinase (AMPK), mitogen-activated protein kinases (MAPKs) and glycogen synthase kinase 3 (GSK3), seem to play a major role (Berrabah et al., 2011).
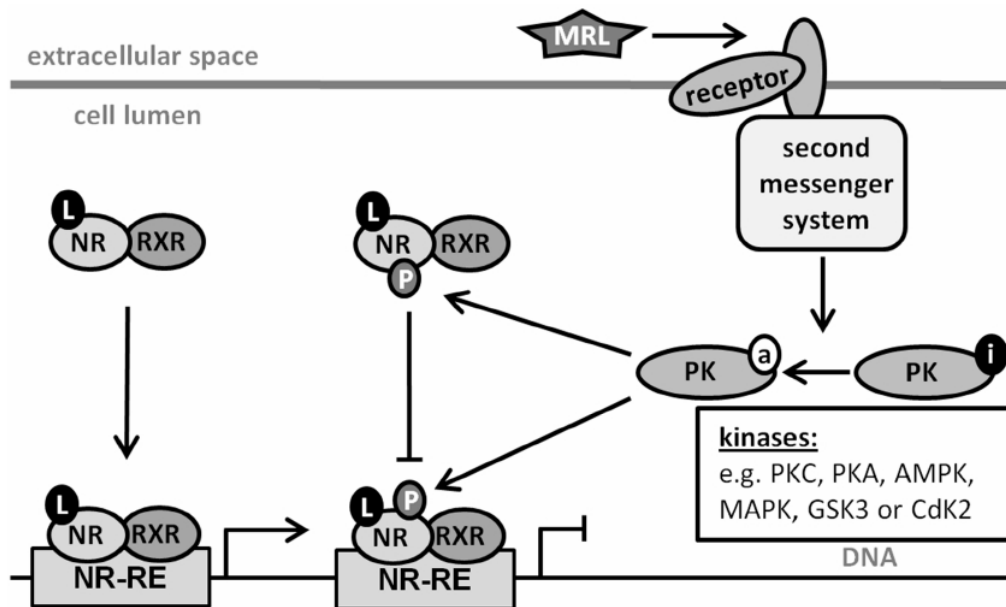
Figure 1.3 Schematic diagram of protein kinase (PK) dependent repression of nuclear receptor (NR) activity. Activity of ligand (L) activated NRs can be decreased or inhibited by protein phosphorylation (P) via PKs transferred from their inactive (i) to active state (a), e.g., by signaling events involving a membrane receptor ligand (MRL)-dependent activation of membrane bound receptors and their associated second messenger systems.

In this context, the NR PXR has been shown to undergo different PTMs including phosphorylation by protein kinases (Staudinger et al., 2011). As shown in Figure 1.3, PKA-, PKC- and Cdk2-dependent phosphorylation of PXR have been shown to decrease PXR mediated activation of the human *CYP3A4* promoter (Ding and Staudinger, 2005; Lichti-Kaiser et al., 2009a; Pondugula et al., 2009). On the other hand, activation of PKA in mice leads to a strong increase of Cyp3a11 expression, also suggesting that the influence of PTMs on PXR is species-specific (Lichti-Kaiser et al., 2009a). They further clearly demonstrated that these species differences were not dependent on the species origin of PXR using reporter gene assays and PXR humanized mice hepatocytes (Lichti-Kaiser et al., 2009a). They also reported increased PXR phosphorylation at serine residues upon activation of PKA and could demonstrate in another publication that mutation of several *in silico* predicted phosphorylation sites alter PXR transactivation capacity (Lichti-Kaiser et al., 2009b). As described in 1.2.3, CAR in its inactivated form is retained as a phospho-protein in the cytoplasm, although the only kinase which is so far shown to directly interact and phosphorylate CAR is PKC (Mutoh et al., 2013). Besides PKC, the extracellular signal-regulated kinase (ERK) was identified to be involved in CAR phosphorylation, whereas ERK did not directly phosphorylate CAR (Osabe and Negishi, 2011). A study performed by Ding and colleagues showed that CAR expression and inducibility of the CAR target gene Cyp2b10 is increased by fasting, epinephrine and the PKA activator 8-bromo cAMP in mice, whereas a direct phosphorylation of CAR by PKA is currently not known (Ding et al., 2006). Nevertheless, the activity of both CAR and PXR appears to be induced by PKA in mice, however PXR activity was shown to be repressed by PKA in human and rat (Ding et al., 2006; Lichti-Kaiser et al., 2009a). The PKA is activated by increased levels of cAMP, which are produced by the adenylate cyclase. The fasting hormone glucagon, as well as the hormone epinephrine, are known to activate PKA in an adenylate cyclase and cAMP-dependent manner. In liver, PKA activation leads to increased gluconeogenesis by the phosphorylation of phosphofructokinase 2 (PFK2) and CREB, and glycogenolysis by activating the phosphorylase in order to provide energy in form of glucose to the body (Berg et al., 2013). Interestingly, the same processes were shown to be repressed by the activation of CAR and PXR (Staudinger et al., 2011; Wada et al., 2009).

1.3 Importance of nuclear receptors in drug therapy and development

Nuclear receptors, especially the xenosensors CAR and PXR, are activated by a broad spectrum of commonly prescribed drugs and widely used herbal drugs, which in turn, leads to altered expression and activity of numerous DMETs. This knowledge gained over the past decades finally provided the molecular basis to explain drug interactions, in which one drug alters the metabolism of another (Hernandez et al., 2009; Kliewer et al., 2002; Molnár et al., 2013). Regarding today´s medical world of polypharmacy, such drug-drug interactions are a major issue in drug therapy as they can lead to drug failure or drug toxicity and may result in life-threatening conditions or even death (Mukherjee and Mani, 2010; Sinz, 2013). Therefore, *in vitro* and *in silico* screening methods were developed to investigate NR activation in drug development but also for drugs already in use, in order to predict or prevent such interactions (Bachmann et al., 2004; Ekins, 2004; Raucy and Lasker, 2013).

1.3.1 St. John´s wort and hyperforin

The plant St. John´s wort (SJW) has been in use for decades as self-medication to treat depression (Chatterjee et al., 1998; Müller, 2003). Several clinical studies showed that extracts of St. John`s wort (*Hypericum perforatum*) performed superior to placebo and were comparable to standard synthetic antidepressant drugs in treating mild to moderate depression (Kasper et al., 2006; Linde et al., 2008). Hyperforin has been identified as the major active compound of SJW regarding its antidepressive effects (Mai et al., 2004; Singer et al., 1999). In line with this finding, clinical outcome has been correlated to the hyperforin content of St. John`s wort extracts (Laakmann et al., 1998). Hyperforin inhibits the reuptake of serotonin and norepinephrine, but does not interact directly with the serotonin reuptake transporter (SERT) like other selective serotonin reuptake inhibitors (Müller, 2003; Treiber et al., 2005). Recently, Leuner et al. showed that hyperforin specifically activates the canonical transient receptor potential channel 6 (TRPC6), leading to an increased Ca^{2+}-influx into neurons, thereby triggering inhibition of serotonin reuptake by Ca^{2+}-dependent signaling (Leuner et al., 2007). The different available SJW formulations contain variable amounts of hyperforin (0.2-6 %) due to the different types of preparation (Klemow et al., 2011). Furthermore, altered preparation methods led to a

strong increase of hyperforin content in SJW extracts in recent years (Schwabe, 1997, 1998).

1.3.2 Drug-drug interactions related to St. John´s wort

Despite a generally favorable side effect profile of SJW (Kasper et al., 2006), there is a well-documented potential of SJW to induce clinically relevant drug-drug interactions (DDI). For example, changes in plasma levels of drugs metabolized by CYP3A4, e.g., cyclosporine A and indinavir, occurred when patients concomitantly had taken SJW (Ahmed et al., 2001; Piscitelli et al., 2000). SJW-related DDIs were also reported for amitriptyline, irinotecan, digoxin, warfarin and statins (Madabushi et al., 2006; Vlachojannis et al., 2011). These observations can be explained by the finding that hyperforin is a potent ligand-activator of human PXR (Bauer et al., 2006; Chen et al., 2004; Moore et al., 2000a). For example, hyperforin-dependent activation of PXR has been shown to increase expression of CYP3A4, CYP2B6 and CYP2C9 as well as MDR1 (Bauer et al., 2006; Chen et al., 2004; Goodwin et al., 2001). As described above (1.2.2), besides hyperforin, activation of PXR by numerous frequently prescribed drugs is a known and established source for drug-drug interaction (1.3) (Hernandez et al., 2009; Kliewer et al., 2002; Molnár et al., 2013).

1.4 Objectives

The nuclear receptors CAR, PXR and PPARα are implicated in the regulation of several important liver functions. Some of these functions like metabolism of xenobiotics and energy homeostasis have been shown to be overlappingly influenced by the activity of CAR, PXR and PPARα. Currently, there are no comparative analyses of the genome-wide changes in gene expression following the activation of these three receptors in humans. Furthermore, such data from rodent experiments are not sufficient due to species differences in NR properties.

Therefore, to assess the role of these nuclear receptors in the regulation of liver function, a major objective of this work was to generate genome-wide expression data following the activation of the nuclear receptors CAR, PXR and PPARα in primary human hepatocytes. Such comprehensive data are imperative to display all transcriptional alterations that contribute to changes of liver-metabolic properties like drug detoxification as well as energy metabolism and others.

This work will further investigate the impact of PKA activation on drug metabolism in human liver. Until now an effect of PKA activation has been only shown for CYP3A and this effect was reported to be contrary regarding mice and human. Therefore, the consequences of PKA signaling on the expression and activity of a broader set drug metabolizing enzymes in a CAR- and PXR-dependent manner will be investigated, in order to assess if PKA, an important transducer of hormonal signals, could be an additional determinant of liver human drug detoxification functions.

A further aim of this work is to investigate a set of new potential drugs structurally related to the antidepressant and PXR agonist hyperforin for their potential to activate PXR. This study shall provide an example of a strategy evaluating the undesired PXR activation by explorative therapeutics in development in order to predict and avoid DDIs and drug failure.

2   Results

2.1   Comparative transcriptome profiling of primary human hepatocyte in response to NR activation

The nuclear receptors CAR, PXR and PPARα have been shown to regulate genes involved in diverse metabolic processes of liver like steroid and bile acid metabolism, drug and xenobiotic metabolism, fatty acid and lipid metabolism. Systematic human data are lacking because most of these studies were conducted in mouse or rat models, whereas in humans a transcriptional regulation by PXR and CAR was only shown for a relatively small set of genes. Moreover, several reports indicate that there are genes co-regulated by CAR, PXR and PPARα, a topic that has not been addressed in the human gene context. Therefore, the aim of the following experiments was the comprehensive and pathway driven analyses comparing the regulomes of the nuclear receptors CAR, PXR and PPARα in primary human hepatocytes, in order to investigate the putative role of these three NRs in the regulation of human liver metabolism.

2.1.1 Identification of differentially expressed genes in human hepatocytes treated with CITCO, rifampicin and WY-14643

To assess the changes in whole-genome gene expression following the activation of the nuclear receptors CAR, PXR and PPARα, primary human hepatocytes of ten different donors were treated for 24 h with their prototypical agonists CITCO (CAR), rifampicin (PXR) and WY-14643 (PPARα) as well as DMSO, the treatment vehicle, as a control (5.1.4). But due to low RNA quantity (RNA amount <600 ng) or quality (RIN <8), only RNA samples of hepatocyte cultures from six donors were used for further experiments. Using Affymetrix GeneChip® HuGene 1.0ST microarrays, the whole-genome mRNA expression profiles were obtained from treated (CITCO, rifampicin and WY-14643) and control samples (DMSO) (5.4). The expression data were preprocessed by log scale robust multi-array analysis (RMA; Gene Level - Default) using Affymetrix Expression Console (Affymetrix). According to the RMA, the 33,252 probe sets presented on each chip were mapped to 20,072 annotated genes. These genes were used for further analyses.

The obtained gene expression values of the primary human hepatocyte samples from the six different donors treated with CITCO, rifampicin, WY-14643 and DMSO, were investigated by principal component analysis (PCA) using Analyst® 8.0 software solution (Genedata AG, Basel Switzerland). The PCA showed that the donors were more separated from each other than the treatments within a single donor (Figure 2.1).
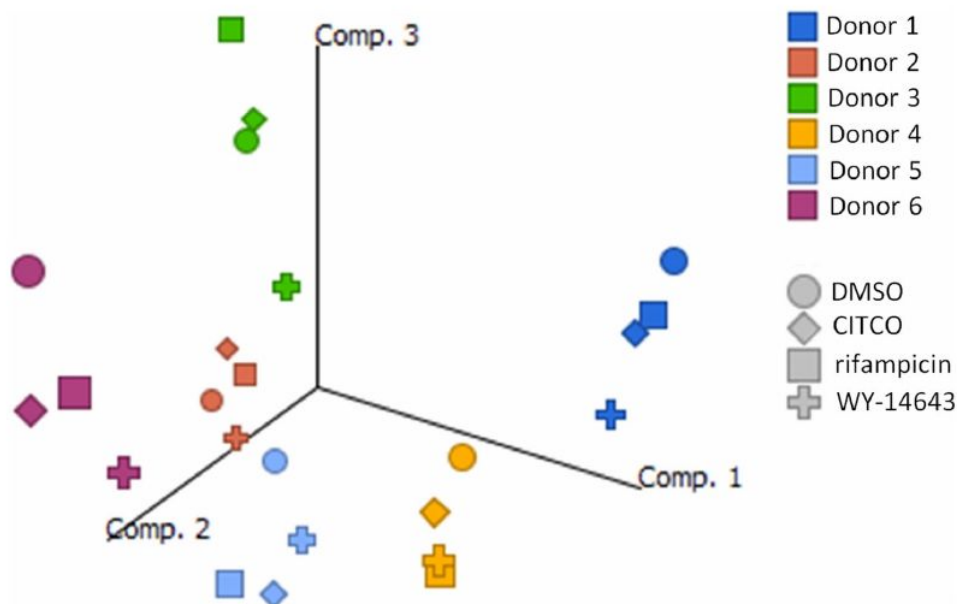
Figure 2.1 Principal component analysis (PCA) of gene expression profiles determined by Affymetrix GeneChip® HuGene 1.0ST microarrays in primary human hepatocyte of six different donors treated with CITCO, rifampicin, WY-14643 and DMSO.

A linear mixed model approach considering donor random effect to account for the high inter-donor variability was used to identify genes differentially expressed between the different treatments across all donors (5.6). 678 genes were identified as significantly differentially expressed between at least two of the treatments (Benjamini-Hochberg adjusted p-value ≤ 0.05). For each of these genes, coefficients of variation (CVs) were computed based on the expression values of a) each donor (across all treatments) and b) the DMSO-treated samples (across all donors). As shown in Figure 2.2, for most of the genes the CV calculated for the DMSO-treated

hepatocyte samples was higher than the CV in the single donors. This confirmed that in these experiments the gene expression was more influenced by the donors than by the treatments.
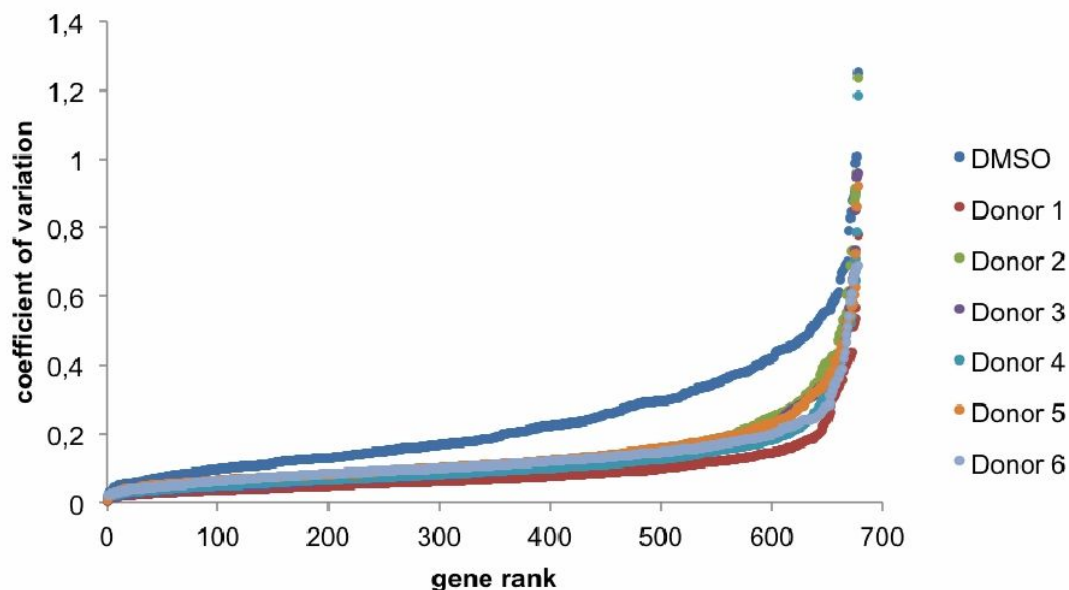
Figure 2.2 Distribution of coefficients of variation (CVs), calculated on the expression values of each gene, which was significant in the linear mixed model approach. For each of these genes, CVs were computed for a) the six DMSO-treated human hepatocyte samples (DMSO) as well as b) the four treatments (DMSO, CITCO, rifampicin and WY-14643) within each donor (donor 1 to 6). CVs are sorted in increasing order for each group (DMSO and Donor 1 to 6)

To identify the genes differentially expressed between the agonist treatments (CITCO, rifampicin and WY-14643) compared to the control treatment (DMSO), the 678 genes received from the linear mixed model were analyzed with post-hoc paired student t-tests (0). Sets of 316, 498 and 478 genes were identified as significantly differentially expressed between the treatments CITCO, rifampicin or WY-14643, respectively, and the control treatment DMSO (p-value $p \leq 0.05$). An effect size cut off was not applied, in order to detect small but consistent changes in the expression of individual genes as well. The relative mRNA expression upon the individual treatments compared to control treatment, expressed as fold change on a linear scale, ranged from 2 to 0.79 fold for CITCO (Table 2.1), from 4.09 to 0.32 fold for rifampicin (Table 2.2), and from 2.81 to 0.54 fold for WY-14643 (Table 2.3).

Table 2.1 List of the significantly (paired t-test p≤0.05) top 20 up- and top 20 downregulated genes in primary human hepatocytes upon CITCO treatment. Fold changes were calculated comparing CITCO and DMSO treated samples.

Gene Symbol	Gene Description	FC	p-value
Upregulated genes			
CYP2B6	cytochrome P450, family 2, subfamily B, polypeptide 6	2.00	3.2E-03
CYP2A7	cytochrome P450, family 2, subfamily A, polypeptide 7	1.83	5.6E-03
CYP1A1	cytochrome P450, family 1, subfamily A, polypeptide 1	1.78	1.4E-03
CYP2A13	cytochrome P450, family 2, subfamily A, polypeptide 13	1.72	7.8E-03
CYP2A6	cytochrome P450, family 2, subfamily A, polypeptide 6	1.71	5.8E-03
CYP2C8	cytochrome P450, family 2, subfamily C, polypeptide 8	1.67	1.1E-02
CYP3A4	cytochrome P450, family 3, subfamily A, polypeptide 4	1.59	1.2E-02
CYP3A7	cytochrome P450, family 3, subfamily A, polypeptide 7	1.45	2.7E-03
CYP1A2	cytochrome P450, family 1, subfamily A, polypeptide 2	1.32	1.8E-02
PTCH2	patched homolog 2 (Drosophila)	1.31	1.4E-03
OSTbeta	organic solute transporter beta	1.29	2.2E-02
AKR1B10	aldo-keto reductase family 1, member B10 (aldose reductase)	1.29	1.8E-02
TMPRSS11A	transmembrane protease, serine 11A	1.28	8.8E-03
CYP2C9	cytochrome P450, family 2, subfamily C, polypeptide 9	1.28	2.5E-03
NCBP2L	nuclear cap binding protein subunit 2-like	1.24	6.8E-03
ALAS1	aminolevulinate, delta-, synthase 1	1.23	2.2E-02
CD3E	CD3e molecule, epsilon (CD3-TCR complex)	1.22	1.3E-02
HLA-DOA	major histocompatibility complex, class II, DO alpha	1.19	1.7E-02
ARHGAP9	Rho GTPase activating protein 9	1.18	9.6E-03
CYP3A5	cytochrome P450, family 3, subfamily A, polypeptide 5	1.17	1.9E-03
Downregulated genes			
CYBB	cytochrome b-245, beta polypeptide	0.79	9.9E-03
PRDM2	PR domain containing 2, with ZNF domain	0.80	8.2E-04
PDCD1LG2	programmed cell death 1 ligand 2	0.82	4.5E-04
SNAI2	snail homolog 2 (Drosophila)	0.82	3.7E-03
DAPK1	death-associated protein kinase 1	0.83	3.3E-03
SLC22A9	solute carrier family 22 (organic anion transporter), member 9	0.83	3.6E-02
PFKFB3	6-phosphofructo-2-kinase/fructose-2,6-biphosphatase 3	0.83	1.2E-03
AASS	aminoadipate-semialdehyde synthase	0.84	4.2E-02
TBL1	transducin (beta)-like 1X-linked	0.84	2.3E-02
X	insulin receptor substrate 1	0.84	1.6E-02
IRS1	growth factor receptor-bound protein 10	0.84	9.4E-03
GRB10	zinc finger protein 36, C3H type, homolog (mouse)	0.84	7.7E-03
ZFP36	family with sequence similarity 169, member A	0.85	3.3E-02
FAM169A	G protein-coupled estrogen receptor 1	0.85	1.3E-03
GPER SLC6A12	solute carrier family 6 (neurotransmitter transporter, betaine/GABA), member 12	0.85	1.7E-02
	tumor necrosis factor receptor superfamily, member 11b	0.85	1.4E-02
TNFRSF11B KIAA0226	KIAA0226	0.85	7.7E-04
ST6GALNAC 6	ST6 (alpha-N-acetyl-neuraminyl-2,3-beta-galactosyl-1,3)-N-acetylgalactosaminide alpha-2,6-sialyltransferase 6	0.85	9.9E-04
SPRY4	sprouty homolog 4 (Drosophila)	0.85	8.1E-04
ZNF470	zinc finger protein 470	0.85	1.0E-02

FC, linear fold change; p-value, post-hoc paired student t-tests

In total, 57 genes were upregulated and 259 genes were downregulated in response to CITCO treatment (Supplemental Table 1). In Table 2.1, the 20 most strongly up- and downregulated significantly differentially expressed genes are shown. Eleven of the 20 most strongly upregulated genes were cytochrome P450 monooxygenases, with *CYP2B6* showing the highest induction (2-fold) upon CITCO treatment. All these CYPs are involved in the metabolism of drugs or xenobiotics, except for *CYP2A7* for which no substrate is currently known. The 20 top upregulated genes furthermore included the gene encoding the solute carrier transporter *OSTbeta* (*SLC51B*), involved in bile acid transport, the gene encoding aldoketoreductase *AKR1B10,* involved in lipid metabolism and detoxification of aliphatic aldehydes, as well as the gene *ALAS1,* which encodes the rate-limiting enzyme in heme biosynthesis.

The most strongly downregulated gene upon CITCO treatment was cytochrome B-245 beta polypeptide (*CYBB*), a gene assumed to be involved in the phagocyte mediated oxidation of microbes, with a fold change of 0.79. Among the top downregulated genes were also genes involved in insulin signaling (*IRS1* and *GRB10*), and the gene *PFKFB3,* associated with gluconeogenesis. Other genes of the top 20 downregulated set were associated with the immune system (*PDCD1LG2* and *DAPK1*), cell development and differentiation (*TNFRSF11B* and *TBL1X*), or cancer (*PRDM2* and *SNAI2*).

The most pronounced effect of CITCO treatment was shown to be the transcriptional induction of several *CYP*s involved in xenobiotic metabolism as well as the upregulation of the most important gene in heme anabolism *ALAS1* that provides heme for the synthesis of CYPs, whereas the genes that responded with decreased expression were associated with diverse biological function.

Table 2.2 List of the significantly (paired t-test p≤0.05) top 20 up- and top 20 downregulated genes in primary human hepatocytes upon rifampicin treatment. Fold changes were calculated comparing rifampicin and DMSO treated samples.

Gene Symbol	Gene Description	FC	p-value
Upregulated genes			
CYP3A4	cytochrome P450, family 3, subfamily A, polypeptide 4	4.09	9.3E-04
PRAMEF10	PRAME family member 10	3.39	3.2E-03
OSTbeta	organic solute transporter beta	3.27	6.8E-04
CYP2C8	cytochrome P450, family 2, subfamily C, polypeptide 8	2.59	6.2E-04
AGXT2L1	alanine-glyoxylate aminotransferase 2-like 1	2.57	5.0E-06
CYP3A7	cytochrome P450, family 3, subfamily A, polypeptide 7	2.38	2.2E-04
AKR1D1	aldo-keto reductase family 1, member D1 (delta 4-3-ketosteroid-5-beta-reductase)	2.33	4.5E-05
CYP2B6	cytochrome P450, family 2, subfamily B, polypeptide 6	2.21	2.1E-03
ALAS1	aminolevulinate, delta-, synthase 1	2.15	1.3E-04
THRSP	thyroid hormone responsive (SPOT14 homolog, rat)	2.12	6.6E-03
AKR1B10	aldo-keto reductase family 1, member B10 (aldose reductase)	1.92	6.0E-04
PRAMEF17	PRAME family member 17	1.87	6.9E-03
CYP3A43	cytochrome P450, family 3, subfamily A, polypeptide 43	1.84	1.3E-03
CYP2C9	cytochrome P450, family 2, subfamily C, polypeptide 9	1.74	1.5E-03
SERPINB9	serpin peptidase inhibitor, clade B (ovalbumin), member 9	1.72	2.3E-03
SEC14L4	SEC14-like 4 (S. cerevisiae)	1.68	1.1E-04
CA12	carbonic anhydrase XII	1.65	1.9E-03
MPV17L	MPV17 mitochondrial membrane protein-like	1.64	3.0E-03
BCAS1	breast carcinoma amplified sequence 1	1.62	6.0E-03
CYP3A5	cytochrome P450, family 3, subfamily A, polypeptide 5	1.59	7.7E-04
Downregulated genes			
CYP7A1	cytochrome P450, family 7, subfamily A, polypeptide 1	0.32	9.5E-03
ADH1B	alcohol dehydrogenase 1B (class I), beta polypeptide	0.39	1.1E-03
SULT1E1	sulfotransferase family 1E, estrogen-preferring, member 1	0.51	2.3E-03
HMGCS2	3-hydroxy-3-methylglutaryl-Coenzyme A synthase 2 (mitochondrial)	0.54	4.8E-03
ADH1A	alcohol dehydrogenase 1A (class I), alpha polypeptide	0.56	5.9E-03
CYP4A11	cytochrome P450, family 4, subfamily A, polypeptide 11	0.62	3.6E-03
AFM	afamin	0.65	4.9E-03
ADH4	alcohol dehydrogenase 4 (class II), pi polypeptide	0.65	1.7E-02
GYS2	glycogen synthase 2 (liver)	0.66	1.0E-03
CYP2E1	cytochrome P450, family 2, subfamily E, polypeptide 1	0.67	6.8E-03
PEG10	paternally expressed 10	0.67	7.6E-03
STEAP4	STEAP family member 4	0.67	3.5E-03
CXCL2	chemokine (C-X-C motif) ligand 2	0.67	1.6E-03
ASPA	aspartoacylase (Canavan disease)	0.68	2.4E-02
SULT1B1	sulfotransferase family, cytosolic, 1B, member 1	0.68	2.2E-04
PDK4	pyruvate dehydrogenase kinase, isozyme 4	0.68	4.8E-04
LECT2	leukocyte cell-derived chemotaxin 2	0.68	4.0E-03
TAT	tyrosine aminotransferase	0.69	7.5E-03
WDR72	WD repeat domain 72	0.69	9.4E-03
IGF1	insulin-like growth factor 1 (somatomedin C)	0.69	4.7E-03

FC, linear fold change; p-value, post-hoc paired student t-tests

Rifampicin treatment led to a significant up- and downregulation of 164 and 334 genes, respectively, when compared to DMSO treatment (Supplemental Table 2). Table 2.2 shows the 20 most strongly up- and downregulated genes. Seven of the 20 most upregulated genes were *CYP*s (*CYP3A4*, *CYP2C8*, *CYP3A7*, *CYP2B6*, *CYP3A43*, *CYP2C9* and *CYP3A5*), which are involved in drug metabolism or steroid hormone metabolism (*CYP3A43*). *CYP3A4* was identified as the most upregulated (fold change of 4.09) gene. Furthermore, two aldoketoreductases (*AKR1D1* and *AKR1B10*), which encode for enzymes detoxifying reactive aldehydes, *OSTbeta* (*SLC51B*), important for steroid transport, *THRSP,* a regulator of lipid metabolism, and *ALAS1*, encoding for the rate-limiting step in heme biosynthesis, were included in the top upregulated genes. Other genes were associated with different types of cancer (*PRAMEF10*, *PRAMEF17* and *BCAS1*).

Among the top 20 downregulated genes, three CYPs were found: *CYP7A1*, encoding the rate-limiting enzyme of bile acid formation, *CYP4A11,* encoding for an enzyme metabolizing fatty acids, and *CYP2E1*, encoding an enzyme metabolizing ethanol. *CYP7A1* was the most downregulated gene (fold change of 0.32). Moreover, three alcohol dehydrogenases (*ADH1A*, *ADH1B* and *ADH4*) were within the list of the top 20 downregulated genes. Furthermore, *HMGCS2*, encoding the rate-limiting step of ketogenesis, *GYS2*, encoding the liver specific glycogen synthesis, and *PDK4*, encoding a kinase, which inhibits the pyruvate dehydrogenase, were among the 20 most downregulated genes. In addition, the two sulfotransferases *SULT1E1* involved in estrone metabolism, and *SULT1B1*, involved in drug metabolism, were found to be among the most downregulated genes.

The strongest response to rifampicin treatment was observed for genes contributing to drug, steroid and fatty acid and glucose metabolism. However, expression of most of the genes involved in drug metabolism, e.g., *CYP*s of the 2C and 3A families, was induced, while genes associated with fatty acid catabolism or glucose metabolism were mainly downregulated.

Table 2.3 List of the significantly (paired t-test p≤0.05) top 20 up- and top 20 downregulated genes in primary human hepatocytes upon WY-14643 treatment. Fold changes were calculated comparing WY-14643 and DMSO treated samples.

Gene Symbol	Gene Description	FC	p-value
Upregulated genes			
HMGCS2	3-hydroxy-3-methylglutaryl-Coenzyme A synthase 2 (mitochondrial)	2.81	1.3E-04
CYP4A22	cytochrome P450, family 4, subfamily A, polypeptide 22	2.39	2.8E-03
FABP4	fatty acid binding protein 4, adipocyte	2.27	8.4E-03
CREB3L3	cAMP responsive element binding protein 3-like 3	2.18	1.1E-03
PDK4	pyruvate dehydrogenase kinase, isozyme 4	1.94	1.0E-05
FABP1	fatty acid binding protein 1, liver	1.90	2.0E-04
CYP4A11	cytochrome P450, family 4, subfamily A, polypeptide 11	1.77	1.8E-04
CYP3A4	cytochrome P450, family 3, subfamily A, polypeptide 4	1.70	9.2E-04
PLIN2	perilipin 2	1.69	2.9E-04
MBL2	mannose-binding lectin (protein C) 2, soluble (opsonic defect)	1.69	5.8E-04
CPT1A	carnitine palmitoyltransferase 1A (liver)	1.68	3.4E-03
CYP2C8	cytochrome P450, family 2, subfamily C, polypeptide 8	1.68	2.0E-03
LRRC31	leucine rich repeat containing 31	1.57	2.4E-02
CD36	CD36 molecule (thrombospondin receptor)	1.56	1.3E-02
PRAMEF10	PRAME family member 10	1.54	1.1E-03
RDH16	retinol dehydrogenase 16 (all-trans)	1.52	1.4E-03
ACSL1	acyl-CoA synthetase long-chain family member 1	1.51	4.1E-04
SGK2	serum/glucocorticoid regulated kinase 2	1.49	6.6E-05
ABCB4	ATP-binding cassette, sub-family B (MDR/TAP), member 4	1.46	2.6E-03
AADAC	arylacetamide deacetylase (esterase)	1.43	4.2E-03
Downregulated genes			
PNRC2	proline-rich nuclear receptor coactivator 2	0.54	2.1E-06
AASS	aminoadipate-semialdehyde synthase	0.61	3.8E-04
PEG10	paternally expressed 10	0.64	2.0E-02
CXCL10	chemokine (C-X-C motif) ligand 10	0.66	7.8E-03
CYBB	cytochrome b-245, beta polypeptide	0.67	3.2E-03
ADH1B	alcohol dehydrogenase 1B (class I), beta polypeptide	0.68	3.9E-02
UNC5CL	unc-5 homolog C (C. elegans)-like	0.71	1.2E-03
ARG2	arginase, type II	0.73	5.2E-04
C3orf52	chromosome 3 open reading frame 52	0.73	1.1E-03
MUC13	mucin 13, cell surface associated	0.74	2.6E-03
TAT	tyrosine aminotransferase	0.74	6.8E-03
IGSF6	immunoglobulin superfamily, member 6	0.74	2.8E-03
WEE1	WEE1 homolog (S. pombe)	0.74	1.6E-03
STEAP4	STEAP family member 4	0.74	2.7E-02
ADH1A	alcohol dehydrogenase 1A (class I), alpha polypeptide	0.75	4.2E-02
NRBP2	nuclear receptor binding protein 2	0.76	1.7E-02
RND1	Rho family GTPase 1	0.76	3.3E-03
MASP1	mannan-binding lectin serine peptidase 1 (C4/C2 activating component of Ra-reactive factor)	0.76	9.9E-03
IGF1	insulin-like growth factor 1 (somatomedin C)	0.76	2.4E-03
AKR1CL1	aldo-keto reductase family 1, member C like 1	0.76	5.0E-03

FC, linear fold change; p-value, post-hoc paired student t-tests

Table 2.3 includes the 20 most strongly up- and downregulated genes upon the WY-14643 mediated activation of PPARα. In total, WY-14643 led to the upregulation of 139 and downregulation of 339 genes compared to DMSO treatment (Supplemental Table 3). The mitochondrial 3-hydroxy-3-methylglutaryl- Coenzyme A synthase 2 (*HMGSC2*), encoding the rate-limiting enzyme of ketogenesis, was the most upregulated gene (fold change of 2.81). Seven among the most upregulated genes were involved in fatty acid metabolism (*CYP4A11* and *CYP4A22*), activation (*ACSL1*) or transport and translocation (*FABP4*, *FABP1*, *CD36* and *CPT1A*). Two of the top 20 upregulated genes were found to be CYPs involved in drug metabolism (*CYP3A4* and *CYP2C8*). Also within the most upregulated genes were *PDK4*, encoding the kinase inhibiting the pyruvate dehydrogenase, and *CREB3L3,* an important regulator of lipid metabolism. The gene proline-rich nuclear receptor coactivator 2 (*PNRC2*), which is assumed to be involved in non-sense mediated mRNA decay, was identified as the most downregulated gene following WY-14643 treatment, with a fold change of 0.54. Also among the top 20 downregulated genes were the genes *ADH1A* and *ADH1B*, encoding two alcohol dehydrogenases, as well as genes involved in the immune system like *CXCL10*, *CYBB* and *MASP1*. The genes *ARG2,* encoding the enzyme catalyzing the reaction from arginine to urea and *STEAP4,* which is suggested to play a role in adipocyte development and metabolism, were also included in the list of the 20 most downregulated genes.

These results revealed that WY-14643 treatment led to the strongest expression changes of genes coding for proteins that facilitate important reactions or transport processes involved in fatty acid, glucose metabolism and ketogenesis (*CD36*, *FABP4*, *CYP4A11*, *CPT1A*, *PDK4* and *HMGCS2*) as well as drug metabolism (*CYP3A4* and *CYP2C8*).

2.1.2 Comparison of the genes differentially expressed by treatment with CITCO, rifampicin and WY-14643

In order to identify genes whose expression was altered in response to more than one of the treatments, the differentially expressed genes upon CITCO, rifampicin or WY-14643 treatment were compared.
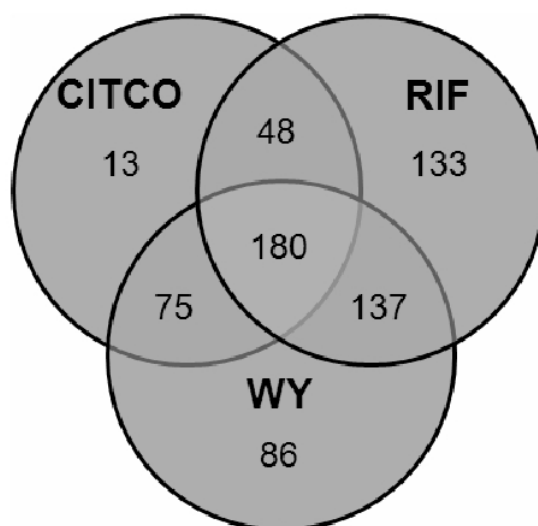
Figure 2.3 Venn diagram showing the overlaps of the sets of differentially expressed genes upon treatment of primary human hepatocytes with CITCO, rifampicin (RIF) or WY-14643 (WY) compared to control. The numbers indicate the counts of genes per intersection.

Figure 2.3 shows the comparison of genes differentially expressed upon CITCO, rifampicin and WY-14643 treatment. A set of 13 genes was exclusively regulated upon CITCO treatment. Rifampicin and WY-14643 treatment exclusively regulated sets of 133 and 86 genes, respectively. 48 genes were regulated by CITCO and rifampicin but not by WY-14643 treatment. Rifampicin and WY-14643 treatment regulated a common set of 137 genes. The intersection of CITCO- and WY-14643-regulated genes included 75 genes. 180 genes were shown to be regulated by all three NR agonist treatments. This comparison showed that a large fraction of the genes influenced individually by one of the three treatments was also affected by one

or both of the other treatments. For all three treatments the number of co-regulated genes was higher than those exclusively affected.

Table 2.4 List of genes differentially expressed by all three treatments with a positive fold change of > 1.2 and a negative fold change <1/1.2

Gene Symbol	Gene Description	FC CITCO[a]	FC rifampicin[b]	FC WY-14643[c]
ALAS1	aminolevulinate, delta-, synthase 1	1.23	2.15	1.40
CYP2B6	cytochrome P450, family 2, subfamily B, polypeptide 6	2.00	2.21	1.32
CYP2C8	cytochrome P450, family 2, subfamily C, polypeptide 8	1.67	2.59	1.68
CYP3A4	cytochrome P450, family 3, subfamily A, polypeptide 4	1.59	4.09	1.70
CYP3A7	cytochrome P450, family 3, subfamily A, polypeptide 7	1.45	2.38	1.42
PTCH2	patched homolog 2 (Drosophila)	1.31	1.25	1.27
PDCD1LG2	programmed cell death 1 ligand 2	0.82	0.81	0.82
PRDM2	PR domain containing 2, with ZNF domain	0.80	0.83	0.83
SNAI2	snail homolog 2 (Drosophila)	0.82	0.72	0.81

linear fold change [a] CITCO, [b] rifampicin or [c] WY-14643 vs. DMSO treatment

Table 2.4 shows the nine overlapping regulated genes, filtered by a FC-threshold (FC= 1.2 for upregulated and 1/1.2 for downregulated genes), included in the intersection of the differentially expressed genes by all three treatments. From these nine genes, *ALSA1*, *CYP2B6*, *CYP2C8*, *CYP3A4*, *CYP3A7* and *PTCH2* were upregulated, whereas *PDCD1LG2*, *PRDM2* and *SNAI2* were coordinately downregulated by all three NRs. These results showed that all three treatments coordinately induced the expression of major drug metabolizing *CYP*s and *ALAS1*, which encodes the rate-limiting enzymes for the biosynthesis of heme that is mandatory for the catalytic function of such CYPs.

Applying this threshold to all differentially expressed genes, 27, 214 and 158 genes remained for CITCO, rifampicin and WY-14643 treatment, respectively. The intersection of CITCO and rifampicin treatment included 11 genes, the intersection of rifampicin and WY-14643 treatment included 58 genes, and the intersection of differentially expressed genes upon WY-14643 and CITCO treatment included 3 genes (data not shown).

2.1.3 Validation of GeneChip® HuGene 1.0ST Array whole-genome expression data by qRT-PCR

In order to validate the whole-genome expression data, the expression of 12 significantly differentially expressed genes, including three of the top regulated liver-specific target genes for each of the nuclear receptors CAR (*CYP1A1*, *CYP2A6* and *CYP2B6*), PXR (*CYP2C8*, *CYP3A7* and *CYP7A1*), and PPARα (*FABP1*, *HMGCS2* and *PDK4*), and three genes shown to be regulated by all three NRs (*ALAS1*, *CYP3A4* and *POR*), were determined using qRT-PCR.
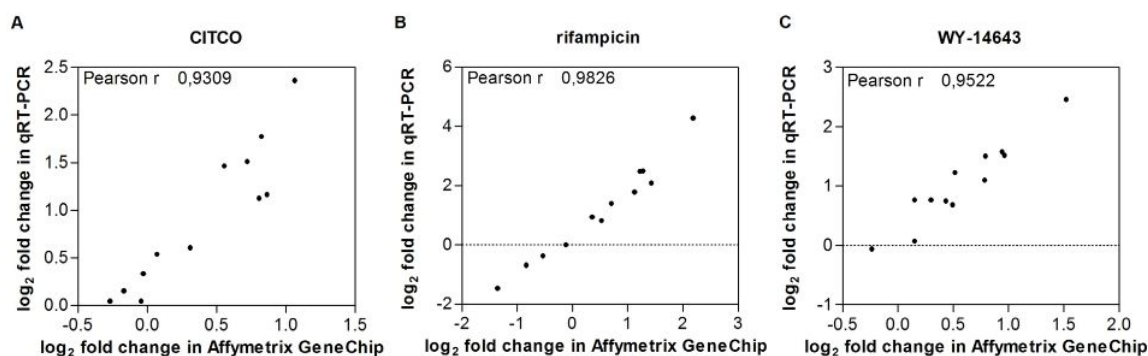
Figure 2.4 Comparison of the mean (six donors) $\log_2$ fold changes for the treatments CITCO (A), rifampicin (B) and WY-14643 (C) compared to control, obtained from qRT-PCR and from GeneChip® HuGene 1.0ST Arrays (Affymetrix) from 12 marker genes using Pearson correlation.

In Figure 2.4, the expression changes of the 12 genes upon CITCO, rifampicin and WY-14643 treatment measured by Affymetrix arrays and by qRT-PCR are shown. The mean relative expression values from all six donors for these 12 genes determined with both methods were highly correlated for all three treatments (CITCO, pearson r= 0.93; rifampicin, pearson r= 0.98 and WY-14643 pearson r= 0.95). However, fold changes obtained from qRT-PCR analysis were generally higher than those from microarray analysis.

2.1.4 Gene Ontology term and KEGG pathway analyses of differentially expressed genes

To investigate the contribution of differentially expressed genes following the activation of the NRs CAR, PXR and PPARα by their respective agonists CITCO, rifampicin and WY-14643 to specific biological processes and metabolic pathways, gene ontology and KEGG pathway enrichment was applied (5.5.1). These procedures involved the use of modified Fisher´s exact test to identify overrepresentations of genes within pathways or ontologies including a defined number of genes, associated with specific biological entity. The enrichments were assumed to be significant with a Bonferroni corrected p-value ≤ 0.05.

2.1.4.1 Pathway analysis of differentially expressed genes by CITCO treatment

For 19 GO terms of biological processes, a significant enrichment of differentially expressed genes upon CITCO treatment was identified. In Table 2.5, the overrepresented GO terms for the differentially expressed genes upon CITCO treatment are listed. In 13 of these terms, the majority of enriched genes were up- and in six of the terms downregulated. The most significantly overrepresented GO term was "drug metabolic process" including 10 upregulated genes and one downregulated gene. In total, nine of the 19 significantly enriched terms were associated with the metabolism or response to exogenous molecules ("drug metabolic process", "response to xenobiotic stimulus", "drug catabolic process", "exogenous drug catabolic process", "xenobiotic metabolic process", "coumarin metabolic process", "cellular response to chemical stimulus" and "response to chemical stimulus"). Two terms were associated with lipid metabolism ("lipid metabolic process" and "cellular lipid metabolic process") and one with carbohydrate metabolism ("carbohydrate metabolic process").

Table 2.5 List of GO terms for biological processes identified as enriched for genes differentially expressed upon CITCO treatment

GO ID	GO term	Up-regulated[a]	Down-regulated[b]	Bonferroni-adjusted p-value
GO:0017144	Drug metabolic process	10	1	1.9E-08
GO:0009410	Response to xenobiotic stimulus	16	4	4.1E-08
GO:0042737	Drug catabolic process	8	0	5.1E-08
GO:0042738	Exogenous drug catabolic process	7	0	7.7E-07
GO:0006805	Xenobiotic metabolic process	15	3	8.4E-07
GO:0071466	Cellular response to xenobiotic stimulus	15	3	1.0E-06
GO:0006629	Lipid metabolic process	17	32	3.1E-05
GO:0008202	Steroid metabolic process	12	8	2.8E-04
GO:0044281	Small molecule metabolic process	22	52	1.0E-03
GO:0044255	Cellular lipid metabolic process	12	25	1.0E-03
GO:0070989	Oxidative demethylation	5	0	2.0E-03
GO:0070988	Demethylation	7	1	2.4E-03
GO:0009804	Coumarin metabolic process	4	0	7.0E-03
GO:0016098	Monoterpenoid metabolic process	3	1	7.0E-03
GO:0005975	Carbohydrate metabolic process	5	29	1.4E-02
GO:0042493	Response to drug	11	10	2.9E-02
GO:0055114	Oxidation-reduction process	20	18	3.2E-02
GO:0070887	Cellular response to chemical stimulus	19	37	3.6E-02
GO:0042221	Response to chemical stimulus	23	66	3.7E-02

[a] number of upregulated genes with in one pathway; [b] number of downregulated genes with in one pathway

Differentially expressed genes following CITCO treatment showed significant enrichment in six KEGG pathways (Table 2.6). The top enriched pathway was "Retinol metabolism", including 13 upregulated genes and one downregulated gene. In general, all terms included more up- than downregulated genes. Four pathways were associated with drug and xenobiotic metabolism ("Drug metabolism by cytochrome P450", "Metabolism of xenobiotics by cytochrome P450", "Drug metabolism by other enzymes" and "Caffeine metabolism") and one with fatty acid metabolism ("Linoleic acid metabolism").

These pathway analyses (Table 2.5 and Table 2.6) revealed that the genes affected by CITCO were most significantly enriched in pathways that are associated with the response to drugs and xenobiotics or the metabolism of such compounds.

Table 2.6 List of KEGG pathways identified as enriched for genes differentially expressed upon CITCO treatment

KEGG ID	KEGG term	Up-regulated[a]	Down-regulated[b]	Bonferroni-adjusted p-value
hsa00830	Retinol metabolism	13	1	9.9E-09
hsa00982	Drug metabolism by cytochrome P450s	13	1	6.4E-08
hsa00980	Metabolism of xenobiotics by cytochrome P450	12	1	5.6E-07
hsa00591	Linoleic acid metabolism	7	1	2.3E-04
hsa00983	Drug metabolism by other enzymes	8	0	4.7E-03
hsa00232	Caffeine metabolism	4	0	4.5E-02

[a] number of upregulated genes with in one pathway;   [b] number of downregulated genes with in one pathway

2.1.4.2 Pathway analysis of differentially expressed genes by rifampicin treatment

Genes differentially expressed by rifampicin treatment were found to be significantly overrepresented in 64 GO terms of biological processes. In Table 2.7 the top 20 GO terms are shown, identified to contain a significantly overrepresented number of genes differentially expressed upon PXR activation. Five of these terms included more upregulated genes and 15 more downregulated genes. The most significantly overrepresented GO term was "small molecules metabolic process" and contained 62 up- and 96 downregulated genes. Nine of the 20 most significantly enriched terms were associated with fatty acid or lipid metabolism ("lipid metabolic process", "cellular lipid metabolic process", "organic acid metabolic process", "carboxylic acid metabolic process", "monocarboxylic acid metabolic process", "carboxylic acid catabolic process", "fatty acid metabolic process", "regulation of lipid metabolic process" and "lipid biosynthetic process") and seven with the response or metabolism of

exogenous compounds ("response to xenobiotic stimulus", "xenobiotic metabolic process", "cellular response to xenobiotic stimulus", "response to drug", "cellular response to chemical stimulus", "drug metabolic process" and "response to chemical stimulus"). Also the term "steroid metabolic process" was among the 20 most significantly enriched GO terms for biological processes.

Table 2.7 List of the 20 most significant GO terms for biological processes identified as enriched for genes differentially expressed upon rifampicin treatment

GO ID	GO term	Up-regulated[a]	Down-regulated[b]	Bonferroni-adjusted p-value
GO:0044281	Small molecule metabolic process	62	96	1.9E-22
GO:0006629	Lipid metabolic process	40	64	2.4E-22
GO:0055114	Oxidation-reduction process	40	55	1.5E-21
GO:0044255	Cellular lipid metabolic process	27	53	8.1E-18
GO:0006082	Organic acid metabolic process	33	52	6.7E-17
GO:0019752	Carboxylic acid metabolic process	32	49	6.7E-17
GO:0009410	Response to xenobiotic stimulus	20	14	3.6E-16
GO:0032787	Monocarboxylic acid metabolic process	21	32	6.6E-16
GO:0006805	Xenobiotic metabolic process	20	12	3.3E-15
GO:0071466	Cellular response to xenobiotic stimulus	20	12	5.1E-15
GO:0046395	Carboxylic acid catabolic process	8	24	3.7E-10
GO:0008202	Ssteroid metabolic process	20	15	4.4E-10
GO:0006631	Fatty acid metabolic process	13	22	2.1E-09
GO:0019216	Regulation of lipid metabolic process	8	21	8.7E-08
GO:0042493	Response to drug	15	23	3.9E-07
GO:0008610	Lipid biosynthetic process	18	25	5.4E-07
GO:0051186	Cofactor metabolic process	12	19	6.3E-07
GO:0070887	Cellular response to chemical stimulus	35	61	4.0E-06
GO:0017144	Drug metabolic process	10	1	4.5E-06
GO:0042221	Response to chemical stimulus	47	103	1.1E-05

[a] number of upregulated genes with in one pathway;   [b] number of downregulated genes with in one pathway

In Table 2.8, the eight KEGG pathways are listed, which showed a significant enrichment of genes differentially expressed upon rifampicin treatment. The most significantly enriched term was "Retinol metabolism". In six of these terms, the majority of the included genes were upregulated. These pathways included "Retinol metabolism", "Steroid hormone biosynthesis" and "Linoleic acid metabolism" and three pathway associated with xenobiotic metabolism ("Drug metabolism by cytochrome P450", "Metabolism of xenobiotics by cytochrome P450" and "Drug metabolism by other enzymes"). In the two pathways "Fatty acid metabolism" and "PPAR signaling pathways", the majority of genes were downregulated.

Taken together, the genes that responded to rifampicin treatment were shown to be most significantly associated with xenobiotic and lipid metabolism. For most of the terms and pathway referring to xenobiotic and drug metabolism the majority of the included genes were upregulated, whereas the terms and pathways that are associated with lipid metabolism contained more down- than upregulated genes (Table 2.7 and Table 2.8).

Table 2.8 List of KEGG pathways identified as enriched for genes differentially expressed upon rifampicin treatment

KEGG ID	KEGG term	Up-[a] regulated	Down-[b] regulated	Bonferroni-adjusted p-value
hsa00830	Retinol metabolism	13	8	7.6E-12
hsa00982	Drug metabolism by cytochrome P450	14	6	1.6E-09
hsa00980	Metabolism of xenobiotics by cytochrome P450	13	5	9.6E-08
hsa00071	Fatty acid metabolism	2	11	3.7E-05
hsa00140	Steroid hormone biosynthesis	9	3	1.7E-04
hsa03320	PPAR signaling pathway	5	9	3.3E-04
hsa00591	Linoleic acid metabolism	7	2	1.3E-03
hsa00983	Drug metabolism by other enzymes	9	1	5.4E-03

[a] number of upregulated genes with in one pathway;   [b] number of downregulated genes with in one pathway

2.1.4.3 Pathway analysis of differentially expressed genes by WY-14643 treatment

Differentially expressed genes upon PPARα activation by WY-14643 (n= 478) were found to be overrepresented (Bonferroni corrected p-value ≤ 0.05) in 45 GO terms of biological processes (Table 2.9 and Supplemental table 5).

Table 2.9 List of the 20 most significant GO terms for biological processes identified as enriched for genes differentially expressed upon WY-14643 treatment

GO ID	GO term	Up-regulated[a]	Down-regulated[b]	Bonferroni-adjusted p-value
GO:0006629	Lipid metabolic process	46	37	3.0E-13
GO:0044255	Cellular lipid metabolic process	38	29	2.5E-12
GO:0046395	Carboxylic acid catabolic process	17	15	3.5E-11
GO:0044281	Small molecule metabolic process	62	61	1.6E-10
GO:0055114	Oxidation-reduction process	36	33	1.9E-09
GO:0009062	Fatty acid catabolic process	14	4	3.5E-09
GO:0019752	Carboxylic acid metabolic process	35	27	1.4E-08
GO:0006082	Organic acid metabolic process	36	28	6.1E-08
GO:0044242	Cellular lipid catabolic process	16	6	1.5E-07
GO:0032787	Monocarboxylic acid metabolic process	25	13	2.8E-07
GO:0009410	Response to xenobiotic stimulus	14	9	3.3E-07
GO:0006631	Fatty acid metabolic process	22	8	6.2E-07
GO:0016042	Lipid catabolic process	21	7	1.3E-06
GO:0042221	Response to chemical stimulus	42	100	3.1E-06
GO:0006805	Xenobiotic metabolic process	13	8	3.4E-06
GO:0071466	Cellular response to xenobiotic stimulus	13	8	4.3E-06
GO:0070887	Cellular response to chemical stimulus	29	61	4.7E-06
GO:0042493	Response to drug	15	19	8.1E-06
GO:0019395	Fatty acid oxidation	13	1	2.5E-05
GO:0034440	Lipid oxidation	13	1	3.1E-05

[a] number of upregulated genes with in one pathway;   [b] number of downregulated genes with in one pathway

Table 2.9 shows the top 20 GO terms that were identified to include a significantly enriched number of differentially expressed genes following WY-14643 treatment. 17 of these terms contained mostly upregulated genes, three terms contained mostly downregulated genes. The top enriched term was "lipid metabolic process", including 46 upregulated and 37 downregulated genes. Furthermore, 12 terms were associated with lipid and fatty acid metabolism ("lipid metabolic process", "cellular lipid metabolic process", "carboxylic acid catabolic process", "fatty acid catabolic process", "carboxylic acid metabolic process", "organic acid metabolic process", "cellular lipid catabolic process", "monocarboxylic acid metabolic process", "fatty acid metabolic process", "lipid catabolic process", "fatty acid oxidation" and "lipid oxidation") and six with response to exogenous compounds or their metabolism ("response to xenobiotic stimulus", "response to chemical stimulus", "xenobiotic metabolic process", "cellular response to xenobiotic stimulus", "cellular response to chemical stimulus" and "response to drug").

Table 2.10 List of KEGG pathways identified as enriched for genes differentially expressed upon WY-14643 treatment

KEGG ID	KEGG term	Up-regulated[a]	Down-regulated[b]	Bonferroni-adjusted p-value
hsa03320	PPAR signaling pathway	17	0	2.5E-07
hsa00071	Fatty acid metabolism	12	2	1.3E-06
hsa00830	Retinol metabolism	11	3	5.0E-05
hsa00980	Metabolism of xenobiotics by cytochrome P450	11	2	1.2E-03
hsa00982	Drug metabolism by cytochrome P450	10	3	1.6E-03

[a] number of upregulated genes with in one pathway;   [b] number of downregulated genes with in one pathway

Five KEGG pathways were identified to contain a significantly enriched number of genes affected by WY-14643 treatment (Table 2.10). For all these terms, the number of included upregulated genes was higher than the number of downregulated genes. The most significantly overrepresented KEGG pathway was "PPAR signaling pathways". Also, the pathways "Fatty acid metabolism", "Retinol metabolism",

"Metabolism of xenobiotics by cytochrome P450" and "Drug metabolism by cytochrome P450" were significantly enriched.

These results presented in Table 2.9 and Table 2.10 showed that genes differentially expressed upon WY-14643 treatment were most pronounced enriched in GO terms und KEGG pathways that are referring to fatty acid and lipid metabolism as well as drug and xenobiotic metabolism.

2.1.4.4 Comparative pathway analysis of differentially expressed genes

To identify biological processes and metabolic pathways that are influenced by more than one of the three NRs, the pathways and terms, identified to include an enriched number of differentially expressed genes upon CITCO, rifampicin and WY-14643 treatment (2.1.4.1, 0 and 0), were compared.
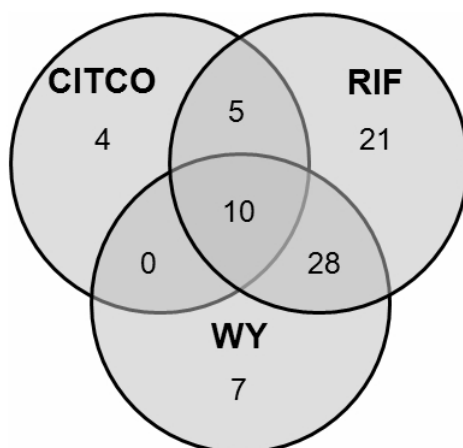
Figure 2.5 Venn diagram depicting comparison of overrepresented GO terms for biological processes for differentially expressed genes by CITCO, rifampicin (RIF) and WY-14643 (WY) treatment.

Figure 2.5 shows the overlaps of overrepresented GO terms for the genes differentially expressed upon CITCO, rifampicin or WY-14643 treatment. Ten terms were overlappingly enriched by all three treatments. Additionally, the intersection of exclusively enriched GO terms upon CITCO and rifampicin treatment included five terms and upon rifampicin and WY-14643 treatment 28 terms. This comparison

revealed that the GO terms, which showed enrichment for the differentially expressed genes upon each treatment, highly overlapped between two or all three treatments. A detailed list of all GO terms included in these intersections, as well as the exclusively enriched terms for each treatment, are shown in Table 2.5, Supplemental table 4 and Supplemental table 5.
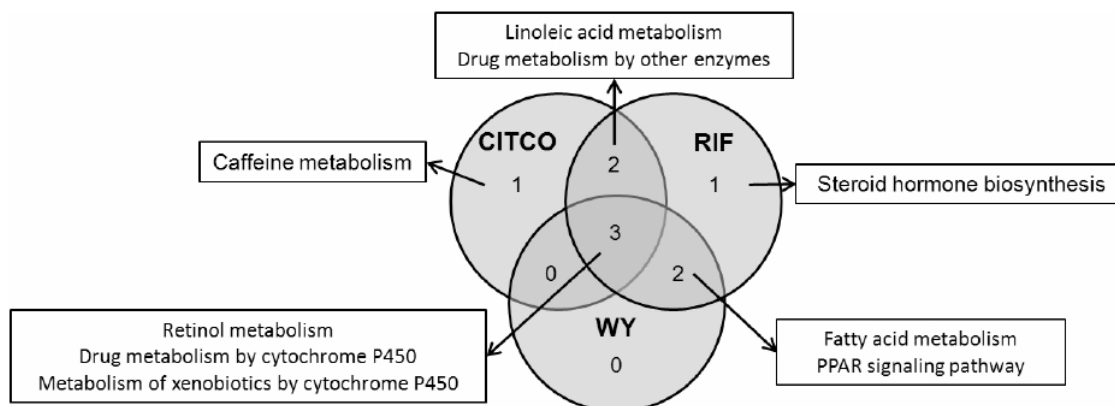
Figure 2.6 Venn diagram depicting comparison of overrepresented KEGG pathways for differentially expressed genes by CITCO, rifampicin (RIF) and WY-14643 (WY) treatment

The Venn diagram in Figure 2.6 shows a comparison of the KEGG pathways found to be overrepresented for differentially expressed genes upon CITCO, rifampicin or WY-14643 treatment. The intersection of all three treatments included the pathways "Retinol metabolism", "Drug metabolism by cytochrome P450" and "Metabolism of xenobiotics by cytochrome P450". The intersection of KEGG pathways enriched exclusively for CITCO and rifampicin treatment included "Linoleic acid metabolism" and "Drug metabolism by other enzymes". The intersection of rifampicin and WY-14643 consisted of the pathways "Fatty acid metabolism" and "PPAR signaling pathway". No pathway was found exclusively enriched upon WY-14643 treatment, and there was no pathway included in the intersection of WY-14643 and CITCO treatment. KEGG pathways are mainly comprised of genes encoding for enzymes contributing to specific metabolic pathways. Therefore, this information can be used to investigate the behavior of such a pathway under a certain condition.

To this end, the genes found to be enriched for the individual treatments, included in those overlapping KEGG pathways, were extracted and compared. The KEGG pathways in the intersections mostly referred to very similar biological functions, and thus, included an overlapping set of genes. Therefore, in order to avoid redundancy, multiply occurring genes were listed only once.

Table 2.11 List of genes and their respective fold changes extracted from the intersection of co-enriched KEGG terms between CITCO, rifampicin and WY-14643 treatment

Gene symbol	FC (CITCO)	FC (rifampicin)	FC (WY-14643)
ADH1A [efg]	-	0.56	0.75
ADH1B [efg]	--	0.39	0.68
ADH4 [efg]	-	0.65	------
ADH6 [efg]	1.78	0.79	-
CYP1A1 [eg]	1.32	1.39	1.32 1.68
CYP1A2 [efg]	1.72	-	--
CYP2A13 [ef]	1.71	1.55	1.70 1.20
CYP2A6 [ef]	1.83	1.56	1.16 1.42
CYP2A7 [ef]	2.00	1.56	1.77 2.39
CYP2B6 [efg]	1.67	2.21	1.16 0.79
CYP2C8 [efg]	1.28	2.59	1.10 1.04
CYP2C9 [efg]	0.86	1.74	1.52 0.92
CYP2E1 [fg]	1.59	0.67	-
CYP3A4 [efg]	-	4.09	1.12 1.06
CYP3A43 [efg]	1.17	1.84	
CYP3A5 [efg]	1.45	1.59	
CYP3A7 [efg]	0.88	2.38	
CYP4A11 [e]	-	0.62	
CYP4A22 [e]	1.15	-	
EPHX1 [g]	--	1.32	
FMO5 [f]	1.08	0.79	
GSTA2 [fg]	--	1.23	
MGST1 [fg]	-	1.05	
RDH16 [e]	1.12	0.80	
RDH5 [e]	1.10	0.81	
RETSAT [e]		0.91	
UGT1A1 [efg]		1.23	
UGT2B4 [efg]		1.12	

[e] gene included in KEGG pathway "Retinol metabolism"; [f] "Drug metabolism by cytochrome P450"; [g] "Metabolism of xenobiotics by cytochrome P450"

Table 2.11 shows the 28 genes and their corresponding fold changes, extracted from the three overlapping regulated KEGG pathways "Retinol metabolism"; "Drug metabolism by cytochrome P450"; "Metabolism of xenobiotics by cytochrome P450", which were differentially expressed by at least one of the three treatments. CITCO treatment altered the expression of 17 of these genes, whereas 15 were up- and two were downregulated. Upon rifampicin treatment, 16 genes were upregulated, whereas 10 were downregulated. WY-14643 treatment led to the up- and downregulation of 14 and four genes, respectively. A total of ten genes were regulated by all three treatments, of which nine were upregulated accordingly (*EPHX1*, *MGST1*, *CYP2B6*, *CYP2C8*, *CYP3A4*, *CYP3A5*, *CYP3A7*, *UGT1A1* and *UGT2B4*). One gene (*CYP4A11*) was downregulated by rifampicin and CITCO but upregulated by WY-14643 treatment. Five genes included in the co-enriched pathways were regulated only by rifampicin and CITCO (CYP2E1, CYP2A13, CYP2A6, CYP2A7 and CYP1A1). The genes GSTA2 and CYP3A43 were upregulated, and the genes RDH5, ADH1A, ADH1B and FMO5 were downregulated by rifampicin and WY-14643 treatment, accordingly. Additionally, RDH16 was down- and upregulated by rifampicin and by WY-14643 treatment, respectively.

Together these showed that CITCO, rifampicin and WY-14643 treatment affected highly overlapping sets of genes involved in drug and xenobiotic metabolism, whereas rifampicin treatment influenced the highest number of genes associated with these pathways.

Table 2.12 List of genes and their respective fold changes extracted from the intersection of co-enriched KEGG terms between CITCO and rifampicin treatment.

Gene symbol	FC (CITCO)	FC (rifampicin)
AKR1B10 [a]	1.29	1.92
CES2 [b]	-	0.93
CYP1A2 [a]	1.32	-
CYP2A13 [b]	1.72	1.55 1.56
CYP2A6 [b]	1.71	1.56 2.59
CYP2A7 [b]	1.83	1.74 0.67
CYP2C8 [a]	1.67	0.84 4.09
CYP2C9 [a]	1.28	1.84 1.59
CYP2E1 [a]	0.86	2.38 1.23
CYP2J2 [a]	-	1.12
CYP3A4 [ab]	1.59	
CYP3A43 [ab]	-	
CYP3A5 [ab]	1.17	
CYP3A7 [ab]	1.45	
UGT1A1 [b]	1.12	
UGT2B4 [b]	1.10	

[a] gene included in KEGG pathway "Linoleic acid metabolism"; [b] "Drug metabolism by cytochrome P450"

Table 2.12 shows the 16 genes and their corresponding fold change, which were included in the intersection of pathways ("Linoleic acid metabolism"; "Drug metabolism by cytochrome P450") exclusively enriched by CITCO and rifampicin treatment. Twelve genes were regulated by both CITCO and rifampicin treatment, of these genes eleven were up- and one gene was downregulated. In total, 13 genes were up- and three were downregulated by any of the two treatments. In this list, eleven CYPs were included, of which nine (*CYP2A13, 2A6, 2A7, 2C8, 2C9, 2E1, 3A4, 3A5 and 3A7*) were regulated by both treatments in the same direction. Also, three further genes retrieved from these pathways were co-regulated by both treatments (*AKR1B10, UGT1A1*, and *UGT2B4*), whereas one gene was exclusively regulated by CITCO treatment (*CYP1A2*) and three upon rifampicin treatment (*CYP2J2, CES2* and *CYP3A43*). This revealed that CAR and PXR coordinately regulated a common set of genes involved the metabolism of linoleic acid and drug metabolism.

Table 2.13 List of genes and their respective fold changes extracted from the intersection of co-enriched KEGG terms between rifampicin and WY-14643 treatment

Gene symbol	FC (rifampicin)	FC (WY-14643)
ACAA2 [c]	0.87	1.20
ACADM [cd]	0.94	1.37 1.15
ACADVL [c]	0.91	1.29
ACOX1 [cd]		-
ACOX2 [d]	0.77	1.51 1.24
ACSL1 [cd]	1.16	0.75 0.68
ACSL5 [cd]	1.12	--
ADH1A [c]	0.56	1.37 1.56
ADH1B [c]	0.39	1.68 1.33
ADH4 [c]	0.65	1.77 2.39
ADH6 [c]	0.79	--
ANGPTL4 [d]	--	1.90 2.27
CD36 [d]	0.80	-
CPT1A [cd]	0.83	1.27 1.41
CPT2 [cd]	0.62	2.81 1.18
CYP4A11 [cd]	-	1.29
CYP4A22 [cd]	0.32	-
CYP7A1 [d]	0.81	1.14 1.07
CYP8B1 [d]	--	
FABP1 [d]	1.09	
FABP4 [d]	-	
FADS2 [d]	0.90	
HADHA [c]	0.54	
HADHB [c]	1.26	
HMGCS2 [d]	-	
ME1 [d]	0.85	
PLIN1 [d]	1.18	
RXRA [d]	-	
SLC27A2 [d]		
SLC27A4 [d]		

[c] gene included in KEGG pathway "Fatty acid metabolism"; [d] "PPAR signaling pathway"

Table 2.13 shows the 30 genes included in the intersection of pathways only enriched by rifampicin and WY-14643 treatment and their corresponding fold changes. Upon rifampicin treatment, five and 16 of the genes were down- and upregulated, respectively. 21 and two of the genes were up- and downregulated, respectively, upon WY-14643 treatment. 14 of the genes were regulated by both treatments, whereas eight genes (*ACAA2*, *ACADVL*, *HADHB*, *HMGCS2*, *ACADM*, *CPT1A*, *CPT2* and *CYP4A11*) were differentially regulated by rifampicin (down) and

WY-14643 treatment (up). *ADH1A* and *ADH1B* were upregulated and *ME1*, *SLC27A2*, *ACSL1* and *ACSL5* were downregulated by both treatments. The genes *ANGPTL4*, *CD36*, *FABP1*, *FABP4, PLIN1*, *SLC27A4* and *CYP4A22*, included in these pathways, were exclusively regulated upon WY-14643 treatment and the genes *CYP7A1*, *CYP8B1*, *FADS2* and *RXRA* exclusively upon rifampicin treatment. Taken together, the genes differentially expressed upon rifampicin and WY-14643 treatment included in these two pathways only partially overlapped, whereas most of the genes affected by both treatments were regulated in opposed directions.

2.2   Expression changes following knock-down and ligand-dependent activation of CAR, PXR and PPARα of selected genes involved drug metabolism and energy homeostasis

To further determine the impact of the nuclear receptors CAR, PXR and PPARα on the regulation of gene expression, knock-down experiments were performed using specific siRNAs, targeting the three nuclear receptors. The experiments were performed in hepatocytes from two of the donors also utilized for the genome-wide expression analysis. The mRNA expression of selected genes, involved in drug metabolism (*CYP2B6*, *CYP2C8*, *CYP3A4*, *ADH1A*, *CYP7A1* and *UGT1A1*) and maintenance of energy homeostasis (*CPT1A*, *HMGCS2* and *PDK4*), were analyzed to investigate reduced expression of the three NRs (knock-down) compared to their agonist-dependent activation (Figure 2.7, Figure 2.8 and Figure 2.9). The selection of these genes was based on their significant response to at least one of the NR agonists, identified in the genome-wide expression analyses (2.1.1).
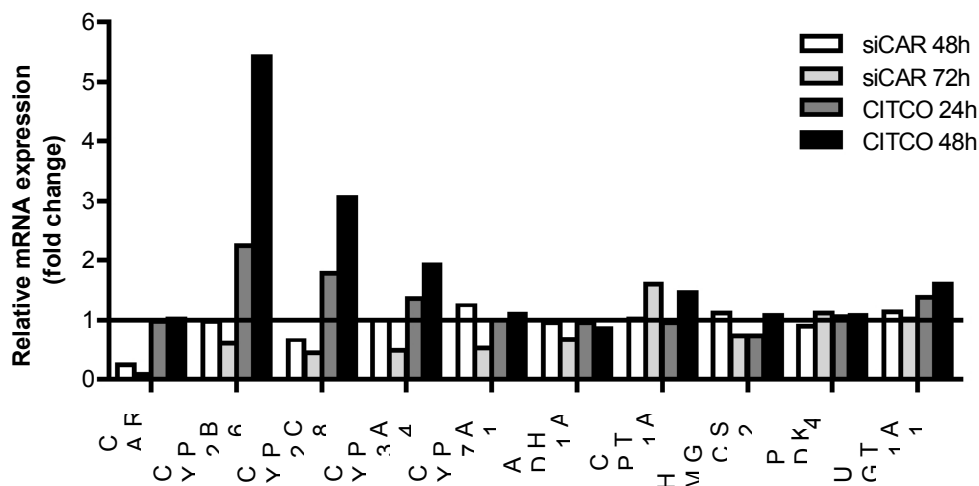
Figure 2.7 Relative mRNA expression of selected genes following 48 h and 72 h siRNA (siCAR) mediated knock-down and 24 h and 48 h activation of CAR by CITCO (1 µM) in primary human hepatocytes. The mRNA expression was normalized to GAPDH and compared to control treatment (knock-down = siControl; chemical treatment = DMSO). Shown is the mean of two independent experiments.

As shown in Figure 2.7, treatment of hepatocytes with a CAR specific siRNA (siCAR) led to a continuous reduction of *NR1I3* (CAR) mRNA expression of up to 89% at 72 h. CAR knock-down also decreased expression of *CYP2B6*, *CYP2C8* and *CYP3A4* up to 33%, 50% and 54% at 72 h, respectively. On the other hand, CITCO increased the expression of *CYP2B6*, *CYP2C8*, *CYP3A4* and *UGT1A1* up to 5.4-fold, 3-fold, 1.9-fold and 1.6-fold after 48 h of treatment, respectively. A more inconsistent pattern was detected for *CYP7A1*, where the expression was increased after 48 h (1.3-fold) and decreased after 72 h (47%) in siCAR treated cells. CITCO treatment hardly altered *CYP7A1* expression at any time point. *ADH1A* expression was decreased after 72 h of siCAR treatment (31%). *CPT1A* expression was increased after 72 h of CAR knock-down and 48 h of CITCO treatment, respectively. *HMGCS2* expression was reduced by 25% upon 72 h CAR knock-down but also after 24 h of CITCO treatment. For the other genes, only minor changes (<25%) were observed.
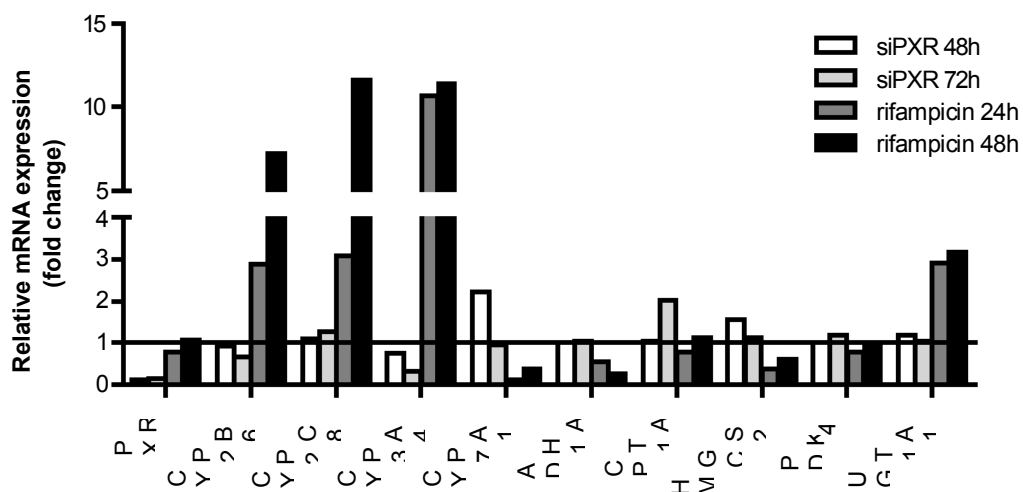
Figure 2.8 Relative mRNA expression of selected genes following 48 h and 72 h siRNA (siPXR) mediated knock-down and 24 h and 48 h activation of PXR by rifampicin (10 µM) in primary human hepatocytes. The mRNA expression was normalized to GAPDH and compared to control treatment (knock-down = siControl; chemical treatment = DMSO). Shown is the mean of two independent experiments.

Figure 2.8 shows that *NR1I2* (PXR) expression was knocked down up to 88% (48 h) by treatment with siPXR. Expression of *CYP2B6* and *CYP3A4* was reduced by 34% and 68% after 72 h treatment with siPXR, respectively. On the other hand, rifampicin treatment continuously increased *CYP2B6* and *CYP3A4* but also *CYP2C8* and *UGT1A1* expression up to 7.2-fold, 11.6-fold, 11.4-fold and 3.2-fold after 48 h, respectively. Treatment with siPXR increased expression of *CYP7A1* (2.2-fold at 48 h), *CPT1A* (2-fold at 72 h) and *HMGCS2* (1.6-fold at 48 h). However, *CYP7A1* and *HMGCS2*, as well as *ADH1A* expression was decreased upon rifampicin treatment up to 88% (24 h), 63% (24 h) and 73% (48 h), respectively.
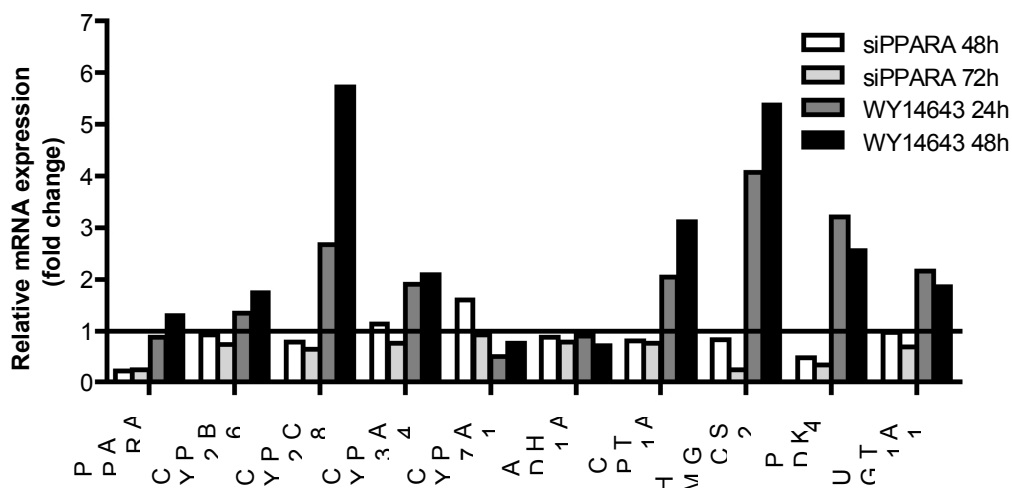
Figure 2.9 Relative mRNA expression of selected genes following 48 h and 72 h siRNA (siPPARA) mediated knock-down and 24 h and 48 h activation of PPARα by WY-14643 (50 µM) in primary human hepatocytes. The mRNA expression was normalized to GAPDH and compared to control treatment (knock-down = siControl; chemical treatment = DMSO). Shown is the mean of two independent experiments.

Treatment of hepatocytes with a specific siRNA targeting PPARα (siPPARA) led to a reduction of *PPARA* (PPARα) expression of 75%. PPARα knock-down furthermore decreased the expression of *CYP2B6*, *CYP2C8*, *HMGCS2*, *PCK1*, *PDK4* and *UGT1A1* by 26%, 35%, 76%, 39%, 66% and 30% at 72 h, respectively. *CYP3A4* expression was also decreased upon *PPARA* knock-down by about 23% at 72 h. Treatment with WY-14643 increased the expression of *CYP2B6*, *CYP2C8*, *CYP3A4*, *HMGCS2*, *PDK4*, *UGT1A1* and also *CPT1A* up to 1.7-fold, 5.7-fold, 2.1-fold, 5.4-fold, 3.2-fold, 2.2-fold and 3.1-fold after either 24 h or 48 h, respectively. *CYP7A1* showed a 1.6-fold increased expression after *PPARA* knock-down (48 h) and a 49% decreased expression after WY-14643 treatment (24h).

2.3 Modulation of PXR and CAR transactivation capacity by PKA dependent phosphorylation

The transactivation capacity of PXR for the human *CYP3A4* was previously shown to be decreased in the presence of the PKA activator 8-bromo cAMP, whereas mouse *CYP3a11* expression was increased (Lichti-Kaiser et al., 2009a). Whether the expression of other human PXR target genes is affected by PKA activation and in which direction was not investigated so far. Moreover, CAR, which also regulates expression of *CYP3A4* and other important drug metabolizing enzymes and transporters, has been shown to undergo post-translational modification by protein kinases, whereas an impact of PKA dependent phosphorylation on its transactivation capacity was not reported so far. To determine the influence of PKA activation on the transactivation capacity of CAR and PXR, the activities of the *CYP3A4* and *CYP2B6* promoters in response to the PKA activator 8-bromo cAMP were assessed in HepG2 cells, using luciferase reporter gene assays. Furthermore, the impact of PKA activation on DMET gene expression was assessed in 8-bromo cAMP-treated primary human hepatocytes in the presence or absence of CAR and PXR agonists, using qRT-PCR (Fluidigm).

2.3.1 PKA-dependent changes in CYP3A4 and CYP2B6 promoter activity

HepG2 cells co-transfected with hCAR or hPXR expression plasmids and luciferase reporter gene promoter constructs of *CYP3A4* and *CYP2B6* were treated with the PXR agonist rifampicin (10 µM) or the CAR agonists CITCO (1 µM) in combination with or without the PKA activator, 8-Bromo-cAMP (1 mM), as described in 5.1.2. Changes in the promoter activities were determined (5.3) at 48 h after transfection by measuring the relative luciferase activity (Figure 2.10, Figure 2.11, Figure 2.12 and Figure 2.13).
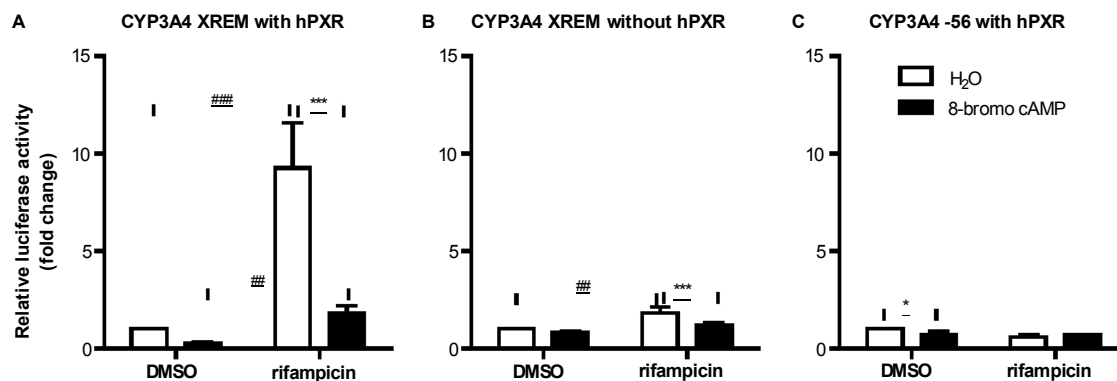
Figure 2.10 PXR dependent effect of 8-Bromo cAMP on CYP3A4 promoter. HepG2 cells were co-transfected with CYP3A4 XREM construct (pGL3-CYP3A4(-7830/Δ7208-364)) (A) or CYP3A4 -56 construct (pGL3-CYP3A4(-56)) (C), pRL-CMV and pcDhPXR (A and C) or pcDNA3 (B). Six h post transfection, cells were treated with the rifampicin (10 µM) or 8-bromo cAMP (1 mM) or both. Firefly and renilla luciferase activity was determined 48 h after transfection. Firefly luciferase values were normalized to renilla luciferase and shown as fold change over control treatment (DMSO). Data represent means ± SD of 5 (A and C) or 3 (B) independent experiments. Significant differences upon rifampicin treatment are indicated by [#], p < 0.05; [##]; p < 0.01 or , p < 0.001 and upon 8-bromo cAMP treatment by *, p < 0.05; **; p < 0.01 or ***, p < 0.001.

As shown in Figure 2.10A, rifampicin treatment significantly increased the activity of the *CYP3A4* XREM promoter in the absence (9.3-fold) and presence of 8-bromo cAMP (6.7-fold). Treatment with 8-bromo cAMP significantly reduced the activity of the induced state (rifampicin treatment) more than 80%. In the absence of co-transfected hPXR, rifampicin treatment also led to a significant increase in promoter activity (1.8-fold) but to a weaker extent. This increase was significantly reduced by 8-bromo cAMP (Figure 2.10B). Using the *CYP3A4* -56 promoter, a significant reduction of the basal promoter activity by 8-bromo cAMP was observed (Figure 2.10C).
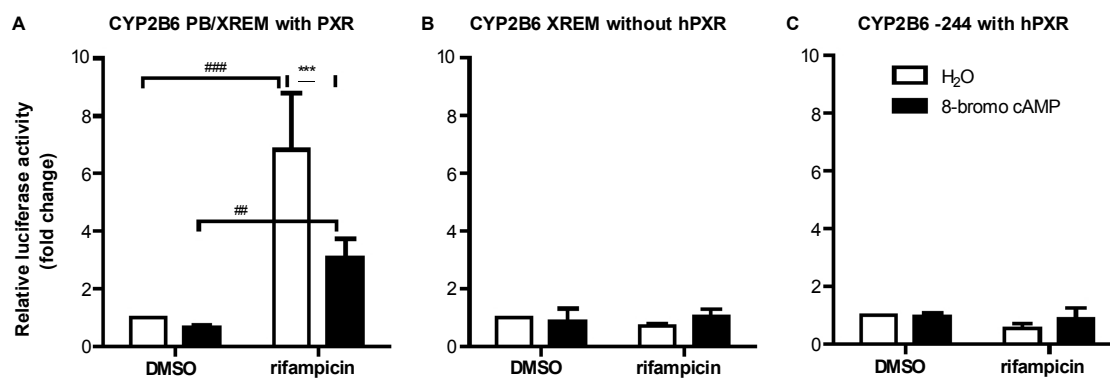
Figure 2.11 PXR dependent effect of 8-Bromo cAMP on CYP2B6 promoter. HepG2 cells were co-transfected with CYP2B6 PB/XREM construct (pB-1.6k/PB/XREM)) (A) or CYP2B6 -244 construct (pGL3-CYP2B6(-244)) (C), pRL-CMV and pcDhPXR (A and C) or pcDNA3 (B). Six h post transfection, cells were treated with the rifampicin (10 µM) or 8-bromo cAMP (1 mM) or both. Firefly and renilla luciferase activity was determined 48 h after transfection. Firefly luciferase values were normalized to renilla luciferase and shown as fold change over control treatment (DMSO). Data represent means ± SD of 5 (A and C) or 3 (B) independent experiments. Significant differences upon rifampicin treatment are indicated by #, p < 0.05; ##, p < 0.01 or ###, p < 0.001 and upon 8-bromo cAMP treatment by *, p < 0.05; **; p < 0.01 or ***, p < 0.001.

Figure 2.11A shows that rifampicin treatment significantly induced the activity of the *CYP2B6*-promoter fragment in the presence (6.8 fold) as well the absence of 8-bromo cAMP (4.5-fold). The promoter activity following rifampicin treatment was significantly decreased by more than 50% in the case of 8-bromo cAMP co-treatment. In the absence of co-transfected hPXR (Figure 2.11B) or using the *CYP2B6* -244 promoter construct (Figure 2.11C), no changes in promoter activity by any of the treatments was observed.
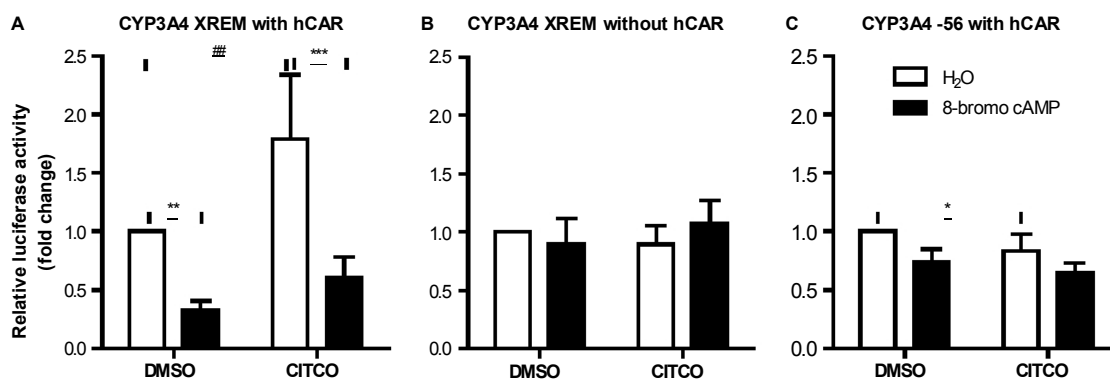
Figure 2.12 CAR dependent effect of 8-Bromo cAMP on the CYP3A4 promoter. HepG2 cells were co-transfected with CYP3A4 XREM construct (pGL3-CYP3A4(-7830/Δ7208-364)) (A) or CYP3A4 -56 construct (pGL3-CYP3A4(-56)) (C), pRL-CMV and pcDhCAR1 (A and C) or pcDNA3 (B). Six h post transfection, cells were treated with the CITCO (1 µM) or 8-bromo cAMP (1 mM) or both. Firefly and renilla luciferase activity was determined 48 h after transfection. Firefly luciferase values were normalized to renilla luciferase and shown as fold change over control treatment (DMSO). Data represent means ± SD of 5 (A and C) or 3 #(B) independent experiments. Significant differences upon CITCO treatment are indicated by #, p < 0.05; ##; p < 0.01 or ###, p < 0.001 and upon 8-bromo cAMP treatment by *, p < 0.05; **; p < 0.01 or ***, p < 0.001.

The activity of the *CYP3A4* promoter fragment showed a significant activation of 1.8-fold upon CITCO treatment (Figure 2.12A). This activation state following CITCO treatment was significantly decreased more than 65% by co-treatment with 8-bromo cAMP. Moreover, the basal activity of the promoter fragment was significantly repressed by about 65% in the presence of 8-bromo cAMP. In the absence of co-transfected hCAR, none of the treatments had an effect on the *CYP3A4* XREM promoter construct (Figure 2.12B), except for a slight but significant reduction of the *CYP3A4* -56 promoter activity observed by rifampicin in the absence of 8-bromo cAMP (Figure 2.12C).
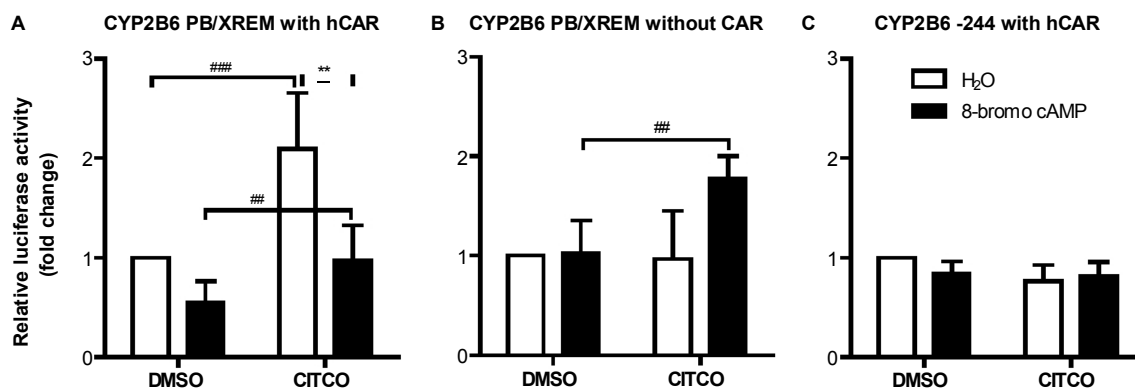
Figure 2.13 CAR dependent effect of 8-Bromo cAMP on the CYP2B6 promoter. HepG2 cells were co-transfected with CYP2B6 PB/XREM construct (pB-1.6k/PB/XREM)) (A) or CYP2B6 -244 construct (pGL3-CYP2B6(-244)) (C), pRL-CMV and pcDhPXR (A and C) or pcDNA3 (B). Six h post transfection, cells were treated with the CITCO (1 µM) or 8-bromo cAMP (1 mM) or both. Firefly and renilla luciferase activity was determined 48 h after transfection. Firefly luciferase values were normalized to renilla luciferase and shown as fold change over control treatment (DMSO). Data represent means ± SD of 5 (A and C) or 3 (B) independent experiments. Significant differences upon CITCO treatment are indicated by #, $p < 0.05$; ##; $p < 0.01$ or ###, $p < 0.001$ and upon 8-bromo cAMP treatment by *, $p < 0.05$; **; $p < 0.01$ or ***, $p < 0.001$.

As shown in Figure 2.13B, CITCO treatment led to a significant activation of the *CYP2B6* promoter fragment in the presence and absence of 8-bromo cAMP by 1.8-fold and 2.1-fold, respectively. Furthermore, co-treatment with 8-bromo cAMP significantly decreased the activation state of the *CYP2B6* promoter fragment following CITCO treatment more than 50%. Without co-transfected hCAR, a significant 1.8-fold increase in promoter activity upon 8-bromo cAMP treatment in the presence of CITCO was observed (Figure 2.13B). Using the *CYP2B6* -244 promoter construct, no changes in promoter activity were visible (Figure 2.13C).

2.3.2 Changes in DMET gene expression and CYP activity in primary human hepatocytes following 8-bromo cAMP-dependent PKA activation

To investigate the effect of PKA on the expression of DMET genes, primary human hepatocytes were treated with the agonist for CAR (CITCO; 1 µM) and PXR (rifampicin; 10 µM) together with or without the PKA activator 8-bromo cAMP (1 mM) for 24 h (5.1.4). The relative mRNA expression of the DMET genes *ABCB1*, *CYP1A2*, *CYP2B6*, *CYP2C8*, *CYP3A4* and *UGT1A1*, the expression of the CREB target gene *PCK1,* a marker for PKA activation, and the expression of the NRs CAR and PXR,

were determined using qRT-PCR (Fluidigm) as described in 5.4.3.2 (Figure 2.14 and Figure 2.15).
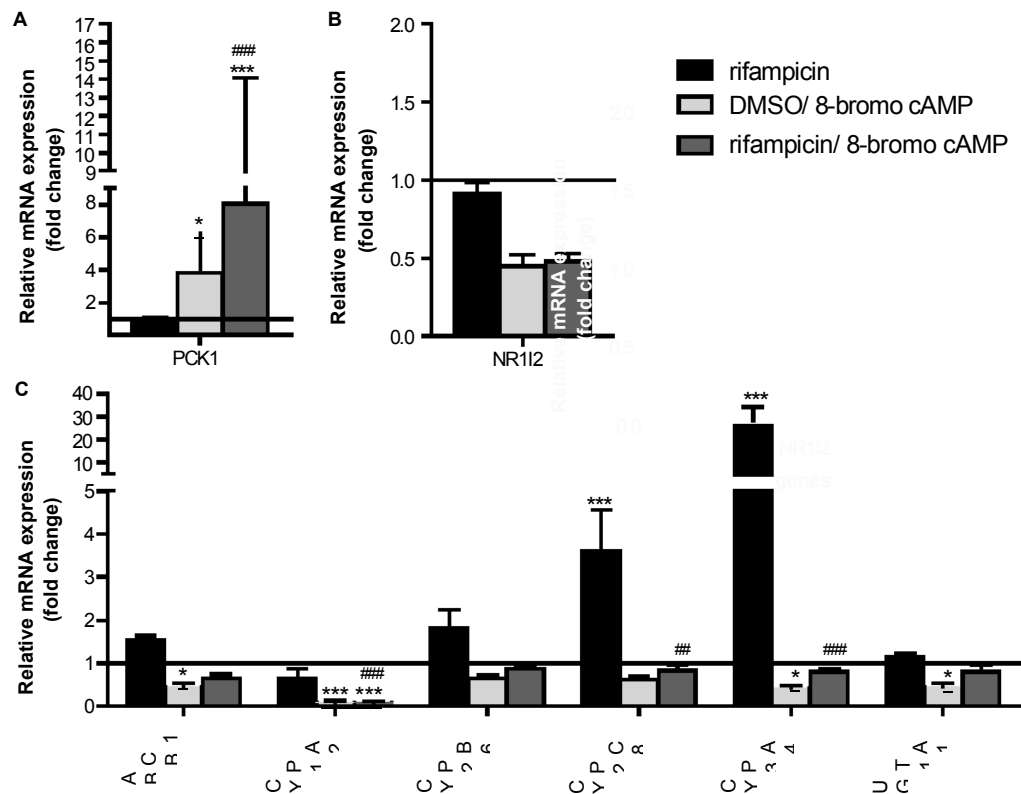
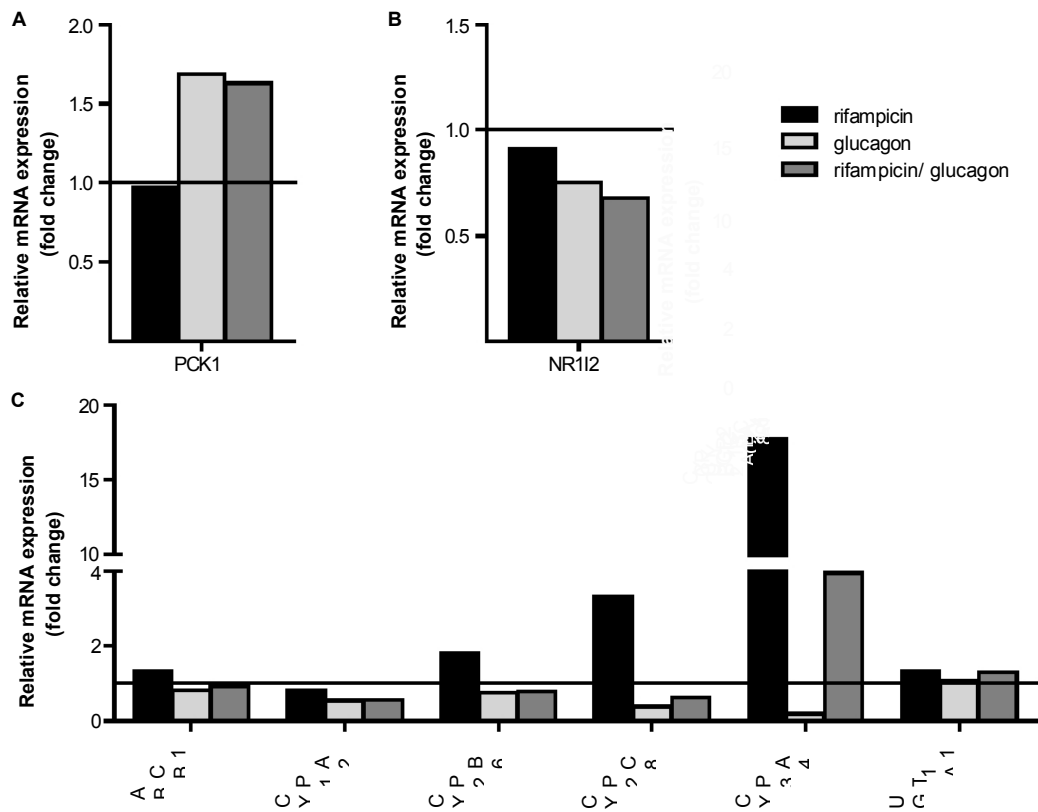Figure 2.14 Effect of 8-bromo cAMP dependent PKA activation on DMET gene expression in the absence or presence of rifampicin in hepatocytes. Primary human hepatocytes were treated with 8-bromo cAMP treatment (1 mM) in the presence or absence of rifampicin (10 µM). 24 h after treatment relative mRNA expression was determined using qRT-PCR. The mRNA expression was normalized to GAPDH and compared to control treatment (DMSO). Shown is the mean ± SD of three independent experiments. Significant differences compared to control treatment DMSO are indicated by *,## < 0.05; **; p#< 0.01 or ***, p < p 0.001 and compared to rifampicin treatment by , p < 0.05; ; p < 0.01 or##, p < 0.001. #

Treatment with 8-bromo cAMP significantly increased the expression of *PCK1* 3.8-fold and co-treatment with rifampicin further increased the expression up to 8.1-fold, compared to DMSO treatment (Figure 2.14A). *NR1I2* (PXR) expression was decreased by about 55% by 8-bromo cAMP with and without rifampicin co-treatment, however, the decrease was not significant (Figure 2.14B). Rifampicin treatment increased the expression of *ABCB1* (1.5-fold), *CYP2B6* (1.8-fold), *CYP2C8* (3.6-fold),

CYP3A4 (26.1-fold) and *CYP3A5* (2.4-fold), which reached significance only in the case of *CYP2C8* and *CYP3A4*. Co-treatment with 8-bromo cAMP abolished the increase in expression of the above mentioned genes, whereas only in the case of *CYP2C8* and *CYP3A4,* this reduction of rifampicin-induced expression by 8-bromo cAMP reached significance. On the other hand, 8-bromo cAMP treatment significantly decreased expression of *ABCB1* (54%) and *CYP3A4* (57%) but also of *CYP1A2* (91%) and *UGT1A1* (54%), compared to control. Moreover, expression of *CYP2B6* (34%) and *CYP2C8* (38%) was also decreased by 8-bromo cAMP, but these changes remained insignificant.
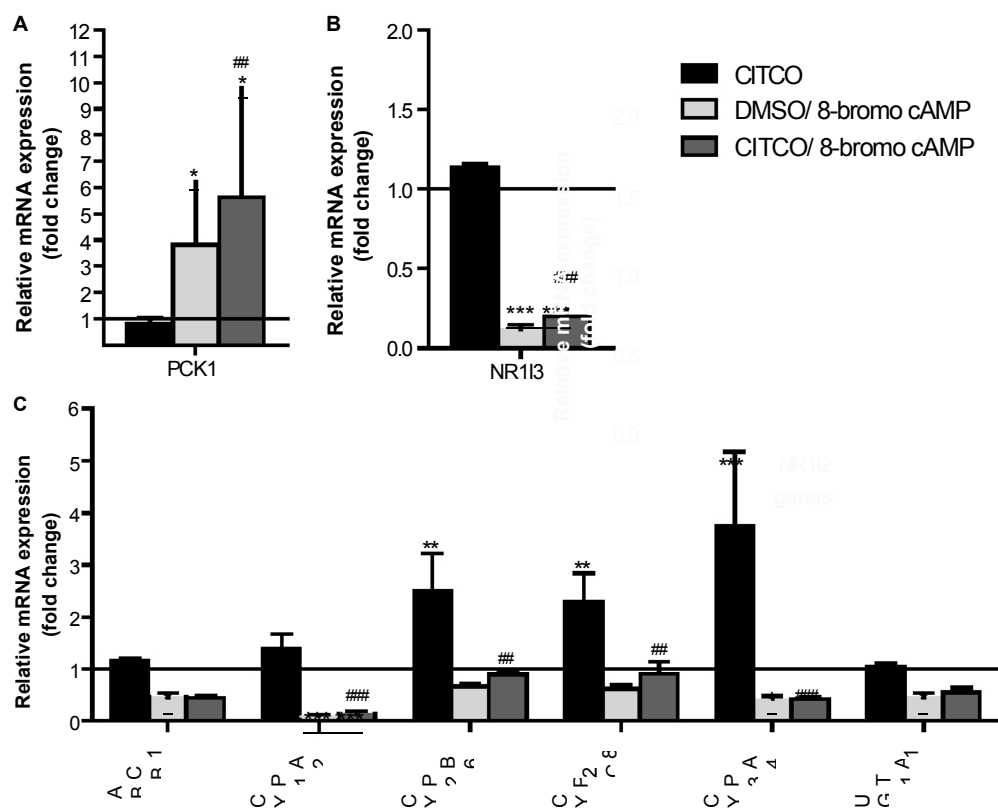
Figure 2.15 Effect of 8-bromo cAMP dependent PKA activation on DMET gene expression in the absence or presence of CITCO in hepatocytes. Primary human hepatocytes were treated with 8-bromo cAMP treatment (1 mM) in the presence or absence of CITCO (1 µM). 24 h after treatment relative mRNA expression was determined using qRT-PCR. The mRNA expression was normalized to GAPDH and compared to control treatment (DMSO). Shown is the mean ± SD of three independent experiments. Significant differences compared to

control treatment DMSO are indicated by *,##p < 0.05; **;### < 0.01 or ***, p < 0.001 and p compared to CITCO treatment by#, p < 0.05; ; p < 0.01 or , p < 0.001.Shown is the mean ± SD of three independent experiments.

As shown in Figure 2.15A, combined treatment of CITCO and 8-bromo cAMP further significantly increased expression of *PCK1* from 3.8-fold (8-bromo cAMP alone) to 5.6-fold. Expression of *NR1I3* (CAR) was significantly decreased by 8-bromo cAMP treatment in the absence (88%) and presence (80%) of CITCO (Figure 2.15B). CITCO treatment led to significantly increased expression of *CYP2B6* (2.5-fold), *CYP2C8* (2.3-fold) and *CYP3A4* (3.8-fold). Furthermore, *CYP1A2* expression was increased 1.4-fold, but this induction remained insignificant. The CITCO-induced expression of *CYP1A2*, *CYP2B6*, *CYP2C8* and *CYP3A4* was significantly decreased by co-treatment with 8-bromo cAMP. Moreover, expression of *ABCB1* and *UGT1A1* was decreased more than 50% by 8-bromo cAMP treatment with or without CITCO co-treatment (Figure 2.15C), which reached significance only in the case of *UGT1A1* in response to 8-bromo cAMP treatment alone. Activation of PKA by 8-bromo cAMP was shown to decrease rifampicin and CITCO induced expression of *CYP2B6*, *2C8* and *3A4* as well as the basal expression of *CYP2B6*, *2C8*, *3A4* and *CYP1A2* (Figure 2.14 and Figure 2.15). To investigate whether this translated to decreased activity of these CYPs, the metabolite formation rates of the CYPs 1A2, 2B6, 2C8 and 3A4 were determined in primary human hepatocytes from one donor treated with DMSO, rifampicin or CITCO alone or in combination with 8-bromo cAMP for 72 h (Figure 2.16). As shown in Figure 2.16A, neither rifampicin nor CITCO increased activity of CYP1A2 in this experiment, whereas 8-bromo cAMP reduced CYP1A2 activity by 70% or more, in the presence or absence of the agonists. CYP2B6 activity was increased 6.3-fold and 3-fold upon rifampicin and CITCO treatment, respectively. Co-treatment with 8-bromo cAMP was shown to decrease rifampicin- and CITCO-induced and also basal (DMSO) activity of CYP2B6 by 88%, 92% and 75%, respectively (Figure 2.16B). Rifampicin treatment increased CYP2C8 activity by 3.4-fold, whereas CITCO treatment failed to induce activity of CYP2C8 and rather led to a decreased activity. In the presence of 8-bromo cAMP, rifampicin-mediated as well as basal activity (DMSO) of CYP2C8 was decreased 70% and 32%, respectively (Figure 2.16C). As shown in Figure 2.16D, CYP3A4 showed a 6-fold increased activity in the presence of rifampicin, whereas CITCO did not alter CYP3A4 activity in this experiment. Rifampicin-induced as well as basal CYP3A4 activity was reduced by 8-bromo cAMP co-treatment by 83% and 50%, respectively.
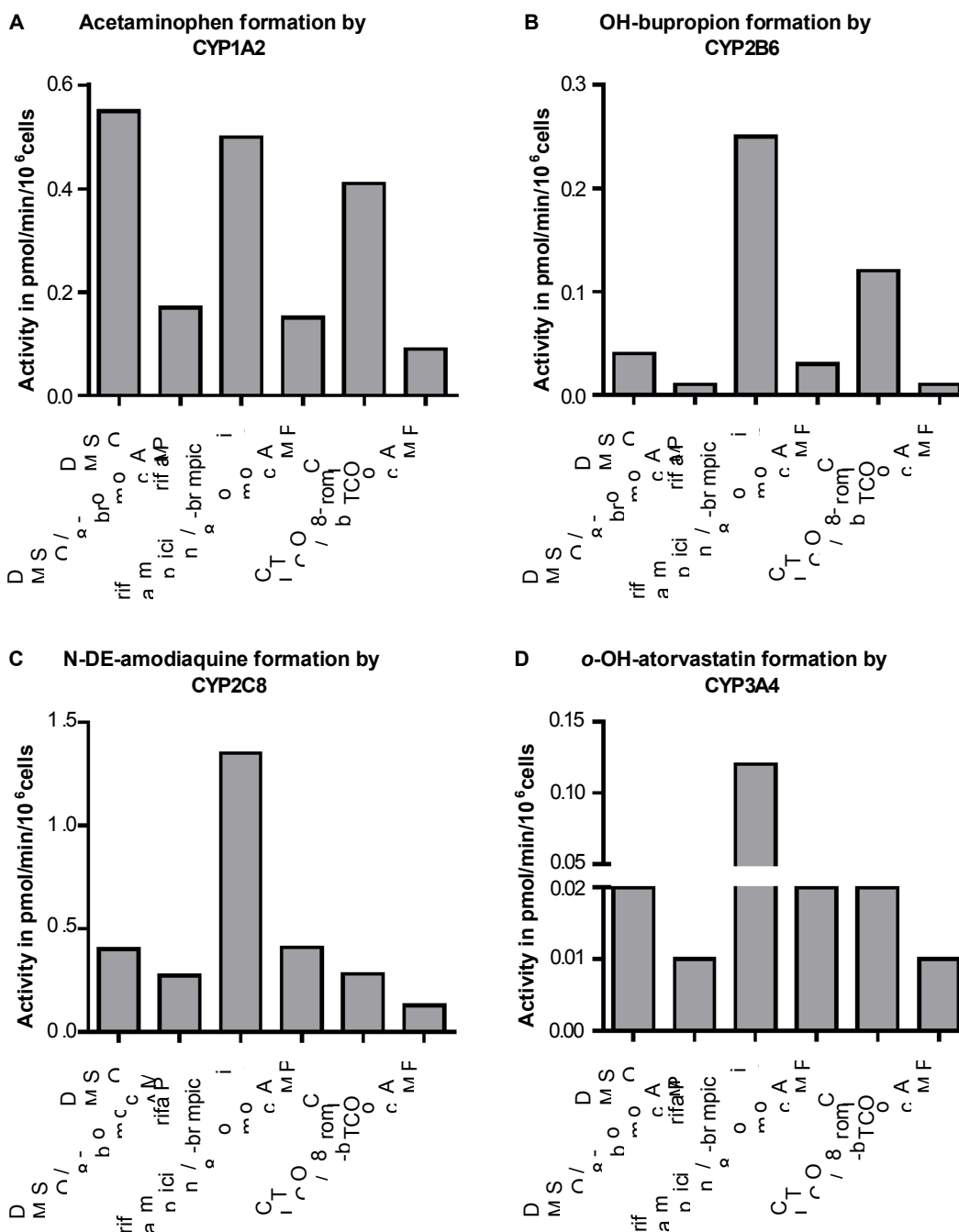
Figure 2.16 Activities of CYP isoenzymes in PHHs, as determined by the formation rate of (A) acetaminophen (CYP1A2), (B) OH-bupropion (CYP2B6), (C) N-DE-amodiaquine (CYP2C8), (D) *o*-OH-atorvastatin (CYP3A4). Graphs show the formation rate of the respective metabolite in hepatocytes from one donor treated for 72 h with DMSO, rifampicin or CITCO alone or in combination with 8-bromo cAMP.

2.3.3 Changes in DMET gene expression in primary human hepatocytes following glucagon treatment

To evaluate whether an endogenous signal, which activates PKA, exerts a similar response concerning the expression of DMET genes, primary human hepatocytes were treated with the fasting hormone glucagon, a known activator of PKA, in the presence or absence of the PXR agonist rifampicin. After 24 h cells were lysed and mRNA expression was quantified by qRT-PCR (Figure 2.17).

Figure 2.17 Effect of glucagon on DMET gene expression in the absence or presence of rifampicin in hepatocytes. Primary human hepatocytes were treated with 8-bromo cAMP treatment (1 mM) in the presence or absence of glucagon (5mg/l). 24 h after treatment relative mRNA expression was determined using qRT-PCR. The mRNA expression was normalized to GAPDH and compared to control treatment (DMSO). Shown is a single experiment.

As shown in Figure 2.17A, glucagon treatment increased *PCK1* expression 1.7-fold and co-treatment with rifampicin revealed comparable values. *NR1I2* expression was reduced by glucagon by 25% in the absence of rifampicin co-treatment and by 32% in the presence of rifampicin treatment (Figure 2.17). In this experiment, rifampicin increased expression of *ABCB1* (1.3-fold), *CYP2B6* (1.8-fold), *CYP2C8* (3.3-fold), *CYP3A4* (17.8-fold) and *UGT1A1* (1.3-fold). In the case of *ABCB1* and *CYP2B6,* the increase in expression by rifampicin treatment was diminished by glucagon co-treatment. In the case of *CYP2C8,* co-treatment with glucagon resulted in an expression, which was 38% lower compared to control treatment (DMSO). *CYP3A4* expression in the case of rifampicin and glucagon co-treatment was almost 4.5-fold lower compared to rifampicin treatment alone, but still 4-fold higher than compared to the control. Glucagon treatment alone decreased expression of *CYP1A2* (46%), *CYP2C8* (62%) and *CYP3A4* (80%). All other changes were less than 25% (Figure 2.17).

2.4   Impact of hyperforin-related phloroglucinol derivatives on the expression of DMET genes

As shown by the results presented in chapter 2.1, activation of PXR by drugs like rifampicin alters the expression of a battery of DMET genes. Drug induced and PXR mediated changes in DMET gene expression have been shown to alter drug metabolism in the liver, and therefore, co-administration of such PXR activators with other drugs implies the risk of drug-drug interactions (DDIs), which is a major issue in drug therapy (Kliewer et al., 2002). Numerous of such PXR associated DDIs have also been reported for the herbal drug St. John's wort (SJW), which is frequently used to treat depression (Chatterjee et al., 1998; Madabushi et al., 2006; Müller, 2003). These DDIs are mainly caused by hyperforin, the most active constituent of SJW (Mai et al., 2004; Singer et al., 1999), and which was also shown to be a strong PXR agonist and to induce expression of, e.g., *CYP3A4* and *CYP2C9* (Chen et al., 2004; Moore et al., 2000a).

In order to develop compounds that show the same beneficial pharmacological effect of hyperforin but lack its PXR activation potential, the Dr. Willmar Schwabe GmbH designed and synthesized molecules based on the phloroglucinol core structure of

hyperforin in a drug development project. Recently, a set of nine of the simple 2-acylphloroglucinol and 2,4-acylphloroglucinol derivatives (Figure 2.18), were evaluated for their bio-activation properties (Leuner et al., 2010). Leuner and colleagues showed that five of these molecules inhibit serotonin re-uptake comparable to hyperforin *in vitro* in a TRPC6-mediated and Ca^{2+} flux-dependent manner. This part of the thesis aimed to investigate the second imposed requirement of these nine phloroglucinols, their inability to activate PXR and to affect DMET gene expression.
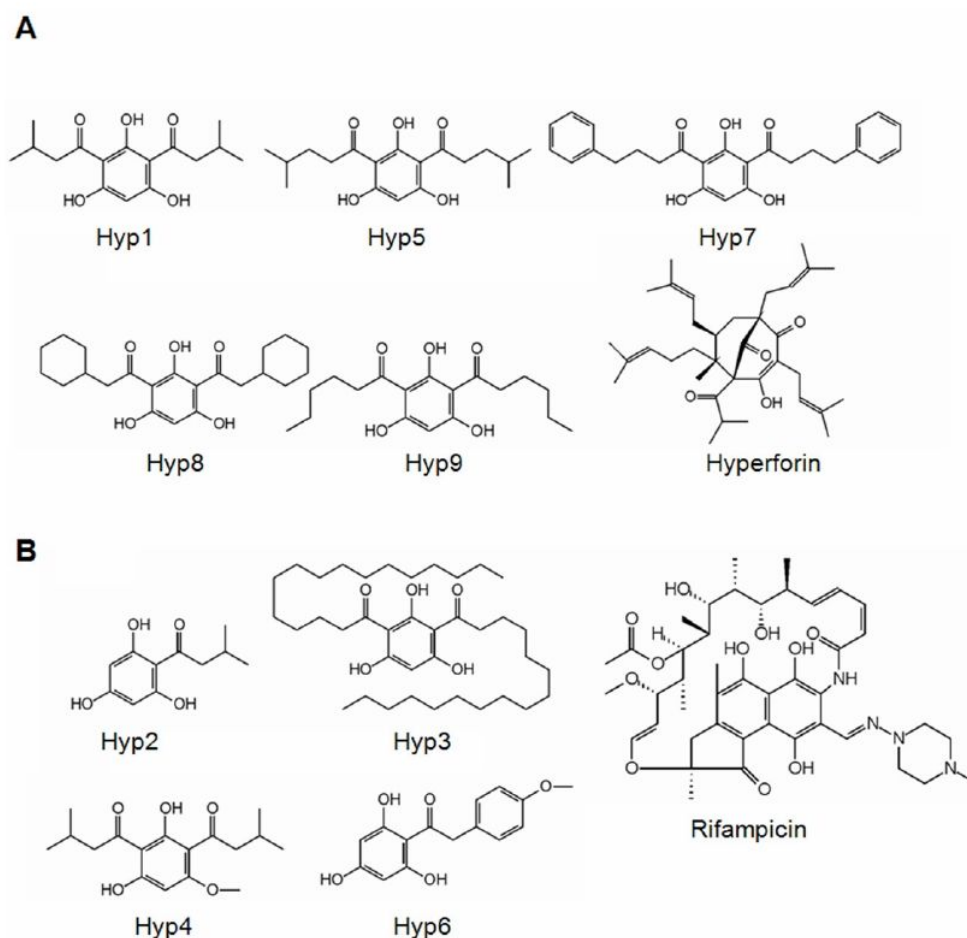
Figure 2.18 Structures of hyperforin and theTRPC6-activating phloroglucinol derivatives Hyp1, Hyp5, and Hyp7-9 (A) and of rifampicin and the TRPC6-nonactivating phloroglucinol derivatives Hyp2-4 and Hyp6 (B).

2.4.1 Effects of the phloroglucinol derivatives on PXR-mediated *CYP3A4* promoter activity

To investigate the potential of phloroglucinol derivatives (Figure 2.18) to activate PXR, HepG2 cells were co-transfected with a *CYP3A4* XREM promoter-based luciferase reporter system and hPXR cDNA expression plasmid and treated with the substances (Hyp1-9) or with hyperforin or rifampicin as a positive control and EC_{50} values were determined in a range from 0.001 µM up to 50 µM (Figure 2.19). It should be noted that TRPC6-activating phloroglucinols including hyperforin showed cytotoxic effects above 5 µM, as previously reported for hyperforin treatment of human hepatocytes and CV-1 cells (Komoroski et al., 2004; Moore et al., 2000a).
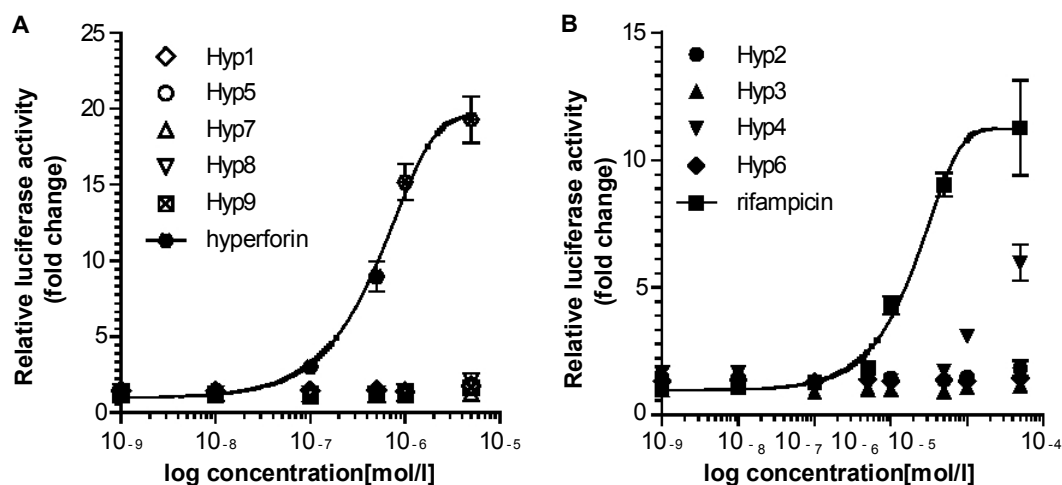
Figure 2.19 EC_{50} determination of phloroglucinol derivatives, hyperforin, and rifampicin. HepG2 cells were co-transfected with pGL3-CYP3A4(-7830/Δ7208-364), pGL3-CMV-Renilla and pcDhPXR. Six h post transfection, the cells were treated with the TRPC6 activating phloroglucinol derivatives or hyperforin (A), or with TRPC6 non-activating phloroglucinol derivatives or rifampicin (B) in a concentration range from 0.001 µM to 50 µM. Firefly and renilla luciferase activity was determined 48 h after transfection. Firefly luciferase values were normalized to renilla luciferase and shown as fold change over control treatment (DMSO or ethanol). Data represent means ± SD of three independent experiments. EC_{50} curves are only shown for compounds where unambiguous nonlinear fitting was achieved.

Hyperforin (Figure 2.19A) and rifampicin (Figure 2.19B) showed dose-dependent activation of the promoter with maximal induction of 19.8-fold and 11.7-fold, respectively. Surprisingly, only the TRPC6 non-activating compound Hyp4 showed a

dose-dependent activation of the promoter with the highest induction of 5.8-fold observed at 50 µM (Figure 2.19B). Non-linear curve fitting revealed EC_{50} values of 0.59 µM and 1.9 µM for hyperforin and rifampicin, respectively. All other phloroglucinol derivatives did not activate the promoter in a dose-dependent manner (Figure 2.19).

2.4.2 Impact of PXR on Hyp4- and hyperforin-mediated *CYP3A4* promoter activation

In order to evaluate whether the activation of the *CYP3A4* promoter by hyperforin, Hyp4 or rifampicin was PXR-dependent, HepG2 cells co-transfected with the *CYP3A4* XREM promoter constructs and pcDhPXR or pcDNA3 (empty vector) were treated with hyperforin (1 µM), rifampicin (10 µM), Hyp4 (50 µM9 or DMSO).
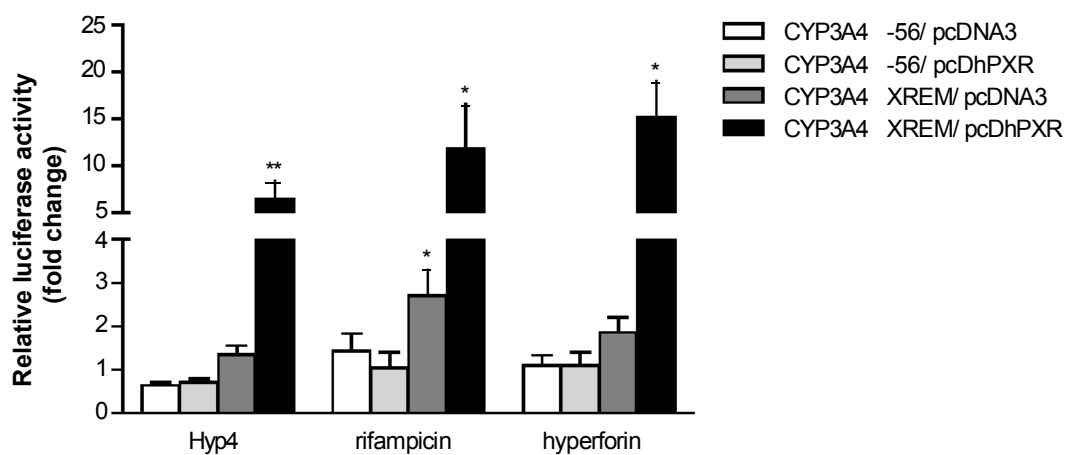
Figure 2.20 Impact of PXR expression on CYP3A4 promoter activation. HepG2 cells were co-transfected with CYP3A4 XREM (pGL3-CYP3A4(-7830/Δ7208-364)) or CYP3A4 -56 (pGL3-CYP3A4(-56) (-XREM)), pRL-CMV and pcDhPXR or pcDNA3 and treated with Hyp4 (50 µM), hyperforin (1 µM), rifampicin (10 µM) or DMSO. Firefly and renilla luciferase activity was determined 48 h after transfection. Firefly luciferase values were normalized to renilla luciferase and shown as fold change over control treatment (DMSO). Data represent means ± SD of three independent experiments. Significant differences compared with control treatment are indicated by *, p < 0.05; **, p < 0.01 or ***, p<0.001.

In the presence of co-transfected hPXR hyperforin, rifampicin and Hyp4 showed a significant induction of the *CYP3A4* XREM promoter of about 6.5-fold, 11.8-fold and 15.1-fold, respectively. In the absence of PXR binding sites (*CYP3A4* -56), none of the substances showed a significant induction of promoter activity. Without co-transfection of hPXR expression plasmid only a weak but significant induction of the promoter occurred. This is most likely due to endogenous PXR (Figure 2.20).

2.4.3 Investigation of antagonistic properties of the phloroglucinols

As antagonist properties have been described for some PXR ligands (Ekins et al., 2007, 2008a), it was investigated whether the phloroglucinols could compete or antagonize rifampicin-mediated PXR activation at the *CYP3A4* promoter. Therefore, HepG2 cells transfected with the *CYP3A4* XREM reporter construct were treated with rifampicin (10 µM) in combination with the different phloroglucinol derivatives or sulforaphane (SFN), a known PXR antagonist (Figure 2.21).
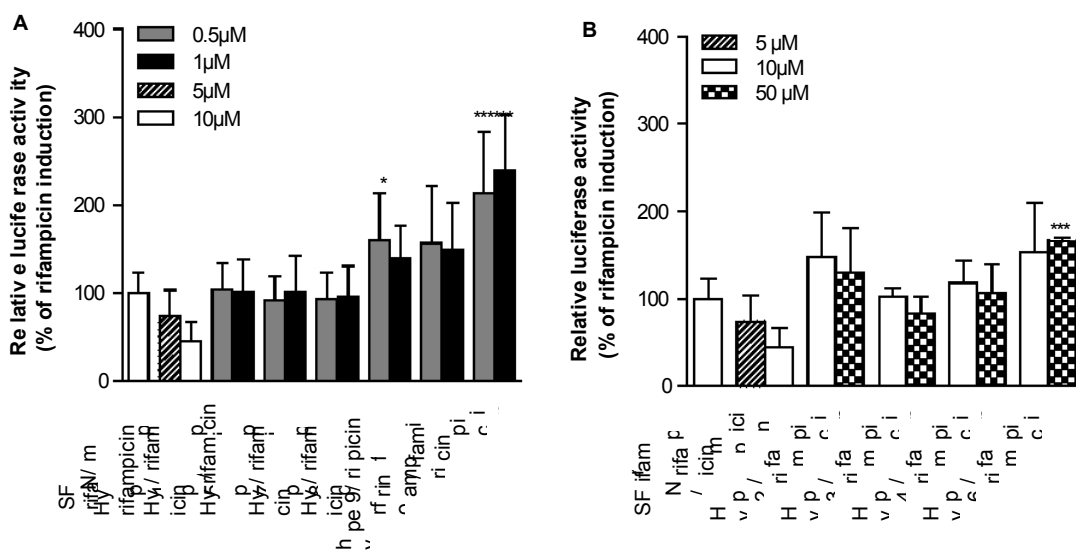
Figure 2.21 Analysis of antagonistic properties of phloroglucinol derivatives. HepG2 cells were co-transfected with pGL3-CYP3A4(-7830/Δ7208-364), pGL3-CMV-Renilla and pcDhPXR and treated 6h after transfection with (A) 0.5 µM or 1 µM of Hyp1, Hyp5, Hyp7, Hyp8, Hyp9, hyperforin and 5 µM or 10 µM of sulforaphane (SFN), or with (B) 10 µM or 50 µM of Hyp2, Hyp3, Hyp4 and Hyp6 in the presence or absence of 10 µM rifampicin. Firefly and renilla luciferase activity was determined 48 h after transfection. Firefly luciferase values were normalized to renilla luciferase and compared to rifampicin induction over control treatment (DMSO; ethanol). Data represent means ± SD of three independent experiments. Significant differences compared with rifampicin treatment are indicated by *, p < 0.05; **; p < 0.01 or ***, p < 0.001.

As expected, SFN showed a dose-dependent reduction of the promoter activity of 24 % and 55 % at 5 µM and 10 µM, respectively (Figure 2.21A). No reduction of the rifampicin-induced promoter activity was found for any of the TRPC6 activating-(Figure 2.21A) or non-activating phloroglucinol derivatives (Figure 2.21B). Co-treatment with hyperforin (0.5 µM and 1 µM), Hyp8 (0.5 µM) (Figure 2.21A), or Hyp6 (50 µM) (Figure 2.21B) resulted in a significant activation of the *CYP3A4* XREM promoter.

2.4.4 Effects of phloroglucinol derivatives on the expression of DMET genes in primary human hepatocytes

To assess whether the phloroglucinol derivatives have other or potentially PXR-unrelated effects on DMET gene expression in human liver, the mRNA expression of a set of 33 DMET genes including the PXR target genes *CYP3A4*, *ABCB1* and UGT1A1 were analyzed in primary human hepatocytes from three individual donors. Spearman correlation analysis was performed to compare mRNA expression changes obtained by treatment with rifampicin and those caused by the different phloroglucinol derivatives (Figure 2.22).

Gene expression changes upon treatment with 1 µM hyperforin were highly correlated (r_s=0.96; p < 0.0001) to those of rifampicin (10 µM). Treatment of hepatocytes with 5 µM hyperforin led to a weaker correlation (r_s =0.63; p< 0.0001) with the rifampicin profile, which may be explained by cytotoxic or other less selective effects of hyperforin at higher concentrations. The correlations of the rifampicin expression profile with all other phloroglucinol derivatives in the different concentrations used were less pronounced (r_s values $\leq$ 0.5) except for Hyp4 (50 µM; r_s=0.73; Figure 2.22).

Figure 2.22 Effects of phloroglucinol derivatives, hyperforin and rifampicin on mRNA expression of selected DMET genes in primary human hepatocytes. Cells were treated with TRPC6 activating phloroglucinols, hyperforin, rifampicin and DMSO or ethanol as a control (concentrations are given in the column headers). The mRNA expression of the indicated genes was determined using RT-PCR 24h after treatment and normalized to GAPDH. Relative changes in expression compared to control treatment are displayed as heatmap and fold changes (log2) are as indicated by the color code. Data represent mean fold change of three independent experiments. Significant differences are indicated by *, $p < 0.05$; **, $p < 0.01$ or ***, $p < 0.001$, compared with control treatment. Spearman coefficients (r_s) were calculated for the correlations of mRNA expression profiles after rifampicin and all other treatments.

In particular, rifampicin and hyperforin (1 µM) both led to a significant and comparable induction of *CYP3A4* of 24-fold and 16-fold, respectively, while all other phloroglucinols did not affect *CYP3A4* expression in the three donors tested (Figure 2.23). Treatment with 5 µM hyperforin led to a 5-fold weaker induction of *CYP3A4* expression compared to treatment with 1 µM hyperforin, probably indicating onset of toxicity (Figure 2.23A).
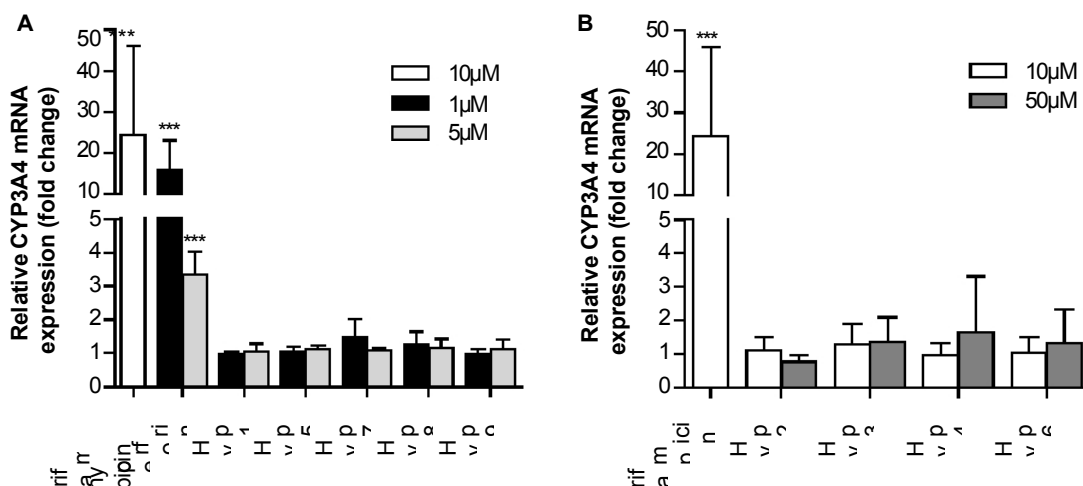
Figure 2.23 Effects of the phloroglucinol derivatives, hyperforin and rifampicin on CYP3A4 mRNA expression in primary human hepatocytes. Cells were treated with A: TRPC6 activating phloroglucinols or hyperforin (1 µM, 5 µM), or rifampicin (10 µM); B: TRPC6 non-activating phloroglucinol derivatives (10 µM, 50µM) or with control treatment (DMSO; ethanol). CYP3A4 mRNA expression was determined using qRT-PCR 24h after treatment. CYP3A4 mRNA expression was normalized to GAPDH and compared to DMSO or ethanol treatment. Data represent means ± SD of three independent experiments. Significant differences are indicated by *, $p < 0.05$; **, $p < 0.01$ or ***, $p < 0.001$, compared with control treatment.

The PXR target genes *CYP2B6*, *ABCB1* (*MDR1*), *UGT1A1, CYP2C9, CYP3A5 and ALAS1* showed significant induction by hyperforin (2.9-fold, 2.4-fold, 2.9-fold, 3.9-fold, 5.3-fold, 5.8-fold and 2.7-fold, respectively) and by rifampicin (3.8-fold, 2-fold, 2.9-fold, 4.1-fold, 5.3-fold, 5.8-fold and 2.7-fold, respectively) (Figure 2.22, Supplemental Table 7 and Supplemental Table 8). In contrast, *CYP7A1* mRNA expression was significantly downregulated by rifampicin (6.3-fold) and by hyperforin (6.7-fold), (Figure 2.22 and Supplemental Table 7 and Supplemental Table 8). Furthermore,

hyperforin significantly up-regulated *POR* expression about 1.6-fold (Figure 2.22 and Supplemental Table 7).

Treatment with the TRPC6-activating phloroglucinol derivatives (Hyp1, Hyp5, Hyp7, Hyp8 and Hyp9) did not significantly change the expression of *CYP2B6*, *CYP7A1*, *CYP1A1*, *CYP1A2*, *CYP2C8*, *ABCB1* or *UGT1A1*, while *CYP2C9* and *CYP2B6* were significantly induced 1.9-fold and 1.7-fold by treatment with 1 µM Hyp7 (Figure 2.22 and Supplemental Table 7), respectively. Hyp7 (1 µM) also significantly induced *CYP2E1* expression. Hyp9 (5 µM) was found to significantly induce ALAS1 expression. For the TRPC6 non-inducing phloroglucinols the only significant expression change observed was 2.7- and 2-fold induction of CYP1A2 by 10 µM Hyp2 and Hyp4, respectively (Figure 2.22 and Supplemental Table 8).

3   Discussion

The human ligand-dependent NRs CAR, PXR and PPARα, sensors of a variety of endogenous and exogenous compounds like drugs, have been shown to impact major hepatic metabolic functions like drug metabolism and energy homeostasis and thereby contribute to inter- and intra- individual variability in liver metabolism (Aleksunes and Klaassen, 2012; Moore et al., 2006; Pyper et al., 2010; Tien and Negishi, 2006). In the first part of this thesis, therefore, the whole-genome transcription changes in response to the activation of these three NRs was investigated, in order to identify their individual target genes that potentially contribute to alterations in liver metabolism introduced upon the activation of CAR, PXR and PPARα.

Beside the ligand-dependent activation, NR activity is further modified by protein kinase mediated phosphorylation in response to various signaling events (Berrabah et al., 2011). In this context, it had previously been reported that the PKA-dependent phosphorylation of PXR attenuates the induction of *CYP3A4* expression (Lichti-Kaiser et al., 2009a). To assess the impact of the PKA on drug metabolism, in the second part of this thesis, the effect of PKA activation on PXR and CAR dependent DMET genes expression was investigated.

The inter- and intra-individual variability in the drug metabolizing capacity of the liver introduced by NRs is a major issue in clinical practice. Most important, drug-dependent activation of PXR, reported for several commonly prescribed therapeutics, had been shown to be the causative mechanism for numerous DDIs (Hernandez et al., 2009; Kliewer et al., 2002; Molnár et al., 2013). Therefore, in the last part of this thesis the PXR activation potential of drugs in development, designed as substitutes of hyperforin, were assessed, in order to identify molecules that lack the potential of hyperforin to activate PXR and cause DDIs and thereby represent promising candidates for further drug development.

3.1 Novel aspects of CAR, PXR and PPARα as regulators of drug metabolism and energy homeostasis

The aim of the first part of this thesis was the identification of the ligand dependent transcriptomes of the human nuclear receptors CAR, PXR and PPARα in human liver cells. Such data are required to assess the specific contribution of these NRs to the inter- and intra-individual variability in human liver functions. Several genome-wide studies have been conducted previously to identify genes differentially expressed upon the activation of PXR, CAR and PPARα. However, all studies on PXR were performed in rodents using PXR knockout (ko) and wild type (wt) mice (Cui et al., 2010), mice expressing human and murine or only human PXR (Rosenfeld et al., 2003), or rats (Guzelian et al., 2006). Additionally, one genome-wide study investigating CAR target genes was conducted in CAR ko and wt mice (Ueda et al., 2002). Lambert and colleagues investigated the whole-genome expression changes in HepaRG cells and primary human hepatocytes, using the rather unspecific (at least in humans) CAR and PXR activator phenobarbital (Kobayashi et al., 2004; Lambert et al., 2009). A direct comparison of CAR and PXR transcriptomes was investigated only in one study in mice using CAR ko, PXR ko, CAR and PXR double ko and wt animals (Tojima et al., 2012). Regarding the known species-specificity of NRs, these data can only partially be extrapolated to humans. Only for PPARα activation, genome-wide expression data of primary human hepatocytes treated with its specific agonist WY-14643 are available (Rakhshandehroo et al., 2009). Until now, genome-wide data comparing the transcriptional impact of CAR, PXR and PPARα in a human background are not available.

Regarding the species differences in liver functions such as drug metabolism, primary human hepatocytes are considered the most useful model to investigate hepatic gene expression and metabolism in human liver (Ballet et al., 1984; Hewitt et al., 2001; Lecluyse and Alexandre, 2010). Nevertheless, PHHs are restricted in availability and usability as they maintain their functionality only during short-term culturing while exhibiting a limited life-span in culture (Godoy et al., 2013; Guillouzo et al., 1993). Moreover, quantitative gene expression levels of hepatic genes are highly variable between batches of PHHs from different donors, reflecting the inter-

individual variability (Rogue et al., 2012). However, PHHs are the model of choice to investigate expression and regulation of genes involved in drug metabolism or other liver specific functions, as their expression profile is highly comparable to human liver tissue in contrast to the available human hepatoma cell lines such as HepG2 (Hart et al., 2010; Wilkening et al., 2003). Yet, HepaRG cells that had been reported to share a largely overlapping transcription profile with PHHs, were shown to express several genes normally expressed in cancerous or stem cells (Rogue et al., 2012).

Therefore, in this study the whole-genome mRNA expression changes in response to the ligand-dependent activation of the NRs CAR, PXR, and PPRAα were determined in primary human hepatocytes. The hepatocytes were obtained from three hospitals within the virtual liver project (5.1.3), of which this study was part of. The accessibility of hepatocytes was, however, unpredictable and highly restricted to one or two suitable batches per month. Furthermore, culturing of several hepatocyte batches failed or was discontinued due to bacterial contaminations or low cell viability (<70%).

For this study, hepatocytes were treated for 24 h with the prototypical agonists for CAR (CITCO), PXR (rifampicin) or PPARα (WY-14643) as well as DMSO (control treatment). These experiments were performed in hepatocyte cultures of ten individual donors. In four of these cultures the yielded RNA quantity and quality was low (2.1.1), and therefore mRNA preparations from the remaining six donors were used for genome-wide mRNA expression analysis using Affymetrix GeneChip® HuGene 1.0ST Arrays (5.1.4 and 5.4).

Principal component analysis (Figure 2.1) and assessment of the coefficients of variation of the gene expression values across donors and treatments (Figure 2.2), revealed that variability in gene expression was generally higher among individuals than within treated individuals (2.1.1). Such variability among hepatocyte cultures from different donors were previously reported (Rogue et al., 2012). In order to identify mRNA expression changes in response to NR activation that are conserved among the examined set of donors and possibly contribute to inter- or intra-individual variability of liver metabolism in general, a linear mixed model and a post-hoc paired t-test were applied that corrected for the observed donor variability (0). These statistical analyses revealed 316, 498 and 478 genes significantly differentially

expressed for CITCO, rifampicin or WY-14643 treatment compared to control, respectively (2.1.1). The validation of the microarray results by re-analysis of 12 marker genes, three top regulated known target genes of each of the three NRs and three differentially expressed genes known to be regulated by all three NRs, using qRT-PCR, revealed highly comparable values, indicating reliability of the microarray data (2.1.3).

For all three treatments, the number of repressed genes was higher than the number of genes with induced expression. The high proportion of downregulated genes in response to the activation of the three NRs was somewhat surprising, as these NRs have been mainly described to upregulate genes when activated. Interestingly, similar results have been reported in other genome-wide studies investigating transcriptional changes upon PPARα activation in human and mice and upon murine CAR and human PXR activation in mice (Rakhshandehroo et al., 2009; Rosenfeld et al., 2003; Ueda et al., 2002). These observations can be associated with the ability of NRs to bind to other TFs or their co-activating proteins and repress their transcriptional activity, like described for PXR dependent inhibition of *CYP7A1* (Li and Chiang, 2005) or CAR and PXR dependent repression of *Pck1* and *G6pc* expression (Kodama et al., 2007; Miao et al., 2006). This was further supported by a ChiP-Seq and microarray study of Cui and colleagues, which showed that more than 65% of genes suppressed in pregnenolone-16α-carbonitrile (PCN; mouse PXR agonist) treated mice were lacking PXR binding (Cui et al., 2010).

Treatment of primary human hepatocytes with CITCO led to the significant upregulation of 57 genes, whereby 11 of these genes including the nine most strongly upregulated genes were shown to be *CYP*s. The well described CAR target gene *CYP2B6* (Wang et al., 2003), showed the strongest up-regulation (Table 2.1). For the *CYP*s *1A1*, *2A6*, *2C8*, *3A4*, *3A7*, *1A2*, *2C9* and *3A5* that showed induction upon CITCO treatment, a direct regulation by CAR has been reported previously (Bertilsson et al., 2001; Burk et al., 2004; Chen and Goldstein, 2009; Goodwin et al., 2002; Itoh et al., 2006; Yoshinari et al., 2010), whereas upregulation of *CYP2A7* and *CYP2A13* was not reported before. Most of these *CYP*s are involved in the metabolism of drugs and other xenobiotics, promoting the role of CAR as an important regulator of these processes.

Furthermore, GO term and KEGG pathway enrichment analyses revealed that the first six of the 19 GO terms and four of the six KEGG pathways, showing a significant over-representation of CITCO regulated genes, were associated with the metabolism or the response to drugs or xenobiotics (Table 2.5 and Table 2.6). Besides the phase I enzyme *EPHX1* and the phase II enzymes *UGT1A1*, *UGT2B4*, *SULT1B1* and *MGST1*, the majority of the CITCO regulated genes contained in these terms and pathways were shown to be CYPs, including the above mentioned as well as *CYP4A11* and *CYP2E1*. In contrast to *EPHX1* and *UGT1A1* (Peng et al., 2013; Sugatani et al., 2001), a direct regulation of *UGT2B4*, *SULT1B1*, *MGST1* or *CYP2E1* by human CAR has not been shown to date. A decreased expression of *CYP4A11*, which was identified upon CITCO treatment was previously reported by Lambert and colleagues in HepaRG cells and primary human hepatocytes treated with the unspecific CAR and PXR activator phenobarbital (Lambert et al., 2009).

Additionally, the comparison of the genes differentially expressed upon CITCO treatment and the "Core ADME" gene list and the "Extended ADME" gene list (www.pharmaadme.org), displayed that 22 of the 316 CITCO regulated genes were overlapping with the 299 genes included in these lists (Supplemental Table 6). These 22 genes included *CYP*s and *UGT*s, *SULT1B1* and *EPHX1*, as well as the CAR heterodimer partner *RXRα*, *POR* (P450 cytochrome oxidoreductase) and the organic anion transporters *SLC22A9*. A transcriptional regulation of *RXRα*, *POR* or *SLC22A9*, has previously not been reported and thus further extends the list of potential CAR target genes. The regulatory mechanisms for the genes identified herein as responsive to CITCO-dependent CAR activation remains to be elucidated in future. Taken together, these results confirmed the role of CAR as an important regulator of drug metabolism by predominantly regulating CYPs of the families 1A, 2C and 3A, but also phase II enzymes. Furthermore, several new potential CAR target genes like *UGT2B4*, *SULT1B1*, *MGST1, CYP2E1, CYP2A7* and *CYP2A13* involved in drug metabolism, were identified.

Rifampicin-dependent activation of PXR in the six donors of primary human hepatocytes led to the significant differential expression of 498 genes. The strongest activation in average was shown for *CYP3A4* (4.1-fold), which is the best described PXR target gene in humans and the most important drug metabolizing enzyme, as it

is involved in the metabolism of more than 35% of all prescribed drugs (Zanger et al., 2008). Along with *CYP3A4*, rifampicin treatment altered the expression of 21 further *CYP* genes (Table 2.2 and Supplemental Table 2). The observed rifampicin-mediated induction of the *CYP*s *1A1*, *2A6*, *2B6*, *2Cs* and *3A5* was in line with other reports, which showed a PXR dependent regulation of these genes (Burk et al., 2004; Chen and Goldstein, 2009; Goodwin et al., 2001; Itoh et al., 2006; Maglich et al., 2001). The rifampicin-mediated repression of *CYP2E1* or induction of *CYP2J2*, was not reported so far. Interestingly, fatty acid oxidation involved *CYP*s *4A11* and *4V2*, were downregulated by rifampicin treatment, supporting a repressive effect of PXR on fatty acid catabolism (Konno et al., 2008). Moreover, *CYP7A1* but also *CYP8B1*, important for bile acid synthesis, were shown to be downregulated by rifampicin treatment, which is in agreement with results for *7A1* reported by Li and Chiang from experiments in HepG2 cells and human hepatocytes (Li and Chiang, 2005).

Using GO term enrichment analysis PXR regulated genes were identified to be over-represented in 64 GO terms, whereby several of these terms, including six of the 20 most significantly enriched terms, were associated with xenobiotic or drug metabolism or the response to such compounds (Table 2.7 and Supplemental table 4). These terms included most of the above-mentioned *CYP*s, but also several alcohol dehydrogenases (*ADH*), phase II enzymes (e.g., the *SULT*s and *UGT*s) and drug transporter like *ABCB1* and *ABCB4* (Table 2.2 and Supplemental Table 2). Interestingly, the terms referring to the response to chemical or xenobiotic stimuli also included several genes involved in energy homeostasis [e.g., members of the acyl-CoA dehydrogenase family (*ACAD*), *HMGCS2*, *CPT1A*, *ketohexokinase* (*KHK*) or *malic enzyme 1* (*ME1*)], suggesting that their belonging to these terms may in part be due to a PXR-dependent regulation of these genes and the ability of PXR to sense various lipophilic compounds, which will be discussed below in more detail.

KEGG pathway enrichment analysis revealed that three of the eight pathways, displaying a significant over-representation of rifampicin responsive genes, were associated with drug or xenobiotic metabolism. In total, 12 *CYP*s (*CYP1A1*, *2A13*, *2A6*, *2A7*, *2B6*, *2C8*, *2C9*, *2E1*, *3A4*, *3A5*, *3A7* and *CYP3A43*), four *ADH*s (*ADH1A*, *1B*, *4* and *6*), *EPHX1*, *FMO5*, *MGST1* and the two *UGT*s *1A1* and *2B4* were found to be rifampicin-regulated and included in these pathways. Moreover, a comparison of

the 498 rifampicin-regulated genes and the "ADME lists" (www.pharmaadme.org), resulted in a set of 43 genes (Supplemental Table 6), including all 21 genes retrieved by the KEGG pathway analysis. Besides several known PXR target genes, this list comprised the NRs *RXRα* and *HNF4α*, both downregulated upon rifampicin treatment, and which are also involved in the regulation of DMET genes. Transcriptional regulation of *NR1I2* (PXR) by HNF4α is already known (Tirona et al., 2003), whereas an impact of PXR activation on the expression of *HNF4α* as well as *RXRα* was not reported so far. A PXR-dependent regulation of the genes *EPHX1*, *GSTA2*, *SULT1B1*, which were also included in the list, was suggested earlier based

on results from experiments conducted in cell lines and rodents (El-Sayed, 2011; Falkner and Prough, 2007; Roques et al., 2013), were confirmed here. Moreover, besides well described PXR target genes, several genes, which responded to rifampicin treatment, like *ABCB4*, *ADHs* (*ADH1A*, *1B*, *4* and *6*), *ALDH6A1*, *CES2*, *FMO5*, *GPX2*, *MGST1*, *SLC22A7* and *SLC22A9*, have not been previously described to be PXR regulated in humans. Altogether, these results further expanded the number of potential PXR target genes and substantiate the role of PXR as a master transcriptional regulator of genes involved in drug metabolism and transport; however, the underlying mechanisms of these observed regulatory events remain to be elucidated.

Using the specific PPARα agonist WY-14643, 478 genes were identified as differentially expressed upon PPARα activation. In accordance with recently published results from our lab (Klein et al., 2012; Thomas et al., 2013), a significant induction of *CYP3A4* upon PPARα activation was observed (Table 2.3). Here, *CYP3A4* was shown to be the eighth most induced gene upon WY-14643 treatment and the average fold change of 1.7 was even higher than that provoked by the CAR ligand CITCO (Table 2.2. and Table 2.3). Furthermore, PPARα activation increased the expression of the drug metabolizing *CYP*s *2B6*, *2C8* and *3A5* (Table 2.3 and Supplemental Table 3), which confirmed the previously suggested role of PPARα in the regulation of these CYPs (Rakhshandehroo et al., 2009; Thomas et al., 2013). In addition, six of the 20 most significantly enriched GO terms (Table 2.9) and two of the five enriched KEGG pathways (Table 2.10) were associated with the metabolism of xenobiotics and drugs or the response to such stimuli. The KEGG pathways

"Metabolism of xenobiotics by cytochrome P450" and "Drug metabolism by cytochrome P450" included the WY-14643-regulated genes *ADH1A*, *ADH1B*, *EPHX1*, the *CYP*s *2B6*, *2C8*, *3A4*, *3A5*, *3A7*, and *3A43*, *UGT1A1*, *UGT2B4*, *GSTA2* and *MGST1*. A potential role of PPARα in the regulation of *UGT1A1*, *GSTA* and *MGST1* was reported so far only in rodents using fibrates (Heydel et al., 2012; Knight et al., 2008), whereas for *UGT2B4* such a regulation could be shown in human hepatocytes (Barbier et al., 2003). For the *ADH1A* and *1B*, the here presented data are the first evidence of a PPARα-dependent regulation of *ADH*s. Comparing to the "ADME lists" (www.pharmaadme.org), 27 genes including all 13 genes from the KEGG pathways, were identified to be associated with drug metabolism. The 14 genes not contained in the KEGG pathways related to xenobiotic and drug metabolism, were *ABCB1*, *ABCB4*, *ALDH6A1*, *CAT*, *CYP21A2*, *CYP4A11*, *CYP4F3*, *CYP4F12*, *FMO5*, *GPX2*, *HNF4α*, *POR* and *SULT2A1* (Supplemental Table 6). For *ABCBA*, *CYP4A11*, *POR* and *SULT2A1,* a regulation by PPARα or fibrates was previously shown in primary human hepatocytes (Fang et al., 2005; Ghonem et al., 2014; Rakhshandehroo et al., 2009), whereas for *ABCB1*, *ALDH6A1*, *CAT* and *GPX2* a regulation by fibrates was only shown in rodents (Alnouti and Klaassen, 2008; Kok et al., 2003; Nishimura et al., 2008). For the *CYP*s of the *4F* family, *CYP21A2* and *FMO5,* the data provide the first evidence of a PPAPα-dependent regulation of these

genes.

The comparison of genes differentially expressed by WY-14643 and those differentially expressed by CITCO and rifampicin, revealed an overlap of 180 genes (Figure 2.3). Interestingly, out of these 180 genes, the nine genes that displayed a fold change of at least 1.2 fold with each of the treatments, included four *CYP*s (*2B6*, *2C8*, *3A4* and *3A7*) involved in drug metabolism as well as the rate-limiting enzyme of the heme biosynthesis *ALAS1*. Furthermore, three KEGG pathways were identified to include a significantly enriched number of genes regulated by all three treatments, of which two were associated with drug or xenobiotic metabolism. Among the three NRs, PXR appeared to be the most important regulator of drug and xenobiotic metabolism by regulating the expression of 22 of the 23 genes (regulated by any of the three receptors) included in these pathways (Table 2.11). Furthermore, PXR was involved in the regulation of 43 of the 46 genes regulated by any of the three

receptors retrieved from the comparison with the "ADME" lists (Supplemental Table 6). 12 of the 16 differentially expressed genes upon CAR activation contained in these pathways were shown to be *CYP*s, underlining the prominent role of CAR in the regulation of this gene family. Moreover, CAR was the only receptor that regulated *CYP1A2* and also showed a stronger effect on the expression of *CYP1A1* and the *CYP*s of the *2A* family compared to PXR (Table 2.11). Interestingly, PPARα revealed a more pronounced effect on the regulation of *CYP2C8* and *CYP3A4* as observed for CAR activation. PPARα was shown to regulate a set of 14 genes included in the pathways dealing with drug and xenobiotic metabolism. These 14 genes were also regulated by PXR and nine genes also by CAR (Table 2.11). Taken together, CAR, PXR, PPARα were shown to play a significant role in drug and xenobiotic metabolism by regulating a highly overlapping set of mainly phase I and phase II enzymes. CAR- and PXR-mediated alterations in the drug metabolizing capacity of human liver is a well-studied and recognized issue in clinical practice in recent years (Wang et al., 2012), whereas PPARα was identified very recently to impact pharmacokinetic parameters in patients (de Keyser et al., 2013; Tsamandouras et al., 2014).

PPARα is known as a key regulator of enzymes involved in peroxisomal and mitochondrial β-oxidation, microsomal ω-oxidation and ketogenesis in rodents and humans (Pyper et al., 2010; Rakhshandehroo et al., 2007, 2009). In accordance with these previous observations, WY-14643 treatment led to the induction of several genes involved in the catabolism of fatty acids, whereby *HMGCS2,* which encodes the rate-limiting enzyme of ketogenesis showed the strongest induction (Table 2.3). Furthermore, WY-14643 treatment upregulated 21 (e.g., *ACAA2*, *ACAC*s, *CPT*s, *HADH*s, *ABCB4*, *CYP4A11*, *ACOX1*, *SLC25A20*, *FABP1*, *ACSL*s and *SLC27A*s) of the 34 genes involved in fatty acid catabolism or transport, identified before by Rakhshandehroo and colleagues as increased upon PPARα activation in primary human hepatocytes. Additionally, *CD36* involved in fatty acid transport and *CYP4A22* and *ETFB* contributing to fatty acid oxidation responded to PPARα activation (Supplemental Table 3), whereas these genes were found to be regulated in mice only according to Rakhshandehroo et al., 2009. GO term enrichment analysis revealed that 12 of 20 most significantly enriched terms for PPARα regulated genes

72

were associated with lipid or fatty acid metabolism, including up to 83 genes (Table 2.9). Moreover, the KEGG pathway "Fatty acid metabolism" showed the second strongest over-representation of genes that responded to WY-14643 treatment (Table 2.10). This altogether further supports the strong involvement of PPARα in overall lipid metabolism by influencing the expression of a battery of genes involved in these processes.

Several reports previously highlighted the contribution of PXR in the regulation of energy homeostasis, more precisely in the regulation of genes encoding for key enzymes involved in fatty acid metabolism, lipid *de novo* synthesis and gluconeogenesis. For most of these genes like *PCK1*, *G6PC*, *CPT1A* and *HMGCS2*, PXR dependent regulation was shown to function via the interaction with the TFs HNF4α, FOXA2, FOXO1 and CREB or the co-activating protein PGC-1α (Konno et al., 2008; Wada et al., 2009). In the genome-wide study presented here, rifampicin treatment led to the significant reduction of *G6P*C, *CPT1A* and *HMGCS2* but not *PCK1* expression (Supplemental Table 2). Additionally, expression of glycogen synthase 2 (*GYS2*) and pyruvate dehydrogenase kinase 2 and 4 (*PDK4* and *2*), were also shown to be downregulated upon rifampicin treatment (Supplemental Table 2). PDK2 and 4, which repress the pyruvate dehydrogenase complex (PDC) via phosphorylation and thereby inhibited the metabolism of glucose to acetyl-*CoA*, were shown to be transcriptionally regulated by PPARα and HNF4α together with PGC-1α (Ma et al., 2005). *GYS2* is also a direct PPARα and HNF4α target and encodes the rate-limiting enzyme for glycogen synthesis in the liver (Mandard et al., 2007; Odom et al., 2004). These genes were so far not described as PXR targets and their PXR dependent regulation may also involve the interaction of PXR with HNF4α and PGC-1α as reported for *Pck1* or *G6pc* (Miao et al., 2006). These findings further emphasize the role of PXR as a regulator of glucose homeostasis and its potential as a target for treating hyperglycemia and diabetes (Gao and Xie, 2012). However, constitutively active PXR and ligand dependent activation of PXR in mice had been reported to provoke hepatic steatosis possibly through increased expression of lipid *de novo* synthesis genes like *Elovl6* and *Fasn* and decreased expression of *Pck1* and *G6pc* involved in gluconeogenesis (Zhou et al., 2006). Furthermore, PXR activation had been reported to repress *Cpt1a* and *Hmgcs2* expression in a Foxa2-dependent

manner in mice, which may also contribute to hepatic lipid accumulation by inhibiting β-oxidation (Nakamura et al., 2007). The expression of *CPT1A*, and *HMGCS2* was also shown to be decreased and expression of *ELOVL6* and *FASN* was shown to be increased upon rifampicin treatment in the herein presented study (Supplemental Table 2 and Table 2.13).

Additionally, GO term and KEGG pathway enrichment analysis showed a significant over-representation of rifampicin-regulated genes within terms and pathways associated with fatty acid and lipid metabolism, including nine of the 20 most significant enriched GO terms and three of the eight significantly enriched KEGG pathways (Table 2.7 and Table 2.8). Surprisingly, "Lipid metabolic process" was the second most significantly enriched GO term containing more the 100 rifampicin-regulated genes (Table 2.7). According to the KEGG enrichment analysis, the "Fatty acid metabolism" pathway comprised 13 genes differentially expressed upon rifampicin treatment. Besides the above-mentioned *CPT1A*, this pathway included the following genes that were downregulated upon rifampicin treatment *ACAA2*, *ACADM*, *ACADVL*, *ACOX2*, *CPT2* and *HADHB* and also involved in mitochondrial and peroxisomal (*ACOX2*) β-oxidation. These genes were shown here for the first time to be downregulated upon rifampicin treatment (Table 2.13). Further included in this pathway are the genes *ACSL1* and *ACSL2* encoding for ligases that convert free fatty acids into fatty acyl-CoA esters and make them available for β-oxidation as well as for triglyceride synthesis (Table 2.13). For these two *ACSL*s, upregulated by rifampicin, a PXR-dependent regulation was also not reported so far. Interestingly, *ACAA2*, *ACADM*, *ACADVL*, *CPT2*, and *HADHB* but also *CYP4A11* and *HMGCS2*, which were all downregulated by rifampicin, are described as PPARα target genes (Rakhshandehroo et al., 2007) and were shown to be upregulated by WY-14643 treatment in the herein presented experiments (Table 2.13). These results clearly indicated, in contrast to the genes involved in drug metabolism, an opposing effect of PPARα and PXR concerning fatty acid catabolic processes. Therefore, these findings provide new evidence for an important role of PXR in the regulation of lipid homeostasis, but also challenge the usefulness of PXR as a therapeutic target.

In contrast to PXR, activation of CAR did not influence the expression of the above mentioned genes involved in fatty acid catabolism or lipid *de novo* synthesis, except

for *CYP4A11*. Ueda and colleagues had reported that PB treatment decreased expression of Cpt1a in wt but not in CAR knock-out mice (Ueda et al., 2002). This downregulation of Cpt1a may involve the interaction of CAR with Foxa2 shown in mice (Tien and Negishi, 2006), which is also a described mechanism for the PXR mediated repression of Cpt1a (Nakamura et al., 2007). However, an interaction of CAR and PXR with FOXA2 in human was not investigated so far. Furthermore, in a report of Lambert and colleagues, where they investigated whole-genome expression changes in HepaRG cells and PHHs in response to phenobarbital (PB), both, a CAR and to a lesser extent a PXR activator, except for *CYP4A11*, none of the above discussed PXR-regulated genes involved in lipid metabolism were found to be regulated (Lambert et al., 2009). On the other hand, CAR activation by CITCO led to decreased expression of *PDK2, PDK4*, *IRS1*, *GRB10* and *PFKFB3* (Supplemental Table 1), involved in the regulation of glucose metabolism and insulin signaling, promoting a previously suggested role of CAR in the regulation of glucose homeostasis (Wada et al., 2009).

The mechanisms by which PXR, CAR and PPARα alter the expression of genes contributing to glucose or lipid metabolism but also drug metabolism, are not fully understood so far. Therefore, to obtain additional information on how CAR, PXR and PPARα activity and abundance impact gene expression, CAR, PXR and PPARα were knocked down using specific siRNAs and activated by their ligands CITCO (CAR), rifampicin (PXR) and WY-14643 (PPARα). These experiments were performed in hepatocytes cultures from two of the six donors utilized for the genome- wide mRNA expression study. Using qRT-PCR, mRNA expression of nine genes involved in energy homeostasis or drug metabolism were selected based on the microarray data results and analyzed at different time points (5.1.4).

PXR and CAR knock-down led to decreased CYP2B6 and CYP3A4 expression at 72 h, whereas their expression was hardly changed after 48 h knock-down. Surprisingly, expression of *UGT1A1* and in the case of PXR knock-down, *CYP2C8* remained unchanged, whereas the four described CAR and PXR target genes (Goodwin et al., 1999, 2001, 2002; Sugatani et al., 2008; Wang et al., 2003) showed increased expression upon treatment with CITCO or rifampicin after 24 h and even more pronounced at 48 h (Figure 2.7 and Figure 2.9). PXR knock-down led to the

upregulation of *CYP7A1* and *HMGCS2* only after 48 h and *CPT1A* only at 72 h, which was somewhat surprising as the PXR-mediated regulation of *HMGCS2* and *CPT1A* was suggested to function via the same FOXA2-dependent mechanism (Nakamura et al., 2007). In contrast, their downregulation was strongest in all three cases after 24 h rifampicin treatment (Figure 2.8). Interestingly, *ADH1A,* which showed a strong decrease upon rifampicin and WY-14643 treatment in the microarray data as well as in these two donors was not altered upon PXR knock-down and even slightly decreased upon PPARα knock-down (Figure 2.8 and Figure 2.9). On the other hand, all investigated genes, which showed upregulation upon WY-14643 treatment (*CYP2B6*, *2C8*, *3A4*, *CPT1A*, *HMGCS2*, *PDK4* and *UGT1A*1) were downregulated by at least 23% following 72 h of PPARα knock-down (Figure 2.9). For *CYP2B6* and *CYP2C8*, this further supported the results from the genome- wide study that suggested a PPARα-dependent regulation of these two genes. In contrast to the genome-wide data where the mean expression (six donors) of *CYP7A1* was not significantly changed upon PPARα activation, in these experiments, *CYP7A1* was decreased upon WY-14643 treatment and increased upon PPARα knock-down (Figure 2.9). In HepG2 cells, *CYP7A1* downregulation by PPARα had been previously reported and was suggested to involve interaction of PPARα and HNF4α, whereas this study could not reproduce these results *in vivo* using PPARα ko or wt mice (Patel et al., 2000).

The results presented in this thesis indicate different time profiles for the response of the individual CAR, PXR and PPARα target genes, following the activation or knock- down of these NRs, which may reflect the different and so far not completely understood regulatory mechanisms contributing to these different transcriptional events. Additionally, not all genes regulated by the activation of the three NRs responded to the corresponding knock-down, which suggests that their basal expression was independent on these NRs. This further complicates the prediction of the overall impact of CAR, PXR and PPARα on hepatic gene expression and therewith on the overall metabolic capacity of the liver.

3.2 Protein kinase A as an important determinant of ADME genes expression

In this part of the thesis, the impact of PKA signaling on the transactivation capacity of PXR and CAR and on the expression of the target genes of these NRs was investigated. The protein kinase mediated phosphorylation of NRs is considered to be an important mechanism to adapt the activity of such receptors in response to various signaling events to meet the organisms' needs (1.2.6). Hence, phosphorylation of PXR and other NRs potentially contributes to alterations of the hepatic drug detoxifying capacity. Previous work from Lichti-Kaiser and colleagues showed that activation of PKA decreased PXR dependent activation of human *CYP3A4* and rat *CYP3A1* expression, whereas PKA activation further increased PXR dependent expression of murine CYP3a11 (Lichti-Kaiser et al., 2009a).

In accordance with the results published by Lichti-Kaiser and colleagues (Lichti-Kaiser et al., 2009a) activation of PKA by 8-bromo cAMP drastically decreased rifampicin-mediated *CYP3A4* promoter activity by about 80% in HepG2 cells (Figure 2.10A). Both the rifampicin-mediated induction and the repression of this induction were also present in the absence of co-transfected PXR, but to a much weaker extent. This was most probably due to endogenously expressed PXR (Figure 2.10B). Besides this, it could be further demonstrated that PKA activation decreased rifampicin-mediated *CYP2B6* promoter activity by about 50% in HepG2 cells only in the presence of co-transfected PXR (Figure 2.11A and Figure 2.11B). Additionally, PKA activation by 8-bromo cAMP also completely abolished CAR-dependent CITCO-mediated induction of the *CYP3A4* and *CYP2B6* promoters (Figure 2.12A and Figure 2.13A), whereas in the absence of CAR, neither rifampicin nor 8-bromo cAMP had an effect on the activity of these promoters except for an unexplainable increase of the *CYP2B6* promoter activity by 8-bromo cAMP (Figure 2.12 and Figure 2.13). These results indicated for the first time that PKA activation by 8-bromo cAMP repressed CAR-dependent activation of the *CYP3A4* and *CYP2B6* promoter and PXR-dependent activation of the *CYP2B6* promoter. For CAR, these findings are in contrast to those from experiments performed in mice by Ding and colleagues, which showed increased CAR activity and *Cyp2b10*, the murine ortholog of CYP2B6,

expression in response to PKA activation by 8-bromo cAMP (Ding et al., 2006). Interestingly, the same species dependent opposite effect of PKA activation was reported for the PXR transactivation capacity and the promoter activity of human *CY3A4* and murine *Cyp3a1* (Lichti-Kaiser et al., 2009a). By contrast, the repression of PXR transactivation capacity and *CYP2B6* promoter activity following PKA activation was in line with the findings of Lichti-Kaiser and colleagues regarding the PXR mediated repression of *CYP3A4* promoter upon PKA activation (Lichti-Kaiser et al., 2009a).

Using primary human hepatocytes, it was further shown that PKA activation by 8-bromo cAMP completely abolished rifampicin-mediated induction of *CYP2C8* and *CYP3A4* mRNA expression (Figure 2.14C) and CITCO-mediated induced expression of *CYP2B6*, *2C8* and *3A4* (Figure 2.15C). 8-bromo cAMP treatment also decreased expression of *NR1I2* (PXR) up to 55% and *NR1I3* (CAR) up to 88% in the presence or absence of their agonists (Figure 2.14B and Figure 2.15B). This may contribute to the reduced expression of CAR and PXR target genes like *CYP3A4* following PKA activation. In contrast, Ding and colleagues showed an increased expression of CAR in response to PKA activation in mice (Ding et al., 2006). Moreover, also rifampicin-induced CPY2B6, CYP2C8 and CYP3A4 activity and CITCO-induced CYP2B6 activity was shown to be abolished by 8-bromo cAMP after 72 h treatment (Figure 2.16), as determined in primary human hepatocytes using the CYP cocktail assay (5.2). It is noteworthy that CITCO failed to induce activity of CYP2C8 and CYP3A4 in the hepatocytes utilized for the determination of CYP activities (Figure 2.16C and Figure 2.16D). Whether mRNA expression was induced by CITCO was not determined in this experiment. In the absence of a PXR or CAR ligand, PKA activation also strongly decreased basal expression of *ABCB1*, *CYP1A2*, *CYP2C8*, *CYP3A4* and *UGT1A1* by 54%, 94%, 57% and 54%, respectively (Figure 2.14C). 8-bromo cAMP treatment was further shown to decreased basal activity CYP1A2, 2B6, 2C8 and 3A4 by 69%, 75%, 32% and 50%, respectively (Figure 2.16).

To investigate the physiological relevance of the above-discussed finding, an explorative experiment was performed to assess the influence of the fasting hormone glucagon, a physiological activator of the PKA signaling, on the induced and basal mRNA expression of DMET genes (Figure 2.17). Therefore, mRNA expression was

determined in primary human hepatocytes from a single donor, treated for 24 h with rifampicin, glucagon (5mg/l) or both or DMSO (control treatment). The obtained results were highly comparable to those received from the experiments with 8-bromo cAMP. Glucagon was shown to reduce expression of *CYP1A2*, *CYP2C8* and *CYP3A4* by at least 50% and also *ABCB1* and *CYP2B6* about 19% and 24%. Additionally, glucagon strongly reduced rifampicin induced expression of *CYP2B6*, *CYP2C8* and *CYP3A4* by 56%, 81% and 78%, respectively (Figure 2.17).

These results presented here, for the first time showed that PKA activation by 8-bromo cAMP decreased CITCO and rifampicin-induced but also basal activity of major drug metabolizing CYPs. Furthermore, besides the previously published repression of *CYP3A4* expression by PKA (Lichti-Kaiser et al., 2009a), it could be further shown that 8-bromo cAMP and glucagon repressed basal or induced expression of further important *CYP*s, *UGT1A1* and *ABCB1*. Whether the observed reduction in basal or induced DMET mRNA expression and CYP activity are a consequence of PKA dependent PXR or CAR phosphorylation, or resulted from the decreased expression of the NRs needs to be investigated. For PXR, it had been shown that PKA-dependent phosphorylation increased the interaction of PXR with its co-repressor NCoR, which could explain the reduced PXR transactivation capacity (Lichti-Kaiser et al., 2009a), whereas for CAR, a PKA-dependent phosphorylation was not reported so far, but was strongly suggested by the data presented here. It could be further suggested that PKA-dependent phosphorylation of other NRs and co-regulating proteins involved in the expression of these DMET genes contributed to the observed effects. For instance, HNF4α was shown to be directly phosphorylated by PKA, which represses HNF4α transactivation capacity (Viollet et al., 1997). Furthermore, PKA was reported to increase expression of *PGC-1*α (Rhee et al., 2003) and phosphorylates SRC1, which are both PXR and CAR co-activators (Rowan et al., 2000). Despite all that, these results indicate that activation of PKA signaling is a possible determinant of the drug metabolizing capacity of the liver, but it still has to be investigated, to which extent PKA activation affects *in vivo* drug metabolism in humans.

3.3 Hyperforin-related phloroglucinol derivatives lacking PXR activation as new potential antidepressives drugs

In the final part of this thesis, the potential of a set of experimental drugs structurally related to the antidepressant and PXR agonist hyperforin, to activate PXR was investigated. Hyperforin has been identified as the major active compound of St. John's wort (SJW) (Mai et al., 2004; Singer et al., 1999) by inhibiting serotonin reuptake in response to the selective activation of the TRPC6 channel (Leuner et al., 2007). As described in chapter 1.3.2, concomitant intake of the antidepressant herbal remedy SJW with drugs that are, e.g., metabolized by CYP3A4, was shown to cause DDIs, most probably due to PXR activation by hyperforin (Chatterjee et al., 1998; Madabushi et al., 2006; Müller, 2003).

TRPC6 and PXR are structurally unrelated proteins with highly distinct physiological functions. The fact that hyperforin, a potent PXR ligand, is also a TRPC6 activator, is thus very surprising and may be a coincidence rather than biologically meaningful. Regarding their structural heterogeneity, it should be possible to separate the activator functions of TRPC6 from those of PXR and to develop ligands activating exclusively TRPC6 and not PXR. To this end, in a drug development project of the Dr. Willmar Schwabe GmbH, molecules were designed based on the phloroglucinol core-structure of hyperforin, in order to identify compounds that lack the PXR activation potential of hyperforin but retain its beneficial pharmacological effect. In an *in vitro* study of Leuner and colleagues, the nine most promising phloroglucinol derivatives (Hyp1- Hyp9) were investigated for their pharmacological activity (Leuner et al., 2010). They identified five phloroglucinol derivatives that activate the TRPC6 channel and inhibit serotonin re-uptake comparable to hyperforin.

The aim of the study presented here was to assess the PXR activation potential of the compounds (Hyp1-Hyp9) examined by Leuner and colleagues (Leuner et al., 2010) in order to identify molecules that lack PXR activation. The result obtained from reporter gene assays in HepG2 cells showed that only high concentrations of the TRPC6 non-activating Hyp4 could induce the *CYP3A4*-promoter (Figure 2.19) and that this only occurred in the presence of hPXR (Figure 2.20). In order to exclude potential antagonistic activity of the phloroglucinol derivatives, the effect of these

compounds on the rifampicin-induced *CYP3A4* promoter activity was investigated in HepG2 cells, but no reduction of the rifampicin-induced promoter activity was found for any of the phloroglucinol derivatives (Figure 2.21). Instead Hyp6, Hyp8 and hyperforin further increased rifampicin-induced promotor activity (Figure 2.21). The reason for this is currently unclear. It is difficult to rationalize how two very large molecules like rifampicin and hyperforin could bind the LBD together. It may be the result of an allosteric mechanism that requires further investigation.

Treatment of human hepatocytes with hyperforin confirmed induction of previously described PXR target genes *CYP2B6*, *CYP3A4*, *CYP2C9* and *ABCB1* (Figure 2.22) (Chen et al., 2004; Goodwin et al., 2001; Haslam et al., 2008; Moore et al., 2000a). In addition, we observed induction of *CYP3A5*, *ALAS1*, *POR*, and *UGT1A1*, which had not been previously reported to be induced by hyperforin. The high correlation of expression changes of a broad set (n=33) of DMET genes following hyperforin (1 µM) or rifampicin treatment of human hepatocytes (r_s= 0.96) is in agreement with the assumption that both substances induce gene expression only via PXR activation (Figure 2.22). Although this finding may not be surprising, it has not been reported before and it helps to further specify the DDI potential of hyperforin. Treatment with the phloroglucinol derivatives also led to expression changes of the investigated DMET genes, which were, however, more modest compared to hyperforin and appeared to be PXR-independent as most PXR target genes were not affected, except for an approximately 2-fold induction of *CYP2C9* and *CYP2B6* by Hyp7 (1 µM). This is further supported by the weak correlations to the changes caused by rifampicin treatment (Figure 2.22). Whether other ligand-dependent nuclear receptors like CAR, GR, FXR, LXR, or VDR are involved in this response appears unlikely as the gene expression changes did not appear to match their known gene target profiles (Zanger and Schwab, 2013).

Only Hyp4 showed a moderate correlation (r_s= 0.73) with the rifampicin expression profile at higher concentration (50 µM), although none of the DMET genes, except *CYP1A2*, was significantly regulated by this compound (Figure 2.22). In contrast to the results obtained from the reporter assays, Hyp4 did not induce CYP3A4 expression in the primary human hepatocytes (Figure 2.22 and Figure 2.23B). Given the high concentrations needed to activate the CYP3A4 promoter in HepG2 cells, it is

conceivable that these concentrations were not reached in hepatocytes, e.g., due to differences in transporter function in HepG2 compared to hepatocytes or due to metabolic degradation.

The potential of the phloroglucinol derivatives to activate or bind to PXR was further investigated utilizing ligand-based pharmacophores and structure-based docking approaches. These studies were performed by Prof. Sean Ekins and were published in (Kandel et al., 2014) together with results presented and discussed in this thesis (2.4 and 3.3). Ligand-based pharmacophores use known information on agonists and antagonists to identify key features for interactions and structure-based methods like docking enable one to determine if molecules will fit and have favorable interactions in crystal structures and homology models. Both these approaches have been widely used for identifying PXR agonists and antagonists (Biswas et al., 2009; Ekins et al., 2007, 2008a, 2009; Kortagere et al., 2009, 2012; Li et al., 2013; Yasuda et al., 2008), for which crystal structures exist (Chrencik et al., 2005; Noble et al., 2006; Teotico et al., 2008; Watkins et al., 2001, 2002, 2003a, 2003b; Xue et al., 2007a, 2007b)

The phloroglucinol derivatives appeared structurally distinct from hyperforin (Figure 2.18) and the physicochemical parameters would also be expected to differ, this would suggest that their protein interactions would also likely differ. For example, the lipophilicity parameter AlogP of hyperforin is considerably higher compared to the majority of the phloroglucinol derivatives, with only the TRPC6 non-activating Hyp3 being higher (Supplemental Table 9). This could also explain why Hyp3 was frequently retrieved by pharmacophores and docking (Supplemental Table 9, Supplemental Table 10 and Supplemental Table 11). It is widely known from previous work and the many crystal structures (Chrencik et al., 2005; Noble et al., 2006; Teotico et al., 2008; Watkins et al., 2001, 2002, 2003a, 2003b; Xue et al., 2007a, 2007b) that hydrophobicity is important for interaction in the LBD and at the SRC-1 antagonist site (Ekins et al., 2007). The majority of the phloroglucinol derivatives were found to have docking scores lower than the comparator compounds hyperforin and ketoconazole, suggesting they were unlikely to behave as agonists or antagonists, respectively (Supplemental Table 10 and Supplemental Table 11). The pharmacophores retrieved few of the phloroglucinols also, suggesting that they were in general, less likely to interact with PXR (Supplemental Table 9).

Together, the results presented here and those contributed by Prof. Sean Ekins (Kandel et al., 2014) showed that TRPC6-activating phloroglucinols are unable to activate or antagonize PXR. Thus, these compounds represent promising new candidates for further drug development as antidepressants with improved safety because they lack the DDI potential of hyperforin and SJW.

3.4   Conclusion and future perspective

Nuclear receptors have been shown to be a source of inter- and intra-individual variability in liver metabolism of humans. As it has been discussed in the previous sections, the aim of this work was to assess the regulomes of the NRs CAR, PXR and PPARα, by which they contribute to this variability. This was investigated using genome-wide mRNA expression analysis following the activation of these NRs by their prototypical ligands in primary human hepatocyte cultures from six individual donors.

Within these different batches of hepatocytes a highly variable basal gene expression was detectable. This variability reflects the genetic diversity of the donors but also the variety of non-genetic factors permanently influencing gene expression within individuals. One factor that may contributes to heterogeneity within hepatocyte batches but also to the metabolic capacity of human liver in general is the post-translational modification (PTMS) of NRs, which was shown to modulate basal and induced activity of these transcription factors. An interesting example for such PTMs is the reported PKA dependent phosphorylation of PXR that was shown to alter PXR activity and expression of *CYP3A4*. Thus, the impact of PKA on the transcriptional expression of genes involved in drug metabolism was investigated in a PXR and CAR dependent manner in order to assess the contribution of PKA to the variability of the drug metabolizing capacity of human liver.

The NR PXR is an important regulator of DMET but also a sensor of a variety of drugs. The variability of the drug metabolizing capacity introduced by drug-dependent PXR activation was shown to impact the metabolism of other concomitantly taken therapeutics, which is one major source of DDIs. Thus, new therapeutics that lack PXR activation potential and hence the ability to cause such DDIs are needed. For this purpose, the Dr. Willmar Schwabe GmbH engineered molecules as substitutes for the antidepressant compound hyperforin, a strong PXR activator, based on its phloroglucinol core structure. Herein, a set of these phloroglucinol derivatives was investigated to identify molecules that lack PXR activation potential, and therefore represent promising candidates that could serve as new drugs.

This work showed that in primary human hepatocytes, PXR, CAR, and PPARα regulated a highly overlapping but distinct set of genes coding for DMET, including several genes previously not shown to be regulated by these NRs and thus displaying novel target genes. For PXR and CAR, this extends the list of genes, by which these NRs influence drug metabolism or contribute to DDIs. These observations further clearly indicate that besides PXR and CAR, PPARα is a potent regulator of drug metabolism *in vitro*. This strongly suggests that PPARα contributes to intra- and inter-individual variability of drug detoxifying function of human liver and thus may potentially be involved in adverse drug reactions like DDIs.

Compared with animal models or liver-derived cell lines, primary human hepatocytes are still the best currently available *in vitro* system to investigate human liver metabolism and its regulation. However, gene expression is highly variable among PHH batches from different donors due to genetic but also non-genetic factors. Thus, data analysis is challenging and limits the general prediction of transcriptional changes following a specific perturbation, as the provoked effects have to be strong or highly conserved among individuals to remain significant. Still, such data can be used to improve pharmacokinetic and pharmacodynamics models or used to predict DDIs. However, this variability reflects the heterogeneity of the population and therefore, such data might be valuable to investigate or predict drug response and DDIs in terms of personalized therapy.

It was further shown that PXR downregulates several genes involved in fatty acid catabolism and gluconeogenesis and upregulates genes of lipid *de novo* synthesis, including several genes where such relation was not reported so far. These observations provide further starting points to explain how PXR activation contributes to altered glucose and lipid levels or disease states like hepatic steatosis or metabolic syndrome. These genome-wide expression data are further used in a systems biology approach to generate a metabolic flux model of the central energy metabolism of human hepatocytes in order to predict metabolic changes following the activation of CAR, PXR and PPARα. It remains to be elucidated, how and under which physiological conditions these NRs contribute to the regulation of their potential target genes presented here. Such data are imperative to understand and predict

transcriptional and subsequent metabolic changes associated with CAR, PXR and PPARα.

Additionally, PKA activity has been identified as a determinant of drug metabolism *in vitro* by strongly reducing PXR- and CAR-mediated or basal expression and activity of CYP1A1, CYP2B6, CYP2C8 and CYP3A4, but also expression of ABCB1 and UGT1A1. These could be linked to the PKA-mediated repression of PXR and CAR transactivation capacity that may involve phosphorylation of these NRs. Thus, signals that activate PKA may contribute to intra-individual variability in the drug metabolizing capacity of the liver by decreasing expression of DMET genes in humans. It remains to be investigated whether conditions like fasting or stress that are shown to activate PKA are also able to influence hepatic drug metabolism *in vivo*. Nevertheless, these findings may be useful in the future in order to adjust drug dosing to, for example, PKA activating hormone levels to avoid drug failure. The extent, to which PKA-dependent phosphorylation or other PTMs of NRs contribute to altered drug metabolizing capacity or further important hepatic metabolic properties *in vivo*, remains to be investigated in detail. However, it is conceivable that such modifications of NR activity contribute to intra- and inter-individual variability in drug response and thus presents an additional issue in drug therapy, which has to be considered.

Considering the unintentional impact of drug-dependent NR activation on drug metabolism, in the last part of this work, developmental drugs designed as substitutes for hyperforin, lacking its PXR dependent DDI potential, were investigated in an *in vitro* study for their potential to activate PXR. It was previously shown that five of the herein investigated synthetic acylated phloroglucinol derivatives activate TRPC6 with similar potency as hyperforin. In this work it was shown that all TRPC6-activating compounds also lack PXR activation and provoked only moderate gene expression changes in primary human hepatocytes, which was further supported by *in silico* pharmacophore approaches and docking studies. Taken together, these results demonstrate that these compounds represent promising new candidates for further drug development as antidepressants with improved safety because they lack the DDI potential of hyperforin and SJW. This study can serve as an instructive example that pharmacologic activity and PXR-mediated activation of drug

metabolism are not necessarily linked to each other, an insight that should be helpful in future drug development strategies to avoid induction-based DDIs already during the early phases of development.

4   Materials

The following tables include all essential products and equipment used for this work.

Table 4.1 List of reagents, chemicals and kits

Reagents, chemicals and kits	Company
GE Sample Loading Reagent (20x)	Fluidigm, Amsterdam, Netherlands
2-mercaptoethanol	Sigma-Aldrich, Steinheim, Germany
Assay Loading Reagent (2x)	Fluidigm, Amsterdam, Netherlands
400µL Human Insulin, INSUMAN Rapid (40 I.E.)	Sanofi, Frankfurt, Germany
4'-hydroxy mephentoin, [$_2$H^3] 4'-hydroxy mephentoin	chemical synthesis (Richter et al., 2004)
Passive Lysis Buffer (5x)	Promega, Madison, USA
8-bromoadenosine 3':5'- Cyclic Monophosphate sodium (8-bromo cAMP)	Sigma-Aldrich, Steinheim, Germany
Acetonotrile LC-MS	Riedel de Haen, Seelze, Germany
Acrylamide/Bis (30:0.8)	Bio-Rad, Munich, Germany
Affymetrix GeneChip® WT Terminal Epression, 3'-Amplification Reagent and Hybridization Controls	Affymetrix, Santa Clara, USA
Affymetrix GeneChip® WT Terminal Labeling	Affymetrix, Santa Clara, USA
Affymetrix® GeneChip® Eukaryotic Poly-A RNA Control Kit	Affymetrix, Santa Clara, USA
Ammoniumpersulfate (APS)	Merck, Darmstadt
Amodiaquin N-desethyl amodiaquin, [$_2$H^5] N-desethyl amodiaquin	Toronto Research Chemicals, Toronto
Atorvastatin o-/p-hydroxy atorvastatin, [$_2$H^5] o-/p-hydroxy atorvastatin	Toronto Research Chemicals, Toronto
Beetle-Juice KIT	P.J.K.-GmbH, Kleinblittersdorf, Germany
Bromophenolblue	Sigma-Aldrich, Steinheim, Germany
Bupropion hydrochloride, hydroxy bupropion hydrochloride, [$_2$H^3] hydroxy bupropion hydrochloride	chemical synthesis (Richter et al., 2004)
Chlorzoxazone	Sigma-Aldrich, Steinheim
CITCO (6-(4-Chlorophenyl)imidazo[2,1-b][1,3]thiazole-5-carbaldehyde O-(3,4-dichlorobenzyl)oxime)	Sigma-Aldrich, Steinheim, Germany
D,L-Sulforaphane	Sigma-Aldrich, Steinheim, Germany
Dexamethasone (1mM)	Sigma-Aldrich, Steinheim, Germany
Dimethyl sulfoxide (DMSO)	Sigma-Aldrich, Steinheim, Germany
DMEM without Phenol Red	GIBCO, Carslbad, USA
Dulbecco's Phosphate Buffered Saline (DPBS)	GIBCO, Carslbad, USA
Ethanol absolute for analysis	Merck, Darmstadt, Germany
Ethylenediaminetetraacetic acid (EDTA)	Sigma-Aldrich, Steinheim, Germany
Fetal Bovine Serum Gold	PAA Laboratories GmbH, Pasching, Austria
GeneChip® HuGene 1.0ST Array	Affymetrix, Santa Clara, USA
GeneChip® Hybridization, Wash & Stain Kit	Affymetrix, Santa Clara, USA
Glucagon	Sigma-Aldrich, Steinheim, Germany
Glycine	Serva, Heidelberg, Germany
Hepes (1M)	GIBCO, Carslbad, USA
Hydrocortisone (50mg/ml)	Pfizer Pharma GmbH, Berlin, Germany
Hyp1; (1,1'-(2,4,6-Trihydroxy-1,3-phenylene)bis-1-isopentanone)	Preclinical Research Department of Dr. Willmar Schwabe, Karlsruhe, Germany
Hyp2; (1,1'-(2,4,6-Trihydroxy-1-phenylene)-1-	Preclinical Research Department of Dr.

Reagents, chemicals and kits	Company
isopentanone)	Willmar Schwabe, Karlsruhe, Germany
Hyp3; (1,1'-(2,4,6-Trihydroxy-1,3-phenylene) bis-1-decahexanone)	Preclinical Research Department of Dr. Willmar Schwabe, Karlsruhe, Germany
Hyp4; (1,1'-(2,6-Trihydroxy-4-Methoxy-1,3-phenylene) bis-1-isopentanone)	Preclinical Research Department of Dr. Willmar Schwabe, Karlsruhe, Germany
Hyp5; (1,1'-(2,4,6-Trihydroxy-1,3-phenylene)bis-1-isohexanone)	Preclinical Research Department of Dr. Willmar Schwabe, Karlsruhe, Germany
Hyp6; (1,1'-(2,4,6-Trihydroxy-1,3-phenylene))	Preclinical Research Department of Dr. Willmar Schwabe, Karlsruhe, Germany
Hyp7; (1,1'-(2,4,6-Trihydroxy-1,3-phenylene))	Preclinical Research Department of Dr. Willmar Schwabe, Karlsruhe, Germany
Hyp8; (1,1'-(2,4,6-Trihydroxy-1,3-phenylene))	Preclinical Research Department of Dr. Willmar Schwabe, Karlsruhe, Germany
Hyp9; (1,1'-(2,4,6-Trihydroxy-1,3-phenylene)bis-1-hexanone)	Preclinical Research Department of Dr. Willmar Schwabe, Karlsruhe, Germany
Hyperforin	Sigma-Aldrich, Steinheim, Germany
L-Glutamin (200mM)	GIBCO, Carslbad, USA
Lipofectamin®RNAiMAX Transfection Reagent	Invitrogen, Carlsbad, USA
Methanol	Roth, Karlsruhe, Germany
Non-essential amino acids 100 x (NEAA)	GIBCO, Carslbad, USA
Nuclease-Free Water	Ambion, Austen, USA
Penicillin/Streptomycin (10000 U/ml, 10mg/ml)	GIBCO, Carlsbad, USA
Phenacetin	Sigma-Aldrich, Steinheim, Germany
Pierce™BCA Protein Assay Kit	Thermo Scientific, Waltham, USA
Ponceau S-solution	Sigma-Aldrich, Steinheim, Germany
Potassium chloride (KCl)	Merck, Darmstadt, Germany
Propafenone, 5-hydroxy propafenone hydrochloride	Knoll, Ludwigshafen, Germany
QAIShredder™	Qiagen, Hilden, Germany
Renilla-Juice KIT	P.J.K.-GmbH, Kleinblittersdorf, Germany
Rifampicin	Sigma-Aldrich, Steinheim, Germany
RNA 6000 Nano Kit	Agilent Technologies, Waldbronn, Germany
RNAeasy Mini Kit	Qiagen, Hilden, Germany
Rnase-Free Dnase Set	Qiagen, Hilden, Germany
Skim milk powder	Sigma-Aldrich, Steinheim, Germany
S-mephentoin	Toronto Research Chemicals, Toronto
Sodium chloride	Merck, Darmstadt, Germany
Sodium dodecyl sulfate (SDS)	Sigma-Aldrich, Steinheim, Germany
Sodium Pyruvat (100mM)	GIBCO, Carslbad, USA
TaqMan® MicroRNA Reverse Transcription Kit	Applied Biosystems, Foster City, USA
TaqMan® Multiscribe Reverse Trasncription Kit	Applied Biosystems, Foster City, USA
TaqMan® PreAmp Master Mix	Applied Biosystems, Foster City, USA
TaqMan® Universal PCR Master Mix (2 X)	Applied Biosystems, Foster City, USA
TEMED	GIBCO, Carslbad, USA
Tolbutamid hydroxy tolbutamid	Toronto Research Chemicals, Toronto, Canada
Tris base	Roth, Karlsruhe, Germany
Triton X-100	Sigma-Aldrich, Steinheim, Germany
Trypsin 0.25 % (EDTA)	GIBCO, Carslbad, USA
Tween 20	Merck, Darmstadt, Germany
William's E Medium without L-Glutamin and Phenol Red	GIBCO, Carslbad, USA

Reagents, chemicals and kits	Company
WT Expression Kit for Affymetrix® Whole Transcript Expression Arrays	Ambion, Austin, USA
WY-14643 (4-Chloro-6-(2,3-xylidino)-2-pyrimidinylthioacetic acid, Pirinixic acid)	Sigma-Aldrich, Steinheim, Germany
Casyton	Innovatis AG, Reutlingen, Germany
Turbofect	Fermentas Life Science, St. Leon-Rot, Germany

Table 4.2 List of expendable materials

Materials	Company
384-well PCR Plate Standard	Thermo Scientific, TF-0384
96.96 Dynamic Array™ IFC	Fluidigm, Amsterdam, Netherlands
96-well PCR plate, non-skirted, clear	4titude Berlin, 4ti-0750
Tissue Culture Flask T-75 Vent Cap Red	Sarstedt Inc., Newton, USA
Nitrocellulose Membran	NeoLab GmbH. Heidelberg
Collagen I Cellware 12-well Plate	Becton Dickinson, Bedford, USA
96 Well Cell Culture Plate	Greiner Bio-One GmbH, Frickenhausen, Germany
Tube 15ml	Sarstedt, Nümbrecht, Germany
Tube 50ml	Sarstedt, Nümbrecht, Germany
C-Chip Neubauer improved	Peqlab, Erlangen, Germany
Safe-Lock Tubes 1,5ml	Eppendorf, Hamburg, Germany
Safe-Lock Tubes 2ml	Eppendorf, Hamburg, Germany
Safe-Lock Tubes 0,5ml	Eppendorf, Hamburg, Germany
MULTIWELL™ 24well	Becton Dickinson, Bedford, USA

Table 4.3 List of used siRNAs

SiRNA	Company
Silencer® select siRNA s19369 (siCAR)	Invitrogen, Carlsbad, USA
Silencer® select siRNA s16911 (siPXR)	Invitrogen, Carlsbad, USA
Silencer® select siRNA s10881 (siPPARA)	Invitrogen, Carlsbad, USA
Silencer® select Negative Control No. siRNA (siControl)	Invitrogen, Carlsbad, USA

Table 4.4 List of used TaqMan® gene expression Assays (Applied Biosystems)

Gen	Order number (Assay ID)
ABCB1	Hs01067802_m1
ABCG2	Hs00184979_m1
ADH1A	Hs00605167_g1
ALAS1	Hs00167441_m1
ALDH2	Hs00355914_m1
CPT1A	Hs00912671_m1
CYP1A1	Hs00153120_m1
CYP1A2	Hs01070374_m1
CYP2A6	Hs00868409_s1
CYP2B6	Hs03044634_m1
CYP2C19	Hs00426380_m1
CYP2C8	Hs00258314_m1
CYP2C9	Hs00426397_m1
CYP2D6	Hs00164385_m1
CYP2E1	Hs00559367_m1
CYP3A4	Hs00430021_m1
CYP3A5	Hs01070905_m1
CYP3A7	Hs00426361_m1
CYP7A1	Hs00167982_m1
DPYD	Hs00559279_m1
FABP1	Hs00155026_m1
GAPD	Hs99999905_m1
H	Hs00747232_m1
GSTA	Hs00168310_m1
2	Hs00985427_m1
GSTP	Hs00157965_m1
1	Hs00166123_m1
HMGCS2	Hs00265080_s1
HMOX1	Hs00605099_m1
ABCC2	Hs00243666_m1
NAT1	Hs00901571_m1
NAT2	Hs00159918_m1
NR1I2	Hs01037712_m1
NR1I3	Hs00287016_m1
PCK1	Hs00231882_m1
PDK4	Hs00161820_m1
POR	Hs00198527_m1
PPARA	Hs00272374_m1
SLC10A1	Hs00234899_m1
SLC22A7	Hs02511055_s1
SLCO1B1	Hs00426591_m1
SULT1B1	
UGT1A1	
UGT2B7	

Table 4.5 List and composition of cell culture media

Medium	Supplements	Used amount
Hepatocyte medium A	William's E Medium without L-Glutamin and Phenol Red (Gibco)	450ml
	Fetal Bovine Serum Gold (PAA Laboratories GmbH)	50ml
	Penicillin/Streptomycin (10000 U/ml, 10mg/ml) (Gibco)	5ml
	L-Glutamin (200mM) (Gibco)	5ml
	Human Insulin, INSUMAN Rapid (40 I.E.) (Sanofi)	400µl
	DMSO (Sigma-Aldrich)	450µl
	Dexametasone (1mM) Sigma-Aldrich)	50µl
Hepatocyte medium B (starvation)	William's E Medium without L-Glutamin and Phenol Red (Gibco)	450ml
	Penicillin/Streptomycin (10000 U/ml, 10mg/ml) (Gibco)	5ml
	L-Glutamin (200mM) (Gibco)	5ml
	Hepes (1M) (Gibco)	7.5ml
Hepatocyte medium C (seeding medium)	William's E Medium without L-Glutamin and Phenol Red (Gibco)	450ml
	Fetal Bovine Serum Gold (PAA Laboratories GmbH)	50ml
	Penicillin/Streptomycin (10000 U/ml, 10mg/ml) (Gibco)	5ml
	L-Glutamin (200mM) (Gibco)	5ml
	Human Insulin, INSUMAN Rapid (40 I.E.) (Sanofi)	400µl
	Sodium Pyruvat (100mM) (Gibco)	5ml
	Non-essential amino acids 100 x (NEAA) (Gibco)	5ml
	Hepes (1M) (Gibco)	7.5ml
	Hydrocortisone (50mg/ml) (Pfizer Pharma GmbH)	8µl
HepG2 medium	DMEM without Phenol Red (Gibco)	450ml
	Sodium Pyruvat (100mM) (Gibco)	5ml
	Fetal Bovine Serum Gold (PAA Laboratories GmbH)	50ml
	Penicillin/Streptomycin (10000 U/ml, 10mg/ml) (Gibco)	5ml

Table 4.6 List of chemicals for treatment in cell culture and their stock concentration and solvent

Chemical	Stock solution concentration	Solvent
8-bromo cAMP (Sigma-Aldrich)	1M	H_2O
Glucagon (Sigma-Aldrich)	5mg/l (1.44 µM)	H_2O
Rifampicin (Sigma-Aldrich)	10mM, 50mM	DMSO
CITCO (Sigma-Aldrich)	1mM	DMSO
D,L-Sulforaphane (Sigma-Aldrich)	10mM	DMSO
WY-14643 (Sigma-Aldrich)	50mM	DMSO
Hyp1 (Preclinical Research Department of Dr. Willmar Schwabe)	10mM, 50mM	DMSO
Hyp2 (Preclinical Research Department of Dr. Willmar Schwabe)	10mM, 50mM	DMSO
Hyp3 (Preclinical Research Department of Dr. Willmar Schwabe)	10mM, 50mM	Ethanol
Hyp4 (Preclinical Research Department of Dr. Willmar Schwabe)	10mM, 50mM	DMSO

Chemical	Stock solution concentration	Solvent
Hyp5 (Preclinical Research Department of Dr. Willmar Schwabe)	10mM, 50mM	DMSO
Hyp6 (Preclinical Research Department of Dr. Willmar Schwabe)	10mM, 50mM	DMSO
Hyp7 (Preclinical Research Department of Dr. Willmar Schwabe)	10mM, 50mM	DMSO
Hyp8 (Preclinical Research Department of Dr. Willmar Schwabe)	10mM, 50mM	DMSO
Hyp9 (Preclinical Research Department of Dr. Willmar Schwabe)	10mM, 50mM	DMSO
Hyperforin (Sigma-Aldrich)	10mM, 50mM	DMSO
DMSO (Sigma-Aldrich)	100%	
Ethanol (Merck)	100%	

Table 4.7 List of equipment

Device	Company
Agilent 2100 Bioanalyzer	Agilent Technologies, Waldbronn, Germany
Biofuge 22R/ Biofuge pico	Heraeus, Hanau, Germany
Biomark® HD System	Fluidigm, Amsterdam, Netherlands
Fastblot B44	Biometra, Göttingen, Germany
Casy®1	Innovatis AG, Reutlingen, Germany
Millipore-Anlage Milli Q	Millipore, Molsheim, France
Mini PROTEAN Tetra Elektrophorese System	Bio Rad Laboratories GmbH, München, Germany
ODYSSEY Infrared Imaging System	LI-COR Biosciences GmbH, Bad Homburg, Germany
Thermocycler PTC-200	MJ Research, Waltham, USA
Universal 32	Hettich Zentrifugen, Tuttlingen, Germany
Zentrifuge 5414 C	Eppendorf AG, Hamburg, Germany
GeneChip® Hybridation Oven 645	Affymetrix, Santa Clara, USA
GeneChip® Fluidics Station 450	Affymetrix, Santa Clara, USA
GeneChip® Scanner 7G	Affymetrix, Santa Clara, USA
Reaxtop (Vortexer)	Heidolph, Schwabach, Germany
Vibramax 100 (Pattenschütler)	Heidolph, Schwabach, Germany
Veriti 96-well thermal cycler	Applied Biosystems, Foster City, USA
Veriti 384-well thermal cycler	Applied Biosystems, Foster City, USA Bio
Power PAC 1000	Rad Laboratories GmbH, München
Centrifuge 5424 R	Eppendorf, Hamburg, Germany
Thermomixer comfort	Eppendorf, Hamburg, Germany
EnSpire® Multimode Plate Reader	PerkinElmer, Waltham, USA
OptiPlate™-96	PerkinElmer, Waltham, USA
Victor 1420 Multilabel Counter	PerkinElmer (Wallac), Waltham, USA
Olympus CKX 41	Olympus, Tokyo, Japan
Universal 320 R	Hettich Zentrifugen, Tuttlingen, Germany
HERA cell 240	Heraeus, Hanau, Germany

Table 4.8 List of software and online tools used in this work

Software and online tools	Company or Website
DAVID Bioinformatics Database	http://david.abcc.ncifcrf.gov/
Enrichr	http://amp.pharm.mssm.edu/Enrichr/
Revigo (reduce+visualize Gene Ontology)	http://revigo.irb.hr/
Affymetrix Expression Console (Build 1.3.1.187)	Affymetrix, Santa Clara, USA
Analyst® 8.0 software solution	Genedata AG, Basel, Switzerland
GraphPad Prism 5.04	GraphPad Software, Inc., La Jolla, USA
Fluidigm Real-Time PCR Analysis	Fluidigm, Amsterdam, The Netherlands
Office 2010	Microsoft, Redmond, USA
PharmaADME (Core list of standardized evidence based drug metabolising (ADME) genetic biomarkers)	www.pharmaadme.org

5   Methods

5.1   Cell culture

5.1.1 Cultivation of HepG2 cells

HepG2 cells were obtained from ATCC (Manassas, VA, USA). The cells are adherent-growing immortal liver carcinoma cells, derived from a cellular liver carcinoma of a male Caucasian. This cell line is often used as a hepatic model system, as these cells express several liver-specific proteins. HepG2 cells have a mean doubling time of about 50 to 60 h. The cells were cultured in HepG2 medium (Table 4.1) under 5 % CO_2 atmosphere at 37 °C in T-75 tissue culture flask. Every three to four days when cells were at least 85% confluent (checked by light-microscopy; Olympus CKX41) they were passaged. Therefore,the medium was aspirated and cells were washed with DPBS (Gibco). Then cells were incubated with 2 ml 0.25% trypsin-EDTA solution (Gibco) for 5 min at RT. After discarding the trypsin-EDTA solution, cells were detached using 10 ml medium (37°C) and 20 to 30% of the cells were seeded into a new flask. Cell numbers were determined using the cell counter Casy1 (Innovatis AG) as follows: 50 µl of trypsinated and in medium resuspended cells were mixed with 10ml Casyton (Innovatis AG) and measured. The calculation parameters were adjusted to the cell type according to manufacturer's guidelines.

5.1.2 Co-transfection and treatment for reporter gene analyses

The pGL3-Basic vector (Promega, Madison, USA) shown in Figure 5.1A was used as reporter gene vector. This vector contains a promoterless gene encoding the firefly luciferase. By cloning a promoter of interest in front of the luciferase gene, in eukaryotic cells transfected with this plasmid, the expression and the activity of the luciferase is dependent on this promoter. To normalize for transfection efficiency and cell number, a pRL-CMV vector (Promega, Madison, USA) was co-transfected. This vector encodes for a Renilla luciferase under the control of the constitutive active cytomegalovirus (CMV) immediate early enhancer/promoter (Figure 5.1B).
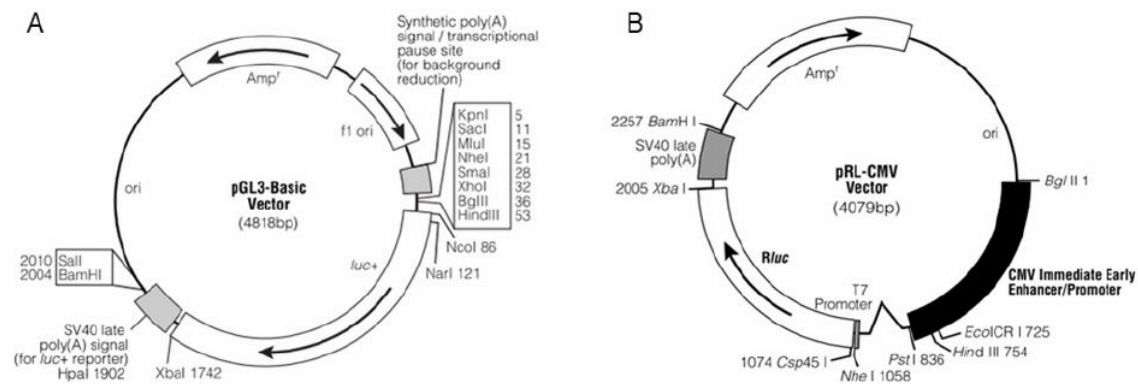
Figure 5.1 Map of circle pGL3-Basic vector (A) and pRL-CMV vector (B) from **P**romega (Madison, USA). Vector maps obtained from the technical manuals pGL3 Luciferase Reporter Vectors and pRL Renilla Luciferase Reporter Vectors (Promega, Madison, USA)

In this work, the following promoter reporter gene constructs were used. To investigate CYP3A4 promoter activation, the pGL3-CYP3A4(-7830/Δ7208-364) vector containing the XREM region of the CYP3A4 promoter with binding sites for hCAR and hPXR described by Hustert and colleagues (Hustert et al., 2001) and the pGL3-CYP3A4(-56) (Kandel et al., 2014) with only 56 nucleotides remaining of the CYP3A4 promoter were used. To examine CYP2B6 promoter activation, the pB-1.6k/PB/XREM vector, a pGL3-Basic vector derivative, described by Wang and colleagues (Wang et al., 2003) containing hCAR and hPXR binding sites of the CYP2B6 promoter and the pGL2B6-244 vector (Dissertation of Jörg Zukunft, IKP,

2005) lacking known hCAR and hPXR binding sites were used. The vectors were kindly provided by Dr. Oliver Burk, except for the pGL2B6-244 vector.

For transfection of HepG2 cells, a transfection cocktail was mixed. The transfection cocktail contained a total of 20 µl DMEM medium (without supplements), 2.5 ng pRL-CMV-Renilla (Promega, Mannheim, Germany), 80 ng of one of the pGL3-Basic vectors and 10 ng of either hPXR expression plasmid pcDhuPXR (Geick et al., 2001), hCAR expression plasmid pcDhuCAR1 (Burk et al., 2002), or the empty pcDNA3-vector (Invitrogen, Carlsbad, USA). Then, pUC18 plasmid was added to a total amount of 200 ng of DNA/well. To the DNA medium mix, 0.4 µl of Turbofect (Fermentas Life Science) was added and after inverting the cocktail for mixing, the cocktail was incubated for 20 min at RT. For reverse transfection, the whole cocktail was then transferred into a well of a 96 well cell culture plate (Greiner Bio-One GmbH) and mixed with 20,000 cells (HepG2) in 180 µl HepG2 medium (Table 4.5). Six hours after transfection, cells were treated with chemicals (Table 4.6) and cultured for further 42h at 37°C and 5% CO_2 until they were lysed. All transfections were performed in triplicates.

5.1.3 Cultivation of primary human hepatocytes

The hepatocytes used in this work were obtained from the department of General-, Visceral- and Transplantation Surgery at Charité University of Medicine, Berlin, Germany, the Center for Liver Cell Research, Department of Pediatrics and Adolescent Medicine, University of Regensburg Hospital, Regensburg, Germany and from the Department of Surgery, Grosshadern Hospital, Ludwig-Maximilians-University Munich, Germany. The use of human hepatocytes for research was approved by the local ethics committees of Berlin and Regensburg, and written informed consent was obtained from all patients. The cells were isolated in a two-step isolation procedure from liver tissue derived from partial hepatectomy (Yuan et al., 2004). The primary human hepatocytes arrived in suspension and on ice one day after surgery. The hepatocytes were transferred to a 50 ml Falcon tube containing 30 ml ice cold DPBS (Gibco) for washing. The cells were then centrifuged at 80 rpm for 5 min at 4°C (Universal 320 R; Hettich). This procedure was repeated once with fresh ice cold DPBS. After carefully removing the DPBS, cells were resuspended in

37°C warm hepatocyte medium C (Table 4.5). After determining the cell number and viability using a Neubauer cell counting chamber (Peqlab) and trypan blue for staining dead cells, cells were then seeded with 400,000 cells/ well in 1ml Medium onto 12-well collagen I coated cell culture plates (Becton Dickinson). Only hepatocyte cultures that showed cell viability above 70% were used for cell culture experiments.

5.1.4 Transfection and treatment of primary human hepatocytes

After 6 h to 24 h when cells were fully attached, the medium was exchanged to hepatocyte medium A or hepatocyte medium B (Table 4.5). For transfection of hepatocytes with siRNAs, a transfection cocktail was prepared. Therefore, 200 µL of supplement-free Williams' E medium (Gibco) were mixed with 20 nmol of one of the Silencer® Select siRNA (Table 4.3) and 3 µl Lipofectamine® RNAiMAX transfection reagent (Invitrogen) per well. The transfection cocktail was incubated for 20 min at RT before it was added to the cells after their medium was previously renewed. For chemical treatment of hepatocytes, cells were adapted for 12 h to the medium A or B (Table 4.5). Then cells were treated with chemicals (Table 4.6) in fresh medium. Cells were treated again and supplied with fresh medium very 24 h until cells were lysed.

5.2   CYP cocktail for Cytochrome P450 activity quantification

For simultaneous quantification of the activity of seven major cytochrome P450 (CYP1A2, CYP2B6, CYP2C8, CYP2C9, CYP2C19, CYP2D6 and CYP3A4), a cocktail assay (Feidt et al., 2010) was used containing a specific substrates for each of the respective isoform as shown in Table 5.1. For CYP activity determination, supernatant of cultured cells was collected and mixed with 10% (v/v) formic acid. Samples were stored at -20°C until further use. Before metabolite formation was analyzed, 10% (v/v) of respective deuterium-labeled internal standards (ITSD) for each metabolite was added to each sample. Samples were mixed by vortexing and centrifuged at 16,000 g for 5 min and afterwards transferred into vials with glas-inlets.

Table 5.1 CYP cocktail assay composition

CYP Isoform	Substrate	Molecular weight [g/mol]	Stock conc. [mM]	Solvent	Final conc. [µM]
CYP1A2	Phenacetin	179	100	DMSO	50
CYP2B6	Bupropion	256	50	H_2O	25
CYP2C8	Amodiaquin	465	10	H_2O	5
CYP2C9	Tolbutamid	270	100	DMSO	100
CYP2C19	S-Mephentoin	218	100	ACN	100
CYP2D6	Propafenone	378	10	MeOH	5
CYP3A4	Atorvastatin	559	5	ACN/H_2O	35

Stock solutions and respective solvents for the analytes and internal standards used for the cocktail assay are shown in Table 5.2. The ISTDs concentrations were 5 µM for all substances except for [$^2H_4$] Acetaminophen (10 µM). A calibration curve for each analyte in a concentration range from 0.005 µM to 5 µM was prepared using the ISTDs (0.01 µM to 10 µM for Acetaminophen). Nine calibration points were generated by serial dilution, starting from 50 µM of each analyte (100 µM for Acetaminophen). Further 5 µl of each calibration point was mixed with 40 µl of the respective cell culture medium, 10 µl ISTD and 6 µl 250 mM formic acid to prepare the calibration samples. To verify the calibration curve samples, several quality controls were included. All steps were performed parallel to samples preparation before each measurement. Measurements of samples were performed using the Agilent 6460 triple quadrupole mass spectrometer as described (Feidt et al., 2010) at the IKP-Analytics facility.

Table 5.2 CYP cocktail assay stock solution of analytes and internal standards

Analyte	Internal standard (ISTD)	Stock conc. analyte/ ISTD [mM]	MW analyte/ ISTD [g/mol]	Solvent analyte/ ISTD
Acetaminophen	[$^2H_4$] Acetaminophen	13.23/ 10	151 / 155	H_2O
Hydroxybupropion-HCl	[$^2H_3$] Hydroxybupropion-HCl	6.84 / 3.39	292 / 295	H_2O
N-Desethylamodiaquin	[$^2H_5$] N-Desethylamodiaquin	3.05 /2.94	328 / 333	MeOH
Hydroxytolbutamid	[$^2H_9$] Hydroxytolbutamid	3.49 / 3.39	287 / 296	MeOH
4-Hydroxymephentoin	[$^2H_3$] 4-Hydroxymephentoin	8.54 / 4.21	234 / 237	MeOH
5-Hydroxypropafenone-HCl	[$^2H_7$] 5-Hydroxypropafenone-HCl	5.08 / 2.5	394 / 401	MeOH/ H_2O
o-Hydroxyatorvastatin	[$^2H_5$] o-Hydroxyatorvastatin	1.58 / 1.6	633 / 624	ACN/ H_2O

5.3   Luciferase assay

For measuring luciferase activity, the cells were lysed using 50 µl passive lysis buffer (Promega) 48h after transfection and 42h after treatment. For measurement, 25 µl of the lysate were transferred to white OptiPlates™-96 (PerkinElmer Inc.). Luciferase activities were determined using beetle juice (firefly luciferase) and renilla juice (P.J.K.-GmbH). Luciferase activity was determined with the EnSpire® Multimode Plate Reader (PerkinElmer Inc.).

5.4   RNA and transcriptome analysis

5.4.1 Isolation of RNA

For the extraction and purification of RNA, RNeasy Mini Kit (Qiagen) was used. Cells were washed with DPBS (Gibco) before they were lysed with RLT buffer (RNeasy Mini Kit, Qiagen) supplemented with 1 % mercaptoethanol. The lysate then was transferred to Qiashredder-columns (Qiagen). The following purification of the RNA, including DNA digestion on the purification-columns to remove genomic DNA using the RNase free DNase Set (Qiagen), was performed according to the manufacturer's protocol. Finally, RNA was dissolved in 30 µl of nuclease free water (Ambion) and an aliquot was taken for quantification and quality control of the RNA. RNA was stored at - 80°C until further use.

5.4.2 RNA quantification

Integrity and quantity of isolated and purified RNA (5.4.1) was analyzed on the Bioanalyzer 2100 (Agilent Technologies) using the RNA 6000 Nano Kit (Agilent Technologies). Sample preparation and measurement was performed according to the manufacturer's guidelines.

5.4.3 mRNA quantification by TaqMan qRT-PCR

5.4.3.1 cDNA synthesis and preamplification

Purified RNA (5.4.1) was reverse transcribed to cDNA with TaqMan Reverse Transcription Reagents (Applied Biosystems). Therefor, between 0.1 µg to 1 µg of

RNA was added to 5 µl 10x TaqMan RT buffer, 11 µl MgCl$_2$, 10 µl dNTP-Mix, 2,5 µl Random Hexamers, 1 µl RNase Inhibitor and 1,25 µl Multiscribe Reverse Transcriptase (Applied Biosystems) to generate a 50 µl reaction mix. The following reverse transcription of the RNA to cDNA was performed in 96-Well plates (4titude) using the Thermocycler PTC-200 (MJ Research) and the temperature-protocol shown in Table 5.3.

Table 5.3 Temperature protocol for cDNA synthesis

Temperature [C°]	Time	Repeats
25	10 min	1
48	30 min	111
95	5 min	
4	for ever	

The cDNA for quantification on the BioMark System had to be pre-amplified to increase the content of cDNA. Therefore, cDNA was pre-amplified using the TaqMan® PreAmp Mastermix (2x) (Applied Biosystems) according to the manufacturer's guidelines (Fluidigm). As primers for the reaction the pooled TaqMan® Gene Expression Assays (Applied Biosystems) were used, which were applied later for the respective quantification on the BioMark HD System (Fluidigm). The generated pre-amplified cDNA was diluted 1:5 in nuclease free water (Ambion) and stored at -20°C.

5.4.3.2 Quantitative Realtime-time PCR

Quantitative Real-time PCR was performed on the BioMark HD System (Fluidigm) using 96.96 Dynamic Array Chip (Fluidigm). The cDNA reverse transcribed and pre-amplified as described in 5.4.3.1, was mixed 1:1 with a solution containing TaqMan® Universal PCR Master Mix (Applied Biosystems) and 20X GE Sample Loading Reagent (Fluidigm) at a ratio of 1:10. The TaqMan® Gene Expression Assays (Applied Biosystems) were mixed 1:1 with 2X Assay Loading Reagents (Fluidigm). Priming and loading of the chips with the sample and assay mixtures were performed with the HX Fluidigm IFC controller (Fluidigm). The final PCR reaction for quantification of cDNA was performed on the BioMark® HD system (Fluidigm). All steps were performed according to the manufacturer's guidelines (Spurgeon et al.,

2008). A list of the TaqMan® Gene Expression Assays used (Applied Biosystems) is show in Table 4.4.

5.4.4 RNA quantification using Human Gene 1.0ST Arrays

For whole-genome expression analysis, RNA isolation, quantification and quality control was performed as described in 5.4.1 and 5.4.2. All (24) used RNA samples had an RNA integrity number (RIN) > 9 (determined with the Bioanalyzer 2100 from Agilent Technologies) to ensure high quality of RNA. Whole-genome gene expression profiles of primary human hepatocytes from 3 female and 3 male donors treated with CITCO (1 µM), rifampicin (10 µM), WY-14643 (50 µM) and the vehicle DMSO were generated using Human Gene 1.0ST Arrays (Affymetrix, Santa Clara, USA). The samples were processed and measured as described in the Ambion® WT Expression Kit manual (Ambion) and the GeneChip Poly-A RNA control, the GeneChip® WT Terminal Labeling and Hybridization and the GeneChip® Expression Wash, Stain and Scan user manual (Affymetrix).

Briefly, RNA samples (50-250ng) were spiked with Poly-A controls (Affymetrix GeneChip Poly-A RNA control kit from Affymetrix). Then, using the WT Expression Kit for Affymetrix® Whole Transcript Expression arrays (Ambion), the RNA was reverse transcribed into first and second strand cDNA with random engineered primers. Afterwards, cDNA was *in vitro* transcribed into cRNA, which was then purified with magnetic nucleic acid binding beads. Purified cRNA was reverse transcribed using random primers (with incorporated dUTP nucleotides) into single stranded DNA (ssDNA) and after RNA digestion using RNase H, ssDNA was purified with magnetic nucleic acid binding beads. The ssDNA was fragmented (uracil DNA glycosylase and apurinic/apyrimidinic endonuclease 1) and labeled (deoxynucleotidyl transferase) at the incorporated dUTP using the GeneChip® WT Terminal Labeling Kit (Affymetrix). Samples were then hybridized onto the GeneChip® HuGene 1.0ST Array (Affymetrix) with the Hybridization Control Kit and after washing (GeneChip® Fluidcs Station 450, Affymetrix) the chips with the solutions supplied in the Wash and Stain Kit (Affymetrix), chips were scanned at the GeneChip® scanner 7G (Affymetrix)

After visual inspection of the obtained GeneChip images, the Affymetrix Expression Console (Affymetrix) was used for quality control of microarrays and pre-processing of expression data by log scale robust multi-array analysis (RMA; Gene Level - Default).

5.5   *In silico* analysis of whole-genome expression data

The log2 scale data obtained from RMA analysis were processed using Analyst 8.0 software solution (Genedata AG, Basel Switzerland). A total of 33,252 probe sets were present on each array. After combining synonymous probe sets and removal of probes that did not correspond to a mapped gene, 20,072 genes were selected for further analyses. Human Gene 1.0ST Array data were investigated via a linear mixed model approach, with donors as pairing variable. Genes with a Benjamini-Hochberg $p \leq 0.05$ were further analyzed using post-hoc paired student t-tests. Expression in samples treated with CITCO, rifampicin or WY-14643 was compared to the expression in the respective control treatment samples (DMSO), and for calculation of the paired effect size to obtain the log2 fold changes. Genes with a p-value $p \leq 0.05$ were assumed as differentially expressed.

5.5.1 GO and KEGG annotation enrichment analysis

The obtained lists of differentially expressed genes ($p \leq 0.05$) upon treatment with CITCO, rifampicin or WY-14643, respectively, generated as described in 5.5, were analyzed for gene ontology (GO) enrichment using Fisher's Exact Test with the Analyst® 8.0 software solution (Genedata AG, Basel Switzerland). The lists of differentially expressed genes were also used for KEGG (Kyoto Encyclopedia for Genes and Genomes) pathway enrichments (Huang et al., 2009) using the DAVID Bioinformatics Database (http://david.abcc.ncifcrf.gov/). GO terms and KEGG pathways with a Bonferroni corrected p-value ≤ 0.05 were assumed as significantly enriched.

5.6   Statistics

In section 2.1, differences in gene expression obtained from the Human Gene 1.0ST Arrays were investigated using a linear mixed model approach, with donors as pairing variable. Genes with a Benjamini-Hochberg p-value $\leq$0.05 were further analyzed using post-hoc paired student t-tests to compare expression in samples treated with CITCO, Rifampicin or WY-14643 the respective control treatment samples (DMSO) to identify significant differentially expressed genes (p-value p $\leq$0.05) and the log2 paired effect sizes. Principal component analysis was performed with default settings using Analyst 8.0 software solution (Genedata, Basel, Switzerland)

In section 2.3, differences in promoter activity (2.3.1) and gene expression (2.3.2) between treatments were analyzed using a repeated measurement (mixed model) two-way ANOVA. The treatments that showed a significant (p-value < 0.05) impact on promoter activity or gene expression were further examined by Bonferroni post-test comparing replicate means of treatments to identify significant differences (p-value < 0.05) in promoter activity or gene expression between the treatments and DMSO (control treatment) or the agonist treatments and combination of agonist and 8-bromo cAMP treatment.

In section 2.4, differences in gene expression and promoter activity between treatments were analyzed using repeated measurement one-way ANOVA. Those with Bonferroni adjusted ANOVA p-value < 0.05 were further examined by Dunnett's Multiple Comparison Test, only comparing the conditions versus the respective control. Results from co-treatment experiments were analyzed using two-way ANOVA adjusted for multiple testing (Bonferroni). Those with Bonferroni adjusted ANOVA p-value < 0.05 were further examined by paired t-test (also Bonferroni corrected) comparing the conditions versus the respective control. Statistical analyses and nonlinear curve fitting (variable slope, four parameters) were performed using GraphPad Prism 5.04 (GraphPad Software, Inc. La Jolla, CA, USA) except for the analyses of the Human Gene 1.0ST Arrays data, which were performed using Analyst 8.0 software solution (Genedata, Basel, Switzerland).

6 Reference

Ahmed, S.M., Banner, N.R., and Dubrey, S.W. (2001). Low cyclosporin-A level due to Saint-John's-wort in heart transplant patients. J. Heart Lung Transplant. *20*, 795.

Aleksunes, L.M., and Klaassen, C.D. (2012). Coordinated Regulation of Hepatic Phase I and II Drug-Metabolizing Genes and Transporters using AhR-, CAR-, PXR-, PPARα-, and Nrf2-Null Mice. Drug Metab. Dispos. *40*, 1366-1379.

Alnouti, Y., and Klaassen, C.D. (2008). Tissue distribution, ontogeny, and regulation of aldehyde dehydrogenase (Aldh) enzymes mRNA by prototypical microsomal enzyme inducers in mice. Toxicol. Sci. Off. J. Soc. Toxicol. *101*, 51-64.

Anzenbacher, P., and Zanger, U.M. (2012). Metabolism of Drugs and Other Xenobiotics (Hoboken, N.J.: Wiley-VCH Verlag GmbH & Co. KGaA).

Bachmann, K., Patel, H., Batayneh, Z., Slama, J., White, D., Posey, J., Ekins, S., Gold, D., and Sambucetti, L. (2004). PXR and the regulation of apoA1 and HDL-cholesterol in rodents. Pharmacol. Res. *50*, 237-246.

Ballet, F., Bouma, M.E., Wang, S.R., Amit, N., Marais, J., and Infante, R. (1984). Isolation, culture and characterization of adult human hepatocytes from surgical liver biopsies. Hepatol. Baltim. Md *4*, 849-854.

Barbier, O., Duran-Sandoval, D., Pineda-Torra, I., Kosykh, V., Fruchart, J.-C., and Staels, B. (2003). Peroxisome Proliferator-activated Receptor α Induces Hepatic Expression of the Human Bile Acid Glucuronidating UDP-glucuronosyltransferase 2B4 Enzyme. J. Biol. Chem. *278*, 32852-32860.

Bauer, B., Yang, X., Hartz, A.M.S., Olson, E.R., Zhao, R., Kalvass, J.C., Pollack, G.M., and Miller, D.S. (2006). In vivo activation of human pregnane X receptor tightens the blood-brain barrier to methadone through P-glycoprotein up-regulation. Mol. Pharmacol. *70*, 1212-1219.

Berg, J.M., Tymoczko, J.L., Stryer, L., and Gatto, G.J. (2013). Biochemie (Heidelberg: Springer Spektrum).

Berrabah, W., Aumercier, P., Lefebvre, P., and Staels, B. (2011). Control of nuclear receptor activities in metabolism by post-translational modifications. FEBS Lett. *585*, 1640-1650.

Bertilsson, G., Berkenstam, A., and Blomquist, P. (2001). Functionally conserved xenobiotic responsive enhancer in cytochrome P450 3A7. Biochem. Biophys. Res. Commun. *280*, 139-144.

Biswas, A., Mani, S., Redinbo, M.R., Krasowski, M.D., Li, H., and Ekins, S. (2009). Elucidating the "Jekyll and Hyde" nature of PXR: the case for discovering antagonists or allosteric antagonists. Pharm. Res. *26*, 1807-1815.

Burk, O., Tegude, H., Koch, I., Hustert, E., Wolbold, R., Glaeser, H., Klein, K., Fromm, M.F., Nuessler, A.K., Neuhaus, P., et al. (2002). Molecular mechanisms of polymorphic CYP3A7 expression in adult human liver and intestine. J. Biol. Chem. *277*, 24280-24288.

Burk, O., Koch, I., Raucy, J., Hustert, E., Eichelbaum, M., Brockmöller, J., Zanger, U.M., and Wojnowski, L. (2004). The Induction of Cytochrome P450 3A5 (CYP3A5)

in the Human Liver and Intestine Is Mediated by the Xenobiotic Sensors Pregnane X Receptor (PXR) and Constitutively Activated Receptor (CAR). J. Biol. Chem. *279*, 38379-38385.

Burk, O., Arnold, K.A., Geick, A., Tegude, H., and Eichelbaum, M. (2005). A role for constitutive androstane receptor in the regulation of human intestinal MDR1 expression. Biol. Chem. *386*, 503-513.

Chakravarthy, M.V., Lodhi, I.J., Yin, L., Malapaka, R.R.V., Xu, H.E., Turk, J., and Semenkovich, C.F. (2009). Identification of a Physiologically Relevant Endogenous Ligand for PPAR? in Liver. Cell *138*, 476-488.

Chang, T.K.H. (2009). Activation of Pregnane X Receptor (PXR) and Constitutive Androstane Receptor (CAR) by Herbal Medicines. AAPS J. *11*, 590-601.

Chatterjee, S.S., Bhattacharya, S.K., Wonnemann, M., Singer, A., and Müller, W.E. (1998). Hyperforin as a possible antidepressant component of hypericum extracts. Life Sci. *63*, 499-510.

Chawla, A., Repa, J.J., Evans, R.M., and Mangelsdorf, D.J. (2001). Nuclear receptors and lipid physiology: opening the X-files. Science *294*, 1866-1870.

Chen, Y., and Goldstein, J.A. (2009). The transcriptional regulation of the human CYP2C genes. Curr. Drug Metab. *10*, 567-578.

Chen, Y., Ferguson, S.S., Negishi, M., and Goldstein, J.A. (2004). Induction of Human CYP2C9 by Rifampicin, Hyperforin, and Phenobarbital Is Mediated by the Pregnane X Receptor. J. Pharmacol. Exp. Ther. *308*, 495-501.

Chrencik, J.E., Orans, J., Moore, L.B., Xue, Y., Peng, L., Collins, J.L., Wisely, G.B., Lambert, M.H., Kliewer, S.A., and Redinbo, M.R. (2005). Structural disorder in the complex of human pregnane X receptor and the macrolide antibiotic rifampicin. Mol. Endocrinol. *19*, 1125-1134.

Cui, J.Y., Gunewardena, S.S., Rockwell, C.E., and Klaassen, C.D. (2010). ChIPing the cistrome of PXR in mouse liver. Nucleic Acids Res.

Ding, X., and Staudinger, J.L. (2005). Repression of PXR-mediated induction of hepatic CYP3A gene expression by protein kinase C. Biochem. Pharmacol. *69*, 867-873.

Ding, X., Lichti, K., Kim, I., Gonzalez, F.J., and Staudinger, J.L. (2006). Regulation of constitutive androstane receptor and its target genes by fasting, cAMP, hepatocyte nuclear factor alpha, and the coactivator peroxisome proliferator-activated receptor gamma coactivator-1alpha. J. Biol. Chem. *281*, 26540-26551.

Ekins, S. (2004). Predicting undesirable drug interactions with promiscuous proteins in silico. Drug Discov. Today *9*, 276-285.

Ekins, S., and Erickson, J.A. (2002). A pharmacophore for human pregnane X receptor ligands. Drug Metab. Dispos. *30*, 96-99.

Ekins, S., Chang, C., Mani, S., Krasowski, M.D., Reschly, E.J., Iyer, M., Kholodovych, V., Ai, N., Welsh, W.J., Sinz, M., et al. (2007). Human Pregnane X Receptor Antagonists and Agonists Define Molecular Requirements for Different Binding Sites. Mol. Pharmacol. *72*, 592-603.

Ekins, S., Kholodovych, V., Ai, N., Sinz, M., Gal, J., Gera, L., Welsh, W.J., Bachmann, K., and Mani, S. (2008a). Computational discovery of novel low micromolar human pregnane X receptor antagonists. Mol. Pharmacol. *74*, 662-672.

Ekins, S., Reschly, E.J., Hagey, L.R., and Krasowski, M.D. (2008b). Evolution of pharmacologic specificity in the pregnane X receptor. BMC Evol. Biol. *8*, 103.

Ekins, S., Kortagere, S., Iyer, M., Reschly, E.J., Lill, M.A., Redinbo, M.R., and Krasowski, M.D. (2009). Challenges Predicting Ligand-Receptor Interactions of Promiscuous Proteins: The Nuclear Receptor PXR. PLoS Comput. Biol. *5*, e1000594.

El-Sayed, W.M. (2011). Effect of pregnane X receptor (PXR) prototype agonists on chemoprotective and drug metabolizing enzymes in mice. Eur. J. Pharmacol. *660*, 291-297.

Falkner, K.C., and Prough, R.A. (2007). Regulation of the rat glutathione S-transferase A2 gene by glucocorticoids: crosstalk through C/EBPs. Drug Metab. Rev. *39*, 401-418.

Fang, H.-L., Strom, S.C., Cai, H., Falany, C.N., Kocarek, T.A., and Runge-Morris, M. (2005). Regulation of Human Hepatic Hydroxysteroid Sulfotransferase Gene Expression by the Peroxisome Proliferator-Activated Receptor α Transcription Factor. Mol. Pharmacol. *67*, 1257-1267.

Fang, H.-L., Strom, S.C., Ellis, E., Duanmu, Z., Fu, J., Duniec-Dmuchowski, Z., Falany, C.N., Falany, J.L., Kocarek, T.A., and Runge-Morris, M. (2007). Positive and negative regulation of human hepatic hydroxysteroid sulfotransferase (SULT2A1) gene transcription by rifampicin: roles of hepatocyte nuclear factor 4alpha and pregnane X receptor. J. Pharmacol. Exp. Ther. *323*, 586-598.

Feidt, D.M., Klein, K., Hofmann, U., Riedmaier, S., Knobeloch, D., Thasler, W.E., Weiss, T.S., Schwab, M., and Zanger, U.M. (2010). Profiling induction of cytochrome p450 enzyme activity by statins using a new liquid chromatography-tandem mass spectrometry cocktail assay in human hepatocytes. Drug Metab. Dispos. Biol. Fate Chem. *38*, 1589-1597.

Ferguson, S.S., LeCluyse, E.L., Negishi, M., and Goldstein, J.A. (2002). Regulation of Human CYP2C9 by the Constitutive Androstane Receptor: Discovery of a New Distal Binding Site. Mol. Pharmacol. *62*, 737-746.

Ferguson, S.S., Chen, Y., LeCluyse, E.L., Negishi, M., and Goldstein, J.A. (2005). Human CYP2C8 is transcriptionally regulated by the nuclear receptors constitutive androstane receptor, pregnane X receptor, glucocorticoid receptor, and hepatic nuclear factor 4alpha. Mol. Pharmacol. *68*, 747-757.

Forman, B.M., Chen, J., and Evans, R.M. (1997). Hypolipidemic drugs, polyunsaturated fatty acids, and eicosanoids are ligands for peroxisome proliferator-activated receptors α and δ. Proc. Natl. Acad. Sci. *94*, 4312-4317.

Gao, J., and Xie, W. (2012). Targeting xenobiotic receptors PXR and CAR for metabolic diseases. Trends Pharmacol. Sci.

Geick, A., Eichelbaum, M., and Burk, O. (2001). Nuclear receptor response elements mediate induction of intestinal MDR1 by rifampin. J. Biol. Chem. *276*, 14581-14587.

Germain, P., Staels, B., Dacquet, C., Spedding, M., and Laudet, V. (2006). Overview of nomenclature of nuclear receptors. Pharmacol. Rev. *58*, 685-704.

Ghonem, N.S., Ananthanarayanan, M., Soroka, C.J., and Boyer, J.L. (2014). Peroxisome proliferator-activated receptor α activates human multidrug resistance

transporter 3/ATP-binding cassette protein subfamily B4 transcription and increases rat biliary phosphatidylcholine secretion. Hepatol. Baltim. Md *59*, 1030-1042.

Godoy, P., Hewitt, N.J., Albrecht, U., Andersen, M.E., Ansari, N., Bhattacharya, S., Bode, J.G., Bolleyn, J., Borner, C., Bottger, J., et al. (2013). Recent advances in 2D and 3D in vitro systems using primary hepatocytes, alternative hepatocyte sources and non-parenchymal liver cells and their use in investigating mechanisms of hepatotoxicity, cell signaling and ADME. Arch. Toxicol. *87*, 1315-1530.

Goodwin, B., Hodgson, E., and Liddle, C. (1999). The orphan human pregnane X receptor mediates the transcriptional activation of CYP3A4 by rifampicin through a distal enhancer module. Mol. Pharmacol. *56*, 1329-1339.

Goodwin, B., Moore, L.B., Stoltz, C.M., McKee, D.D., and Kliewer, S.A. (2001). Regulation of the Human CYP2B6 Gene by the Nuclear Pregnane X Receptor. Mol. Pharmacol. *60*, 427-431.

Goodwin, B., Hodgson, E., D'Costa, D.J., Robertson, G.R., and Liddle, C. (2002). Transcriptional Regulation of the Human CYP3A4Gene by the Constitutive Androstane Receptor. Mol. Pharmacol. *62*, 359-365.

Guillouzo, A., Morel, F., Fardel, O., and Meunier, B. (1993). Use of human hepatocyte cultures for drug metabolism studies. Toxicology *82*, 209-219.

Gutmann, H., Poller, B., Büter, K.B., Pfrunder, A., Schaffner, W., and Drewe, J. (2006). Hypericum perforatum: which constituents may induce intestinal MDR1 and CYP3A4 mRNA expression? Planta Med. *72*, 685-690.

Guzelian, J., Barwick, J.L., Hunter, L., Phang, T.L., Quattrochi, L.C., and Guzelian, P.S. (2006). Identification of Genes Controlled by the Pregnane X Receptor by Microarray Analysis of mRNAs from Pregnenolone 16α-carbonitrile Treated Rats. Toxicol. Sci. Off. J. Soc. Toxicol. *94*, 379-387.

Hagenbuch, B., and Meier, P.J. (2004). Organic anion transporting polypeptides of the OATP/ SLC21 family: phylogenetic classification as OATP/ SLCO superfamily, new nomenclature and molecular/functional properties. Pflüg. Arch. Eur. J. Physiol. *447*, 653-665.

Hart, S.N., Li, Y., Nakamoto, K., Subileau, E., Steen, D., and Zhong, X. (2010). A Comparison of Whole Genome Gene Expression Profiles of HepaRG Cells and HepG2 Cells to Primary Human Hepatocytes and Human Liver Tissues. Drug Metab. Dispos. *38*, 988-994.

Haslam, I.S., Jones, K., Coleman, T., and Simmons, N.L. (2008). Induction of P-glycoprotein expression and function in human intestinal epithelial cells (T84). Biochem. Pharmacol. *76*, 850-861.

Hernandez, J.P., Mota, L.C., and Baldwin, W.S. (2009). Activation of CAR and PXR by Dietary, Environmental and Occupational Chemicals Alters Drug Metabolism, Intermediary Metabolism, and Cell Proliferation. Curr. Pharmacogenomics Pers. Med. *7*, 81-105.

Hewitt, N.J., Bühring, K.U., Dasenbrock, J., Haunschild, J., Ladstetter, B., and Utesch, D. (2001). Studies comparing in vivo:in vitro metabolism of three pharmaceutical compounds in rat, dog, monkey, and human using cryopreserved hepatocytes, microsomes, and collagen gel immobilized hepatocyte cultures. Drug Metab. Dispos. Biol. Fate Chem. *29*, 1042-1050.

Heydel, J.-M., Garnier, P., Faure, P., and Artur, Y. (2012). Ciprofibrate regulation of rat hepatic bilirubin glucuronidation and UDP-glucuronosyltransferases expression. Eur. J. Drug Metab. Pharmacokinet. *37*, 233-240.

Huang, D.W., Sherman, B.T., and Lempicki, R.A. (2009). Bioinformatics enrichment tools: paths toward the comprehensive functional analysis of large gene lists. Nucleic Acids Res. *37*, 1-13.

Hustert, E., Haberl, M., Burk, O., Wolbold, R., He, Y.Q., Klein, K., Nuessler, A.C., Neuhaus, P., Klattig, J., Eiselt, R., et al. (2001). The genetic determinants of the CYP3A5 polymorphism. Pharmacogenetics *11*, 773-779.

Ihunnah, C.A., Jiang, M., and Xie, W. (2011). Nuclear receptor PXR, transcriptional circuits and metabolic relevance. Biochim. Biophys. Acta *1812*, 956-963.

Itoh, M., Nakajima, M., Higashi, E., Yoshida, R., Nagata, K., Yamazoe, Y., and Yokoi, T. (2006). Induction of Human CYP2A6 Is Mediated by the Pregnane X Receptor with Peroxisome Proliferator-Activated Receptor-γ Coactivator 1α. J. Pharmacol. Exp. Ther. *319*, 693 -702.

Iyer, M., Reschly, E.J., and Krasowski, M.D. (2006). Functional evolution of the pregnane X receptor. Expert Opin. Drug Metab. Toxicol. *2*, 381-397.

Kandel, B.A., Ekins, S., Leuner, K., Thasler, W.E., Harteneck, C., and Zanger, U.M. (2014). No activation of human pregnane x receptor by hyperforin-related phloroglucinols. J. Pharmacol. Exp. Ther. *348*, 393-400.

Kasper, S., Anghelescu, I.-G., Szegedi, A., Dienel, A., and Kieser, M. (2006). Superior efficacy of St John's wort extract WS® 5570 compared to placebo in patients with major depression: a randomized, double-blind, placebo-controlled, multi-center trial [ISRCTN77277298]. BMC Med. *4*, 14.

De Keyser, C.E., Becker, M.L., Uitterlinden, A.G., Hofman, A., Lous, J.J., Elens, L., Visser, L.E., van Schaik, R.H., and Stricker, B.H. (2013). Genetic variation in the PPARA gene is associated with simvastatin-mediated cholesterol reduction in the Rotterdam Study. Pharmacogenomics *14*, 1295-1304.

Klein, K., Thomas, M., Winter, S., Nussler, A.K., Niemi, M., Schwab, M., and Zanger, U.M. (2012). PPARA: a novel genetic determinant of CYP3A4 in vitro and in vivo. Clin. Pharmacol. Ther. *91*, 1044-1052.

Klemow, K.M., Bartlow, A., Crawford, J., Kocher, N., Shah, J., and Ritsick, M. (2011). Medical Attributes of St. John's Wort (Hypericum perforatum). In Herbal Medicine: Biomolecular and Clinical Aspects, I.F.F. Benzie, and S. Wachtel-Galor, eds. (Boca Raton (FL): CRC Press),.

Kliewer, S.A., Sundseth, S.S., Jones, S.A., Brown, P.J., Wisely, G.B., Koble, C.S., Devchand, P., Wahli, W., Willson, T.M., Lenhard, J.M., et al. (1997). Fatty acids and eicosanoids regulate gene expression through direct interactions with peroxisome proliferator-activated receptors α and γ. Proc. Natl. Acad. Sci. *94*, 4318-4323.

Kliewer, S.A., Goodwin, B., and Willson, T.M. (2002). The nuclear pregnane X receptor: a key regulator of xenobiotic metabolism. Endocr. Rev. *23*, 687-702.

Knight, T.R., Choudhuri, S., and Klaassen, C.D. (2008). Induction of hepatic glutathione S-transferases in male mice by prototypes of various classes of microsomal enzyme inducers. Toxicol. Sci. Off. J. Soc. Toxicol. *106*, 329-338.

Kobayashi, K., Sueyoshi, T., Inoue, K., Moore, R., and Negishi, M. (2003). Cytoplasmic accumulation of the nuclear receptor CAR by a tetratricopeptide repeat protein in HepG2 cells. Mol. Pharmacol. *64*, 1069-1075.

Kobayashi, K., Yamagami, S., Higuchi, T., Hosokawa, M., and Chiba, K. (2004). Key Structural Features of Ligands for Activation of Human Pregnane X Receptor. Drug Metab. Dispos. *32*, 468-472.

Kodama, S., Koike, C., Negishi, M., and Yamamoto, Y. (2004). Nuclear receptors CAR and PXR cross talk with FOXO1 to regulate genes that encode drug-metabolizing and gluconeogenic enzymes. Mol. Cell. Biol. *24*, 7931-7940.

Kodama, S., Moore, R., Yamamoto, Y., and Negishi, M. (2007). Human nuclear pregnane X receptor cross-talk with CREB to repress cAMP activation of the glucose-6-phosphatase gene. Biochem. J. *407*, 373-381.

Kok, T., Bloks, V.W., Wolters, H., Havinga, R., Jansen, P.L.M., Staels, B., and Kuipers, F. (2003). Peroxisome proliferator-activated receptor alpha (PPARalpha)-mediated regulation of multidrug resistance 2 (Mdr2) expression and function in mice. Biochem. J. *369*, 539-547.

Komoroski, B.J., Zhang, S., Cai, H., Hutzler, J.M., Frye, R., Tracy, T.S., Strom, S.C., Lehmann, T., Ang, C.Y.W., Cui, Y.Y., et al. (2004). Induction and Inhibition of Cytochromes P450 by the St. John's Wort Constituent Hyperforin in Human Hepatocyte Cultures. Drug Metab. Dispos. *32*, 512-518.

Konno, Y., Negishi, M., and Kodama, S. (2008). The roles of nuclear receptors CAR and PXR in hepatic energy metabolism. Drug Metab. Pharmacokinet. *23*, 8-13.

Kortagere, S., Chekmarev, D., Welsh, W.J., and Ekins, S. (2009). Hybrid Scoring and Classification Approaches to Predict Human Pregnane X Receptor Activators. Pharm. Res. *26*, 1001-1011.

Kortagere, S., Krasowski, M.D., and Ekins, S. (2012). Ligand- and structure-based pregnane X receptor models. Methods Mol. Biol. *929*, 359-375.

Kretschmer, X.C., and Baldwin, W.S. (2005). CAR and PXR: xenosensors of endocrine disrupters? Chem. Biol. Interact. *155*, 111-128.

Laakmann, G., Schüle, C., Baghai, T., and Kieser, M. (1998). St. John's wort in mild to moderate depression: the relevance of hyperforin for the clinical efficacy. Pharmacopsychiatry *31 Suppl 1*, 54-59.

Lalloyer, F., and Staels, B. (2010). Fibrates, Glitazones, and Peroxisome Proliferator-Activated Receptors. Arterioscler. Thromb. Vasc. Biol. *30*, 894-899.

Lambert, C.B., Spire, C., Claude, N., and Guillouzo, A. (2009). Dose- and time-dependent effects of phenobarbital on gene expression profiling in human hepatoma HepaRG cells. Toxicol. Appl. Pharmacol. *234*, 345-360.

Lecluyse, E.L., and Alexandre, E. (2010). Isolation and culture of primary hepatocytes from resected human liver tissue. Methods Mol. Biol. Clifton NJ *640*, 57-82.

Leuner, K., Kazanski, V., Müller, M., Essin, K., Henke, B., Gollasch, M., Harteneck, C., and Müller, W.E. (2007). Hyperforin—a key constituent of St. John's wort specifically activates TRPC6 channels. FASEB J. *21*, 4101-4111.

Leuner, K., Heiser, J.H., Derksen, S., Mladenov, M.I., Fehske, C.J., Schubert, R., Gollasch, M., Schneider, G., Harteneck, C., Chatterjee, S.S., et al. (2010). Simple

2,4-diacylphloroglucinols as classic transient receptor potential-6 activators--identification of a novel pharmacophore. Mol. Pharmacol. 77, 368-377.

Li, T., and Chiang, J.Y.L. (2005). Mechanism of rifampicin and pregnane X receptor inhibition of human cholesterol 7 alpha-hydroxylase gene transcription. Am. J. Physiol. Gastrointest. Liver Physiol. 288, G74-84.

Li, H., Redinbo, M.R., Venkatesh, M., Ekins, S., Chaudhry, A., Bloch, N., Negassa, A., Mukherjee, P., Kalpana, G., and Mani, S. (2013). Novel yeast-based strategy unveils antagonist binding regions on the nuclear xenobiotic receptor PXR. J. Biol. Chem. 288, 13655-13668.

Lichti-Kaiser, K., Xu, C., and Staudinger, J.L. (2009a). Cyclic AMP-dependent protein kinase signaling modulates pregnane x receptor activity in a species-specific manner. J. Biol. Chem. 284, 6639-6649.

Lichti-Kaiser, K., Brobst, D., Xu, C., and Staudinger, J.L. (2009b). A systematic analysis of predicted phosphorylation sites within the human pregnane X receptor protein. J. Pharmacol. Exp. Ther. 331, 65-76.

Lim, Y.-P., and Huang, J. (2008). Interplay of pregnane X receptor with other nuclear receptors on gene regulation. Drug Metab. Pharmacokinet. 23, 14-21.

Linde, K., Berner, M.M., and Kriston, L. (2008). St John's wort for major depression. Cochrane Database Syst. Rev. CD000448.

Ma, K., Zhang, Y., Elam, M.B., Cook, G.A., and Park, E.A. (2005). Cloning of the Rat Pyruvate Dehydrogenase Kinase 4 Gene Promoter ACTIVATION OF PYRUVATE DEHYDROGENASE KINASE 4 BY THE PEROXISOME PROLIFERATOR-ACTIVATED RECEPTOR γ COACTIVATOR. J. Biol. Chem. 280, 29525-29532.

Madabushi, R., Frank, B., Drewelow, B., Derendorf, H., and Butterweck, V. (2006). Hyperforin in St. John's wort drug interactions. Eur. J. Clin. Pharmacol. 62, 225-233.

Maglich, J.M., Sluder, A., Guan, X., Shi, Y., McKee, D.D., Carrick, K., Kamdar, K., Willson, T.M., and Moore, J.T. (2001). Comparison of complete nuclear receptor sets from the human, Caenorhabditis elegans and Drosophila genomes. Genome Biol. 2, RESEARCH0029.

Maglich, J.M., Parks, D.J., Moore, L.B., Collins, J.L., Goodwin, B., Billin, A.N., Stoltz, C.A., Kliewer, S.A., Lambert, M.H., Willson, T.M., et al. (2003). Identification of a novel human constitutive androstane receptor (CAR) agonist and its use in the identification of CAR target genes. J. Biol. Chem. 278, 17277-17283.

Mai, I., Bauer, S., Perloff, E.S., Johne, A., Uehleke, B., Frank, B., Budde, K., and Roots, I. (2004). Hyperforin content determines the magnitude of the St John's Wort-cyclosporine drug interaction*. Clin. Pharmacol. Ther. 76, 330-340.

Mandard, S., Stienstra, R., Escher, P., Tan, N.S., Kim, I., Gonzalez, F.J., Wahli, W., Desvergne, B., Muller, M., and Kersten, S. (2007). Glycogen synthase 2 is a novel target gene of peroxisome proliferator-activated receptors. Cell. Mol. Life Sci. 64, 1145-1157.

Mangelsdorf, D.J., and Evans, R.M. (1995). The RXR heterodimers and orphan receptors. Cell 83, 841-850.

Mangelsdorf, D.J., Thummel, C., Beato, M., Herrlich, P., Schütz, G., Umesono, K., Blumberg, B., Kastner, P., Mark, M., Chambon, P., et al. (1995). The nuclear receptor superfamily: The second decade. Cell *83*, 835-839.

Miao, J., Fang, S., Bae, Y., and Kemper, J.K. (2006). Functional inhibitory cross-talk between constitutive androstane receptor and hepatic nuclear factor-4 in hepatic lipid/glucose metabolism is mediated by competition for binding to the DR1 motif and to the common coactivators, GRIP-1 and PGC-1alpha. J. Biol. Chem. *281*, 14537-14546.

Molnár, F., Küblbeck, J., Jyrkkärinne, J., Prantner, V., and Honkakoski, P. (2013). An update on the constitutive androstane receptor (CAR). Drug Metabol. Drug Interact. *28*, 79-93.

Moore, D.D., Kato, S., Xie, W., Mangelsdorf, D.J., Schmidt, D.R., Xiao, R., and Kliewer, S.A. (2006). International Union of Pharmacology. LXII. The NR1H and NR1I receptors: constitutive androstane receptor, pregnene X receptor, farnesoid X receptor alpha, farnesoid X receptor beta, liver X receptor alpha, liver X receptor beta, and vitamin D receptor. Pharmacol. Rev. *58*, 742-759.

Moore, L.B., Goodwin, B., Jones, S.A., Wisely, G.B., Serabjit-Singh, C.J., Willson, T.M., Collins, J.L., and Kliewer, S.A. (2000a). St. John's wort induces hepatic drug metabolism through activation of the pregnane X receptor. Proc. Natl. Acad. Sci. U. S. A. *97*, 7500-7502.

Moore, L.B., Parks, D.J., Jones, S.A., Bledsoe, R.K., Consler, T.G., Stimmel, J.B., Goodwin, B., Liddle, C., Blanchard, S.G., Willson, T.M., et al. (2000b). Orphan nuclear receptors constitutive androstane receptor and pregnane X receptor share xenobiotic and steroid ligands. J. Biol. Chem. *275*, 15122-15127.

Moore, L.B., Maglich, J.M., McKee, D.D., Wisely, B., Willson, T.M., Kliewer, S.A., Lambert, M.H., and Moore, J.T. (2002). Pregnane X receptor (PXR), constitutive androstane receptor (CAR), and benzoate X receptor (BXR) define three pharmacologically distinct classes of nuclear receptors. Mol. Endocrinol. Baltim. Md *16*, 977-986.

Moreau, A., Téruel, C., Beylot, M., Albalea, V., Tamasi, V., Umbdenstock, T., Parmentier, Y., Sa-Cunha, A., Suc, B., Fabre, J.-M., et al. (2009). A novel pregnane X receptor and S14-mediated lipogenic pathway in human hepatocyte. Hepatology *49*, 2068-2079.

Moya, M., Gómez-Lechón, M.J., Castell, J.V., and Jover, R. (2010). Enhanced steatosis by nuclear receptor ligands: a study in cultured human hepatocytes and hepatoma cells with a characterized nuclear receptor expression profile. Chem. Biol. Interact. *184*, 376-387.

Mukherjee, S., and Mani, S. (2010). Orphan nuclear receptors as targets for drug development. Pharm. Res. *27*, 1439-1468.

Müller, W.E. (2003). Current St. John's wort research from mode of action to clinical efficacy. Pharmacol. Res. *47*, 101-109.

Mutoh, S., Sobhany, M., Moore, R., Perera, L., Pedersen, L., Sueyoshi, T., and Negishi, M. (2013). Phenobarbital Indirectly Activates the Constitutive Active Androstane Receptor (CAR) by Inhibition of Epidermal Growth Factor Receptor Signaling. Sci. Signal. *6*, ra31.

Nakae, J., Kitamura, T., Silver, D.L., and Accili, D. (2001). The forkhead transcription factor Foxo1 (Fkhr) confers insulin sensitivity onto glucose-6-phosphatase expression. J. Clin. Invest. *108*, 1359-1367.

Nakamura, K., Moore, R., Negishi, M., and Sueyoshi, T. (2007). Nuclear Pregnane X Receptor Cross-talk with FoxA2 to Mediate Drug-induced Regulation of Lipid Metabolism in Fasting Mouse Liver. J. Biol. Chem. *282*, 9768-9776.

Nakata, K., Tanaka, Y., Nakano, T., Adachi, T., Tanaka, H., Kaminuma, T., and Ishikawa, T. (2006). Nuclear receptor-mediated transcriptional regulation in Phase I, II, and III xenobiotic metabolizing systems. Drug Metab. Pharmacokinet. *21*, 437-457.

Pharmacokinetic interactions with rifampicin : clinical relevance. Clin. Pharmacokinet.

Niemi, M., Backman, J.T., Fromm, M.F., Neuvonen, P.J., and Kivistö, K.T. (2003). *42,*

819-850.

Nishimura, J., Dewa, Y., Okamura, T., Muguruma, M., Jin, M., Saegusa, Y., Umemura, T., and Mitsumori, K. (2008). Possible involvement of oxidative stress in fenofibrate-induced hepatocarcinogenesis in rats. Arch. Toxicol. *82*, 641-654.

Noble, S.M., Carnahan, V.E., Moore, L.B., Luntz, T., Wang, H., Ittoop, O.R., Stimmel, J.B., Davis-Searles, P.R., Watkins, R.E., Wisely, G.B., et al. (2006). Human PXR Forms a Tryptophan Zipper-Mediated Homodimer. Biochemistry (Mosc.) *45*, 8579-8589.

Odom, D.T., Zizlsperger, N., Gordon, D.B., Bell, G.W., Rinaldi, N.J., Murray, H.L., Volkert, T.L., Schreiber, J., Rolfe, P.A., Gifford, D.K., et al. (2004). Control of pancreas and liver gene expression by HNF transcription factors. Science *303*, 1378-1381.

Osabe, M., and Negishi, M. (2011). Active ERK1/2 Protein Interacts with the Phosphorylated Nuclear Constitutive Active/Androstane Receptor (CAR; NR1I3), Repressing Dephosphorylation and Sequestering CAR in the Cytoplasm. J. Biol. Chem. *286*, 35763-35769.

Pascussi, J.M., Gerbal-Chaloin, S., Drocourt, L., Assénat, E., Larrey, D., Pichard-Garcia, L., Vilarem, M.J., and Maurel, P. (2004). Cross-talk between xenobiotic detoxication and other signalling pathways: clinical and toxicological consequences. Xenobiotica Fate Foreign Compd. Biol. Syst. *34*, 633-664.

Patel, D.D., Knight, B.L., Soutar, A.K., Gibbons, G.F., and Wade, D.P. (2000). The effect of peroxisome-proliferator-activated receptor-alpha on the activity of the cholesterol 7 alpha-hydroxylase gene. Biochem. J. *351*, 747-753.

Patel, J., Buddha, B., Dey, S., Pal, D., and Mitra, A.K. (2004). In vitro interaction of the HIV protease inhibitor ritonavir with herbal constituents: changes in P-gp and CYP3A4 activity. Am. J. Ther. *11*, 262-277.

Peng, H., Zhu, Q.-S., Zhong, S., and Levy, D. (2013). Transcription of the human microsomal epoxide hydrolase gene (EPHX1) is regulated by an HNF-

4α/CAR/RXR/PSF complex. Biochim. Biophys. Acta *1829*, 1000-1009.

Piscitelli, S.C., Burstein, A.H., Chaitt, D., Alfaro, R.M., and Falloon, J. (2000). Indinavir concentrations and St John's wort. The Lancet *355*, 547-548.

Pondugula, S.R., Brimer-Cline, C., Wu, J., Schuetz, E.G., Tyagi, R.K., and Chen, T. (2009). A Phosphomimetic Mutation at Threonine-57 Abolishes Transactivation

113

Activity and Alters Nuclear Localization Pattern of Human Pregnane X Receptor. Drug Metab. Dispos. *37*, 719-730.

Prueksaritanont, T., Richards, K.M., Qiu, Y., Strong-Basalyga, K., Miller, A., Li, C., Eisenhandler, R., and Carlini, E.J. (2005). Comparative effects of fibrates on drug metabolizing enzymes in human hepatocytes. Pharm. Res. *22*, 71-78.

Pyper, S.R., Viswakarma, N., Yu, S., and Reddy, J.K. (2010). PPARα: energy combustion, hypolipidemia, inflammation and cancer. Nucl. Recept. Signal. *8*, e002.

Rakhshandehroo, M., Sanderson, L.M., Matilainen, M., Stienstra, R., Carlberg, C., de Groot, P.J., Müller, M., and Kersten, S. (2007). Comprehensive analysis of PPARalpha-dependent regulation of hepatic lipid metabolism by expression profiling. PPAR Res. *2007*, 26839.

Rakhshandehroo, M., Hooiveld, G., Müller, M., and Kersten, S. (2009). Comparative analysis of gene regulation by the transcription factor PPARalpha between mouse and human. PloS One *4*, e6796.

Raucy, J.L., and Lasker, J.M. (2013). Cell-based systems to assess nuclear receptor activation and their use in drug development. Drug Metab. Rev. *45*, 101-109.

Rhee, J., Inoue, Y., Yoon, J.C., Puigserver, P., Fan, M., Gonzalez, F.J., and Spiegelman, B.M. (2003). Regulation of hepatic fasting response by PPAR? coactivator-1? (PGC-1): Requirement for hepatocyte nuclear factor 4? in gluconeogenesis. Proc. Natl. Acad. Sci. U. S. A. *100*, 4012-4017.

Rogue, A., Lambert, C., Spire, C., Claude, N., and Guillouzo, A. (2012). Interindividual variability in gene expression profiles in human hepatocytes and comparison with HepaRG cells. Drug Metab. Dispos. Biol. Fate Chem. *40*, 151-158.

Roques, B.B., Leghait, J., Lacroix, M.Z., Lasserre, F., Pineau, T., Viguié, C., and Martin, P.G.P. (2013). The nuclear receptors pregnane X receptor and constitutive androstane receptor contribute to the impact of fipronil on hepatic gene expression linked to thyroid hormone metabolism. Biochem. Pharmacol. *86*, 997-1039.

Rosenfeld, J.M., Vargas, R., Xie, W., and Evans, R.M. (2003). Genetic profiling defines the xenobiotic gene network controlled by the nuclear receptor pregnane X receptor. Mol. Endocrinol. Baltim. Md *17*, 1268-1282.

Rowan, B.G., Garrison, N., Weigel, N.L., and O'Malley, B.W. (2000). 8-Bromo-Cyclic AMP Induces Phosphorylation of Two Sites in SRC-1 That Facilitate Ligand-Independent Activation of the Chicken Progesterone Receptor and Are Critical for Functional Cooperation between SRC-1 and CREB Binding Protein. Mol. Cell. Biol. *20*, 8720-8730.

Schröder, A., Wollnik, J., Wrzodek, C., Dräger, A., Bonin, M., Burk, O., Thomas, M., Thasler, W.E., Zanger, U.M., and Zell, A. (2011). Inferring statin-induced gene regulatory relationships in primary human hepatocytes. Bioinforma. Oxf. Engl. *27*, 2473-2477.

Schwabe, W. (1997). Stable extract of Hypericum perforatum L., process for preparing the same pharmaceutical composition.

Schwabe, W. (1998). Stable extract of Hypericum perforatum L., a method for producing the same, and corresponding pharmaceutical preparations.

Senekeo-Effenberger, K., Chen, S., Brace-Sinnokrak, E., Bonzo, J.A., Yueh, M.-F., Argikar, U., Kaeding, J., Trottier, J., Remmel, R.P., Ritter, J.K., et al. (2007). Expression of the Human UGT1 Locus in Transgenic Mice by 4-Chloro-6-(2,3-xylidino)-2-pyrimidinylthioacetic Acid (WY-14643) and Implications on Drug Metabolism through Peroxisome Proliferator-Activated Receptor α Activation. Drug Metab. Dispos. *35*, 419-427.

Singer, A., Wonnemann, M., and Müller, W.E. (1999). Hyperforin, a Major Antidepressant Constituent of St. John's Wort, Inhibits Serotonin Uptake by Elevating Free Intracellular Na+1 1. J. Pharmacol. Exp. Ther. *290*, 1363-1368.

Sinz, M.W. (2013). Evaluation of pregnane X receptor (PXR)-mediated CYP3A4 drug-drug interactions in drug development. Drug Metab. Rev. *45*, 3-14.

Sousa, M., Pozniak, A., and Boffito, M. (2008). Pharmacokinetics and pharmacodynamics of drug interactions involving rifampicin, rifabutin and antimalarial drugs. J. Antimicrob. Chemother. *62*, 872-878.

Staudinger, J.L., Goodwin, B., Jones, S.A., Hawkins-Brown, D., MacKenzie, K.I., LaTour, A., Liu, Y., Klaassen, C.D., Brown, K.K., Reinhard, J., et al. (2001). The nuclear receptor PXR is a lithocholic acid sensor that protects against liver toxicity. Proc. Natl. Acad. Sci. U. S. A. *98*, 3369-3374.

Staudinger, J.L., Xu, C., Biswas, A., and Mani, S. (2011). Post-translational modification of pregnane x receptor. Pharmacol. Res. Off. J. Ital. Pharmacol. Soc.

Sueyoshi, T., Kawamoto, T., Zelko, I., Honkakoski, P., and Negishi, M. (1999). The Repressed Nuclear Receptor CAR Responds to Phenobarbital in Activating the Human CYP2B6 Gene. J. Biol. Chem. *274*, 6043-6046.

Sugatani, J., Kojima, H., Ueda, A., Kakizaki, S., Yoshinari, K., Gong, Q.H., Owens, I.S., Negishi, M., and Sueyoshi, T. (2001). The phenobarbital response enhancer module in the human bilirubin UDP-glucuronosyltransferase UGT1A1 gene and regulation by the nuclear receptor CAR. Hepatol. Baltim. Md *33*, 1232-1238.

Sugatani, J., Mizushima, K., Osabe, M., Yamakawa, K., Kakizaki, S., Takagi, H., Mori, M., Ikari, A., and Miwa, M. (2008). Transcriptional regulation of human UGT1A1 gene expression through distal and proximal promoter motifs: implication of defects in the UGT1A1 gene promoter. Naunyn. Schmiedebergs Arch. Pharmacol. *377*, 597-605.

Sui, Y., Ai, N., Park, S.-H., Rios-Pilier, J., Perkins, J.T., Welsh, W.J., and Zhou, C. (2012). Bisphenol A and Its Analogues Activate Human Pregnane X Receptor. Environ. Health Perspect. *120*, 399-405.

Teotico, D.G., Bischof, J.J., Peng, L., Kliewer, S.A., and Redinbo, M.R. (2008). Structural Basis of Human PXR Activation by the Hops Constituent Colupulone. Mol. Pharmacol. *74*, 1512-1520.

Thomas, M., Burk, O., Klumpp, B., Kandel, B.A., Damm, G., Weiss, T.S., Klein, K., Schwab, M., and Zanger, U.M. (2013). Direct transcriptional regulation of human hepatic cytochrome P450 3A4 (CYP3A4) by peroxisome proliferator-activated receptor alpha (PPARα). Mol. Pharmacol. *83*, 709-718.

Tien, E.S., and Negishi, M. (2006). Nuclear receptors CAR and PXR in the regulation of hepatic metabolism. Xenobiotica Fate Foreign Compd. Biol. Syst. *36*, 1152-1163.

Timsit, Y.E., and Negishi, M. (2007). CAR and PXR: the xenobiotic-sensing receptors. Steroids *72*, 231-246.

Tirona, R.G., Lee, W., Leake, B.F., Lan, L.-B., Cline, C.B., Lamba, V., Parviz, F., Duncan, S.A., Inoue, Y., Gonzalez, F.J., et al. (2003). The orphan nuclear receptor HNF4alpha determines PXR- and CAR-mediated xenobiotic induction of CYP3A4. Nat. Med. *9*, 220-224.

Tojima, H., Kakizaki, S., Yamazaki, Y., Takizawa, D., Horiguchi, N., Sato, K., and Mori, M. (2012). Ligand dependent hepatic gene expression profiles of nuclear receptors CAR and PXR. Toxicol. Lett. *212*, 288-297.

Tolson, A.H., and Wang, H. (2010). Regulation of drug-metabolizing enzymes by xenobiotic receptors: PXR and CAR. Adv. Drug Deliv. Rev. *62*, 1238-1249.

Treiber, K., Singer, A., Henke, B., and Muller, W.E. (2005). Hyperforin activates nonselective cation channels (NSCCs). Br. J. Pharmacol. *145*, 75-83.

Tsamandouras, N., Dickinson, G., Guo, Y., Hall, S., Rostami-Hodjegan, A., Galetin, A., and Aarons, L. (2014). Identification of multiple polymorphisms effect on the pharmacokinetics of simvastatin and simvastatin acid using a population modeling approach. Clin. Pharmacol. Ther.

Ueda, A., Hamadeh, H.K., Webb, H.K., Yamamoto, Y., Sueyoshi, T., Afshari, C.A., Lehmann, J.M., and Negishi, M. (2002). Diverse roles of the nuclear orphan receptor CAR in regulating hepatic genes in response to phenobarbital. Mol. Pharmacol. *61*, 1-6.

Viollet, B., Kahn, A., and Raymondjean, M. (1997). Protein kinase A-dependent phosphorylation modulates DNA-binding activity of hepatocyte nuclear factor 4. Mol. Cell. Biol. *17*, 4208-4219.

Vlachojannis, J., Cameron, M., and Chrubasik, S. (2011). Drug interactions with St. John's wort products. Pharmacol. Res. *63*, 254-256.

Wada, T., Gao, J., and Xie, W. (2009). PXR and CAR in energy metabolism. Trends Endocrinol. Metab. TEM *20*, 273-279.

Wahli, W., and Michalik, L. (2012). PPARs at the crossroads of lipid signaling and inflammation. Trends Endocrinol. Metab. *23*, 351-363.

Wang, H., Faucette, S., Sueyoshi, T., Moore, R., Ferguson, S., Negishi, M., and LeCluyse, E.L. (2003). A novel distal enhancer module regulated by pregnane X receptor/constitutive androstane receptor is essential for the maximal induction of CYP2B6 gene expression. J. Biol. Chem. *278*, 14146-14152.

Wang, Y.-M., Ong, S.S., Chai, S.C., and Chen, T. (2012). Role of CAR and PXR in xenobiotic sensing and metabolism. Expert Opin. Drug Metab. Toxicol. *8*, 803-817.

Watkins, R.E., Wisely, G.B., Moore, L.B., Collins, J.L., Lambert, M.H., Williams, S.P., Willson, T.M., Kliewer, S.A., and Redinbo, M.R. (2001). The human nuclear xenobiotic receptor PXR: structural determinants of directed promiscuity. Science *292*, 2329-2333.

Watkins, R.E., Noble, S.M., and Redinbo, M.R. (2002). Structural insights into the promiscuity and function of the human pregnane X receptor. Curr. Opin. Drug Discov. Devel. *5*, 150-158.

Watkins, R.E., Davis-Searles, P.R., Lambert, M.H., and Redinbo, M.R. (2003a). Coactivator binding promotes the specific interaction between ligand and the pregnane X receptor. J. Mol. Biol. *331*, 815-828.

Watkins, R.E., Maglich, J.M., Moore, L.B., Wisely, G.B., Noble, S.M., Davis-Searles, P.R., Lambert, M.H., Kliewer, S.A., and Redinbo, M.R. (2003b). 2.1 A crystal structure of human PXR in complex with the St. John's wort compound hyperforin. Biochemistry (Mosc.) *42*, 1430-1438.

Wilkening, S., Stahl, F., and Bader, A. (2003). Comparison of Primary Human Hepatocytes and Hepatoma Cell Line Hepg2 with Regard to Their Biotransformation Properties. Drug Metab. Dispos. *31*, 1035-1042.

Xie, W., Barwick, J.L., Simon, C.M., Pierce, A.M., Safe, S., Blumberg, B., Guzelian, P.S., and Evans, R.M. (2000). Reciprocal activation of xenobiotic response genes by nuclear receptors SXR/PXR and CAR. Genes Dev. *14*, 3014-3023.

Xue, Y., Moore, L.B., Orans, J., Peng, L., Bencharit, S., Kliewer, S.A., and Redinbo, M.R. (2007a). Crystal structure of the pregnane X receptor-estradiol complex provides insights into endobiotic recognition. Mol. Endocrinol. *21*, 1028-1038.

Xue, Y., Chao, E., Zuercher, W.J., Willson, T.M., Collins, J.L., and Redinbo, M.R. (2007b). Crystal Structure of the PXR-T1317 Complex Provides a Scaffold to Examine the Potential for Receptor Antagonism. Bioorg. Med. Chem. *15*, 2156-2166.

Yasuda, K., Ranade, A., Venkataramanan, R., Strom, S., Chupka, J., Ekins, S., Schuetz, E., and Bachmann, K. (2008). A comprehensive in vitro and in silico analysis of antibiotics that activate pregnane X receptor and induce CYP3A4 in liver and intestine. Drug Metab. Dispos. *36*, 1689-1697.

Yoshinari, K., Yoda, N., Toriyabe, T., and Yamazoe, Y. (2010). Constitutive androstane receptor transcriptionally activates human CYP1A1 and CYP1A2 genes through a common regulatory element in the 5'-flanking region. Biochem. Pharmacol. *79*, 261-269.

Yuan, J., Liu, L., Shimada, M., Wang, A., Ruhnke, M., Heeckt, P., Muller, A.R., Nussler, N.C., Neuhaus, P., and Nussler, A. (2004). Induction, expression and maintenance of cytochrome P450 isoforms in long-term cultures of primary human hepatocytes. ALTEX *21 Suppl 3*, 3-11.

Zanger, U.M., and Schwab, M. (2013). Cytochrome P450 enzymes in drug metabolism: Regulation of gene expression, enzyme activities, and impact of genetic variation. Pharmacol. Ther. *138*, 103-141.

Zanger, U.M., Turpeinen, M., Klein, K., and Schwab, M. (2008). Functional pharmacogenetics/genomics of human cytochromes P450 involved in drug biotransformation. Anal. Bioanal. Chem. *392*, 1093-1108.

Zhou, J., Zhai, Y., Mu, Y., Gong, H., Uppal, H., Toma, D., Ren, S., Evans, R.M., and Xie, W. (2006). A novel pregnane X receptor-mediated and sterol regulatory element-binding protein-independent lipogenic pathway. J. Biol. Chem. *281*, 15013-15020.

11 Supplements

Supplemental Table 1 List of significantly (paired t-test p≤0.05) genes in primary human hepatocytes upon CITCO treatment. Fold changes are calculated comparing CITCO and DMSO treated samples.

Gene symbol	log₂ FC	p-value
AADAC	0.12	1.5E-02
AASS	-0.26	4.2E-02
ABHD12	-0.10	8.5E-03
ACLY	-0.10	7.0E-03
AFF1	-0.11	3.5E-03
AGPAT2	-0.12	4.7E-02
AGT	-0.08	5.1E-03
AGXT2L2	-0.09	2.9E-02
AKR1B10	0.36	1.8E-02
AKR1CL1	-0.19	4.5E-02
ALAS1	0.29	2.2E-02
ALDH6A1	-0.17	1.7E-02
ALG12	-0.12	1.4E-02
ALKBH5	-0.13	1.9E-03
ALOX5	-0.07	2.3E-02
AMOT	-0.13	4.4E-02
ANXA8	-0.13	4.1E-04
ANXA8L1	-0.07	3.4E-02
ANXA8L2	-0.12	6.3E-03
APBA1	-0.19	1.9E-02
AQP3	-0.18	2.1E-02
AQP7P1	-0.08	1.1E-02
AQP9	-0.08	3.0E-02
ARF6	-0.16	6.7E-03
ARHGAP1	-0.14	2.2E-03
ARHGAP9	0.24	9.6E-03
ARHGEF5	-0.12	1.7E-02
ARID5B	-0.23	1.0E-02
ATOH8	-0.18	1.1E-02
ATP11A	-0.21	1.2E-02
ATP13A2	-0.14	3.7E-03
BAAT	0.04	1.0E-02
BCL9	-0.20	1.1E-02
BHLHE40	-0.11	3.3E-03
C15orf41	-0.16	2.1E-02
C17orf63	-0.12	8.4E-03
C1orf49	0.25	8.2E-03
C20orf95	-0.05	3.6E-02
C22orf36	-0.11	3.2E-02
C2orf18	-0.16	7.5E-04
C3orf52	-0.22	1.2E-02
C5orf23	-0.13	1.1E-02
C5orf4	-0.14	9.0E-03
C9orf114	-0.12	3.6E-02
CACNA1H	-0.12	9.2E-03
CD163	-0.18	1.4E-03
CD3E	0.28	1.3E-02
CDNF	-0.18	4.7E-04
CHMP1A	-0.10	5.8E-04
CLSTN3	-0.11	3.5E-02
CORO2A	-0.17	3.5E-03
CSF1	-0.11	4.4E-03
CSNK1E	-0.08	1.7E-03

Gene symbol	log₂ FC	p-value
CTDSP1	-0.20	5.4E-03
CXCL2	-0.13	3.1E-02
CYB5A	0.08	2.9E-02
CYBB	-0.34	9.9E-03
CYFIP2	-0.07	3.2E-02
CYP1A1	0.83	1.4E-03
CYP1A2	0.41	1.8E-02
CYP2A13	0.78	7.8E-03
CYP2A6	0.77	5.8E-03
CYP2A7	0.87	5.6E-03
CYP2B6	1.00	3.2E-03
CYP2B7P1	1.13	2.4E-03
CYP2C8	0.74	1.1E-02
CYP2C9	0.35	2.5E-03
CYP2E1	-0.22	3.9E-02
CYP3A4	0.67	1.2E-02
CYP3A5	0.23	1.9E-03
CYP3A7	0.54	2.7E-03
CYP4A11	-0.19	4.6E-02
DAG1	-0.07	4.0E-02
DAP	-0.06	4.0E-02
DAPK1	-0.28	3.3E-03
DCTN1	-0.12	9.7E-03
DGKA	-0.16	2.7E-03
DLL3	0.17	1.4E-03
DNMBP	-0.13	4.0E-02
DPP9	-0.12	6.4E-03
EHD4	-0.12	1.1E-02
EPHX1	0.20	1.1E-02
ETFA	0.09	4.2E-02
ETNK2	-0.06	2.6E-02
EXT1	-0.13	5.3E-03
FAM10A5	0.22	6.2E-04
FAM120A	-0.07	1.8E-02
FAM129B	-0.20	3.3E-02
FAM169A	-0.24	3.3E-02
FAM186B	0.19	1.7E-03
FARP2	-0.16	3.3E-02
FGFR4	-0.15	2.3E-02
FLJ36000	0.31	4.5E-03
FOXN3	-0.19	1.2E-03
GAL3ST1	-0.09	3.1E-02
GPER	-0.24	1.3E-03
GPR133	-0.12	2.3E-03
GPT	-0.18	4.4E-02
GRB10	-0.25	9.4E-03
GSDM	-0.21	1.0E-03
B	-0.18	2.9E-02
GUCA2	-0.09	2.5E-02
B	-0.18	1.1E-02
H1F0	-0.19	1.7E-02
HERC2P2	-0.10	4.1E-02
HERC2P4	-0.18	1.5E-02
HERPUD2	0.10	4.3E-02
HIATL1	0.25	1.7E-02
HINT1		
HLA-DOA	0.28	7.9E-03
HNRNPA3P	-0.09	3.7E-02
1	-0.16	4.3E-02
HPGD	-0.14	3.1E-02
ID1	-0.18	2.0E-02
IDUA	-0.17	1.3E-02
IGF1	0.06	2.9E-02
IL6R	-0.14	1.3E-02
IL6ST	-0.17	1.4E-02
INPP5A	-0.25	1.6E-02
IQGAP1	0.10	3.3E-03
IRS1	-0.15	7.4E-05
ISCA1	-0.16	2.4E-02
ITGA5	-0.06	2.3E-02
ITGB3	-0.14	7.4E-03
KANK1	-0.19	8.0E-03
KANK2		
KCND3		

Gene symbol	log₂ FC	p-value
KHK	-0.17	3.3E-02
KIAA0226	-0.23	7.7E-04
KIAA0247	-0.13	2.8E-02
KIAA0652	-0.09	3.2E-02
KLC4	-0.10	1.8E-02
KLF6	-0.07	3.5E-02
KLF9	-0.14	2.7E-03
KLHL18	-0.18	1.4E-02
KRTAP5-2	-0.13	6.3E-03
LASS2	-0.05	2.8E-03
LDLRAD1	0.16	1.8E-02
LDLRAP1	-0.14	2.5E-04
LILRB4	-0.14	5.1E-03
LMNA	-0.12	9.2E-03
LOC100134 934	-0.08	3.4E-02
LOC151009	-0.16	3.4E-02
LOC440993	-0.22	1.0E-02
LRIG1	-0.12	2.1E-02
LRRC37A3	-0.08	3.4E-02
LSS	-0.13	3.2E-02
LYVE1	-0.18	1.3E-04
MAFB	-0.12	1.9E-02
MAP4	-0.05	3.5E-02
MARCH2	-0.10	2.7E-03
MASP1	-0.20	4.7E-02
MAST3	-0.18	7.7E-03
MATN2	-0.16	3.3E-02
MBD5	-0.15	2.9E-02
ME1	0.09	4.7E-02
MED24	-0.13	1.5E-02
MEGF9	-0.11	4.8E-02
MFGE8	-0.12	1.9E-02
MGST1	0.11	8.2E-03
MMACHC	-0.15	9.6E-03
MMD	-0.11	4.2E-02
MOGAT2	-0.10	4.1E-02
MON1B	-0.20	1.5E-02
MPV17L2	-0.11	2.4E-03
MTMR4	-0.10	2.8E-02
MUC13	-0.16	2.0E-02
MUS81	0.09	2.0E-02
MVP	-0.17	3.2E-02
MYO1B	0.04	3.0E-02
MYRIP	-0.17	4.4E-02
NADSYN1	-0.08	1.5E-02
NAGA	-0.23	3.7E-04
NAMPT	0.13	4.9E-03
NCBP2	0.32	6.8E-03
L	-0.11	1.8E-02
NFE2L1	-0.14	1.6E-02
NFKBIZ	-0.08	2.4E-02
NHEDC2	-0.07	4.7E-02
NIPA2	-0.14	9.7E-03
NPAS2	-0.10	9.0E-03
NPR3	-0.18	1.7E-02
NUAK2	-0.15	4.7E-02
OAS1	-0.12	1.7E-03
OPN3	0.37	2.2E-02
OSTbeta	-0.17	1.1E-02
P2RX7	0.23	1.7E-02
PAK6	-0.08	1.8E-03
PARP12	-0.16	3.4E-03
PARP3	-0.14	3.2E-03
PCTK1	-0.29	4.5E-04
PDCD1LG2	-0.18	1.2E-02
PDE11A	-0.17	9.0E-03
PDE4DI	-0.11	8.6E-03
P	-0.13	2.0E-02
PDE8A	-0.14	2.9E-02
PDHA1	-0.17	1.9E-02
PDK2	-0.09	2.6E-02
PDK4		
PEMT		

Gene symbol	log$_2$ FC	p-value	Gene symbol	log$_2$ FC	p-value
PER2	-0.10	4.1E-02	C6		
PFKFB3	-0.26	1.2E-03	STAT2	-0.23	1.0E-02
PHF17	-0.11	1.5E-03	SULT1B1	-0.09	2.1E-02
PHF2	-0.18	1.0E-02	SYT11	-0.18	3.5E-03
PHLPP1	-0.15	7.4E-03	TBC1D2B	-0.22	8.7E-03
PIK3R1	-0.07	2.8E-02	TBL1X	-0.26	2.3E-02
PLXDC2	-0.22	3.2E-03	TEP1	-0.21	1.4E-02
PLXNA2	-0.20	2.7E-03	TES	-0.09	3.6E-02
PMM1	-0.21	1.0E-02	TGFBR1	-0.18	7.7E-04
PNLDC1	0.11	2.2E-02	TGFBR2	-0.09	1.4E-02
PNRC1	-0.09	1.5E-02	TIPRL	0.15	2.1E-03
POFUT1	-0.12	3.0E-02	TM6SF2	-0.13	4.3E-02
POLS	-0.20	1.8E-02	TMEM120A	-0.16	3.2E-03
POMT2	-0.10	1.1E-05	TMEM164	-0.14	2.0E-02
POR	0.07	3.5E-02	TMEM26	0.13	3.2E-02
PPAP2A	-0.04	4.7E-02	TMEM47	-0.10	1.3E-02
PPFIA1	-0.19	4.8E-03	TMOD1	-0.16	2.7E-02
PPL	-0.20	2.8E-02	TMPPE	-0.20	2.0E-03
PPP1R3B	-0.13	3.6E-02	TMPRSS11		
PPP2R5B	-0.18	4.0E-03	A	0.35	8.8E-03
PRAMEF11	0.23	1.2E-02	TNC	-0.11	2.2E-02
PRAMEF15	0.12	2.4E-02	TNFRSF11B	-0.23	1.4E-02
PRDM2	-0.32	8.2E-04	TP53	-0.08	8.4E-03
PRKCA	-0.19	3.3E-02	TRAF7	-0.12	2.4E-02
PRSS12	-0.16	1.9E-02	TRIB1	-0.17	2.4E-03
PTCH2	0.39	1.4E-03	TRIM8	-0.10	4.5E-02
PTP4A2	-0.10	3.1E-02	TRIO	-0.14	2.5E-02
PVR	-0.09	2.1E-02	TSC22D3	-0.20	1.8E-02
PYGO2	-0.14	1.8E-02	TSKU	0.12	4.2E-02
QRICH1	-0.15	3.2E-02	TSPAN14	-0.15	1.8E-03
R3HDM2	-0.13	4.1E-02	TTC7B	-0.13	3.8E-02
RAI14	-0.14	1.6E-02	U2AF2	-0.15	2.2E-02
RAPGEF1	-0.21	2.3E-03	UAP1	-0.10	1.4E-03
RHOB	-0.07	1.5E-02	UBQLN2	-0.12	6.7E-03
RHOF	-0.14	1.6E-02	UGT1A1	0.16	2.9E-05
RICS	-0.15	2.7E-02	UGT2B4	0.14	1.7E-03
RND1	-0.14	1.4E-02	UMOD	0.21	1.3E-02
RNF103	-0.09	2.4E-02	UNC5CL	-0.12	4.3E-02
RNF157	-0.09	4.7E-02	VASP	-0.09	1.3E-02
RNF216	-0.17	8.2E-03	VAT1L	0.14	4.6E-02
RNF216L	-0.19	2.6E-02	VPS52	-0.10	4.4E-02
RNF24	-0.22	1.9E-02	WDR91	-0.18	7.6E-03
RNU2-1	0.50	4.6E-03	WDTC1	-0.14	2.4E-02
RORA	-0.10	4.9E-02	WWC1	-0.10	1.8E-02
RPL26	0.19	7.5E-03	ZBTB16	-0.15	3.7E-04
RPS18P9	0.09	1.3E-02	ZC3H12A	-0.14	1.4E-02
RXRA	-0.10	1.6E-02	ZER1	-0.10	1.6E-02
SALL1	-0.12	1.1E-02	ZFP36	-0.24	7.7E-03
SAMD4A	-0.14	2.2E-02	ZNF250	-0.11	1.2E-02
SEPT9	-0.09	4.4E-02	ZNF470	-0.23	1.0E-02
SFT2D2	0.07	3.4E-02	ZNF592	-0.17	5.9E-03
SH3BGRL2	-0.10	2.3E-02	ZNF618	-0.11	5.6E-03
SH3PXD2B	-0.19	5.1E-03			
SH3RF2	-0.13	2.5E-02			
SHPK	-0.20	7.5E-03			
SLC22A9	-0.26	3.6E-02			
SLC27A4	-0.10	1.0E-02			
SLC30A10	-0.12	3.8E-02			
SLC39A14	-0.06	1.6E-03			
SLC44A2	-0.18	8.0E-03			
SLC6A12	-0.23	1.7E-02			
SLC7A2	-0.09	4.3E-02			
SMAP2	-0.15	3.4E-02			
SMOC1	-0.20	1.1E-02			
SNAI2	-0.28	3.7E-03			
SORCS2	-0.13	3.6E-02			
SPRY4	-0.23	8.1E-04			
SRD5A2	-0.13	3.1E-02			
SRGAP2	-0.16	4.0E-02			
ST6GALNA					
C2	-0.18	1.5E-02			
ST6GALNA	-0.23	9.9E-04			

Supplemental Table 2 List of significantly (paired t-test p≤0.05) genes in primary human hepatocytes upon rifampicin treatment. Fold changes are calculated comparing rifampicin and DMSO treated samples.

Gene symbol	log₂ FC	p-value
AADAC	-0.11	1.3E-02
AASS	-0.36	1.4E-02
ABAT	-0.26	1.3E-02
ABCB1	0.60	2.0E-04
ABCB4	-0.11	1.8E-02
ABCC2	0.31	1.9E-04
ABHD12	-0.11	8.9E-03
ACAA2	-0.20	2.5E-02
ACAD11	-0.37	1.4E-02
ACADM	-0.08	2.5E-02
ACADVL	-0.14	4.7E-02
ACBD4	-0.32	8.4E-03
ACLY	0.15	1.5E-02
ACOT2	-0.21	1.6E-02
ACOX2	-0.37	5.6E-04
ACSL1	0.21	1.3E-03
ACSL5	0.16	1.4E-02
ACSM5	-0.33	1.4E-02
ADH1A	-0.83	5.9E-03
ADH1B	-1.36	1.1E-03
ADH4	-0.62	1.7E-02
ADH6	-0.33	5.1E-03
ADRA1A	-0.32	4.2E-02
ADRA1B	-0.23	2.1E-03
AFF1	-0.12	4.2E-02
AFF3	-0.23	2.1E-02
AFM	-0.63	4.9E-03
AGPAT2	-0.13	3.4E-03
AGPHD1	0.52	1.7E-02
AGT	-0.15	2.0E-03
AGXT2L1	1.36	5.0E-06
AKAP12	0.32	4.9E-03
AKR1B10	0.94	6.0E-04
AKR1CL1	-0.44	8.0E-03
AKR1D1	1.22	4.5E-05
ALAD	-0.27	8.0E-03
ALAS1	1.11	1.3E-04
ALDH6A1	-0.23	1.9E-02
ALG12	-0.09	5.7E-03
AMOT	-0.26	7.4E-04
AMOTL1	0.24	2.1E-02
ANG	-0.41	7.9E-03
ANXA8	-0.21	1.4E-02
ANXA8L1	-0.27	3.1E-03
ANXA8L2	-0.20	1.9E-02
APBA1	-0.31	7.2E-03
APOL2	-0.06	1.8E-02
AQP3	-0.30	2.2E-02
AQP7P1	-0.14	6.9E-03
ARF6	-0.13	1.9E-02
ARHGAP1	-0.15	4.3E-03
ARHGAP9	0.19	4.3E-03
ARID5B	-0.36	1.1E-02
ASB16	0.25	3.6E-02
ASPA	-0.55	2.4E-02
ATOH8	-0.41	9.3E-03
ATP11A	-0.17	1.7E-02
ATP13A2	-0.09	1.8E-03

Gene symbol	log₂ FC	p-value
ATP2B4	-0.16	2.4E-02
ATP9A	-0.28	4.3E-03
BAAT	-0.09	8.6E-03
BAIAP2L1	0.10	3.8E-03
BCAS1	0.69	6.0E-03
BCL7A	0.27	3.7E-03
BCL9	-0.18	1.7E-02
BID	0.19	5.2E-03
BTAF1	-0.19	3.3E-02
C10orf140	-0.23	5.3E-02
C15orf41	-0.19	1.3E-02
C17orf63	-0.11	2.3E-02
C17orf68	-0.14	9.2E-03
C1orf49	0.38	2.0E-03
C20orf196	0.14	8.9E-03
C22orf36	-0.18	1.8E-02
C2orf18	0.08	9.9E-03
C3orf52	-0.19	4.3E-02
C4orf32	0.33	1.6E-05
C5orf23	-0.39	4.3E-04
C5orf24	0.18	1.4E-02
C5orf4	-0.20	1.5E-02
C6	-0.47	2.2E-02
C9orf152	-0.41	2.2E-04
CA12	0.72	1.9E-03
CALM1	-0.11	5.2E-03
CALN1	0.26	1.8E-02
CARD10	0.18	3.0E-03
CAV1	-0.10	2.9E-02
CBS	0.14	1.2E-02
CCBL1	-0.23	1.3E-02
CD14	0.63	8.1E-05
CD163	-0.29	3.9E-03
CDK5RAP2	-0.28	6.3E-04
CES2	-0.10	1.1E-02
CFHR2	0.33	4.8E-04
CFHR5	0.36	7.4E-03
CGN	-0.29	6.3E-03
CLIP1	0.12	4.2E-02
CLMN	0.13	1.9E-02
CLSTN3	-0.18	9.1E-03
CNTLN	0.50	6.6E-03
COMMD7	0.18	4.9E-03
CORO2A	-0.19	1.1E-02
COX10	-0.15	2.9E-03
CPN1	-0.53	2.0E-04
CPS1	-0.30	1.2E-02
CPT1A	-0.32	2.3E-02
CPT2	-0.27	6.3E-03
CSNK1E	0.05	4.7E-02
CSRP1	0.07	6.0E-03
CTDSP1	-0.16	2.8E-02
CX3CL1	-0.32	7.1E-03
CXCL10	-0.49	7.7E-03
CXCL2	-0.57	1.6E-02
CYB5A	0.24	1.1E-04
CYBB	-0.26	3.5E-03
CYCS	0.15	3.2E-03
CYFIP2	-0.16	1.3E-02
CYP1A1	0.48	3.8E-02
CYP21A2	0.31	3.1E-02
CYP2A13	0.63	1.8E-02
CYP2A6	0.64	1.7E-02
CYP2A7	0.64	2.9E-02
CYP2B6	1.15	2.1E-03
CYP2B7P1	1.30	9.4E-04
CYP2C8	1.37	6.2E-04
CYP2C9	0.80	1.5E-03
CYP2E1	-0.59	6.8E-03
CYP2J2	-0.25	3.0E-03
CYP3A4	2.03	9.3E-04
CYP3A43	0.88	1.3E-03

Gene symbol	log₂ FC	p-value
CYP3A5	0.67	7.7E-04
CYP3A7	1.25	2.2E-04
CYP4A11	-0.70	3.6E-03
CYP4F12	0.23	3.6E-02
CYP4F3	0.34	2.3E-04
CYP4V2	-0.25	1.8E-03
CYP4X1	-0.32	4.5E-02
CYP7A1	-1.65	9.5E-03
CYP8B1	-0.31	1.3E-03
DAG1	0.08	3.5E-02
DAPK1	-0.25	8.8E-03
DCTN1	-0.12	5.1E-03
DGKA	-0.28	1.7E-03
DHCR24	0.11	3.9E-03
DHCR7	0.11	3.6E-02
DIO1	0.49	1.1E-05
DLL3	0.22	6.8E-03
DNMBP	-0.27	8.3E-03
DOCK9	0.23	1.2E-02
DOK4	0.12	2.3E-02
DTX1	-0.27	1.7E-03
DUS3L	0.09	3.3E-03
DYDC1	0.15	2.0E-02
ECH1	-0.06	3.5E-02
EEF1A2	-0.11	9.7E-03
EHD4	-0.09	2.3E-02
EIF4EBP2	-0.22	3.3E-03
ELL2	-0.16	2.9E-04
ELOVL2	-0.27	4.4E-03
ELOVL6	0.43	1.5E-03
ENTPD5	0.27	2.3E-03
EPHA1	-0.29	1.4E-02
EPHB4	0.27	3.6E-02
EPHX1	0.40	3.3E-05
ERBB3	-0.28	9.9E-03
ETFDH	-0.20	2.5E-02
ETNK2	-0.24	6.8E-03
EXT1	-0.22	3.9E-03
F13B	0.46	1.8E-03
FADS1	0.15	1.2E-03
FADS2	0.12	1.2E-03
FAM10A5	0.18	2.3E-02
FAM129B	-0.26	1.8E-02
FAM134B	-0.17	1.8E-02
FAM149A	-0.28	1.1E-02
FAM169A	-0.46	2.7E-03
FARP2	-0.18	1.5E-02
FASN	0.45	3.1E-03
FBXO8	-0.23	1.4E-02
FGF2	0.25	7.6E-03
FGFR4	-0.28	1.4E-02
FLJ36000	0.43	3.3E-02
FLJ41484	-0.22	3.0E-02
FMO5	-0.34	5.1E-03
FOXN3	-0.23	4.7E-04
FRMD4A	0.22	1.7E-03
FSTL1	-0.16	1.0E-02
G6PC	-0.49	2.0E-03
GAL3ST1	0.42	4.5E-02
GALNT2	-0.11	4.4E-02
GALT	-0.46	1.3E-02
GATM	-0.08	1.7E-02
GJB2	0.15	2.3E-02
GPD1	-0.31	8.2E-03
GPER	-0.33	3.7E-03
GPLD1	-0.39	5.7E-03
GPRC5B	0.32	4.3E-02
GPT	-0.29	6.4E-03
GPX2	0.58	1.3E-02
GRB10	-0.24	2.1E-02
GRIA3	-0.49	5.4E-04
GSTA2	0.30	1.5E-02

Gene symbol	log₂ FC	p-value	Gene symbol	log₂ FC	p-value	Gene symbol	log₂ FC	p-value
GUCA2B	-0.47	1.4E-02	MICAL3	-0.11	3.7E-02	PPAP2A	-0.16	2.0E-02
GUSBL1	-0.17	3.0E-02	MMACHC	-0.24	3.4E-03	PPFIA1	-0.12	2.1E-02
GYS2	-0.60	1.0E-02	MMD	0.30	3.5E-03	PPP1R3B	-0.31	2.1E-04
HAAO	-0.16	1.2E-02	MOGAT2	-0.21	5.5E-03	PPP2R5B	-0.14	1.8E-02
HADHB	-0.15	4.4E-02	MOSC1	-0.38	1.5E-02	PRAMEF10	1.76	3.2E-03
HAL	0.14	9.3E-03	MPV17L	0.72	3.0E-03	PRAMEF11	0.29	5.1E-03
HAO2	-0.52	7.9E-04	MSN	-0.08	1.6E-02	PRAMEF15	0.28	6.7E-03
HDAC6	-0.23	1.5E-02	MTCP1	0.26	2.1E-02	PRAMEF17	0.90	6.9E-03
HERPUD2	-0.22	8.8E-03	MTMR11	-0.43	3.1E-03	PRAMEF22	0.48	7.4E-04
HIF1A	0.17	2.4E-02	MTMR4	-0.13	1.2E-02	PRDM2	-0.26	3.7E-03
HLA-DOA	0.21	1.9E-03	MUC13	-0.34	9.9E-04	PRKAB2	-0.14	8.4E-03
HMGCS2	-0.89	4.8E-03	MVP	-0.21	1.7E-02	PRKCA	-0.20	1.3E-02
HNF4A	-0.15	9.1E-03	MYBPH	0.31	1.3E-02	PRODH2	0.35	7.8E-05
HNRNPA3P 1	0.21	5.6E-03	MYO1B	-0.11	4.7E-03	PROX1	-0.39	1.2E-03
HPGD	-0.24	3.7E-04	MYRIP	-0.35	1.1E-02	PRSS12	-0.21	1.4E-03
HSD17B6	-0.17	1.3E-02	NAGA	-0.24	6.2E-03	PRSS23	-0.27	1.5E-02
HSDL2	-0.11	2.6E-02	NAT8B	-0.19	1.9E-03	PTCH2	0.32	6.3E-03
ID1	-0.33	1.0E-02	NBEAL2	0.25	2.7E-03	PTGR1	0.16	8.0E-03
IDH1	0.25	1.5E-03	NDRG2	-0.19	3.7E-02	PTK2B	-0.27	1.2E-03
IDUA	-0.21	4.7E-03	NEFM	0.42	1.7E-02	PTPRJ	0.20	9.3E-03
IFIT1	-0.45	1.1E-02	NFE2L1	-0.12	1.2E-02	PVR	-0.14	5.9E-03
IFIT3	-0.25	2.1E-02	NFE2L2	0.34	9.2E-03	PYGO2	-0.14	9.2E-04
IGF1	-0.53	4.7E-03	NFKBIZ	-0.17	1.8E-02	QRICH1	-0.13	9.6E-03
IL6R	-0.21	4.8E-03	NHEDC2	-0.19	2.0E-03	R3HDM2	-0.26	9.5E-03
IL6ST	0.18	7.5E-03	NIPA2	-0.04	1.2E-02	RAB8B	0.43	7.4E-04
INHBC	-0.29	3.6E-03	NPPB	0.34	1.0E-02	RAPGEF4	-0.43	1.8E-02
INHBE	-0.48	5.8E-04	NPR3	-0.37	3.2E-03	RASGEF1B	-0.29	3.6E-04
INPP5A	-0.17	1.6E-02	NRBP2	-0.34	1.4E-02	RASSF4	0.16	1.7E-02
IRS1	-0.26	1.7E-02	NRG1	-0.22	6.0E-03	RDH16	-0.32	1.6E-03
ISCA1	0.25	6.4E-03	NUP88	-0.11	8.3E-03	RDH5	-0.30	7.9E-03
ITIH3	-0.14	3.1E-02	OAS1	-0.37	1.3E-03	REPS1	-0.22	6.6E-03
JUP	-0.16	8.1E-03	OASL	-0.20	9.5E-03	RETSAT	-0.14	2.0E-03
KANK1	-0.17	2.9E-03	OLA1	0.16	4.5E-03	RHOB	-0.17	9.8E-04
KANK2	-0.24	1.1E-02	OPN3	-0.14	4.1E-05	RHOC	-0.05	2.4E-02
KCND3	-0.29	1.6E-02	OSTbeta	1.71	6.8E-04	RHOU	-0.22	1.1E-02
KHK	-0.27	3.5E-03	P2RX7	-0.41	3.2E-03	RND1	-0.44	4.7E-03
KIAA0226	-0.12	1.5E-02	PAK6	0.27	1.7E-03	RNF103	-0.16	5.6E-04
KIAA0247	-0.17	3.3E-02	PALMD	-0.26	1.9E-02	RNF216	-0.12	1.4E-02
KIAA0652	-0.09	3.2E-02	PANK1	-0.22	3.5E-02	RNF216L	-0.15	2.1E-02
KIAA1598	0.18	7.8E-03	PAPD5	0.29	7.5E-03	RNU2-1	0.33	2.8E-03
KLC4	-0.24	8.5E-04	PARP12	0.11	1.8E-03	RORA	-0.28	5.2E-03
KLF6	-0.08	1.0E-02	PARP3	-0.21	9.5E-03	RPL26	0.16	2.1E-02
KLHL29	-0.19	2.4E-02	PCTK1	-0.15	1.8E-02	RUSC2	-0.06	2.6E-02
KMO	-0.44	9.4E-04	PCTP	0.24	6.3E-03	RXRA	-0.24	1.8E-03
KRTAP5-2	-0.18	1.4E-03	PDCD1LG2	-0.30	2.8E-03	SALL1	-0.20	7.8E-04
LAMB3	-0.11	2.3E-02	PDE11A	-0.29	4.0E-03	SCMH1	-0.18	9.0E-03
LAMP1	-0.10	7.0E-03	PDE4DIP	-0.20	2.1E-02	SDC4	0.16	9.6E-03
LASS2	-0.10	1.1E-02	PDE8A	-0.17	3.5E-03	SDCBP2	-0.25	4.7E-03
LCLAT1	0.17	2.8E-02	PDHA1	-0.08	3.0E-02	SEC14L4	0.75	1.1E-04
LDLRAD1	0.29	9.8E-03	PDK2	-0.19	2.3E-03	SEC16B	-0.24	2.2E-02
LECT2	-0.55	4.0E-03	PDK4	-0.55	4.8E-04	SEPT9	0.10	3.8E-04
LILRB4	-0.10	3.7E-02	PEG10	-0.57	7.6E-03	SERPINA4	-0.19	7.9E-03
LIMCH1	-0.16	7.3E-04	PER2	-0.07	2.8E-02	SERPINB1	0.46	2.6E-03
LMNA	-0.10	2.2E-02	PEX11A	-0.18	4.5E-02	SERPINB9	0.78	2.3E-03
LOC100134 934	-0.13	4.6E-02	PFKFB3	-0.24	2.6E-03	SERPINE2	0.54	1.1E-02
LPIN2	-0.22	5.8E-03	PGD	0.36	5.2E-04	SERTAD3	-0.14	8.9E-03
LRRC31	-0.26	3.9E-02	PGM2	0.41	5.5E-04	SGK2	0.56	1.7E-05
LSR	0.19	4.8E-03	PHF17	-0.19	4.0E-03	SH3BGRL2	-0.25	5.4E-03
LTBP1	-0.31	5.8E-03	PHF2	-0.16	6.4E-03	SH3PXD2B	-0.31	3.6E-03
MAFB	-0.33	1.0E-02	PIGR	0.20	4.1E-02	SIK2	-0.24	6.1E-03
MARCH2	-0.14	3.4E-04	PIK3R1	-0.15	1.2E-02	SLC13A5	0.29	2.4E-02
MARK2	-0.11	2.9E-02	PKLR	-0.33	2.5E-02	SLC16A12	-0.39	3.8E-03
MAST3	-0.16	1.1E-02	PLA1A	-0.15	3.0E-02	SLC16A13	-0.17	8.8E-04
MBD5	-0.29	6.6E-03	PLEKHG6	0.19	2.9E-02	SLC20A2	-0.26	4.5E-03
MBL2	0.51	7.1E-03	PLIN2	-0.09	3.4E-02	SLC22A7	-0.51	7.3E-03
ME1	0.33	2.7E-03	PLXDC2	-0.21	7.1E-03	SLC22A9	-0.47	5.6E-03
MEGF9	-0.19	8.7E-03	PLXNA2	-0.21	1.2E-02	SLC25A10	-0.28	7.8E-04
MFGE8	-0.17	1.2E-03	PMM1	-0.27	2.8E-03	SLC25A33	-0.18	4.9E-02
MGC39372	1.46	6.3E-04	PNRC1	-0.19	5.4E-03	SLC25A42	-0.22	6.7E-03
MGST1	0.06	2.4E-02	POFUT1	-0.08	1.6E-02	SLC27A2	0.24	1.6E-02
			POLS	-0.18	2.2E-02	SLC2A1	0.19	4.0E-02
			POR	0.36	9.0E-06	SLC30A10	-0.28	4.9E-03

Gene symbol	log2 FC	p-value
SLC44A2	-0.27	6.1E-03
SLC47A1	0.11	2.2E-02
SLC4A4	0.23	1.6E-02
SLC6A20	0.46	4.0E-04
SMA5	-0.19	2.6E-02
SMAD7	-0.15	1.7E-02
SMAP2	-0.20	5.2E-03
SMOC1	-0.25	7.1E-03
SMPDL3A	0.34	9.4E-03
SNAI2	-0.48	1.2E-03
SORCS2	-0.13	1.6E-02
SPON2	-0.26	4.9E-02
SRD5A2	-0.31	2.4E-03
SRGAP2	-0.18	1.6E-02
ST6GALNAC2	-0.38	6.4E-03
STAT2	-0.32	6.7E-03
STEAP4	-0.57	3.5E-03
SUCNR1	-0.32	7.4E-03
SULT1B1	-0.55	2.2E-04
SULT1E1	-0.97	2.3E-03
SULT2A1	0.48	8.2E-04
SYT11	-0.17	2.8E-03
TAS2R40	-0.32	1.4E-02
TAT	-0.54	7.5E-03
TBC1D2B	-0.21	1.5E-02
TBL1X	-0.34	9.1E-03
TCEA3	-0.41	5.2E-03
TEP1	-0.20	4.2E-02
TFCP2L1	0.26	1.4E-02
TGFBR1	-0.20	1.1E-02
TGFBR2	-0.09	8.3E-04
TGFBR3	-0.39	2.1E-03
THRSP	1.08	6.6E-03
TIMP3	0.15	8.7E-03
TIPRL	0.11	1.1E-02
TM6SF2	0.20	3.9E-02
TMEM120A	-0.28	5.0E-03
TMEM140	-0.24	3.8E-03
TMEM164	-0.26	8.0E-03
TMEM26	0.15	1.2E-02
TMEM47	-0.24	2.9E-03
TMEM97	0.41	2.8E-04
TMOD1	-0.31	5.0E-03
TNFRSF11B	-0.28	1.4E-03
TNFRSF19	0.14	1.1E-03
TNFRSF1B	-0.13	8.5E-03
TOX3	0.55	8.5E-05
TP53INP2	0.18	1.5E-02
TRAF3IP2	-0.13	4.3E-02
TRAF7	0.12	2.1E-02
TREH	-0.24	6.1E-03
TRIB1	-0.15	1.5E-02
TRIM31	0.52	4.9E-03
TRPV4	0.18	4.2E-02
TRUB2	-0.06	4.2E-02
TSC22D2	0.07	1.7E-02
TSC22D3	-0.37	1.4E-03
TSKU	0.27	1.9E-03
TTC7B	-0.19	5.9E-03
TULP3	-0.17	9.7E-03
TXNIP	-0.21	2.3E-02
UAP1	-0.29	9.7E-04
UGT1A1	0.30	3.4E-03
UGT2B4	0.17	6.1E-03
UMOD	0.17	3.9E-04
USP2	0.46	1.8E-02
VAT1L	0.18	1.3E-02
VLDLR	0.39	2.0E-03
VPS52	-0.13	2.1E-02
VSNL1	-0.45	4.4E-03
WDR51A	0.28	8.4E-03
WDR72	-0.54	9.4E-03
WDR91	-0.21	1.6E-02
WDTC1	-0.16	1.5E-02
WEE1	-0.19	2.2E-02
YARS	0.20	2.1E-03
ZBTB16	-0.15	1.1E-02
ZER1	-0.17	2.1E-03
ZFP36	-0.47	2.5E-03
ZNF250	-0.17	9.2E-03
ZNF592	-0.18	4.9E-03
ZNF618	-0.18	1.7E-04

Supplemental Table 3 List of significantly (paired t-test p≤0.05) genes in primary human hepatocytes upon WY-14643 treatment. Fold changes are calculated comparing WY-14643 and DMSO treated samples.

Gene	log₂ FC	p-value
AADAC	0.52	4.2E-03
AASS	-0.71	3.8E-04
ABAT	-0.37	3.1E-03
ABCB1	0.18	2.3E-02
ABCB4	0.55	2.6E-03
ABHD12	-0.12	3.8E-03
ACAA2	0.27	2.4E-02
ACADM	0.45	9.3E-03
ACADVL	0.21	2.7E-03
ACOX1	0.36	1.0E-02
ACSL1	0.59	4.1E-04
ACSL5	0.31	2.1E-03
ACSS2	-0.18	7.9E-03
ADH1A	-0.41	4.2E-02
ADH1B	-0.56	3.9E-02
ADRA1B	-0.16	1.2E-02
AFF1	-0.17	5.0E-04
AFF3	-0.13	5.0E-02
AFM	-0.26	3.4E-02
AGAP4	-0.32	1.7E-03
AGAP7	-0.32	3.7E-03
AGFG1	-0.09	7.1E-05
AGXT2L1	0.34	7.1E-03
AGXT2L2	-0.13	2.8E-02
AKR1CL1	-0.39	5.0E-03
ALAS1	0.49	1.1E-03
ALDH6A1	-0.31	2.1E-03
ALG12	-0.15	3.4E-03
ALKBH5	-0.10	4.5E-02
ALOX5	-0.24	7.0E-04
AMOT	-0.28	4.6E-05
ANGPTL4	0.46	4.0E-04
ANXA8	-0.18	5.1E-03
ANXA8L1	-0.19	5.6E-03
ANXA8L2	-0.19	2.2E-03
APBA1	-0.35	6.8E-03
APOL2	0.12	4.2E-02
AQP7P1	0.20	4.6E-03
AQP9	-0.21	4.4E-03
ARF6	-0.11	2.8E-02
ARG2	-0.45	5.2E-04
ARHGAP1	-0.14	1.2E-02
ARHGAP9	0.27	1.1E-03
ARHGEF5	-0.14	9.2E-03
ARID5B	-0.28	8.3E-03
ASB16	0.17	1.3E-02
ATP11A	-0.22	1.1E-02
ATP13A2	-0.15	5.9E-03
ATP2B4	0.28	1.7E-02
BCL9	-0.19	5.7E-03
BHLHE40	-0.17	6.5E-05
BTAF1	-0.27	7.0E-04
C10orf10	-0.14	9.4E-03
C14orf68	0.69	5.8E-04
C15orf41	-0.10	3.4E-02
C17orf63	-0.13	2.6E-02
C17orf68	-0.23	5.6E-03

Gene symbol	log₂ FC	p-value
C18orf58	-0.31	8.7E-03
C19orf12	0.18	4.2E-02
C1orf49	0.33	9.6E-03
C1orf84	-0.26	2.6E-03
C20orf69	-0.26	4.9E-04
C22orf36	-0.27	5.0E-03
C3orf52	-0.44	1.1E-03
C4orf32	0.26	2.6E-03
C5orf23	-0.32	9.0E-04
C5orf4	-0.26	8.1E-03
C5orf51	-0.19	2.8E-03
C6	-0.34	2.3E-02
C8orf47	0.20	4.3E-02
C9orf114	-0.21	6.8E-03
C9orf152	-0.27	4.7E-02
CACNA1H	-0.33	1.5E-03
CALM1	-0.13	1.5E-03
CALN1	0.29	3.4E-03
CAT	0.19	2.4E-02
CAV1	-0.15	6.1E-07
CBS	-0.21	4.2E-03
CCBL1	-0.32	8.6E-03
CD14	0.27	1.4E-03
CD163	-0.30	3.3E-03
CD36	0.64	1.3E-02
CD3E	0.36	1.3E-03
CDC25B	-0.16	5.1E-03
CDK3	0.36	2.0E-03
CDK5RAP2	-0.10	3.5E-02
CGN	-0.15	4.6E-02
CHMP1A	-0.12	4.7E-03
CIDEC	0.28	1.8E-04
CLIP1	-0.09	3.1E-03
CLSTN3	-0.25	1.8E-02
CMTM3	-0.15	1.7E-02
CNNM4	-0.23	3.5E-02
CORO2A	-0.38	5.0E-04
COX10	-0.19	3.9E-03
CPS1	-0.24	4.6E-02
CPT1A	0.75	3.4E-03
CPT2	0.41	2.4E-02
CREB3L3	1.13	1.1E-03
CSF1	-0.09	6.1E-03
CSNK1G2	-0.12	7.4E-03
CTDSP1	-0.24	8.9E-03
CX3CL1	-0.14	1.8E-02
CXCL10	-0.60	7.8E-03
CXCL2	-0.39	6.5E-04
CYB5A	0.11	1.2E-02
CYBB	-0.57	3.2E-03
CYCS	0.10	3.2E-03
CYFIP2	-0.14	1.4E-02
CYP21A2	-0.19	1.1E-02
CYP2B6	0.40	2.9E-02
CYP2C8	0.75	2.0E-03
CYP3A4	0.77	9.2E-04
CYP3A43	0.26	1.6E-02
CYP3A5	0.21	5.8E-03
CYP3A7	0.50	2.2E-03
CYP4A11	0.82	1.8E-04
CYP4A22	1.26	2.8E-03
CYP4F11	-0.18	2.2E-02
CYP4F12	-0.28	6.3E-04
CYP4F3	-0.16	8.2E-03
DAP	-0.09	3.9E-03
DAPK1	-0.36	1.6E-03
DCTN1	-0.16	4.0E-05
DENND5A	-0.18	1.5E-02
DGKA	-0.30	2.9E-03
DHDPSL	-0.26	1.3E-03
DIO1	0.19	3.8E-03
DLL3	0.19	3.3E-02

Gene symbol	log₂ FC	p-value
DNMBP	-0.22	1.1E-02
DOCK9	-0.13	1.2E-02
DOK4	-0.06	1.6E-02
DPP9	-0.14	2.4E-03
DPYSL2	-0.15	5.8E-03
DTX1	-0.19	6.3E-03
DYDC1	0.24	1.7E-03
ECH1	0.24	7.3E-03
ECHDC3	0.14	2.7E-02
EHD4	-0.16	2.8E-03
ELMO1	-0.19	5.5E-03
EPHA1	-0.13	4.4E-02
EPHB4	0.16	2.2E-02
EPHX1	0.21	3.9E-03
ERBB3	-0.27	1.1E-02
ETFA	0.29	2.1E-02
ETFB	0.15	2.7E-02
ETFDH	0.40	8.0E-03
ETNK2	-0.19	6.0E-03
EXT1	-0.21	3.9E-03
FABP1	0.93	2.0E-04
FABP4	1.18	8.4E-03
FAH	0.15	1.3E-02
FAM10A5	0.17	7.6E-03
FAM120A	-0.13	1.4E-02
FAM129B	-0.18	2.4E-02
FAM134B	-0.19	2.4E-03
FAM186B	0.16	4.8E-02
FAM83D	-0.18	1.5E-02
FARP2	-0.19	1.5E-02
FETUB	-0.23	4.5E-02
FGF2	-0.21	7.9E-03
FGF21	0.36	1.4E-03
FGFR4	-0.21	1.9E-02
FLJ41484	-0.41	1.0E-02
FLJ45248	0.38	2.3E-02
FMO5	-0.33	1.5E-03
FOXN3	-0.08	2.1E-02
GAL3ST1	-0.20	6.0E-03
GALT	0.23	4.2E-02
GLUL	0.11	4.3E-03
GPER	-0.18	3.0E-02
GPLD1	-0.25	3.7E-02
GPR133	-0.26	1.3E-02
GPRC5B	-0.15	2.1E-02
GPT	-0.35	4.8E-03
GPX2	0.16	1.7E-02
GRB10	-0.25	9.4E-03
GRIA3	-0.30	2.4E-02
GSDMB	-0.31	4.5E-03
GSTA2	0.14	4.6E-02
GUSBL1	-0.25	2.0E-03
GYS2	-0.25	2.3E-02
H1F0	-0.17	2.5E-02
HADHA	0.34	4.3E-03
HADHB	0.49	3.7E-03
HAL	-0.16	2.5E-03
HAO2	-0.17	2.1E-02
HDAC6	-0.21	8.1E-03
HEG1	-0.29	4.5E-03
HERC2P2	-0.31	4.8E-04
HERC2P4	-0.30	1.3E-03
HERPUD2	-0.11	3.3E-02
HIATL1	-0.23	1.7E-03
HINT1	0.18	1.8E-04
HLA-DOA	0.23	3.7E-03
HMGCS2	1.49	1.3E-04
HNF4A	-0.13	1.6E-02
HNRNPA3P1	0.23	1.2E-02
HPGD	-0.18	1.9E-02
HSD17B4	0.23	1.0E-02

Gene symbol	log₂ FC	p-value	Gene symbol	log₂ FC	p-value	Gene symbol	log₂ FC	p-value
HSD17B6	0.26	1.6E-04	MSN	-0.14	7.8E-04	PRKCA	-0.31	3.1E-03
HSPA1A	-0.11	7.3E-03	MTMR11	-0.31	2.6E-05	PRSS12	-0.14	1.1E-02
HSPA1B	-0.13	2.6E-02	MTMR4	-0.16	1.5E-02	PTCH2	0.34	2.0E-03
ID1	-0.15	5.3E-03	MUC13	-0.44	2.6E-03	PTGR1	0.17	1.6E-02
IDUA	-0.20	2.3E-02	MVP	-0.21	8.3E-03	PTK2B	-0.07	2.7E-02
IFIT1	0.26	2.3E-02	MYBPH	0.25	3.7E-03	PTP4A2	-0.10	2.8E-02
IGF1	-0.39	2.4E-03	MYRIP	-0.32	8.7E-03	PVR	-0.12	5.7E-03
IGSF6	-0.44	2.8E-03	NADSYN1	-0.16	3.2E-03	PYGO2	-0.25	3.6E-04
IL6R	-0.19	1.1E-02	NAGA	-0.27	1.8E-03	QRICH1	-0.13	3.7E-04
INHBC	-0.15	3.4E-02	NAGS	-0.14	4.8E-02	R3HDM2	-0.15	8.7E-03
INPP5A	-0.20	2.4E-05	NEFM	0.24	4.3E-03	RAB11FIP1	-0.22	1.3E-03
IQGAP1	-0.24	4.6E-03	NFATC2IP	-0.20	3.6E-05	RAI14	-0.22	3.9E-03
IRS1	-0.36	7.9E-03	NFE2L1	-0.12	1.6E-02	RAPGEF1	-0.11	2.1E-02
ISCA1	0.24	4.1E-03	NFKBIZ	-0.25	2.0E-04	RAPGEF4	0.32	1.8E-02
ITGA5	-0.19	1.6E-02	NHEDC2	-0.15	1.4E-02	RASGEF1B	-0.24	2.1E-02
ITGA7	-0.37	2.5E-04	NID1	-0.26	3.3E-03	RASSF4	-0.08	2.5E-02
ITGB3	-0.32	7.3E-05	NIPA2	-0.11	2.7E-04	RDH16	0.60	1.4E-03
JDP2	-0.13	4.9E-03	NPAS2	-0.13	7.0E-03	RDH5	-0.12	1.8E-02
JUP	-0.28	7.7E-03	NPR3	-0.28	8.2E-05	RHOC	-0.11	2.0E-02
KANK2	-0.15	1.8E-02	NRBP2	-0.40	1.7E-02	RHOU	-0.15	4.4E-02
KHDRBS1	-0.14	1.8E-03	NRG1	-0.25	9.3E-04	RICS	-0.29	3.9E-03
KIAA0226	-0.18	6.0E-03	NUDT16	-0.24	2.4E-03	RND1	-0.40	3.3E-03
KIAA0247	-0.17	4.0E-04	NUMB	-0.18	9.8E-03	RNF103	-0.15	3.9E-03
KIAA0652	-0.13	4.0E-04	OASL	0.36	1.9E-03	RNF157	-0.23	1.3E-03
KLC4	-0.12	3.7E-03	OPN3	-0.11	1.4E-02	RNF216	-0.13	6.4E-05
KLF10	0.17	3.3E-02	OR2A4	-0.21	8.6E-03	RNF216L	-0.26	2.3E-03
KLF11	0.38	1.3E-03	OR2A7	-0.21	4.9E-03	RNF24	-0.18	1.7E-03
KLF3	-0.20	3.7E-03	OSTbeta	0.19	1.2E-02	RNU2-1	0.18	3.8E-02
KLF6	-0.16	1.2E-03	P2RX7	-0.31	8.2E-04	RORA	-0.23	1.3E-02
KLF9	-0.13	1.5E-02	PAK6	0.27	9.2E-04	RPL26	0.22	8.6E-03
KLHL18	-0.16	1.7E-03	PANK1	0.36	2.6E-02	RPS18P9	0.09	4.8E-03
KLHL29	-0.23	5.6E-03	PARP3	-0.23	5.5E-04	RPS6KA2	-0.25	2.7E-03
KRTAP5-2	-0.17	8.6E-03	PCTK1	-0.20	1.1E-02	RUSC2	-0.24	1.1E-02
LAMB3	-0.17	6.0E-03	PCTP	0.24	6.9E-04	SAMD4A	-0.20	3.8E-03
LAMP1	-0.07	7.7E-03	PCYT2	-0.21	1.1E-02	SCHIP1	0.21	1.3E-02
LASS2	-0.06	3.5E-03	PDCD1LG2	-0.29	6.4E-03	SCMH1	-0.23	1.0E-03
LDLRAD1	0.18	1.6E-03	PDE11A	-0.32	3.2E-03	SDCBP2	0.16	4.6E-02
LILRB4	-0.19	1.0E-02	PDE4DIP	-0.30	1.4E-02	SECTM1	0.22	2.6E-04
LIMCH1	-0.17	5.1E-03	PDE8A	-0.10	3.9E-02	SERTAD3	-0.22	1.9E-03
LMNA	-0.16	2.9E-03	PDK4	0.96	1.0E-05	SGK2	0.57	6.6E-05
LOC100134 934	0.20	3.8E-03	PEG10	-0.65	2.0E-02	SH3BGRL2	0.49	5.7E-03
LOC151009	-0.32	2.4E-03	PER2	-0.20	1.8E-02	SH3PXD2B	-0.28	9.3E-03
LOC284422	0.22	3.2E-03	PEX11A	0.45	1.7E-02	SH3RF2	-0.23	4.9E-03
LOC440993	-0.32	6.2E-03	PFKFB3	-0.26	7.8E-03	SHPK	-0.13	2.7E-02
LOH12CR1	-0.25	1.7E-02	PHF17	-0.14	3.5E-03	SIK2	-0.12	2.2E-03
LPCAT3	0.32	9.6E-04	PHF2	-0.20	6.3E-03	SLC16A13	0.33	2.3E-03
LPIN1	-0.09	1.8E-02	PHLPP1	-0.12	1.9E-02	SLC25A10	-0.19	4.9E-03
LRCH1	-0.20	1.0E-02	PIK3R1	-0.16	5.7E-03	SLC25A20	0.46	2.4E-03
LRIG1	-0.17	4.1E-03	PKLR	-0.30	4.9E-03	SLC25A33	0.39	4.3E-02
LRRC31	0.65	2.4E-02	PKP4	-0.19	3.7E-03	SLC25A34	0.26	8.7E-03
LRRC37A3	-0.22	4.7E-03	PLA1A	0.35	1.6E-02	SLC25A42	0.33	4.8E-03
LSS	-0.22	6.8E-03	PLIN1	0.37	2.0E-03	SLC25A5	0.13	3.0E-04
LYVE1	-0.36	2.6E-04	PLIN2	0.76	2.9E-04	SLC27A2	0.19	1.1E-02
MAFB	-0.17	6.1E-03	PLXDC2	-0.32	2.5E-03	SLC27A4	0.10	2.3E-02
MAP4	-0.11	1.2E-03	PLXNA2	-0.24	1.7E-03	SLC39A14	-0.12	6.5E-03
MARCH2	-0.18	1.5E-02	PMM1	-0.19	4.2E-02	SLC44A2	-0.31	8.1E-04
MARK2	-0.20	3.1E-05	PNLDC1	0.23	4.6E-04	SLC47A1	-0.12	9.6E-03
MASP1	-0.39	9.9E-03	PNRC1	-0.16	1.5E-02	SLC7A2	-0.20	8.9E-03
MAST3	-0.24	6.4E-03	PNRC2	-0.89	2.1E-06	SMA5	-0.28	2.7E-03
MBD5	-0.18	6.0E-03	POLS	-0.32	1.6E-02	SMAD6	-0.23	1.6E-03
MBL2	0.76	5.8E-04	POMT2	-0.15	1.1E-02	SMAD7	-0.22	3.8E-03
ME1	0.23	1.9E-02	POR	0.29	1.7E-03	SMAP2	-0.20	6.8E-04
MED24	-0.19	3.4E-02	PPFIA1	-0.18	4.9E-03	SNAI2	-0.31	1.1E-02
MFGE8	-0.20	1.3E-03	PPL	-0.34	3.7E-03	SNAP23	-0.11	2.5E-02
MGC39372	0.33	3.2E-02	PPP2R5B	-0.23	5.2E-03	SORCS2	-0.19	1.4E-03
MGST1	0.06	4.0E-02	PRAMEF10	0.62	1.1E-03	SPON2	-0.28	7.6E-03
MICAL3	-0.16	4.3E-04	PRAMEF11	0.32	4.2E-03	SPRY4	-0.20	2.5E-03
MMACHC	-0.13	1.1E-02	PRAMEF15	0.21	1.2E-03	SRD5A2	-0.16	5.6E-03
MOGAT2	-0.14	5.0E-02	PRAMEF17	0.21	3.2E-02	SRGAP2	-0.22	5.8E-03
MON1B	-0.23	1.4E-02	PRAMEF22	0.27	1.4E-02	ST6GALNA C6	-0.19	2.2E-02
MPV17L2	-0.12	4.4E-03	PRDM2	-0.27	1.2E-03	STAT2	-0.23	3.6E-03
			PRKAB2	-0.13	1.3E-03			

131

Gene symbol	log2 FC	p-value	Gene symbol	log2 FC	p-value	Gene symbol	log2 FC	p-value
STAU1	0.19	3.5E-02	TMPPE	-0.17	1.3E-02	UBQLN2	-0.14	1.7E-03
STEAP4	-0.43	2.7E-02	TMPRSS11A	0.26	4.3E-03	UGT1A1	0.17	1.8E-02
SULT2A1	0.42	3.5E-04	TMPRSS9	-0.12	3.0E-02	UGT2B4	0.08	1.7E-02
SYT11	-0.25	6.1E-03	TNC	-0.27	8.9E-03	UMOD	0.12	4.1E-02
TAT	-0.44	6.8E-03	TNFRSF11B	-0.33	1.6E-02	UNC5CL	-0.50	1.2E-03
TBC1D1	-0.10	2.3E-03	TNFRSF21	0.22	3.5E-02	USP31	-0.11	4.7E-02
TBC1D2B	-0.31	2.9E-03	TP53	-0.14	4.7E-03	VASP	-0.13	1.9E-02
TBL1X	-0.22	1.1E-02	TREH	-0.32	4.4E-03	VAT1L	0.29	2.5E-04
TEAD1	-0.18	4.4E-03	TRIB1	-0.16	7.2E-04	VCL	-0.09	1.7E-02
TEP1	-0.33	6.1E-04	TRIM8	-0.18	1.7E-04	VPS52	-0.14	4.8E-03
TES	-0.15	7.5E-04	TRIO	-0.22	4.2E-03	WDR91	-0.19	4.0E-03
TGFBR1	-0.31	1.8E-03	TRPV4	-0.09	3.6E-02	WDTC1	-0.20	6.6E-03
TGFBR2	-0.10	1.6E-02	TRUB2	0.13	1.5E-02	WEE1	-0.44	1.6E-02
TGFBR3	-0.33	7.6E-03	TSC22D2	-0.13	4.9E-02	WWC1	-0.21	2.9E-03
TIPRL	0.17	2.5E-03	TSC22D3	-0.32	9.3E-04	ZBTB16	-0.23	6.7E-03
TM6SF2	-0.20	2.3E-02	TSKU	0.16	1.0E-02	ZC3H12A	-0.18	1.8E-03
TMBIM1	-0.09	1.8E-03	TSPAN14	-0.15	9.1E-03	ZER1	-0.13	1.5E-02
TMEM120A	-0.31	4.3E-03	TTC7B	0.23	1.3E-02	ZFP36	-0.37	8.9E-03
TMEM135	0.37	1.6E-02	TULP3	-0.16	2.1E-03	ZNF250	-0.13	1.1E-02
TMEM164	-0.27	1.3E-05	TXNIP	0.38	3.6E-03	ZNF470	-0.39	3.2E-03
TMEM26	0.18	1.4E-02	U2AF2	-0.15	1.5E-02	ZNF592	-0.23	8.6E-04
TMEM97	0.14	1.5E-02						

Supplemental table 4 List of GO-terms for biological processes identified as significantly enriched for genes differentially expressed upon rifampicin treatment

GO ID	GO term	Property Size	Universe Size	Selection Property Size	Selection Size	p-value	Bonferroni corrected p-value
GO:0044281	small molecule metabolic process	2354	15186	158	444	3.6E-26	1.9E-22
GO:0006629	lipid metabolic process	1155	15186	104	444	4.6E-26	2.4E-22
GO:0055114	oxidation-reduction process	1005	15186	95	444	2.8E-25	1.5E-21
GO:0044255	cellular lipid metabolic process	836	15186	80	444	1.6E-21	8.1E-18
GO:0006082	organic acid metabolic process	962	15186	85	444	1.3E-20	6.7E-17
GO:0019752	carboxylic acid metabolic process	884	15186	81	444	1.3E-20	6.8E-17
GO:0009410	response to xenobiotic stimulus	162	15186	34	444	7.0E-20	3.6E-16
GO:0032787	monocarboxylic acid metabolic process	420	15186	53	444	1.3E-19	6.6E-16
GO:0006805	xenobiotic metabolic process	151	15186	32	444	6.5E-19	3.3E-15
GO:0071466	cellular response to xenobiotic stimulus	153	15186	32	444	9.9E-19	5.1E-15
GO:0046395	carboxylic acid catabolic process	222	15186	32	444	7.2E-14	3.7E-10
GO:0008202	steroid metabolic process	267	15186	35	444	8.6E-14	4.4E-10
GO:0006631	fatty acid metabolic process	281	15186	35	444	4.0E-13	2.1E-09
GO:0019216	regulation of lipid metabolic process	224	15186	29	444	1.7E-11	8.7E-08
GO:0042493	response to drug	390	15186	38	444	7.5E-11	3.9E-07
GO:0008610	lipid biosynthetic process	488	15186	43	444	1.0E-10	5.4E-07
GO:0051186	cofactor metabolic process	275	15186	31	444	1.2E-10	6.3E-07
GO:0070887	cellular response to chemical stimulus	1763	15186	96	444	7.8E-10	4.0E-06
GO:0017144	drug metabolic process	32	15186	11	444	8.7E-10	4.5E-06
GO:0042221	response to chemical stimulus	3304	15186	150	444	2.1E-09	1.1E-05
GO:0006639	acylglycerol metabolic process	96	15186	17	444	2.3E-09	1.2E-05
GO:0006638	neutral lipid metabolic process	97	15186	17	444	2.7E-09	1.4E-05
GO:0009062	fatty acid catabolic process	74	15186	15	444	2.9E-09	1.5E-05
GO:0010033	response to organic substance	2067	15186	105	444	4.9E-09	2.5E-05
GO:0016042	lipid catabolic process	254	15186	27	444	7.1E-09	3.7E-05
GO:0006641	triglyceride metabolic process	91	15186	16	444	7.6E-09	3.9E-05
GO:0005996	monosaccharide metabolic process	278	15186	28	444	1.2E-08	6.4E-05
GO:0019395	fatty acid oxidation	71	15186	14	444	1.4E-08	7.4E-05
GO:0001676	long-chain fatty acid metabolic process	32	15186	10	444	1.5E-08	7.7E-05
GO:0034440	lipid oxidation	72	15186	14	444	1.7E-08	8.9E-05
GO:0006637	acyl-CoA metabolic process	74	15186	14	444	2.5E-08	1.3E-04
GO:0042737	drug catabolic process	13	15186	7	444	2.6E-08	1.3E-04
GO:0009725	response to hormone stimulus	835	15186	54	444	3.2E-08	1.7E-04
GO:0044242	cellular lipid catabolic process	142	15186	19	444	3.2E-08	1.7E-04
GO:0014070	response to organic cyclic compound	662	15186	46	444	4.5E-08	2.3E-04
GO:0009056	catabolic process	2156	15186	105	444	4.7E-08	2.4E-04
GO:0030334	regulation of cell migration	391	15186	33	444	4.9E-08	2.5E-04
GO:0051272	positive regulation of cellular component movement	233	15186	24	444	9.1E-08	4.7E-04
GO:0005975	carbohydrate metabolic process	817	15186	52	444	9.9E-08	5.1E-04
GO:0019217	regulation of fatty acid metabolic process	83	15186	14	444	1.1E-07	5.9E-04
GO:0030335	positive regulation of cell migration	220	15186	23	444	1.3E-07	6.6E-04

GO ID	GO term	Property Size	Universe Size	Selection Property Size	Selection Size	p-value	Bonferroni corrected p-value
GO:0046486	glycerolipid metabolic process	274	15186	26	444	1.4E-07	7.1E-04
GO:2000145	regulation of cell motility	411	15186	33	444	1.6E-07	8.1E-04
GO:2000147	positive regulation of cell motility	224	15186	23	444	1.8E-07	9.2E-04
GO:0042738	exogenous drug catabolic process	11	15186	6	444	2.5E-07	1.3E-03
GO:0019432	triglyceride biosynthetic process	42	15186	10	444	2.6E-07	1.4E-03
GO:0001889	liver development	89	15186	14	444	2.8E-07	1.4E-03
GO:0007584	response to nutrient	180	15186	20	444	3.2E-07	1.6E-03
GO:0006694	steroid biosynthetic process	118	15186	16	444	3.3E-07	1.7E-03
GO:0051270	regulation of cellular component movement	446	15186	34	444	3.5E-07	1.8E-03
GO:0006635	fatty acid beta-oxidation	54	15186	11	444	3.6E-07	1.9E-03
GO:0019318	hexose metabolic process	251	15186	24	444	3.6E-07	1.9E-03
GO:0040017	positive regulation of locomotion	234	15186	23	444	3.9E-07	2.0E-03
GO:0040012	regulation of locomotion	443	15186	33	444	8.7E-07	4.5E-03
GO:0046890	regulation of lipid biosynthetic process	105	15186	14	444	2.2E-06	1.1E-02
GO:0006006	glucose metabolic process	205	15186	20	444	2.5E-06	1.3E-02
GO:0031667	response to nutrient levels	323	15186	26	444	3.2E-06	1.6E-02
GO:0009991	response to extracellular stimulus	352	15186	27	444	5.1E-06	2.6E-02
GO:0009743	response to carbohydrate stimulus	164	15186	17	444	6.4E-06	3.3E-02
GO:0033993	response to lipid	672	15186	41	444	7.0E-06	3.6E-02
GO:0006066	alcohol metabolic process	277	15186	23	444	7.1E-06	3.7E-02
GO:0035338	long-chain fatty-acyl-CoA biosynthetic process	18	15186	6	444	8.3E-06	4.3E-02
GO:0042445	hormone metabolic process	151	15186	16	444	9.0E-06	4.6E-02
GO:0051495	positive regulation of cytoskeleton organization	103	15186	13	444	9.4E-06	4.8E-02

Supplemental table 5 List of GO-terms for biological processes identified as significantly enriched for genes differentially expressed upon WY-14643 treatment

GO ID	GO term	Property Size	Universe Size	Selection Property Size	Selection Size	p-value	Bonferroni corrected p-value
GO:0006629	lipid metabolic process	1155	15186	83	408	5.8E-17	3.0E-13
GO:0044255	cellular lipid metabolic process	836	15186	67	408	4.9E-16	2.5E-12
GO:0046395	carboxylic acid catabolic process	222	15186	32	408	6.8E-15	3.5E-11
GO:0044281	small molecule metabolic process	2354	15186	123	408	3.1E-14	1.6E-10
GO:0055114	oxidation-reduction process	1005	15186	69	408	3.6E-13	1.9E-09
GO:0009062	fatty acid catabolic process	74	15186	18	408	6.7E-13	3.5E-09
GO:0019752	carboxylic acid metabolic process	884	15186	62	408	2.8E-12	1.4E-08
GO:0006082	organic acid metabolic process	962	15186	64	408	1.2E-11	6.1E-08
GO:0044242	cellular lipid catabolic process	142	15186	22	408	2.9E-11	1.5E-07
GO:0032787	monocarboxylic acid metabolic process	420	15186	38	408	5.5E-11	2.8E-07
GO:0009410	response to xenobiotic stimulus	162	15186	23	408	6.5E-11	3.3E-07
GO:0006631	fatty acid metabolic process	281	15186	30	408	1.2E-10	6.2E-07
GO:0016042	lipid catabolic process	254	15186	28	408	2.4E-10	1.2E-06
GO:0042221	response to chemical stimulus	3304	15186	142	408	6.1E-10	3.1E-06
GO:0006805	xenobiotic metabolic process	151	15186	21	408	6.5E-10	3.4E-06
GO:0071466	cellular response to xenobiotic stimulus	153	15186	21	408	8.4E-10	4.3E-06
GO:0070887	cellular response to chemical stimulus	1763	15186	90	408	9.2E-10	4.7E-06
GO:0042493	response to drug	390	15186	34	408	1.6E-09	8.1E-06
GO:0019395	fatty acid oxidation	71	15186	14	408	4.9E-09	2.5E-05
GO:0034440	lipid oxidation	72	15186	14	408	5.9E-09	3.0E-05
GO:0010033	response to organic substance	2067	15186	97	408	1.4E-08	7.4E-05
GO:0006635	fatty acid beta-oxidation	54	15186	12	408	1.5E-08	7.7E-05
GO:0015908	fatty acid transport	44	15186	11	408	1.6E-08	8.2E-05
GO:0015909	long-chain fatty acid transport	35	15186	10	408	1.8E-08	9.1E-05
GO:0019216	regulation of lipid metabolic process	224	15186	23	408	3.9E-08	2.0E-04
GO:0014070	response to organic cyclic compound	662	15186	43	408	7.8E-08	4.0E-04
GO:0001676	long-chain fatty acid metabolic process	32	15186	9	408	1.1E-07	5.6E-04
GO:0019217	regulation of fatty acid metabolic process	83	15186	13	408	3.0E-07	1.6E-03
GO:0007584	response to nutrient	180	15186	19	408	3.9E-07	2.0E-03
GO:0015718	monocarboxylic acid transport	86	15186	13	408	4.6E-07	2.4E-03
GO:0050896	response to stimulus	6976	15186	235	408	1.1E-06	5.7E-03
GO:0009725	response to hormone stimulus	835	15186	47	408	1.2E-06	6.3E-03
GO:0051272	positive regulation of cellular component movement	233	15186	21	408	1.3E-06	6.8E-03
GO:0030335	positive regulation of cell migration	220	15186	20	408	2.1E-06	1.1E-02
GO:0031667	response to nutrient levels	323	15186	25	408	2.2E-06	1.1E-02
GO:0030334	regulation of cell migration	391	15186	28	408	2.5E-06	1.3E-02
GO:2000147	positive regulation of cell motility	224	15186	20	408	2.7E-06	1.4E-02
GO:0046320	regulation of fatty acid oxidation	35	15186	8408		3.2E-06	1.6E-02
GO:0009991	response to extracellular stimulus	352	15186	26	408	3.3E-06	1.7E-02
GO:0009605	response to external stimulus	1140	15186	57	408	3.6E-06	1.9E-02
GO:0071310	cellular response to organic substance	1403	15186	66	408	4.5E-06	2.3E-02

GO ID	GO term	Property Size	Universe Size	Selection Property Size	Selection Size	p-value	Bonferroni corrected p-value
GO:0040017	positive regulation of locomotion	234	15186	20	408	5.3E-06	2.8E-02
GO:2000145	regulation of cell motility	411	15186	28	408	6.5E-06	3.4E-02
GO:0009743	response to carbohydrate stimulus	164	15186	16	408	9.0E-06	4.6E-02
GO:0009056	catabolic process	2156	15186	90	408	9.2E-06	4.7E-02

Supplemental Table 6 List of differentially expressed genes upon CITCO, rifampicin and WY-14643 treatment included in the "Core ADME" or "Extended ADME" list on www.pharmaadme.org

Gene Symbol	ADME list	log$_2$ FC (CITCO)	log$_2$ FC (RIF)	log$_2$ FC (WY)
ABCB1	core		0.60	0.18
ABCB4	extended		-0.11	0.55
ABCC2	core		0.31	
ADH1A	extended		-0.83	-0.41
ADH1B	extended		-1.36	-0.56
ADH4	extended		-0.62	
ADH6	extended		-0.33	
ALDH6A1	extended	-0.17	-0.23	-0.31
CAT	extended			0.19
CES2	extended		-0.10	
CYP1A1	core	0.83	0.48	
CYP1A2	core	0.41		
CYP21A2	extended		0.31	-0.19
CYP2A13	extended	0.78	0.63	
CYP2A6	core	0.77	0.64	
CYP2A7	extended	0.87	0.64	
CYP2B6	core	1.00	1.15	0.40
CYP2C8	core	0.74	1.37	0.75
CYP2C9	core	0.35	0.80	
CYP2E1	core	-0.22	-0.59	
CYP2J2	extended		-0.25	
CYP3A4	core	0.67	2.03	0.77
CYP3A43	extended		0.88	0.26
CYP3A5	core	0.23	0.67	0.21
CYP3A7	extended	0.54	1.25	0.50
CYP4A11	extended	-0.19	-0.70	0.82
CYP4F11	extended			-0.18
CYP4F12	extended		0.23	-0.28
CYP4F3	extended		0.34	-0.16
CYP7A1	extended		-1.65	
CYP8B1	extended		-0.31	
EPHX1	extended	0.20	0.40	0.21
FMO5	extended		-0.34	-0.33
GPX2	extended		0.58	0.16
GSTA2	extended		0.30	0.14
HNF4A	extended		-0.15	-0.13
MGST1	extended	0.11	0.06	0.06
POR	extended	0.07	0.36	0.29
RXRA	extended	-0.10	-0.24	
SLC22A7	extended		-0.51	
SLC22A9	extended	-0.26	-0.47	
SULT1B1	extended	-0.09	-0.55	
SULT1E1	extended		-0.97	
SULT2A1	extended		0.48	0.42
UGT1A1	core	0.16	0.30	0.17
UGT2B4	extended	0.14	0.17	0.08

Supplemental Table 7 mRNA expression of ADME genes in PHHs after treatment with rifampicin, hyperforin and TRPC6 activating phloroglucinols.

Gene Symbol	rifampicin 10 µM FC (SD)	hyperforin 1 µM FC (SD)	hyperforin 5 µM FC (SD)	Hyp1 1 µM FC (SD)	Hyp1 5 µM FC (SD)	Hyp5 1 µM FC (SD)	Hyp5 5 µM FC (SD)	Hyp7 1 µM FC (SD)	Hyp7 5 µM FC (SD)	Hyp8 1 µM FC (SD)	Hyp8 5 µM FC (SD)	Hyp9 1 µM FC (SD)	Hyp9 5 µM FC (SD)
CYP1A1	1.22 (0.62)	1.15 (0.70)	3.60 (1.28)	1.15 (0.49)	0.89 (0.28)	0.93 (0.44)	1.41 (0.82)	0.88 (0.96)	0.82 (0.12)	1.06 (0.22)	1.32 (0.82)	0.86 (0.64)	1.10 (0.36)
CYP1A2	1.01 (0.23)	1.06 (0.13)	0.68 (0.24)	1.06 (0.14)	1.79 (0.48)*	0.94 (0.24)	1.17 (0.34)	1.24 (0.26)	1.03 (0.27)	0.96 (0.15)	0.93 (0.28)	1.07 (0.10)	1.45 (0.36)
CYP2A6	2.60 (0.72)	1.92 (0.96)	1.40 (0.60)	1.30 (0.63)	1.06 (0.40)	1.15 (0.45)	1.18 (0.56)	1.66 (0.33)	1.09 (0.22)	1.09 (0.31)	0.88 (0.38)	0.93 (0.21)	1.33 (0.22)
CYP2B6	3.83 (0.53)***	2.88 (0.61)***	2.51 (1.22)***	1.13 (0.30)	1.55 (0.82)	1.18 (0.39)	1.09 (0.49)	1.69 (0.07)*	1.16 (0.41)	1.25 (0.32)	1.18 (0.43)	1.13 (0.26)	1.22 (0.33)
CYP2C19	1.82 (1.10)	1.68 (1.26)	0.66 (0.13)	1.61 (0.15)	1.43 (0.35)	1.10 (0.19)	1.10 (0.59)	1.23 (0.21)	1.23 (0.52)	1.06 (0.42)	1.02 (0.18)	1.18 (0.37)	1.37 (0.57)
CYP2C8	2.52 (0.62)	1.63 (1.06)	1.78 (0.98)	1.00 (0.30)	0.88 (0.69)	0.88 (0.47)	0.85 (0.35)	1.46 (0.02)	0.84 (0.17)	0.87 (0.26)	1.10 (0.64)	0.84 (0.15)	0.99 (0.14)
CYP2C9	4.06 (0.78)***	3.93 (2.37)***	1.52 (0.35)	1.31 (0.31)	1.47 (0.50)	1.21 (0.32)	1.13 (0.30)	1.90 (0.32)*	1.23 (0.24)	1.33 (0.41)	1.15 (0.63)	1.31 (0.22)	1.29 (0.13)
CYP2D6	0.86 (0.18)	0.82 (0.39)	1.20 (0.69)	1.19 (0.52)	0.98 (0.31)	0.72 (0.31)	1.10 (0.70)	1.24 (0.14)	1.25 (0.63)	0.96 (0.33)	0.99 (0.53)	1.15 (0.28)	1.67 (0.81)
CYP2E1	1.00 (0.13)	1.13 (0.14)	2.42 (0.52)***	1.13 (0.09)	1.11 (0.14)	1.09 (0.10)	1.12 (0.20)	1.24 (0.13)*	1.01 (0.04)	1.09 (0.07)	1.08 (0.06)	0.99 (0.03)	1.05 (0.08)
CYP3A4	24.28 (21.65)***	15.80 (7.18)***	3.33 (0.69)***	0.99 (0.06)	1.05 (0.23)	1.04 (0.16)	1.12 (0.12)	1.19 (0.22)	1.09 (0.07)	1.26 (0.37)	1.17 (0.26)	1.00 (0.14)	1.13 (0.28)
CYP3A5	3.75 (1.51)***	5.30 (2.96)***	3.96 (2.42)***	1.33 (0.21)	1.47 (0.08)	1.23 (0.10)	1.41 (0.19)	1.51 (0.22)	1.17 (0.14)	1.25 (0.22)	1.22 (0.25)	1.22 (0.05)	1.49 (0.34)
CYP3A7	4.48 (2.10)**	5.77 (2.55)***	6.11 (4.38)**	1.21 (0.05)	1.23 (0.22)	1.17 (0.24)	1.35 (0.28)	2.04 (1.45)	1.22 (0.24)	1.17 (0.71)	1.21 (0.70)	1.28 (0.21)	0.92 (0.15)
CYP7A1	0.16 (0.06)**	0.15 (0.08)**	0.12 (0.04)**	0.73 (0.29)	1.02 (0.35)	0.99 (0.59)	0.72 (0.71)	1.42 (0.77)	0.73 (0.62)	1.24 (0.72)	0.79 (0.68)	0.96 (0.04)	0.84 (0.34)
ADH1A	0.80 (0.19)	0.86 (0.23)	1.80 (0.38)	1.18 (0.33)	1.04 (0.14)	1.13 (0.25)	1.02 (0.37)	1.22 (0.15)	1.21 (0.18)	1.10 (0.08)	0.82 (0.13)	0.91 (0.27)	1.00 (0.33)
ALDH2	0.98 (0.09)	1.09 (0.18)	1.41 (0.39)	1.11 (0.26)	1.16 (0.33)	1.19 (0.30)	1.20 (0.43)	0.96 (0.12)	1.00 (0.20)	1.01 (0.32)	1.08 (0.46)	0.92 (0.24)	1.10 (0.19)
DPYD	0.98 (0.02)	1.10 (0.05)	0.82 (0.10)	1.19 (0.14)	1.27 (0.25)	1.07 (0.09)	1.32 (0.22)	1.02 (0.06)	0.95 (0.09)	1.03 (0.32)	0.97 (0.11)	1.08 (0.04)	1.16 (0.12)
ALAS1	2.46 (0.28)***	2.72 (0.20)***	1.78 (0.44)	1.08 (0.14)	1.16 (0.24)	1.13 (0.16)	1.19 (0.16)	1.07 (0.01)	1.06 (0.10)	1.08 (0.19)	1.03 (0.12)	0.98 (0.16)	1.25 (0.18)*
HMOX1	1.28 (0.31)	1.48 (0.08)**	1.85 (0.73)	1.11 (0.12)	1.24 (0.20)	1.19 (0.23)	1.17 (0.16)	1.05 (0.21)	0.97 (0.11)	1.03 (0.15)	0.92 (0.03)	0.98 (0.17)	1.04 (0.11)
POR	1.39 (0.20)	1.63 (0.28)**	1.97 (0.33)***	1.06 (0.20)	1.10 (0.43)	1.10 (0.26)	1.18 (0.24)	1.06 (0.10)	1.14 (0.25)	1.39 (0.83)	0.93 (0.15)	0.98 (0.33)	1.05 (0.24)
GSTA2	1.13 (0.40)	1.31 (0.27)	0.97 (0.72)	0.99 (0.20)	1.20 (0.33)	1.00 (0.27)	1.07 (0.27)	1.05 (0.29)	0.91 (0.10)	0.98 (0.31)	0.89 (0.22)	0.94 (0.18)	0.97 (0.25)
GSTP1	0.60 (0.10)	0.74 (0.12)	1.48 (0.69)	0.86 (0.15)	1.01 (0.22)	0.94 (0.12)	0.98 (0.04)	0.91 (0.17)	0.79 (0.09)	0.84 (0.08)	0.81 (0.11)	0.84 (0.09)	0.88 (0.28)
NAT1	1.13 (0.33)	1.11 (0.10)	0.57 (0.12)	1.20 (0.32)	1.37 (0.94)	1.18 (0.67)	0.98 (0.14)	1.37 (0.24)	0.93 (0.09)	1.23 (0.24)	0.91 (0.26)	1.19 (0.47)	1.30 (0.31)
NAT2	0.77 (0.20)	0.82 (0.07)	0.64 (0.25)	1.02 (0.27)	1.18 (0.24)	1.05 (0.30)	1.04 (0.08)	1.01 (0.12)	0.88 (0.12)	0.97 (0.25)	0.94 (0.14)	1.09 (0.17)	0.97 (0.25)
SULT1B1	0.91 (0.15)	0.87 (0.39)	0.58 (0.29)	1.36 (0.42)	1.27 (0.43)	1.23 (0.46)	1.15 (0.39)	1.29 (0.32)	1.15 (0.35)	1.10 (0.28)	0.90 (0.22)	0.89 (0.32)	1.31 (0.34)
TPMT	1.01 (0.10)	1.06 (0.21)	0.77 (0.40)	1.05 (0.21)	1.07 (0.38)	1.07 (0.30)	1.04 (0.33)	0.88 (0.18)	0.94 (0.18)	0.94 (0.33)	0.90 (0.36)	0.84 (0.29)	0.99 (0.28)
UGT1A1	2.89 (0.56)***	2.90 (0.93)***	1.57 (0.48)*	1.14 (0.04)	1.33 (0.23)	1.10 (0.13)	1.20 (0.13)	1.25 (0.07)	1.06 (0.10)	1.11 (0.13)	1.09 (0.10)	1.08 (0.10)	1.15 (0.03)
UGT2B7	0.90 (0.18)	0.96 (0.12)	0.62 (0.35)	0.97 (0.04)	1.01 (0.27)	0.93 (0.16)	1.05 (0.37)	0.98 (0.12)	0.88 (0.17)	0.97 (0.15)	0.95 (0.19)	0.94 (0.21)	0.95 (0.23)
ABCB1	2.00 (0.20)*	2.35 (0.37)**	1.50 (0.79)	1.49 (0.30)	1.36 (0.46)	1.49 (0.11)	1.14 (0.61)	1.08 (0.16)	0.99 (0.05)	0.99 (0.32)	1.09 (0.45)	0.90 (0.26)	1.23 (0.26)
ABCC2	1.34 (0.06)	1.35 (0.30)	1.16 (0.28)	1.08 (0.33)	1.17 (0.43)	0.96 (0.38)	0.94 (0.29)	0.91 (0.19)	0.94 (0.20)	0.87 (0.26)	0.81 (0.19)	0.97 (0.35)	1.05 (0.45)
ABCG2	0.84 (0.18)	1.10 (0.25)	1.10 (0.32)	1.18 (0.26)	1.18 (0.51)	1.10 (0.39)	1.09 (0.36)	0.81 (0.07)	0.90 (0.18)	0.92 (0.37)	0.90 (0.27)	1.01 (0.34)	1.13 (0.44)
SLC10A1	0.87 (0.23)	0.92 (0.05)	0.44 (0.34)***	1.09 (0.07)	1.16 (0.07)	1.05 (0.17)	0.96 (0.17)	1.13 (0.14)	1.02 (0.04)	1.09 (0.06)	1.01 (0.13)	1.02 (0.18)	1.02 (0.12)
SLC22A7	0.64 (0.25)	0.74 (0.17)	0.54 (0.20)	1.21 (0.90)	1.05 (0.26)	1.24 (0.93)	1.20 (0.69)	1.21 (0.08)	1.31 (0.61)	0.90 (0.19)	0.99 (0.25)	1.10 (0.43)	1.27 (0.33)
SLCO1B1	0.99 (0.20)	1.04 (0.22)	0.86 (0.51)	1.09 (0.20)	1.07 (0.35)	1.07 (0.35)	1.08 (0.42)	0.88 (0.30)	0.90 (0.19)	0.89 (0.32)	0.99 (0.48)	0.95 (0.35)	0.99 (0.29)

FC, fold change; SD, standard deviation; significant differences are indicated by *, $p < 0.05$; **, $p < 0.01$ or ***, $p < 0.001$, compared with control treatment.

Supplemental Table 8 mRNA expression of ADME genes in PHHs after treatment with TRPC6 non-activating phloroglucinols.

Gene Symbol	Hyp2 10 µM FC (SD)		Hyp2 50 µM FC (SD)		Hyp3 10 µM FC (SD)		Hyp3 50 µM FC (SD)		Hyp4 10 µM FC (SD)		Hyp4 50 µM FC (SD)		Hyp6 10 µM FC (SD)		Hyp6 50 µM FC (SD)
CYP1A1	1.51 (0.40)		3.35 (1.85)		0.92 (1.00)		0.95 (0.27)		0.91 (0.36)		3.61 (2.70)		1.41 (0.81)		4.06 (2.22)
CYP1A2	2.73 (0.84)***		5.37 (2.47)		1.13 (0.08)		1.24 (0.45)		1.99 (0.52)**		5.21 (3.68)		1.19 (0.19)		2.67 (1.91)
CYP2A6	1.26 (0.16)		0.96 (0.10)		1.35 (0.66)		1.30 (0.59)		1.15 (0.01)		0.97 (0.55)		1.03 (0.29)		1.03 (0.25)
CYP2B6	1.24 (0.33)		0.99 (0.29)		0.85 (0.15)		1.00 (0.27)		1.39 (0.19)		1.85 (0.80)		1.09 (0.39)		1.68 (0.49)
CYP2C19	1.29 (0.36)		1.33 (0.89)		1.43 (0.35)		1.52 (0.35)		1.32 (0.46)		1.31 (0.38)		1.23 (0.39)		1.69 (0.85)
CYP2C8	1.03 (0.40)		0.76 (0.26)		1.62 (0.65)		1.33 (0.63)		0.77 (0.21)		1.15 (0.80)		1.04 (0.49)		1.52 (1.03)
CYP2C9	1.43 (0.22)		1.07 (0.20)		1.39 (0.40)		1.33 (0.27)		1.14 (0.23)		0.96 (0.40)		1.27 (0.23)		1.32 (0.47)
CYP2D6	1.08 (0.33)		0.84 (0.24)		1.11 (0.22)		1.21 (0.21)		1.04 (0.43)		0.77 (0.30)		1.15 (0.24)		0.65 (0.25)
CYP2E1	1.13 (0.19)		1.16 (0.20)		1.01 (0.03)		1.38 (0.09)		1.05 (0.06)		0.89 (0.24)		1.14 (0.06)		1.12 (0.30)
CYP3A4	1.12 (0.39)		0.77 (0.19)		1.28 (0.60)		1.34 (0.76)		0.96 (0.37)		1.63 (1.68)		1.03 (0.48)		1.33 (1.01)
CYP3A5	1.28 (0.32)		1.31 (0.42)		1.12 (0.32)		1.33 (0.14)		1.11 (0.25)		1.35 (0.89)		1.17 (0.22)		1.56 (0.93)
CYP3A7	0.71 (0.40)		0.86 (0.23)		1.60 (1.35)		1.21 (0.56)		0.87 (0.10)		1.23 (0.95)		1.03 (0.33)		1.82 (1.84)
CYP7A1	0.97 (0.19)		0.61 (0.28)		2.13 (1.16)		4.05 (3.13)		0.87 (0.33)		0.37 (0.25)		0.74 (0.20)		1.19 (1.73)
ADH1A	1.25 (0.34)		1.04 (0.16)		1.22 (0.39)		1.72 (0.33)		0.98 (0.10)		0.77 (0.27)		1.00 (0.29)		1.28 (0.76)
ALDH2	1.18 (0.36)		1.10 (0.21)		1.07 (0.17)		1.30 (0.14)		1.03 (0.37)		1.08 (0.32)		1.05 (0.41)		0.86 (0.22)
DPYD	1.21 (0.33)		1.06 (0.31)		1.06 (0.33)		1.18 (0.22)		0.98 (0.20)		0.90 (0.34)		1.01 (0.12)		1.19 (0.98)
ALAS1	1.12 (0.22)		1.26 (0.29)		1.00 (0.16)		1.07 (0.15)		1.01 (0.23)		1.24 (0.52)		1.13 (0.25)		1.11 (0.28)
HMOX1	1.01 (0.13)		1.08 (0.02)		0.94 (0.09)		0.83 (0.09)		0.99 (0.13)		0.99 (0.20)		1.08 (0.11)		1.07 (0.05)
POR	1.36 (0.44)		1.16 (0.03)		1.05 (0.24)		1.09 (0.14)		1.04 (0.46)		1.12 (0.26)		1.18 (0.41)		1.01 (0.20)
GSTA2	1.00 (0.23)		0.93 (0.20)		0.98 (0.13)		1.14 (0.08)		0.86 (0.13)		0.94 (0.22)		0.98 (0.26)		1.20 (0.48)
GSTP1	0.88 (0.09)		0.94 (0.17)		0.92 (0.05)		0.68 (0.45)		0.73 (0.16)		0.90 (0.22)		0.90 (0.13)		1.01 (0.28)
NAT1	1.14 (0.38)		1.22 (0.20)		0.89 (0.18)		1.23 (0.22)		0.95 (0.13)		1.06 (0.31)		1.07 (0.43)		1.88 (1.48)
NAT2	1.01 (0.37)		1.10 (0.45)		1.01 (0.41)		1.37 (0.11)		0.89 (0.23)		0.77 (0.25)		1.06 (0.28)		1.24 (0.76)
SULT1B1	1.31 (0.29)		1.35 (0.35)		1.12 (0.27)		1.72 (0.29)		0.95 (0.09)		1.03 (0.58)		1.32 (0.61)		1.80 (0.97)
TPMT	1.08 (0.39)		1.10 (0.17)		0.91 (0.05)		1.30 (0.09)		0.88 (0.27)		1.03 (0.33)		0.97 (0.35)		1.08 (0.32)
UGT1A1	1.22 (0.13)		1.48 (0.24)		0.98 (0.11)		1.09 (0.21)		1.12 (0.21)		1.83 (0.71)		1.14 (0.13)		1.57 (0.49)
UGT2B7	1.07 (0.20)		1.11 (0.04)		1.05 (0.39)		1.26 (0.03)		0.84 (0.17)		0.93 (0.11)		0.97 (0.37)		1.24 (0.85)
ABCB1	1.34 (0.49)		1.25 (0.33)		1.18 (0.56)		1.32 (0.26)		1.04 (0.36)		1.19 (0.66)		1.16 (0.37)		1.14 (0.42)
ABCC2	1.28 (0.54)		1.33 (0.61)		1.11 (0.16)		1.27 (0.42)		0.89 (0.27)		1.10 (0.40)		1.18 (0.46)		1.28 (0.37)
ABCG2	0.99 (0.33)		1.30 (0.47)		0.97 (0.13)		1.40 (0.07)		0.93 (0.37)		1.10 (0.38)		1.03 (0.52)		1.07 (0.54)
SLC10A1	1.24 (0.37)		0.82 (0.15)		1.11 (0.24)		1.15 (0.13)		0.97 (0.26)		0.76 (0.21)		1.08 (0.31)		0.93 (0.28)
SLC22A7	1.39 (0.61)		0.90 (0.45)		1.40 (0.52)		1.46 (0.39)		0.69 (0.20)		0.73 (0.31)		1.29 (0.79)		1.29 (1.08)
SLCO1B1	1.21 (0.52)		1.18 (0.15)		0.99 (0.14)		1.31 (0.05)		0.85 (0.25)		0.92 (0.24)		1.05 (0.50)		1.00 (0.34)

FC, fold change; SD, standard deviation; significant differences are indicated by *, $p < 0.05$; **, $p < 0.01$ or ***, $p < 0.001$, compared with control treatment.

Supplemental Table 9 Summary of different PXR agonist and antagonist pharmacophores using model names previously described (Ekins and Erickson, 2002; Ekins et al., 2008b; Yasuda et al., 2008) (- = no mapping to pharmacophore, higher fit scores are preferable). Analysis performed by Prof. Sean Ekins (Kandel et al., 2014).

Compound	BMS agonist pharmacophore	Diverse PXR agonist pharmacophore	Original PXR agonist pharmacophore	PXR antagonist pharmacophore	Lipophilicity
	Fit value	Fit value	Fit value	Fit value	AlogP
Hyperforin	4.71	-	2.92	-	9.06
Hyp1	1.93	-	-	-	3.33
Hyp5	2.32	-	-	-	4.25
Hyp7	4.03	-	-	2.51	5.81
Hyp8	2.92	-	-	-	5.33
Hyp9	4.13	6.87	-	-	4.65
Hyp2	-	-	-	-	2.22
Hyp3	5.35	5.88	2.84	-	13.78
Hyp4	3.39	-	-	-	3.56
Hyp6	0.58	-	-	-	2.53

Supplemental Table 10 Docking in 1M13 LBD. Summary of calculated libdock scores (higher scores are preferable). Analysis performed by Prof. Sean Ekins (Kandel et al., 2014).

Compound	PXR LBD Libdock score	Murine serotonin uptake EC_{50} data (µM) (Leuner et al., 2010)
Hyperforin	135.85	1.93
Phloroglucinol	60.56	-
Hyp1	85.77	2.5
Hyp5	107.81	4.84
Hyp7	129.28	1.5 3.5
Hyp8	111.73	11.10
Hyp9	103.83	----
Hyp2	76.73	
Hyp3	failed to dock	
Hyp4	88.55	
Hyp6	100.72	

Supplemental Table 11 PXR antagonist sites and their docking scores (higher scores are preferable). Analysis performed by Prof. Sean Ekins (Kandel et al., 2014).

Compound	SRC-1 site Libdock score	S208 Libdock score
Hyperforin	85.25	99.35
Phloroglucinol	45.53	61.78 129.4
Ketoconazole	103	104.43
Hyp1	66.81	114.3
Hyp5	67.46	140.19
Hyp7	90.43	103.77
Hyp8	83.34	125.64
Hyp9	75.23	99.13
Hyp2	63.74	153.33
Hyp3	103.43	114.06
Hyp4	77.1	120.42
Hyp6	74.41	